NASA CONTRACTOR REPORT

NASA CR-2277

NASA CR-2277

DEVELOPMENT OF DESIGN INFORMATION FOR MOLECULAR-SIEVE TYPE REGENERATIVE CO_2-REMOVAL SYSTEMS

by R. M. Wright, J. M. Ruder, V. B. Dunn, and K. C. Hwang

Prepared by
AIRESEARCH MANUFACTURING COMPANY
Los Angeles, Calif.
for Langley Research Center

NATIONAL AERONAUTICS AND SPACE ADMINISTRATION • WASHINGTON, D. C. • JULY 1973

AIR FORCE 13680 8-14-73/1000 copies

1. Report No.	2. Government Accession No.	3. Recipient's Catalog No.
NASA CR-2277		

4. Title and Subtitle	5. Report Date
DEVELOPMENT OF DESIGN INFORMATION FOR MOLECULAR-SIEVE TYPE REGENERATIVE CO_2-REMOVAL SYSTEMS	July 1973
	6. Performing Organization Code
7. Author(s)	8. Performing Organization Report No.
R. M. Wright, J. M. Ruder, V. B. Dunn, and K. C. Hwang	72-8417
	10. Work Unit No.
9. Performing Organization Name and Address	11. Contract or Grant No.
AIRESEARCH MANUFACTURING COMPANY LOS ANGELES, CALIFORNIA	NAS1-8559
	13. Type of Report and Period Covered
12. Sponsoring Agency Name and Address	CONTRACTOR REPORT
NATIONAL AERONAUTICS AND SPACE ADMINISTRATION WASHINGTON, D.C. 20546	14. Sponsoring Agency Code

15. Supplementary Notes

16. Abstract

Experimental and analytic studies were conducted with molecular sieve sorbents to provide (1) basic design information, and (2) to develop a system design technique for regenerable CO_2-removal systems for manned spacecraft. Single sorbate equilibrium data were obtained over a wide range of conditions for CO_2, water, nitrogen, and oxygen on several molecular sieve and silica gel sorbents. The coadsorption of CO_2 with water preloads, and with oxygen and nitrogen was experimentally evaluated. Mass-transfer, and some limited heat-transfer performance evaluations were accomplished under representative operating conditions, including the coadsorption of CO_2 and water. CO_2-removal-system performance prediction capability was derived and is provided in two computer programs which, while only described briefly in the report, are documented fully in NASA CR-112098.

17. Key Words (Suggested by Author(s))	18. Distribution Statement
Adsorption, CO_2, Concentration Process Math Modeling, Regenerative CO_2 Sorber, CO_2 Removal, Molecular Sieve Adsorption Data, CO_2 Removal System Design Criteria	UNCLASSIFIED

19. Security Classif. (of this report)	20. Security Classif. (of this page)	21. No. of Pages	22. Price*
UNCLASSIFIED	UNCLASSIFIED	253	$3.00

*For sale by the National Technical Information Service, Springfield, Virginia 22151

FOREWORD

This report describes the work performed by the AiResearch Manufacturing Company of Los Angeles, California under Tasks I and 2 of Contract NASI-8859, "Development of Regenerative CO_2-Removal-System Design Techniques," issued by NASA Langley Research Center. The purpose of Tasks I and 2 of the contract was to produce basic design data and design tools (in the form of computer programs) to facilitate the design process of, and to aid efforts in improving spacecraft regenerable CO_2-removal systems which employ molecular-sieve and silica-gel inorganic sorbents. The time period of the analysis and experimentation that this report represents was from November 1968 to May 1972.

Two CO_2-removal-system performance-prediction computer programs were produced under this contract. These programs are discussed only briefly in this report; full documentation of these programs is contained in a separate report "A Transient Performance Prediction Method for CO_2 Removal with Regenerable Adsorbents", NASA CR-II2098 (Reference I).

NASA Manned Spacecraft Center provided a portion of the financial support for the dynamic coadsorption mass-transfer tests; these tests were monitored at NASA MSC by Mr. Will Ellis. Dr. Sam Davis served as a consultant to NASA MSC in this area of interest.

At AiResearch, Mr. J. P. Byrne was the initial program manager; later, Mr. C. W. Browning was program manager. Initially, Mr. J. M. Ruder was principal investigator in charge of all equilibrium data taken in Tasks I and 2. Later, Dr. R. M. Wright was principal investigator responsible for dynamic mass-transfer experimentation. Dr. K. C. Hwang was responsible for the performance-prediction computer programs developed under the contract. Dr. Jack Winnick of the University of Missouri was a consultant to AiResearch during the early phases of the work.

Experimental equipment design was handled by Mr. K. Walther, Mr. M. Gee, and Mr. W. Dunn. Laboratory technicians were Mr. R. Forrey, Mr. D. Falzett, and Mr. R. Clifton.

CONTENTS

CONTENTS (Continued)

CONTENTS (Continued)

CONTENTS (Continued)

ILLUSTRATIONS

ILLUSTRATIONS (Continued)

ILLUSTRATIONS (Continued)

ILLUSTRATIONS (Continued)

TABLES

DEVELOPMENT OF DESIGN INFORMATION FOR MOLECULAR SIEVE TYPE REGENERATIVE CO_2-REMOVAL SYSTEMS

by R.M. Wright, Ph.D., J.M. Ruder,
V.B. Dunn, and K.C. Hwang, Ph.D.

Space and Cryogenic Systems Department
AiResearch Manufacturing Company
A Division of The Garrett Corporation

SUMMARY

This report describes the results of analytical and experimental research studies which were directed toward the acquisition of basic design information on molecular sieve sorbents for CO_2 removal systems. Equilibrium and dynamic mass-transfer data are presented for a number of molecular sieve sorbents over a range of conditions appropriate to future manned spacecraft CO_2-removal systems.

A large amount of equilibrium data for molecular sieve and silica gel sorbents was obtained and is presented here in graphical form. Some of the equilibrium data is for coadsorbed pairs of sorbents, with water and CO_2 coadsorption of primary interest.

The dynamic mass-transfer behavior of special prototype beds was studied under controlled conditions. This involved studies with single sorbates in the carrier gas, and tests where the coadsorption of CO_2 and water was studied. Many observations resulted from the latter series of tests. From the single-sorbate tests, mass-transfer coefficients and intraparticle diffusivities were evaluated and are presented herein. Comparisons were made of different size plate-fin heat-transfer surfaces placed within the packed sorbent beds.

Packed-bed densities and process-gas flow pressure drops were measured for various bed heat-transfer-surface configurations.

Two large-scale computer programs were produced to predict the transient performance of spacecraft, regenerable, CO_2-removal systems which employ molecular sieve sorbents. One program considers water-dump/CO_2-dump systems which use composite sorbent beds. The second, more-general program allows for two- or four-bed systems, with water-save and CO_2-save provisions. It considers the second-order effects due to the coadsorption of CO_2, water, oxygen, and nitrogen. Several auxiliary programs useful in molecular-sieve CO_2-removal-system design work were produced.

Along with presentation of graphical and numerical data, pertinent observations and conclusions have been made. Suggestions for further design and research activity are made.

SYMBOLS

a_{sg}	Specific external sorbent area exposed to the process gas stream, ft^2/ft^3 of bed.
A	Superficial bed cross-section area for flow, ft^2
C_{CO_2}, C_{H_2O}	Concentration, mass of CO_2 or H_2O/mass of N_2
D, D_k	Intraparticle diffusivity for sorbate k, ft^2/hr
f	Bed void fraction
L	Flow length, ft
ΔH	Differential heat of adsorption Btu/lb of sorbate
K	Constant in pressure drop equation
K_g	Gas-phase mass-transfer coefficient, lb-mole/hr-ft^2-mm Hg
M_{Bed}	Mass of sorbent contained in the test bed, lb
M_k, M_g	Molecular weight of sorbate k; molecular weight of process gas stream
p, p_k	Partial pressure of sorbate k, mm Hg
P	Total pressure, mm Hg
ΔP	Pressure drop, psi or in. H_2O
r	Radial distance from sorbent pellet center, ft
R	Universal gas constant, 1.986 Btu/lb-mole-^0R
t	Time, adsorption-breakthrough time, hr
T	Temperature, ^0F or ^0R
u_g	Interstitial gas velocity, ft/hr
V	Supercificial gas velocity, ft/sec

w	Sorbate loading on the sorbent, mass sorbate/mass sorbent; or as a percent loading, mass sorbate/100 mass units of sorbent
W	Process gas flow rate, lb/hr
x	Axial distance from front of bed, ft
θ	Perfect-bed breakthrough time, hr. Defined by Equations 4-3 and 4-4.
ρ	Density, lb/ft^3
σ	Ratio of actual density in lb/ft^3 to that at standard conditions $\sigma = \rho/0.07176$
τ	Dimensionless time, $\tau = t/\theta$
ψ	Dimensionless concentration, defined by Equation 4-6

Subscripts

g	Process gas
k	Sorbate k; for example CO_2 or H_2O
s	Sorbent
sb	Sorbent bed
sg	sorbent-to-gas

Superscript

*	Refers to equilibrium condition

SECTION I

INTRODUCTION

In all Mercury, Gemini, and Apollo manned spaceflights, carbon dioxide has been removed from the spacecraft cabin by means of absorption by lithium hydroxide. This method of CO_2 removal is extremely reliable and efficient, and in general, the design of LiOH systems is relatively easy. The main objection to LiOH is that it is not regenerable and as an expendable it can represent a large weight penalty to the vehicle, especially for long duration missions.

Considering the normal CO_2 output of a man to be 2.2 lb/day, and using a 92-percent utilization efficiency without contingencies, 2.60 lb of LiOH are required per man-day. For first generation manned-spacecraft, the penalties associated with LiOH were reasonably small. A one-day Mercury flight required about 5.4 lb LiOH, contained in a single bed. For the two-man Gemini vehicle, one large LiOH bed was employed which could hold 80.5 lb LiOH for a 14-day mission. The Apollo vehicle employs a dual-bed LiOH CO_2-removal unit; each bed contains a removable LiOH charge of 3.979 lb. Each bed is charged by the crew every 24 hours; bed recharging is alternated to provide one charge every 12 hours. For a 12-day mission, some 24 LiOH charges (95.5 lb) are carried.

For long duration missions with large crews, the total weight and volume penalty due to LiOH could be substantial. Also, the lower cabin levels of CO_2 and higher total pressures desired in future missions makes the design of LiOH systems more complex. This is due to the accumulation in the bed of water produced by the chemical reaction with LiOH, and the subsequent slow-down in the CO_2 removal process. The water accumulation is a result of excessive cooling of the bed due to the large flow of cabin gases. In previous missions, at 7 mm Hg CO_2 partial pressure and 5 psia total pressure, the mass ratio of CO_2 to cabin gases is reasonably large, and the heat of reaction of CO_2 and LiOH is sufficient to keep the bed warm and to drive off water formed by the reaction. For future mission conditions, the mass ratio of CO_2 to cabin gases is much lower and the bed would run much cooler. To make the system work, thermal conservation by means of regenerative heat exchangers is necessary. The system and its design are thereby complicated.

As a consequence of the penalties and added complexities of LiOH systems for long-term flights, there has been a great deal of emphasis to develop low-penalty, regenerable CO_2-removal systems. One of the most promising concepts involves the use of inorganic molecular-sieve sorbents. The concept has been used by AiResearch in a system for Skylab missions. This system is capable of maintaining the partial pressure of CO_2 in Skylab at 5 mm Hg or below for the three-man crew. The entire system weighs 195 lb; two entire systems are included in the vehicle for redundancy, although only one is required for the CO_2 control. The normal energy requirement (exclusive of fans) is 87 watt-hr per day. The flow through the system is 15 lb per hr; cycle time is 30 minutes. Each system contains two beds. Each bed contains

7.5 lb of molecular sieve 13X and 9.9 lb of molecular sieve 5A. In addition, 10 lb of activated charcoal is included in each RCRS package. The Skylab vehicle is to be manned for a total of 112 days. If LiOH were used for CO_2 removal, 874 lb of the material would be required; not to mention the weight of the attendant hardware.

At the time that this program was initiated (during the early development period of the RCRS), it was obvious that there were many areas in the design of molecular-sieve CO_2 removal systems where data quantity and quality were marginal or insufficient, and that many areas existed where improvements could be made in design techniques. Thus, this program was directed at providing information and design tools where there were known deficiencies. This report presents the results of these efforts. Some of the results of the program were immediately used in the RCRS development.

With any learning and development process, as more information becomes available and as desired applications change, new areas emerge which warrant study. This has occurred with respect to molecular-sieve CO_2-removal systems. Throughout this program, where it has been possible, new areas of concern were incorporated into the study investigations; however, it was not possible to cover all such areas. In some cases, the need for further study has become apparent only recently; some of these areas are discussed in the last section of this report. In summary, it is considered that the concept of CO_2 removal by molecular-sieve sorbents is sound and practical for manned spacecraft. Further, the concept has considerable growth potential and thus should be considered as a leading candidate for CO_2 removal on future spacecraft.

Program results are presented in the remainder of this report. The contents of the report are summarized below:

- Section 1 Introduction
- Section 2 Basic Scope of the Study Program--Background information on spacecraft molecular-sieve CO_2-removal systems and a review of the scope of the program.
- Section 3 Equilibrium Data--Equilibrium data for CO_2, water, O_2, and N_2 on various molecular sieve types, including coadsorption of sorbate pairs on molecular sieves.
- Section 4 Single Sorbate Dynamic Mass-Transfer Data--Single-sorbate dynamic breakthrough tests and comparisons of packed-bed heat-transfer surfaces.
- Section 5 Evaluation of Mass-Transfer-Coefficients and Intra-particle Diffusivities--This evaluation based on the tests given in Section 4.
- Section 6 Coadsorption Dynamic Mass-Transfer Tests--Coadsorption dynamic breakthrough tests, involving CO_2 and water simultaneously adsorbed by molecular sieves.

- Section 7 Performance-Prediction Computer Programs--Computer programs developed under this contract.
- Section 8 Pressure Drop and Packed-Bed Densities--Data for molecular sieves in internally finned beds.
- Section 9 Conclusions and Recommendations

SECTION 2

BASIC SCOPE OF THE STUDY PROGRAM

GENERAL

This section presents background information on molecular sieve adsorbents, and on features of spacecraft CO_2-removal systems using molecular sieves. On the basis of the background information, this section reviews the scope of the research and analyses performed during this program.

REGENERABLE MOLECULAR-SIEVE CO_2-REMOVAL SYSTEMS FOR SPACECRAFT

Basic Characteristics of Molecular Sieves

Molecular sieves belong to the class of materials called zeolites which are generally crystalline, hydrated metal alumino silicates. Many types of zeolites are known. The molecular-sieve type of zeolite has a special crystalline structure which contains many interconnecting cavaties, all of uniform size. The cavities, or "cages," are interconnected by narrow openings, sometimes called windows. When formed, the cages are filled with water. Upon heating, the water can be driven out leaving a tremendous internal surface area capable of adsorbing many different gases and liquids, especially polar molecules like CO_2 and water.

When gases are adsorbed by molecular sieves, heat is given off in the process. Simply speaking, the heat release is approximately equal to the latent heat of vaporization of the gas at the adsorption temperature, plus a heat of adsorption. For water, the total heat release is about 1400 Btu per lb of adsorbed water. It is from this rather large heat effect associated with water that the name zeolite is derived: from the Greek, "zeo" meaning boil, and "lithos" meaning stone. Early observers noted that the natural zeolite materials seemed to melt and boil when heated--as water was given off. Also, in the baked-dry condition, rather violent heat releases can occur, simulating boiling, when zeolites are dumped into water. Some zeolites literally explode when plunged into water.

The unique property of molecular sieves--the property for which they are named--is that the openings between cavities are very uniform in size and small enough (3 to 10 angstroms, depending on the crystal type) to prohibit the entry and subsequent adsorption of large molecules. Thus, in many instances separations can be made strictly on the basis of the size of the molecules.

The chemical process industry today uses millions of pounds of molecular sieves in many diverse applications. The great majority of molecular sieves are made synthetically. There are three manufacturers of molecular-sieve or zeolite sorbents in the United States: Linde Division of Union Carbide Corp.,

Davison Chemical Division of W.R. Grace and Co., and Norton Company. Of major interest are the synthetic molecular sieves of the type A crystal structure and the type X crystal structure. With each of these types, the building blocks of the crystal are alumina and silica tetrahedra. These tetrahedra are each formed by four oxygen atoms surrounding an aluminum or silicon atom. Considering that neighboring tetrahedra share oxygen atoms (i.e., each oxygen atom is shared among four tetrahedra), silica tetrahedra, with silicon in the +4 valence state, are electrically neutral. However, with aluminum in the +3 valence state, the alumina tetrahedra are negatively charged. This requires the presence of a cation in the crystal structure. The cations are exchangeable and are located in the vicinity of the windows. By altering the size and valence of the cations, the window size may be made larger or smaller. For example, with sodium cations, molecular sieve type 4A has 4.2-angstrom windows. This is the parent A-type molecular sieve; it has the basic formula:

$$Na_{12}\left[(AlO_2)_{12}(SiO_2)_{12}\right] \times H_2O$$

By exchanging calcium ions for sodium ions (in the ratio of two sodiums for each calcium), type 5A molecular sieve is produced with approximately 5-angstrom windows. With potassium ions exchanged for the smaller sodium ions, the openings are closed to approximately 3 angstroms; the molecular sieve is called type 3A. Similarly, with the X-type crystal, types 10X and 13X are available. Type 13X has the chemical formula:

$$Na_{86}\left[(AlO_2)_{86}(SiO_2)_{106}\right] \times H_2O$$

It has windows of about 9 angstroms.

Because of their inorganic crystalline nature, molecular sieves are extremely inert and stable. For example, with normal commercial regeneration temperatures of about 600^0 to 700^0F, an indefinite number of regenerations of the basic crystal are possible without affecting adsorption performance. Excellent repeatability of performance has been experienced with molecular sieves.

Most molecular sieves are first manufactured in the form of fine crystallites. For 4A and 5A molecular sieves manufactured by Linde, the crystallites are cubic with crystal sides measuring from 1 to 5 μ, with the average being about 3 μ (Reference 2). This material (usually referred to as a powder) is not practical for packed-bed operations (pressure drop in beds would be too large); therefore, the base powder is usually combined with an inert clay binder and formed into pellets or spheres of practical dimensions (e.g., 1/16 to 1/8 in.).

The final molecular-sieve pellet or sphere is about 20 percent clay binder. It is desirable that the binder be as inert as possible, both chemically and with respect to adsorption; it should be strong, to allow long sorbent life; and it should possess an open-pore structure to allow unhindered diffusional access to the molecular-sieve crystallites. Each manufacturer claims to have produced a molecular-sieve sorbent which is near ideal with respect to these properties. In addition, binderless sorbent particles have

been produced. Early binderless particles were reputed to be fragile and to have a rather restrictive pore structure. Newer binderless sorbents are advertised as being much stronger and equal in dynamic performance to the standard sorbent particles with clay binder.

Characteristics of Spacecraft CO_2-Removal Systems using Molecular Sieves

Requirement for Water Predrier Beds. - Molecular sieve 5A has an equilibrium loading capacity for CO_2 of 0.068 gm CO_2/gm 5A at 70°F and a CO_2 partial pressure of 7 mm Hg. At the same temperature and at a water partial pressure of 9.2 mm Hg (50°F dew point), molecular sieve 5A has an equilibrium capacity for water of about 0.18 gm H_2O/gm 5A. However, the material will not simultaneously adsorb both CO_2 and water to these capacities. In fact, when both are present, molecular sieves unfortunately have a strong preference for water and will absorb much less CO_2. Further, if adequate water vapor is available, CO_2 will be stripped off molecular sieves, resulting in no net CO_2 adsorption.

This hydrophilic nature of molecular sieve sorbents has an important impact on spacecraft CO_2-removal systems: each system must contain a predrier bed upstream of the molecular-sieve CO_2-removal bed. This predrier (or desiccant) bed must be capable of trapping almost all of the water in the process air stream, allowing very little to reach the CO_2-removal bed. A removal efficiency of 99.5 percent is considered as a design goal for the predrier. When a molecular-sieve bed has adsorbed water to the point that its CO_2-removal performance is impaired, it is said to have been "poisoned." This poisoning is reversible in nature--like almost all adsorptions with molecular sieves. By heating the bed sufficiently to drive off the water, the CO_2-removal performance is totally restored to the bed.

Two sorbents have been proposed for the predrier bed: molecular sieve 13X and silica gel. Because of this use of silica gel, it has been included as a subject in this study. Molecular sieve 13X has less overall capacity for water at spacecraft cabin conditions than silica gel, but it has substantially greater capacity in the low partial-pressure (low concentration) range. The choice of sorbent to be used for a particular application depends upon design-analysis tradeoffs. For the Skylab RCRS, molecular sieve 13X is used.

Cyclic Adsorption/Desorption of Beds. - Molecular-sieve CO_2-removal systems operate in a cyclic fashion with two or, in rare cases, three sets of adsorption beds. While one set is adsorbing water and CO_2, the other set is undergoing a desorption process. When the respective adsorption processes have reached the desired limits, the process gas is switched to the freshly desorbed bed system, and the water- and CO_2-laden beds undergo the desorption process.

For adsorption, cabin gas is passed through the two beds (predrier and CO_2-removal) and returned to the cabin. Low head fans are sufficient for this application. As the adsorption process occurs, heat is given off in both beds. The design of the system must fully account for this heat release, as the molecular sieve adsorption capacities for CO_2 and water are inversely related

to temperature. As the beds warm, their equilibrium capacities for CO_2 and water become less.

There are two approaches to providing thermal control of adsorbing beds. First, in an active manner, cooling can be supplied to the beds from the spacecraft heat-transport system. This requires that cooling coils or passages be incorporated within the packed beds. The more efficient the cooling process (with the ultimate being an isothermal bed) and the lower the bed temperature, the more efficient will be the adsorption and the smaller will be the allowable bed size. The major disadvantage to internal bed cooling is that an interface is created with, and a dependency placed upon, the spacecraft coolant system. This latter system also sustains a penalty due to this application.

The second approach is to forego all active cooling and allow the adsorption beds to operate adiabatically. Basically, a larger bed mass is provided so that the heat released in adsorption does not raise the bed temperature to an intolerable level. The bed temperature floats somewhat above the inlet temperature of the process gas stream (usually cabin temperature). With this approach, a great deal of simplicity is allowed in the system hardware design; for example, internal coolant passages are dispensed with. However, in order to assure proper performance, very accurate and encompassing analyses are required. The RCRS for Skylab employs adiabatic beds, thus making the system independent of the spacecraft heat-transport system.

In general terms, desorption is accomplished by subjecting the bed to conditions where the equilibrium partial-pressure of the sorbate on the bed is greater than the actual partial pressure above the bed. This can be accomplished by subjecting the bed to an environment where the sorbate is in low concentration; it can also be accomplished by increasing the temperature of the bed, thus increasing the equilibrium partial pressure of the bed; or both methods may be used. If desorption is accomplished by subjecting the bed to low pressure (and thus a low partial pressure of the sorbate), the bed is said to be operating in a "pressure swing" mode. That is, the bed pressure swings from the adsorption level, usually cabin pressure, to the low level employed for desorption. If the low desorption pressure is provided by space vacuum, the bed is said to be "vacuum dumped." If desorption is carried out by heating the bed, the operation is called "thermal swing." If desorption is carried out by flowing through the bed a gas which has a very small concentration of sorbate, the process is called "gas stripping." Combinations of the desorption methods are possible; for example, a bed might undergo a combined pressure/thermal swing if the bed is heated as it is exposed to vacuum. Heating (thermal swing) can also be used with gas stripping.

Types of Spacecraft CO_2-Removal Systems. - The desorption method to be applied to a particular application depends greatly upon the ultimate desired disposition of the separated sorbates, CO_2 and water. If there is no need to save the adsorbed CO_2 and water, then simple vacuum dumping of both predrier and CO_2-removal beds is probably the best available desorption method. In such a water-dump/CO_2-dump system, it is possible to pack both sorbents in a

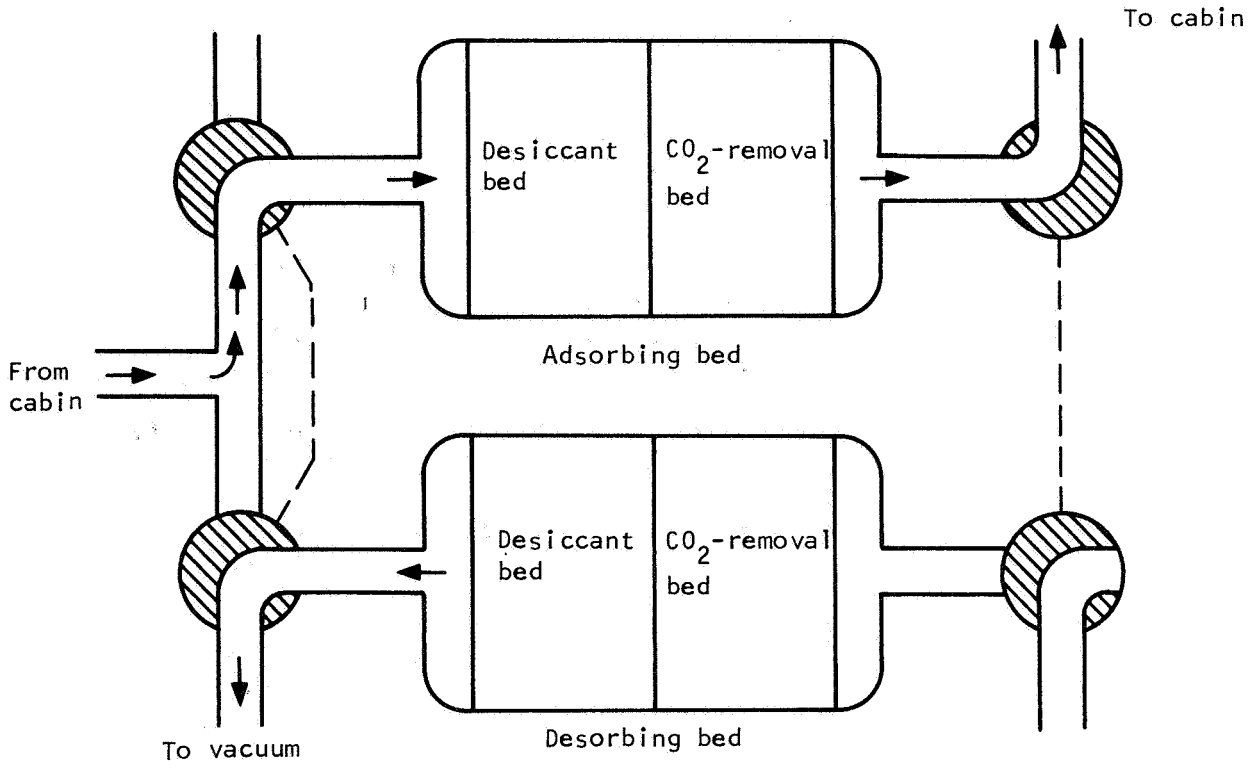

Figure 2-1. Composite-Bed, Water-Dump/CO_2-Dump CO_2 Removal System; After the Regenerative CO_2-Removal System (RCRS) for the Skylab Vehicle

single bed container. Figure 2-1 depicts this type of a composite-bed, water-dump/CO_2-dump CO_2-removal system, which is often called a two-bed system. The Skylab RCRS is precisely this type of system.

With composite bed systems, it is almost mandatory that the desorption take place in such a manner that the water leaving the predrier portion of the bed does not travel through, and have the opportunity to adsorb on, the CO_2-removal bed. In effect, the desorption is counterflow to the adsorption. As a somewhat more complicated alternative, a void space may be provided between predrier and CO_2-removal portions of the bed. Upon desorption, this void area can be opened to vacuum. By also opening the predrier inlet to vacuum, double-end desorption of the predrier bed is afforded. This arrangement is shown in Figure 2-2.

If the adsorbed water, but not the adsorbed CO_2, must be saved, another system arrangement is required. It may be necessary to save water either to maintain cabin humidity conditions or to reclaim and use all water aboard the spacecraft. Such a system would be known as water-save/CO_2-dump system. For this system, it is necessary to physically isolate the predrier beds from their respective CO_2-removal beds and to provide a different means of desorbing

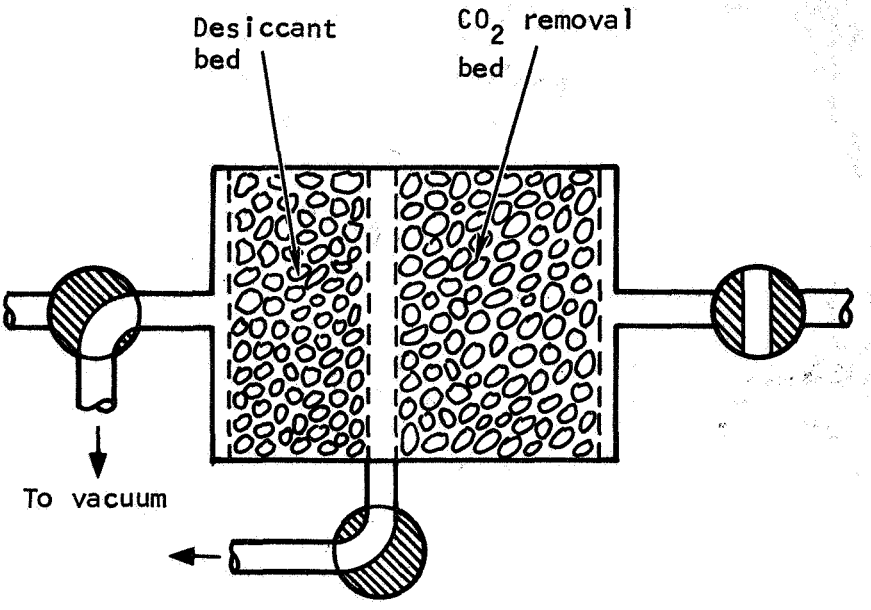

Figure 2-2. Two-Point Desorption Scheme for Regeneration of Composite Sorbent Beds

the predrier beds. This can be accomplished by gas stripping. By proper ducting and valving, it is possible to introduce the very dry, CO_2-lean gas exiting from the adsorbing CO_2-removal bed back into the desorbing predrier bed, as shown schematically in Figure 2-3. That is, the desorption of water from the predrier beds is carried out by a gas-stripping arrangement, using all or a portion of the same process gas stream that just passed through the adsorbing beds. Thus, as can be seen from Figure 2-3, at any particular time the process gas stream flows through three beds: the predrier bed, where water is removed from the processed gas stream; the adsorbing CO_2 bed, where CO_2 is removed; and finally back through the previously water-loaded predrier bed. In this arrangement, care must be taken that the gas-stripping operation is as efficient as the adsorption operation. Meanwhile, the desorbing CO_2-removal bed is opened to vacuum for a more or less simple vacuum dump. Upon completion of the cycle, the bed positions are essentially reversed.

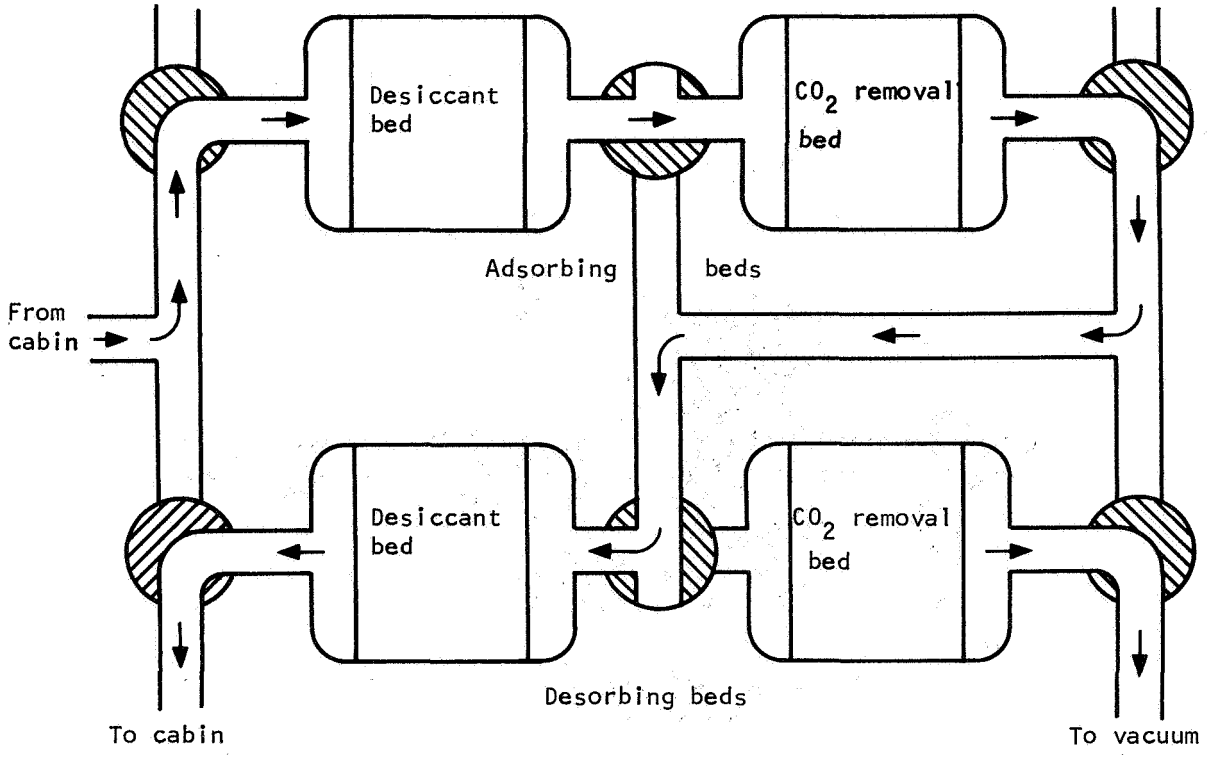

Figure 2-3. Four-Bed Water-Save/CO_2-Dump CO_2 Removal System.

With somewhat greater system complexity, it is possible to produce a semi-water-save/CO_2-dump system. This might be desired where there is an overbundance of water in the cabin, and it is desired to dump water to vacuum for a fraction of the desorption time. In such a system, a gas-stripping operation of the predrier bed might proceed for a fraction of the desorption period, and then the bed would be opened to vacuum to finalize the desorption and to remove excess water from the spacecraft cabin. This, however, requires a rather complex system arrangement, which is probably undesirable. In most instances, the same result can be obtained by using a composite two-bed system and altering the process gas flow rate to fit the production rates of CO_2 and water. This type of system is based on the assumption that the production of CO_2 and water are linked, and that by controlling cabin humidity by the modulation of the process gas flow rate, CO_2 removal is also properly controlled.

For extremely long duration flights, it appears desirable to save both water and CO_2. A water-save/CO_2-save system differs from the water-save/CO_2-dump system only in the manner of CO_2 desorption. Water is again removed from a predrier bed by gas stripping; however, the CO_2 is removed from the CO_2-removal bed by means of heating and vacuum pumping, the CO_2 being delivered to an accumulator which would be upstream of an oxygen reclamation unit.

SCOPE OF RESEARCH AND ANALYSES

The research and analyses conducted under this contract for the purpose of generating basic design data and providing design tools for spacecraft regenerable CO_2-removal systems was in three areas: (1) experimentally defining basic equilibrium data for molecular-sieve sorbents, (2) evaluating the dynamic mass-transfer performance of prototype beds under representative conditions, and (3) producing general performance-prediction computer programs for spacecraft CO_2-removal systems.

Equilibrium Testing

Equilibrium sorption capacity refers to the ultimate capacity of a sorbent to adsorb another material (sorbate) under given conditions of temperature and sorbate partial pressure. Equilibrium sorption capacity data is usually taken by exposing a sorbent sample to a controlled environment of temperature and sorbate pressure. After a sufficiently long period of time, when equilibrium between gaseous and adsorbed sorbate has been established, the weight increase of the sorbent material is noted. The sorbent capacity or sorbent loading is usually expressed in terms of the mass of sorbate adsorbed on a unit mass of sorbent; percentage loadings (mass of sorbate per 100 mass units of sorbent) are sometimes used. Because sorbent loading is a function of temperature and sorbate partial pressure, equilibrium data is usually displayed as a map of loading vs partial pressure, with temperature used as a parameter. The lines drawn for constant temperature are called adsorption isotherms.

Equilibrium data may be applied in a number of ways. First, by its definition (expressing maximum sorption capacities), it is useful in initial comparisons of sorbents or sorption conditions. Because equilibrium data says nothing about rates, such comparisons can be used only as guidelines. Properly used with rate information, the comparisons become more definitive.

Equilibrium data is also used in the prediction of the dynamic performance of beds, as the mass-transfer driving force is usually considered to be the difference between the actual sorbate partial pressure in the gas stream (p_k) and the equilibrium partial pressure (p_k^*, evaluated from the equilibrium map) with respect to the instantaneous bed temperature and loading. Thus, equilibrium data is necessary for the use of performance-prediction computer programs. Another use of equilibrium data is that the shapes of the adsorption isotherms can give insight into the relative ease or difficulty of adsorption processes.

In spite of the basic nature of equilibrium data, at the onset of this program much of the required equilibrium data was scarce, was missing entirely, or was questionable. A substantial part of the reasoning why such data was not available lies in the range of partial pressures of interest for spacecraft systems as contrasted to those of interest in commercial practice. For example, CO_2 removal in industry is not usually accomplished with the use of solid adsorbents. Even when CO_2 adsorption by molecular sieves occurs commerically, CO_2 partial pressures are usually much higher than the levels experienced in spacecraft.

With regard to water equilibirum on molecular sieves, it should be noted that even at very low partial pressures these sorbents can hold large quantities of water. However, it is only recently that high-quality instrumentation has become available (1) to accurately measure water vapor pressures in the range of interest (down to below 1μ), and (2) to measure within the apparatus used for equilibria determination, small weight changes of sorbent samples. Thus, much of the previously available data is questionable. To clarify the interest in low water-vapor pressure, it is noted that Linde 5A has an equilibrium capacity of about 8.5 percent at 70°F and at a water vapor pressure of only 0.006 mm Hg; that is, at -80°F frost point. Further, at 8.5 percent water loading, molecular sieve 5A exhibits a drastic poisoning effect with respect to CO_2 adsorption.

For many new sorbents (for example, sorbents with improved binders) there was little equilibrium data by which to judge their potential usefulness. Furthermore, there was essentially no data at all on the equilibrium capacities of molecular sieves when both water and CO_2 were present. As discussed earlier, because of the poisoning nature of water, it is most desirable to have quantitative information on the equilibrium capacity for CO_2 in the presence of water vapor; therefore, a good deal of the equilibrium data taken in this contract has been for CO_2 and water simultaneously on molecular sieves. There was also interest in sorbate pairs other than CO_2 and water. Thus, data was also taken for CO_2 paired with oxygen, CO_2 paired with nitrogen, water paired with oxygen and water paired with nitrogen. The data and explanations of the equilibrium tests that were conducted are presented in Section 3.

Single-Sorbate Dynamic Testing

Equilibrium data is probably the most basic of all categories of mass-transfer information. However, the knowledge of the equilibrium sorption capacity of the particular sorbent is not sufficient to declare that it is a good sorbent, and that it will perform well under dynamic conditions. One of the goals of this program was to characterize molecular-sieve sorbents for water and CO_2 under representative dynamic conditions. To accomplish this, special beds were produced which incorporated the latest concepts in internal-coolant heat-transfer surfaces. Using these beds, single-sorbate mass-transfer experiments were carried out under isothermal conditions. The reason for using isothermal adsorptions was to eliminate heat-transfer considerations from evaluation of mass-transfer parameters. Therefore, to the greatest extent possible, the beds were kept isothermal during the entire adsorption runs.

The sorbent/sorbate combinations studied in the dynamic tests were: water adsorbing on silica gel; water adsorbing on Linde 13X molecular sieve; CO_2 adsorbing on Linde 5A molecular sieve; CO_2 adsorbing on Davison 5A molecular sieve; and CO_2 adsorbing on Linde 13X molecular sieve. All of the single-sorbate adsorption tests were initiated by subjecting the bed to a prolonged vacuum-bakeout to remove essentially all traces of CO_2 and water. All adsorptions were carried out with nitrogen as the carrier gas for the CO_2 or water vapor. The nitrogen/CO_2 or nitrogen/water gas stream was passed through the sorbate bed until the outlet concentration from the bed finally rose to that of the inlet concentration; that is, until complete breakthrough of the sorbent was obtained. For some cases, gas stripping desorptions using dry nitrogen were carried out after adsorption tests. The data from the breakthrough runs and gas strips, and the discussion of the results of these tests, are contained in Section 4.

Evaluation of Mass-Transfer Coefficients

Using the single-sorbate breakthrough curves as basic data, and with the help of the performance-prediction computer programs produced under this program, mass-transfer parameters were evaluated. For the sorbent systems in question, the mass-transfer parameters of interest are the mass-transfer coefficient K_g and the effective intraparticle diffusivity, D. The mass-transfer coefficient relates to the conductance of the convective mass-transfer process as the sorbate moves from the free stream of gas within the bed to the sorbent-pellet boundary. The effective sorbate diffusivity relates to the diffusional conductance as the sorbate travels through the pore structure of the sorbent pellet. The means of determining the mass-transfer coefficients and diffusivities from the breakthrough data, and the results of these evaluations are contained in Section 5.

Coadsorption Dynamic Testing

In order to obtain a greater understanding of the water poisoning effect on CO_2-removal beds, a series of coadsorption tests were conducted in the dynamic mass-transfer apparatus. A few of these runs involved the simultaneous adsorption of CO_2 and water onto a sorbent bed. However, most of the coadsorption runs were conducted in somewhat different manner: After an initial vacuum-bakeout, the bed was allowed to acquire a preload of water, up to a designated loading, by means of adsorption from a water-bearing nitrogen stream. The water preload was usually 7 to 9 percent, corresponding to an equilibrium water vapor pressure of -80^0F frost point. Following the water preloading, a stream of nitrogen and CO_2 was passed through the bed and its CO_2-removal performance monitored. Section 6 contains the data and the discussions of these rather unique tests.

Performance-Prediction Computer Programs

Section 7 contains discussions of the computer programs produced under this contract. Two major CO_2-removal-system performance-prediction computer programs were produced. The first program concerns composite-bed water-dump/CO_2-dump systems. The second and more general computer program deals with four-bed systems that involve any combination of water-save, water-dump, CO_2-save, or CO_2-dump provisions. Further, it has features to allow the prediction of the gradual buildup of water on the CO_2-removal bed over long periods of operation, and the prediction of the CO_2-removal performance of the bed in the face of the poisoning effect of water. Additional programs useful in CO_2-removal-system design and evaluation efforts are also discussed and presented in Section 7.

Pressure Drop and Packed-Bed Density

Section 8 contains design information on packed-bed density and pressure drop for molecular-sieve and silica-gel beds.

SECTION 3
EQUILIBRIUM DATA

INTRODUCTION

This section presents the results of tests performed on various molecular-sieve materials to determine their equilibrium sorption capacity for specific gases at various pressures and temperatures. The equilibrium sorption capacity refers to the ultimate capacity of a sorbent to adsorb another material under given, constant conditions of temperature and sorbate partial pressure. The sorbate capacity, or loading, is usually expressed in terms of the mass of sorbate adsorbed on a unit mass of sorbent, or alternatively, as a percentage loading, i.e., mass of sorbate per 100 mass units of sorbent.

This section is divided into four subsections:

- Equilibrium test equipment and procedures - Describes the test setup and the test equipment used; defines test techniques used to obtain specific data; and discusses some of the problem areas encountered.
- Single-sorbate equilibrium test data - Includes all data taken pertaining to single gas or vapor adsorption by various molecular sieve and silica gel sorbents. Where applicable, this data is compared with previously existing data.
- Coadsorption equilibrium test data - Presents all data taken where a sorbent was preloaded with gas or vapor to some predetermined level and then subjected to the partial pressure of another gas sorbate. The equilibrium coadsorption behavior of several sorbate pairs on Linde 5A and on Linde 13X have been studied and are presented in this section.
- Heat of adsorption - Discusses related heat of adsorption associated with the single-sorbate adsorptions.

EQUILIBRIUM TEST EQUIPMENT AND PROCEDURES

Test Equipment

The equilibrium test setup schematic is shown in Figure 3-1; a photograph of the apparatus is shown in Figure 3-2. The basic purposes of the apparatus are (1) to provide the proper, controlled adsorption environment for the sorbent test sample, and (2) to measure this environment and, by weight, to obtain the adsorption capacity of the sample. The test schematic is divided into six subsystems for functional presentation:

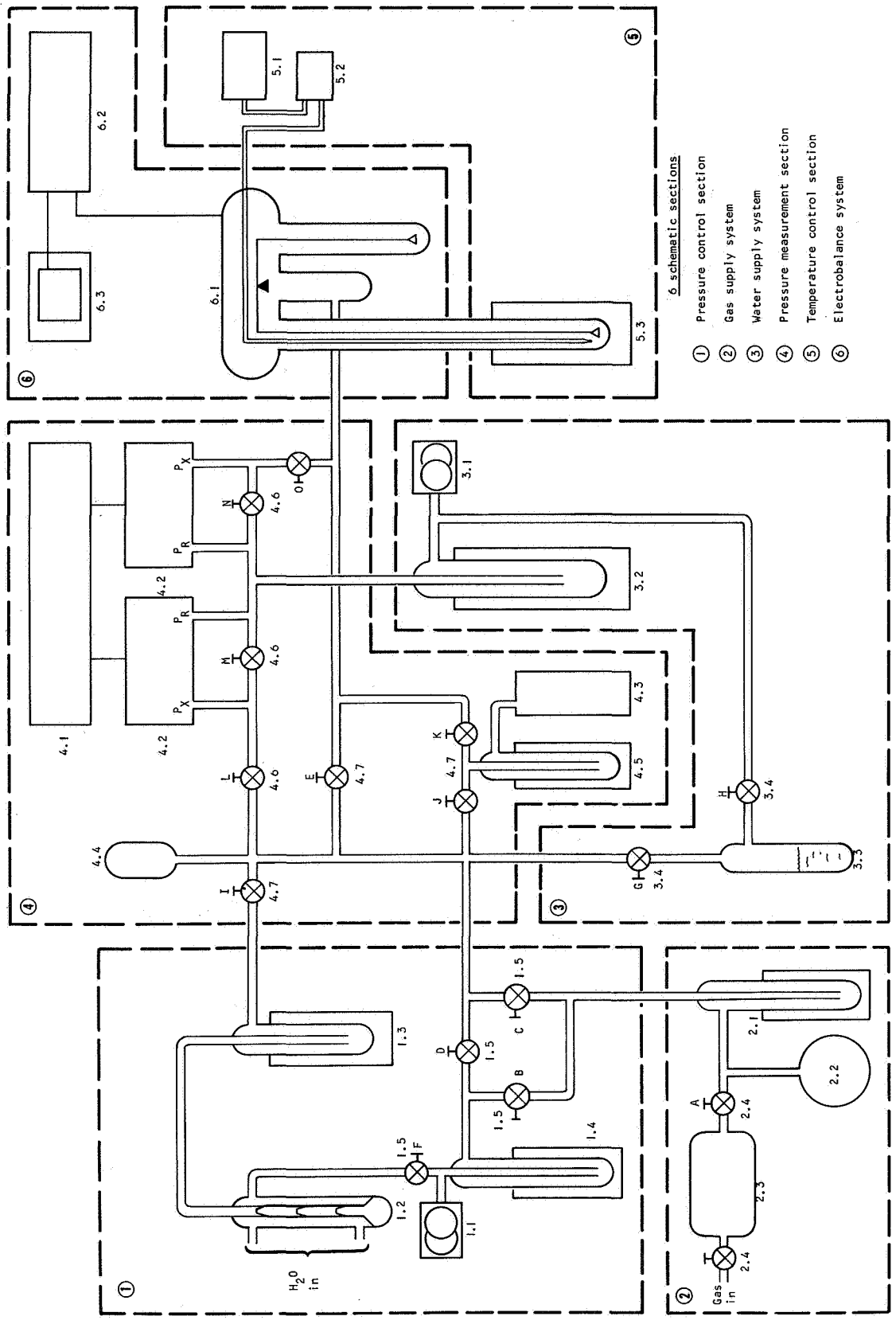

Figure 3-1. Equlibrium Test Setup

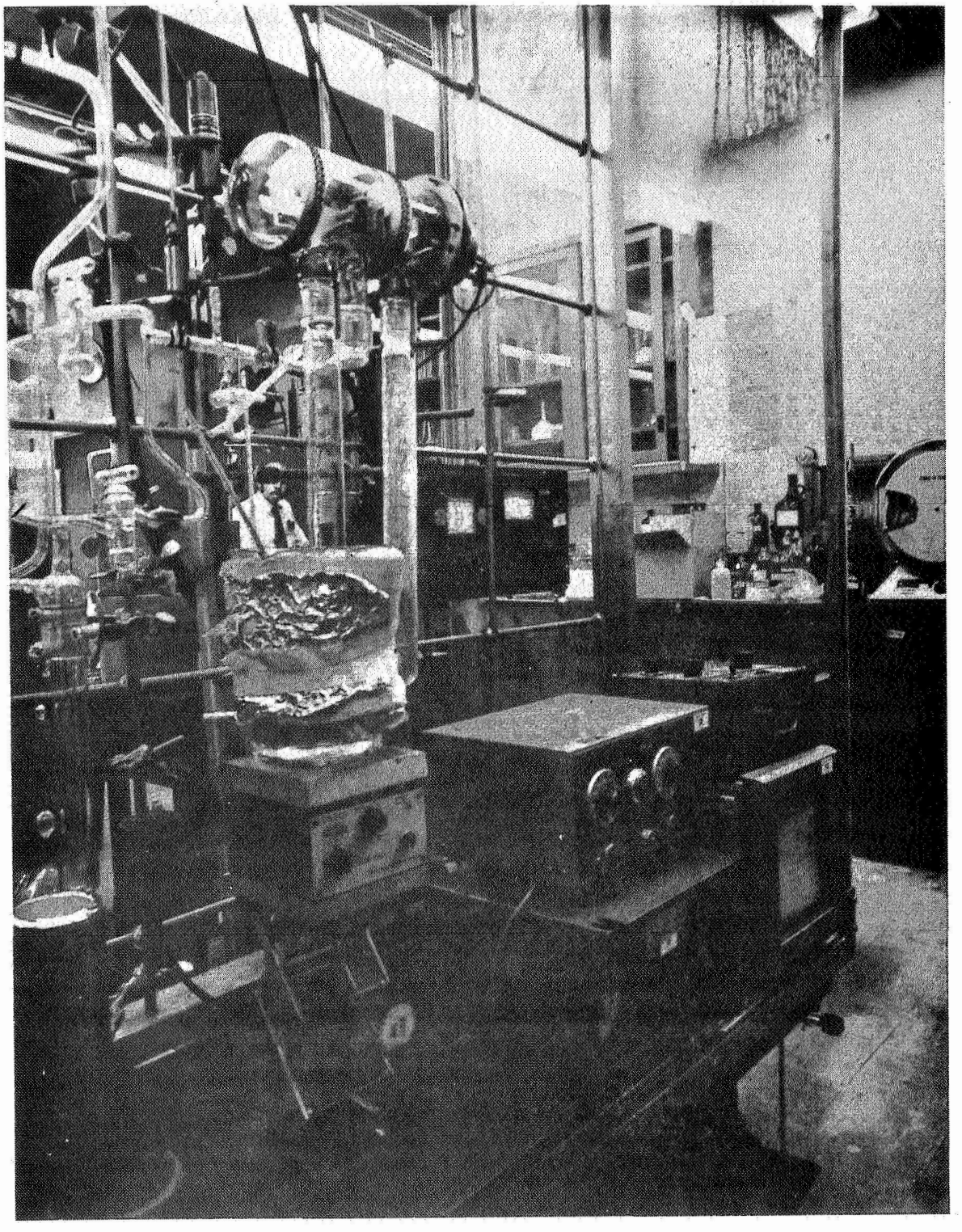

Figure 3-2. Photo of Equilibrium Test Setup

(1) Pressure Control Section--Provides the vacuum source to maintain the system pressure and to allow drying of the system and sorbent sample.

(2) Gas Supply System--Provides gas supply for controlled gas distribution to the sorbent under test.

(3) Water Supply System--Provides water vapor for controlled vapor distribution to the sorbent under test.

(4) Pressure Measurement Section--Provides accurate system pressure measurement.

(5) Temperature Control Section--Provides accurate temperature control and monitoring of the sorbent temperature.

(6) Electrobalance System--Provides accurate real-time weight measurement of the sorbent sample.

The heart of the system is the electrobalance module, consisting of a Cahn RG electrobalance and its auxiliary equipment. This device is a beam balance with a feed-back servo system designed to keep the beam level. The sensing of rotation of the balance beam is done optically. The optical sensor produces a signal which, after amplification, is directed to an electromagnet located at the beam fulcrum. The electromagnet produces a torque which restores the balance to a level position. The electromagnet current is accurately measured and translated into a weight reading.

At the start of a test, the balance is zeroed by using calibrated weights on the reference weigh pan. After this, all weight readings are obtained remotely. Thus, there is no need for mechanical feed-throughs and the balance can be placed entirely within the test envelope. The balance is insensitive to pressure levels within the apparatus. Because of its excellent sensitivity, and the ability to produce accurate weight readings when subjected to the adsorption environment, the Cahn electrobalance is an excellent instrument for equilibrium adsorption-capacity measurements. Throughout this study, it has been very reliable, and repeatability of its readings has been excellent.

The measurement of pressures in the range of interest in this study, generally 760 mm Hg down to less than 1 μ Hg, has traditionally been difficult and has hindered the production of accurate adsorption equilibrium data. For example, McLeod gages cannot be used with water vapor in certain pressure regions due to the condensation of the entrapped vapor in the gage capillaries. Recently, new wide-range pressure measurement instruments have been devised. For this study, a MKS Baratron pressure meter was used. Its sensing transducers involving variable capacitors are linear with pressure and are quite stable.

Sample temperature was measured by a chromel-alumel thermocouple suspended very close to the sample weigh pan. The thermocouple did not actually touch the sorbent or the weigh pan as this would have caused erroneous weight readings. Sorbent temperature was controlled by immersing the glass sample tube in a temperature controlled bath, or by affixing an electric heater around the sample tube. Originally, the thermocouple reference junction was located within the upper portion of the gas-tight glassware of the test setup. The junction was considered to be at room temperature. Later, a feed through arrangement was made and the reference junction was moved outside of the glassware into an ice bath.

Table 3-I provides a list of the test equipment (Referenced by item number to Figure 3-I) used and briefly describes what function the equipment satisfied, and, where applicable, its tolerance and range. All active lines and valves of the setup are Pyrex glass. Equipment which exhibits off-gassing characteristics at low pressures or high temperatures was not used. The test setup (Figure 3-I) will maintain a system pressure of 0.02 μ Hg.

Test Procedure

The test procedure for producing equilibrium sorption capacity data is relatively simple and straight forward, but the preparation and maintenance of the equipment prior to actually taking equilibrium data is more subtle in nature. To produce accurate data, the system must be thoroughly dry and leak tight, and must be maintained in this condition. Many laboratory hours were spent in producing and verifying a leak tight system.

The first step in the equilibrium procedure involves zeroing of the electrobalance. This involves the use of a calibration weight (60 mg) on the weigh pan. Then a sorbent sample of approximately 65 mg is weighed out on a laboratory balance and placed onto the electrobalance weigh pan. To avoid picking up of any considerable amount of water from the atmosphere, this operation is done as quickly as possible. The system is then closed off, and all portions of the system, except the gas supply system, are pumped down, in order to dry out the system. At the same time, water and other sorbates are removed from the sample by means of a vacuum-bakeout. The bakeout, usually at 600^0F, is carried out by placing the electric heater around the glass tube which surrounds the sample weigh pan. Some bakeouts were conducted at 400^0F, however 600^0F was adopted as the standard bakeout temperature; this will be discussed at greater length later.

Bakeout of the sorbent sample is continued until a stable system pressure is obtained, and the Cahn electrobalance shows no weight change taking place. The stabilized pressure is usually less than I μHg. Once the bakeout is successfully completed, the sorbent is allowed to cool to the desired temperature, and provisions are made to maintain this temperature with either a heater or a bath. When the desired sorbent temperature is established, still at vacuum conditions, the weight of sample as given by the Cahn electrobalance is read; this weight is adopted as the base or dry weight of sorbent. Usually there is little difference between this weight and that measured at the bakeout temperature. However, because of the possibility of thermal currents or temperature gradients which might produce inaccurate readings, the hot weights are not used.

TABLE 3-I

TEST EQUIPMENT

Reference Number	General Description and Model Identification	Remarks
I	Pressure Control Section	Controls test system from 0.02 to 760 mm Hg
I.I	Weigh Vacuum ump, Model I402	Controls test system from 3 to 760 mm Hg
I.2	Mercury iffusion Pump	Controls test system from 0.02 to 3 mm Hg
I.3	Fabco Dewar	Thermal sink
I.4	Fabco Dewar	Thermal sink
I.5	Pyrex Valves, V-type	Selects system route
2	Gas Supply System	Provides gas to sorbent
2.I	Fabco Dewar	Thermal sink
2.2	Wallace and Tiernan Pressure Gage, R/N 44S0I5	Monitors gas supply pressure
2.3	Hoke Gas Plenum	Stores gas for test use
2.4	Valves	Fill and system supply valves
3	Water Supply System	Provides water vapor for the test
3.I	Walch Vacuum Pump, Model I405	Provides low pressure source for vaporizing water
3.2	Fabco Dewar	Thermal sink
3.3	Water Reservoir	Water supply for system test
3.4	Pyrex Valves, V-type	Activates water distribution
4	Pressure Measurement Section	Provides accurate system pressure measurement capability
4.I	MKS Baratron Pressuremeter, Type 77 R/N 44S946	System pressure readout
4.2	MKS Baratron Pressure Heads, Type 77	Transducers for item 4.I
4.3	McLeod Gauge Type GM100-A	Reference system pressure readout
4.4	Ion Tube IG I00/C	
4.5	Fabco Dewar	Thermal sink
4.6	Valves	Used for calibration of MKS heads and system monitoring
4.7	Pyrex Valves, V-type	System valves
5	Temperature Control Section	Maintains and monitors sorbent temperature
5.I	Leeds Northrop Temperature Bridge S/N 8690, R/N 43BI79	Readout for temperature
5.2	Reference Thermocouple	Reference for temperature measurement
5.3	Constant Temperature Bath	Temperature control for sorbent
6	Electrobalance System	Provides weight monitoring
6.I	Cahn Electrobalance S/N I0307	Electrobalance devise
6.2	Cahn Electrobalance Control R/N 46B009	Controls for weight output
6.3	Leeds Northrop Speedomax R/N 430296	Chart recorder for weight change

Then the test gas, from the gas supply system is introduced to the system at the pressure required for the first datum point. The system conditions are maintained constant until the pressure stabilizes and the Cahn electrobalance indicates no weight change taking place. The sorbent gas loading is then determined by the change from the bakeout dry weight.

Additional sorbate gas is introduced and the procedure is repeated for a higher pressure. In this manner, any number of data points can be obtained, thereby producing one adsorption isotherm. The bakeout procedure is then repeated and another isotherm can be generated. The developed isotherms are then plotted and, where applicable, certain tests of consistency are made.

The test procedure for coadsorption equilibrium tests is similar, except that a sorbent pre-adsorption or preloading procedure is performed. For tests involving water and another sorbate water vapor, produced by the water supply system, is first distributed to the sorbent at a specific temperature and pressure. When the system reaches pressure and weight stability, the percent of water loading is noted. Then the gas supply system is opened to the system and the second sorbate gas is distributed to the sorbent. The partial pressure of the second sorbate gas is assumed to be equal to the total pressure minus the initial water vapor partial pressure. This assumption is valid as long as none of the initially adsorbed water is desorbed by the gas and no leakage into the system occurs. The condition of no water unloading was verified on a sample test by making a complete mass balance of the gases in the equilibrium apparatus; this involved the measurement of internal volumes and system pressures. Once the system reaches pressure and weight equilibrium, the coadsorption equilibrium data can be obtained and plotted. The developed isotherms are presented later in this section.

Experimental Problem Areas

There are several areas which, because of procedures or limitations of test equipment, may have caused inaccuracy in the data. The major problem areas are discussed below.

Sorbent Bakeout Temperature.-Previous to this contract, 600°F was used as the vacuum-bakeout temperature prior to adsorption testing. This temperature also seems to be widely used in industry. However, at the start of this program, it became apparent that spacecraft systems would not be able to produce bakeouts at 600°F. Instead, 400°F was considered more likely. Therefore, in an attempt to produce more-directly-useable engineering data, 400°F was adopted for vacuum bakeouts. After some testing, it became apparent that 400°F bakeouts, even with CO_2 gave equilibrium data that was lower than previous AiResearch data, or that was available in the literature. Some special comparison tests were performed; the results of these tests indicated that 600°F bakeouts should be used. Therefore, for all subsequent tests 600°F bakeouts were performed. However, not all 400°F-bakeout tests were rerun and some of these data are presented in this report. As such, these data are clearly labelled as to bakeout temperature.

Sorbent Temperature Measurement.-Early in the program, measurement of sorbent temperature caused considerable problems. The problem area developed because there was no way provided with the Cahn electrobalance electrical feedthrough to pass the chromel-alumel thermocouple wire out of the apparatus without creating addition thermocouple junctions. Therefore, a reference junction was setup inside the apparatus. It was located near the Cahn electrobalance, and was supposed to be at room ambient temperature. However, due to its proximity to the Cahn-balance light source, its temperature was actually unknown and varied with system pressure. Later, this problem was completely solved when the junction was removed and a bulkhead seal was provided which allowed the thermocouple wires to pass directly out of the apparatus. A 32^{0}F reference junction was then provided exterior to the system.

Some of the early data has scatter in it which is undoubtedly due to sample temperature-measurement inaccuracy. Although calibrations were made in all cases with the early thermocouple system, it is believed that the calibrations were not sufficient to account for all modes of operation. Therefore, some measurements are suspected of being incorrect. As much as possible, the data was edited and only reliable data have been presented.

Leakage.-Leakage of atmospheric gases into the apparatus was always a prime concern. Depending upon the test conditions and the sorbent loading at the time a leak develops, the measurable effects of a leak are not readily predictable. Certainly if a sorbent is nearly saturated with water, a leak would be noticed with increase in system pressure, without apparent weight increase. However, at low pressure levels and low loadings with sorbates other than water, leakage may not be noticeable from system pressure readings, but unusually high loadings (due to water vapor adsorption) might result. Therefore, great care and diligence on the part of test personnel was exercised in noting trends of the readings, and in frequent leak checks.

Slowness of Adsorption in Low Pressure Ranges.-Under some conditions of very low pressure (in the range of 50 μ Hg and below), the driving force for adsorption or desorption is very low and relatively long periods of time are required to achieve equilibrium. Sometimes it was difficult to determine whether equilibrium had been achieved or if system conditions were varying slightly. Therefore, there is some question concerning all data in the very low partial pressure region. One effect of slow adsorption is that data seem to be slightly low when data points are taken for increasing pressures; that is, when gas is added to the system to produce the next adsorption condition. On the other hand, data seems to be slightly high when tests were taken with decreasing pressure levels; that is, by pumping gas out of the system. Due to the time involved, not all systems received as much investigation in the low pressure region as would be desired.

Reversibility of Adsorption.-It is noted that earlier during equilibrium testing there was concern of reversibility of adsorption and degradation of the sorbent itself due to prolonged exposure to the testing environment. Special tests as well as continued data comparisons indicated that adsorptions were reversible and the stability of the sorbents (molecular sieves and silica gel) was excellent. This was concluded from repeatability of dry-weight measurements after bakeouts, and from equilibrium data repeatability.

SINGLE-SORBATE TEST DATA

Table 3-2 presents the conditions under which mono-gas single-sorbate equilibrium sorbent capacity data were taken. The gas/sorbent combinations studied are shown in the table along with sorbent temperature and pressure ranges. Figures 3-3 through 3-22 present the single-sorbate equilibrium data.

TABLE 3-2

TEST MATRIX FOR SINGLE-SORBATE EQUILIBRIUM DATA ON MOLECULAR SIEVES

Molecular Sieve Sorbent	Manufacturer	H_2O	CO_2	O_2	N_2
5A	Linde	77, 167, 120, 392°F, 0-10 mm Hg	Testing from AAP program used	32, 70°F 0-760 mm Hg	32, 68, 120°F 0-760 mm Hg
5A	Davison	120°F 0-10 mm Hg	70, 120°F 0-760 mm Hg		
13X	Linde	70°F, 0-10 mm Hg	32, 70, 120 120°F, 0-760 mm Hg	32, 72, 120°F, 0-760 mm Hg	32, 72, 120°F 0-760 mm Hg
13X	Davison	70°F, 0-10 mm Hg			
10X	Linde	70°F, 0-10 mm Hg	70°F, 0-760 mm Hg		
4A30	Linde	70°F, 0-10 mm Hg	70°F, 0-760 mm Hg		
5A30	Linde	70°F, 0-10 mm Hg	70°F, 0-760 mm Hg		
4A	Linde			70°F, 0-760 mm Hg	70°F, 0-760 mm Hg

Carbon Dioxide Equilibrium on Molecular Sieves

Figures 3-3 through 3-9 present carbon dioxide isotherms obtained with Davison 5A, Linde 10X, Linde 13X, Linde 4A30, and Linde 5A30 molecular-sieve sorbents. Linde 5A data is also presented. However it has been included from previous Apollo Application Program (AAP) test data. The 4A30 and 5A30 sorbents, also identified as 4AXW and 5AXW respectively, have been included because the manufacturers performance predictions indicated an approximate 40 percent increase in capacity over the standard 4A and 5A sorbents. The basic difference in the two materials is that 4A30 and 5A30 use a different, supposedly improved binder, with respect to CO_2 adsorption capacity. The test data does not support this contention; the capacities are essentially those of standard 4A and 5A.

Figure 3-3 presents 70° and 120°F isotherms for the Davison 5A sorbent. Also included (phantom lines) is the curve for Linde 5A at 70°F (AAP data). A variance can be seen between the two curves; therefore the 7mm Hg point was re-run for the Davison 5A sorbent and is shown with a large diamond. This point coincides with the curve for Linde 5A. This might be expected due to the fact that both sorbents are basically the same crystal structure. There could, of course, be differences in the amount of binder used. This re-run casts some doubt on the original AiResearch isotherms for this material.

Figure 3-4 presents the data on Linde 5A from the AAP program. Isotherms of 0°, 40°, 60°, 100°, and 120°F are included. Actual data points are indicated by circles; other isotherms were interpolated.

Figure 3-5 presents a 70°F isotherm for the Linde 10X sorbent. Figure 3-6 presents a tabulation of various isotherms obtained for Linde 13X sorbent. Reference isotherms obtained after various bakeout temperatures of 400,500, and 600°F are also included. Figure 3-7 presents a summary of the Linde 13X sorbent test data for CO_2 gas. Included on the figure are 32°, 0°, 70°, 90°, and 120°F isotherms. This summary figure includes data taken in the AAP program. Figure 3-8 presents the 70°F isotherms obtained for the Linde 4A30 and 5A30 sorbents.

An interesting observation of the 4A30 and 5A30 absorption characteristics is that a cross over point exists at approximately 12.5 mm Hg and 8.8 percent loading. (This is also true with the standard 4A and 5A sorbents.) The 4A20 sorbent has a greater potential load capacity at low pressures and the 5A30 has a greater capacity in the higher pressure range.

Obtaining equilibrium data for 4A30 was extremely tedious due to the slow adsorption and desorption rates. Figure 3-9 presents a transient desorption curve plotted for both 4A30 and 13X. The desorption was obtained by simply opening the apparatus to the vacuum system.

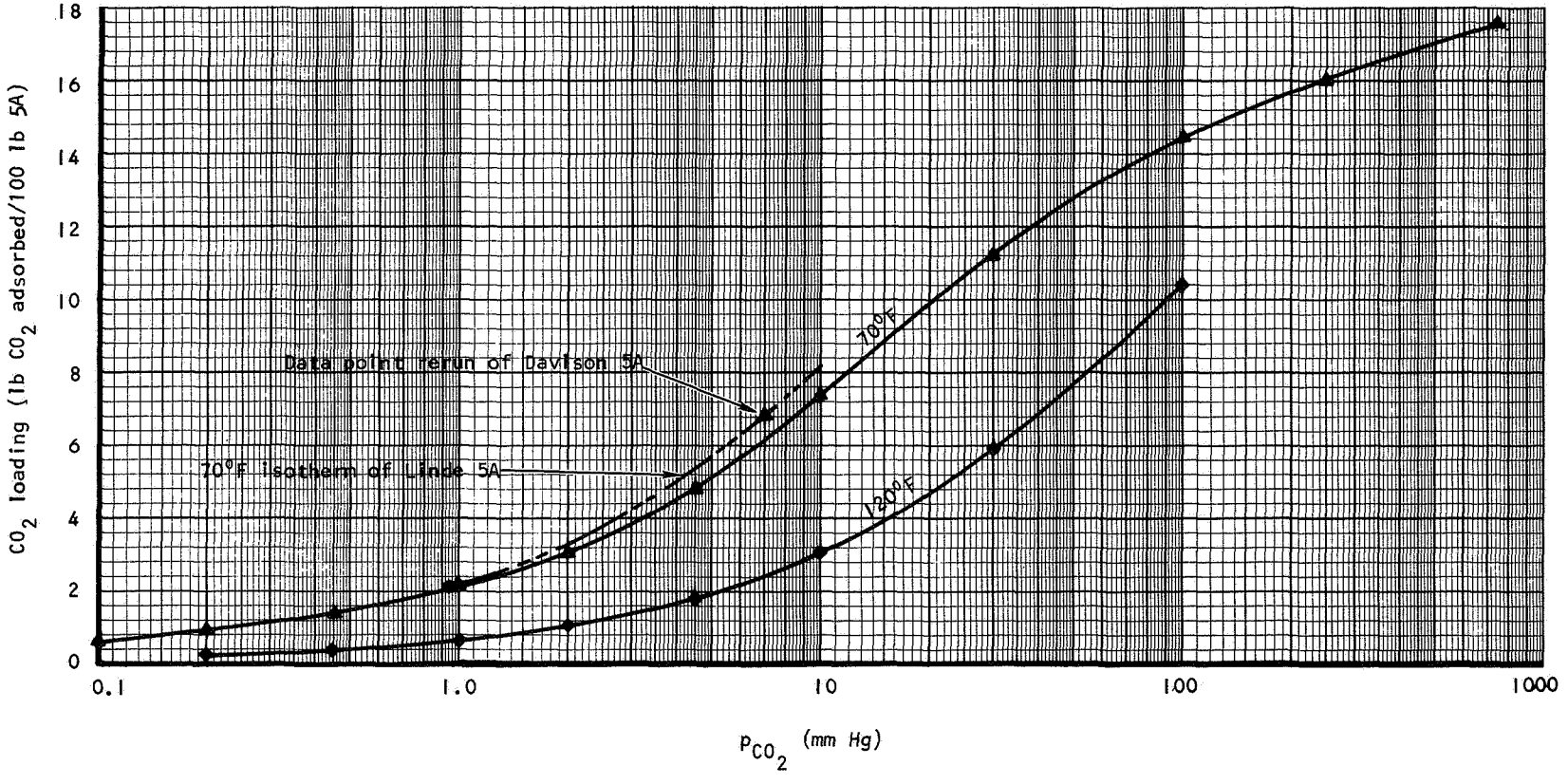

Figure 3-3. Carbon Dioxide Equilibrium Data for Davison 5A Sorbent

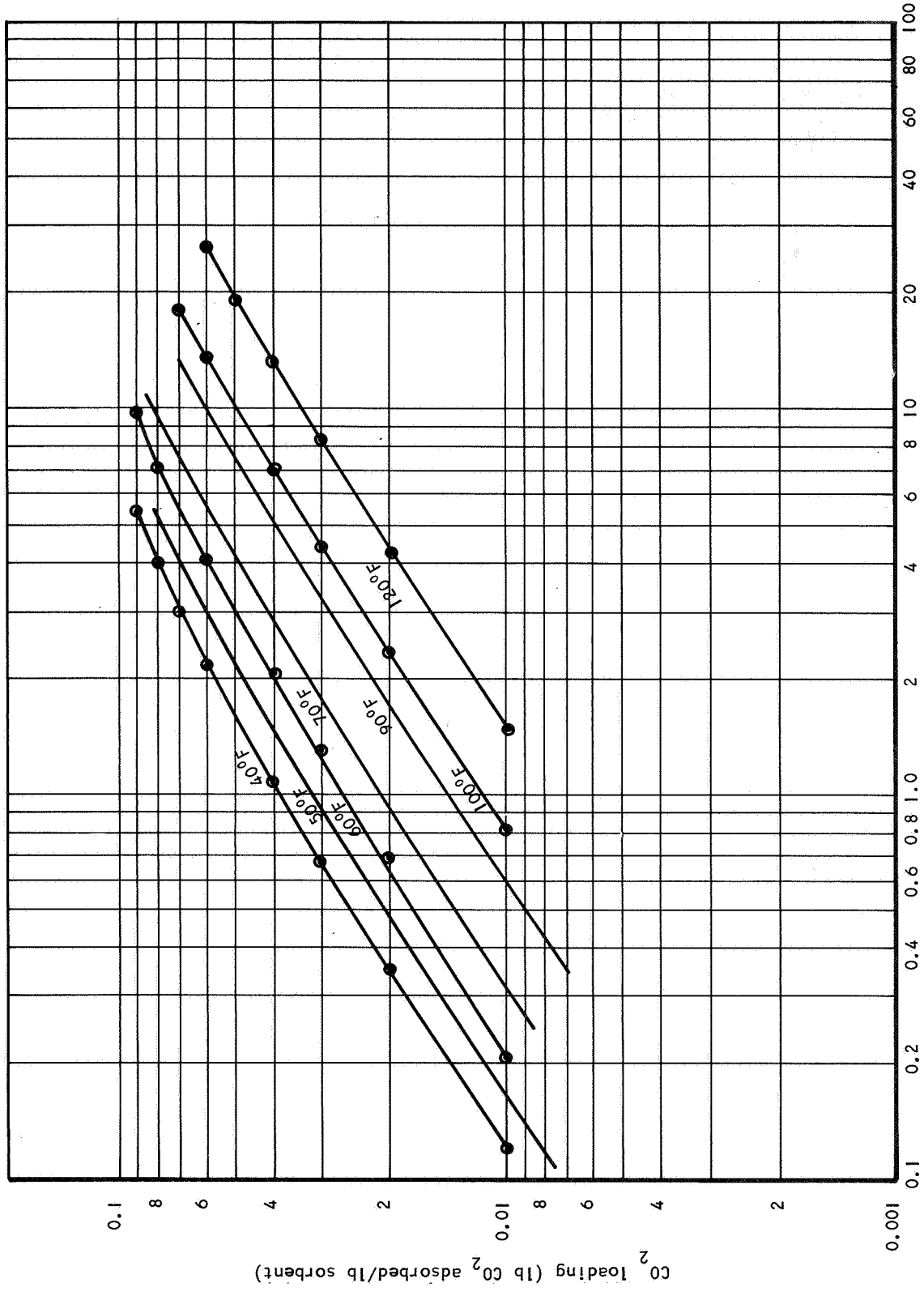

Figure 3-4. Carbon Dioxide Equilibrium Data for Linde 5A Sorbent

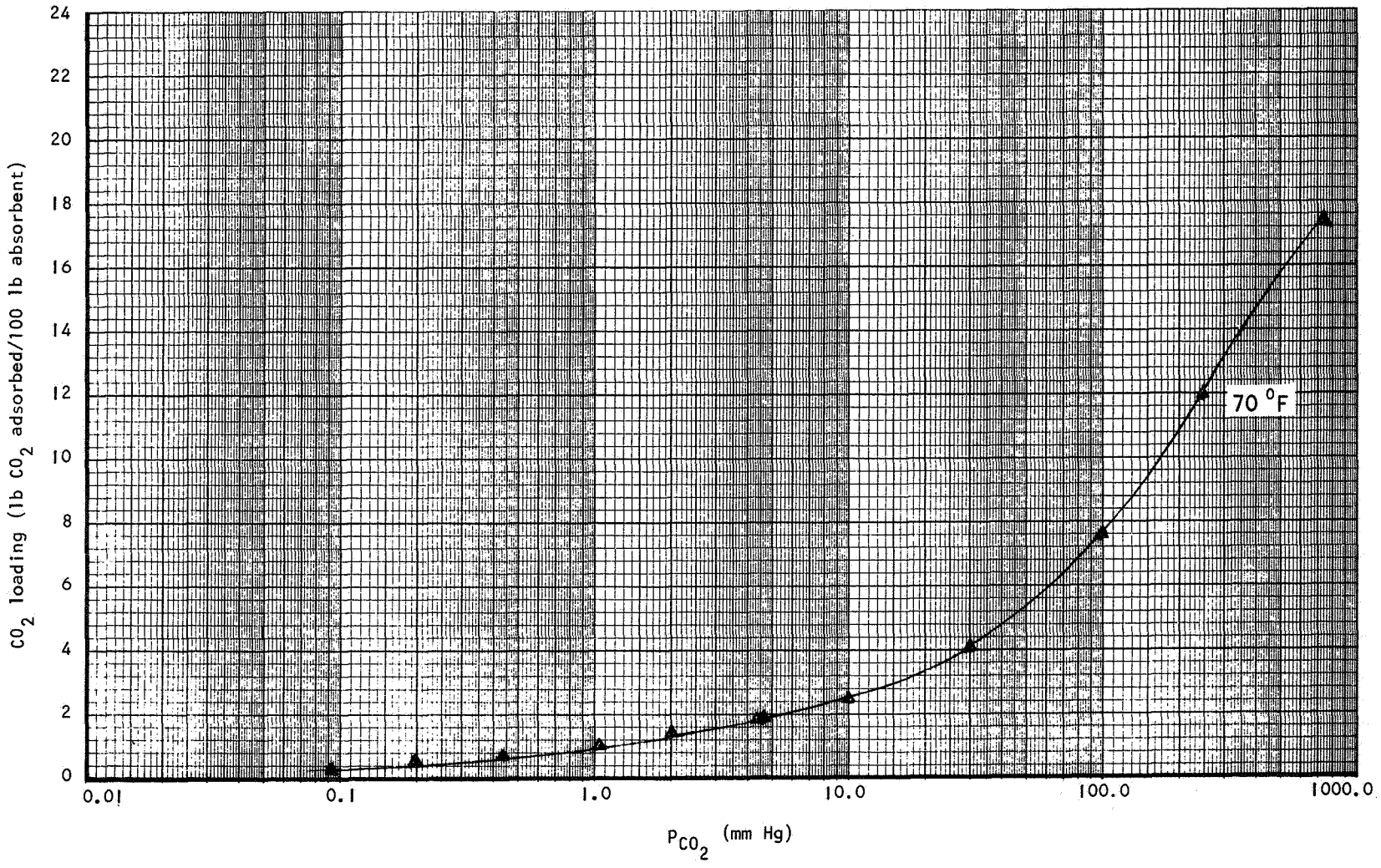

Figure 3-5. Carbon Dioxide Equilibrium Data for Linde 10X Sorbent

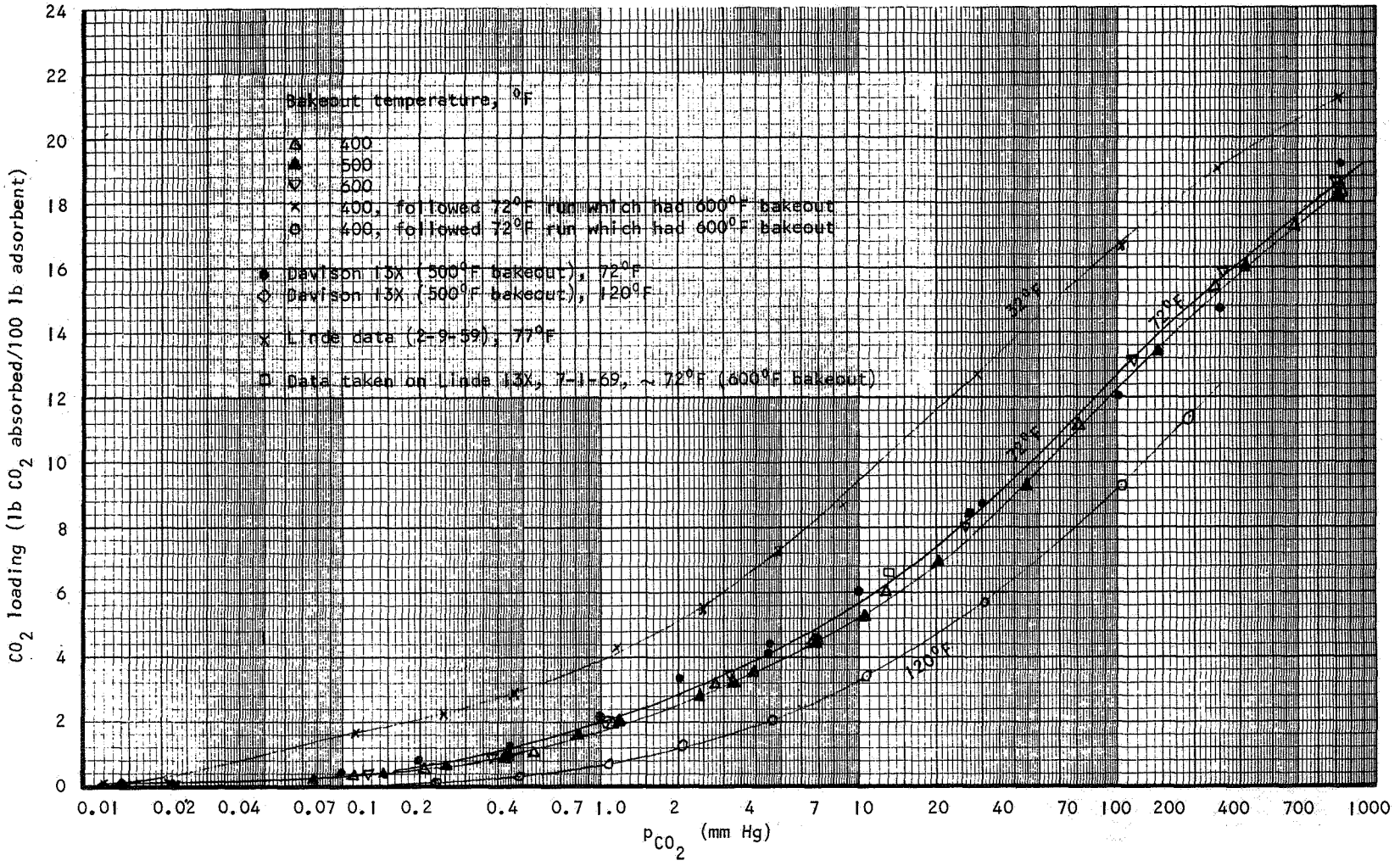

Figure 3-6. Carbon Dioxide Equilibrium Data for Linde 13X Sorbent

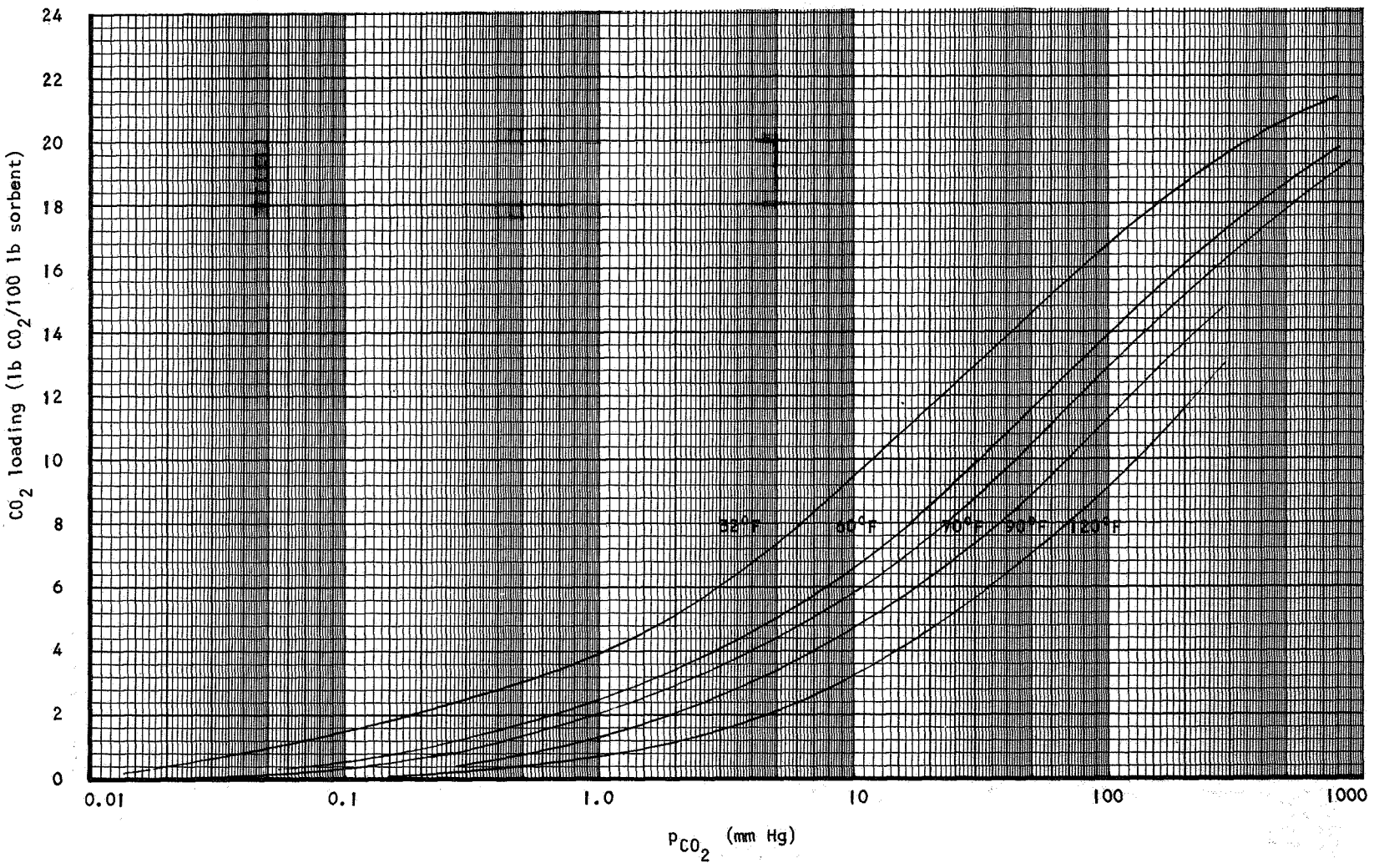

Figure 3-7. Carbon Dioxide Equilibrium Data for Linde 13X Sorbent (Summary)

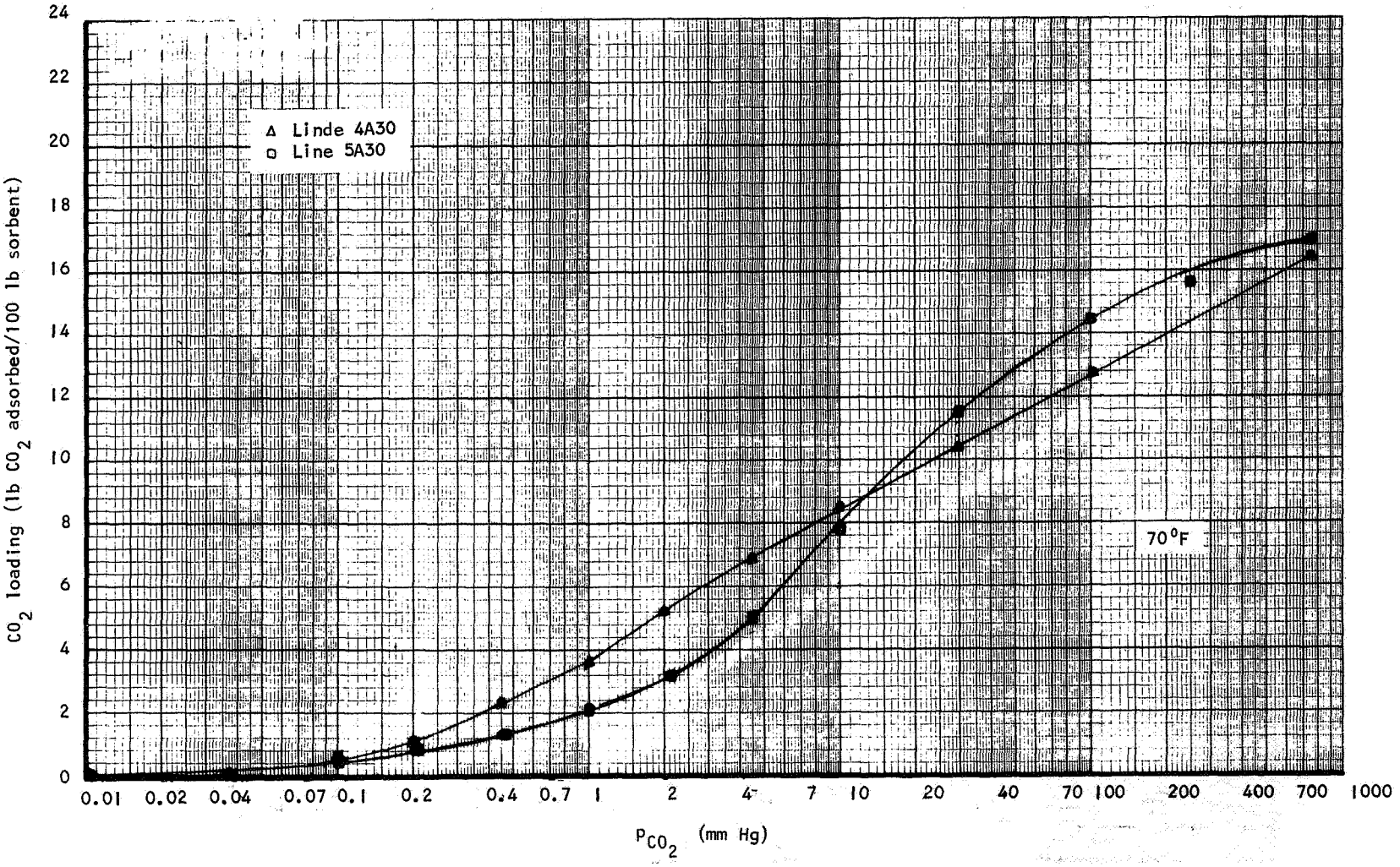

Figure 3-8. Carbon Dioxide Equilibrium Data for Linde 4A30 and 5A30 Sorbents

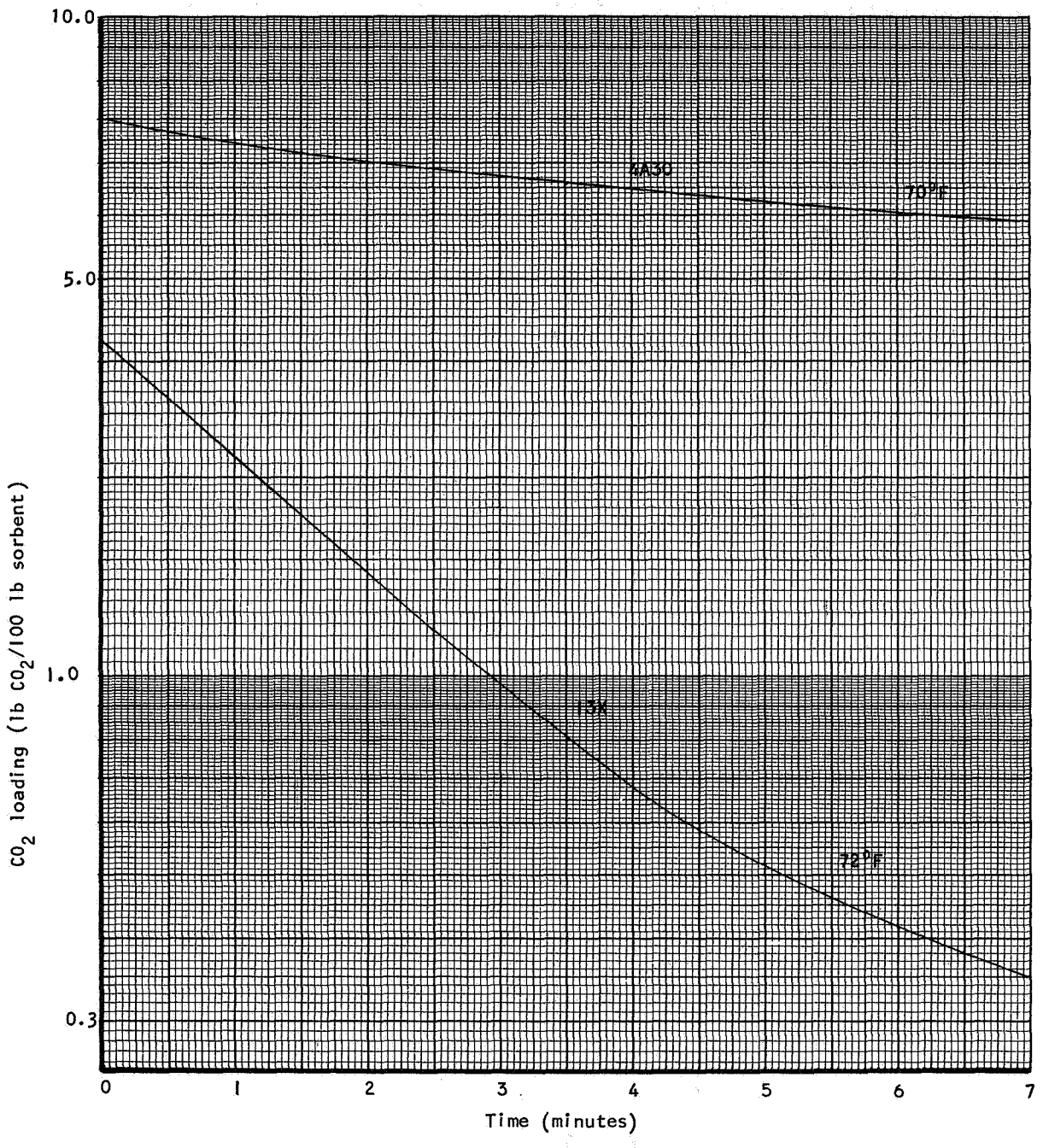

Figure 3-9. Desorption of Carbon Dioxide from Linde 4A30 and 13X Sorbents

Water Vapor Equilibrium on Molecular Sieves

The following figures present the water vapor isotherms obtained with Davison and Linde 5A, Linde 10X, Davison and Linde 13X, Linde 4A30 and Linde 5A30. Figure 3-10 presents a comparison of a 70°F isotherm taken from the AiResearch AAP program and Linde data sheet 5A-1, a least square fit of the Linde isotherm at 70°F, and a 70°F isotherm with Davison 5A. Figure 3-11 presents a comparison of the Davison and Linde 5A sorbent at 120°F. The Davison curve was run by AiResearch and the Linde curve was taken from Linde data sheet 5A-1. Figure 5-12 presents a 70°F isotherm with Linde 10X sorbent. Figure 3-13 presents a comparison of the davison and Linde 13X sorbent at 70°F. The Linde data was again taken from the data sheet and the Davison data produced here. Figure 3-14 presents a family of isotherms at 33°, 60°, 70°, 90°, 120°, 208°, 302°, and 400°F for Linde 13X sorbent. Figure 3-15 presents 70°F isotherms for Linde 4A30 and 5A30 sorbents.

Comparison of all the previous listed data indicate that the 10X sorbent has a slightly higher loading capacity at higher pressures, i.e., from 10 mm Hg down to 0.1 mm Hg. At approximately 0.1 mm Hg the two capacities are the same and for lower pressures the Davison 5A indicates the greater load capacity. Low pressure loading was extremely difficult to obtain due to the time required to stabilize.

Oxygen Equilibrium on Molecular Sieves

The following figures present the oxygen isotherms obtained with Linde 4A, 5A, and 13X sorbents. Figure 3-16 presents a 70°F isotherm for the Linde 4A sorbent. Figure 3-17 presents 32° and 70°F isotherms for the Linde 5A sorbent, and Figure 3-18 presents 32°, 72°, and 120°F isotherms for the Linde 13X sorbent. The 120°F isotherm for the Linde 13X sorbent was difficult to obtain in both the high pressure and low pressure regions; however sufficient mid-range data was obtained to demonstrate slope characteristics compatible with the 32° and 72°F isotherms. Oxygen loading generally was quite small making data difficult to obtain.

Comparison of the 70°F isotherms indicate very little to choose between in the three sorbents. However 4A and 5A do appear to possess a slightly higher potential load capacity at high pressure.

Nitrogen Equilibrium on Molecular Sieves

The following figures present the nitrogen isotherms obtained with Linde 4A, 5A, and 13X sorbents. Figure 3-19 presents a 70°F isotherm for the Linde 4A sorbent and Figure 3-20 presents three isotherms for 32°F, 68°F, and 120°F, for the Linde 5A sorbent. Also included on this figure is a referenced nitrogen isotherm obtained from ESSO (Reference 3) The basic slope characteristics of the AiResearch data and the referenced isotherm are in agreement. Figure 3-21 also presents three isotherms, for 32°F, 72°F, and 120°F, for the Linde 13X sorbent. The Linde 5A appears to have the greatest potential load capacity of the three materials at both high and low pressure levels. This

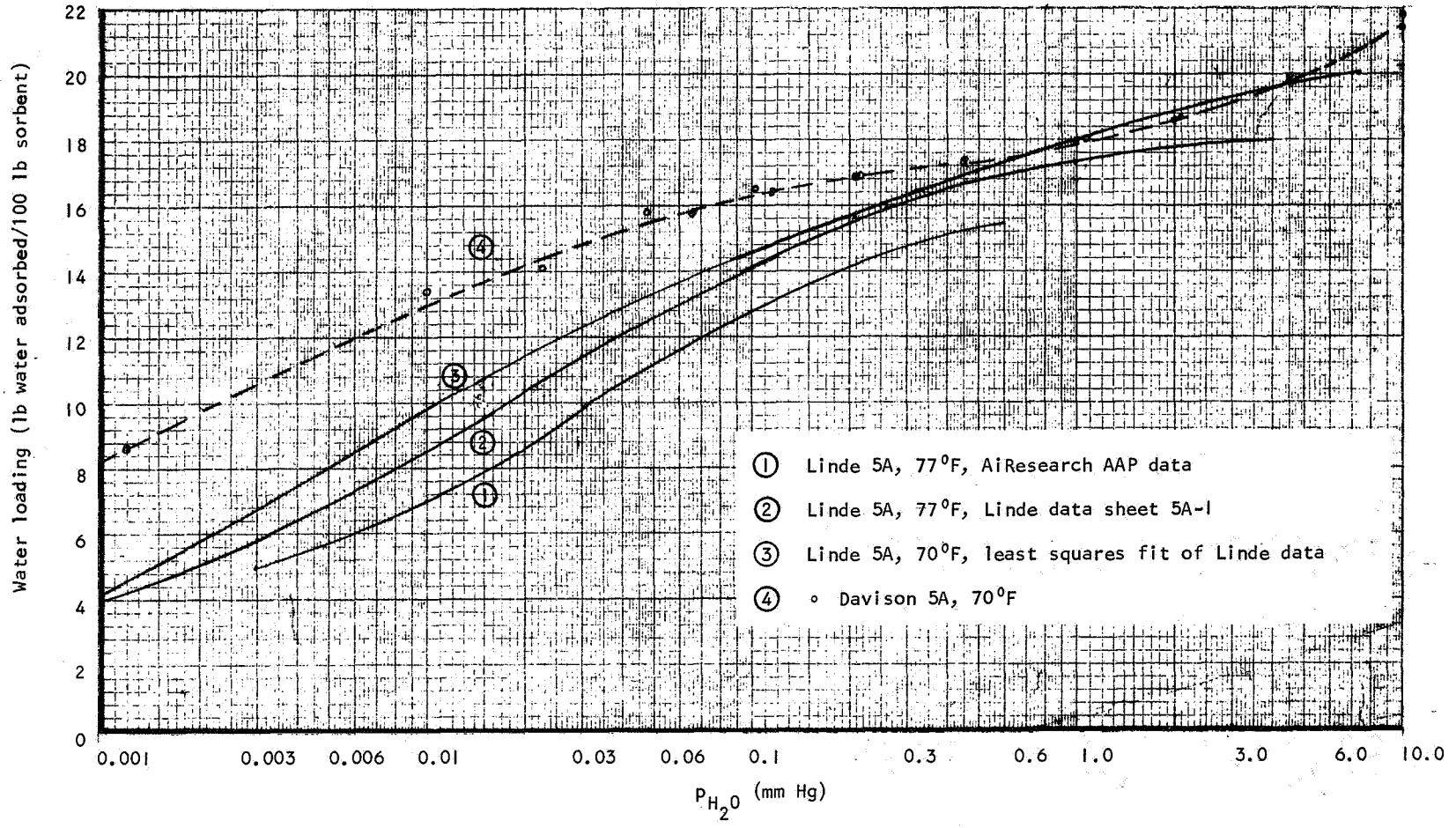

Figure 3-10. Water Vapor Equilibrium Data for Linde and Davison 5A Sorbents

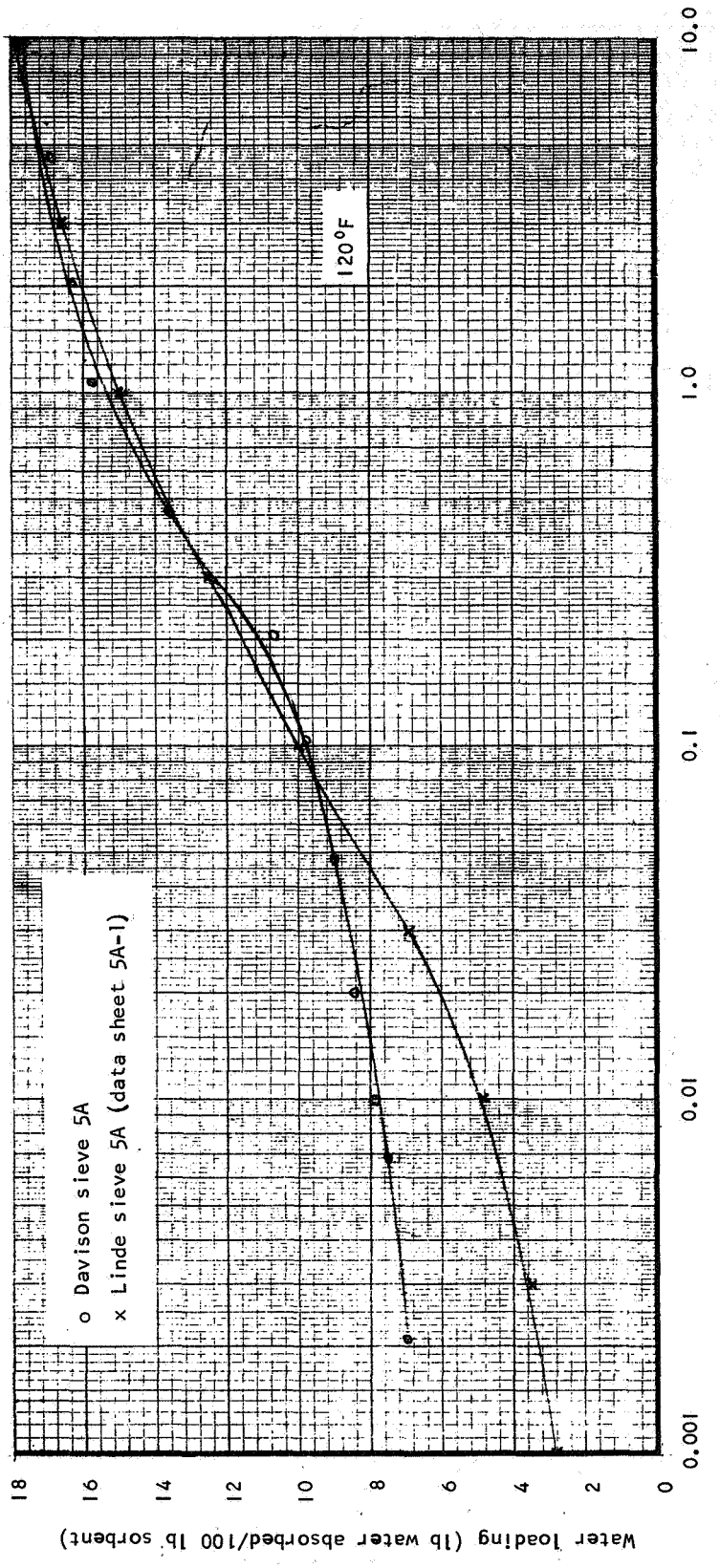

Figure 3-11. Water Vapor Equilibrium Data for Linde and Davison 5A Sorbents

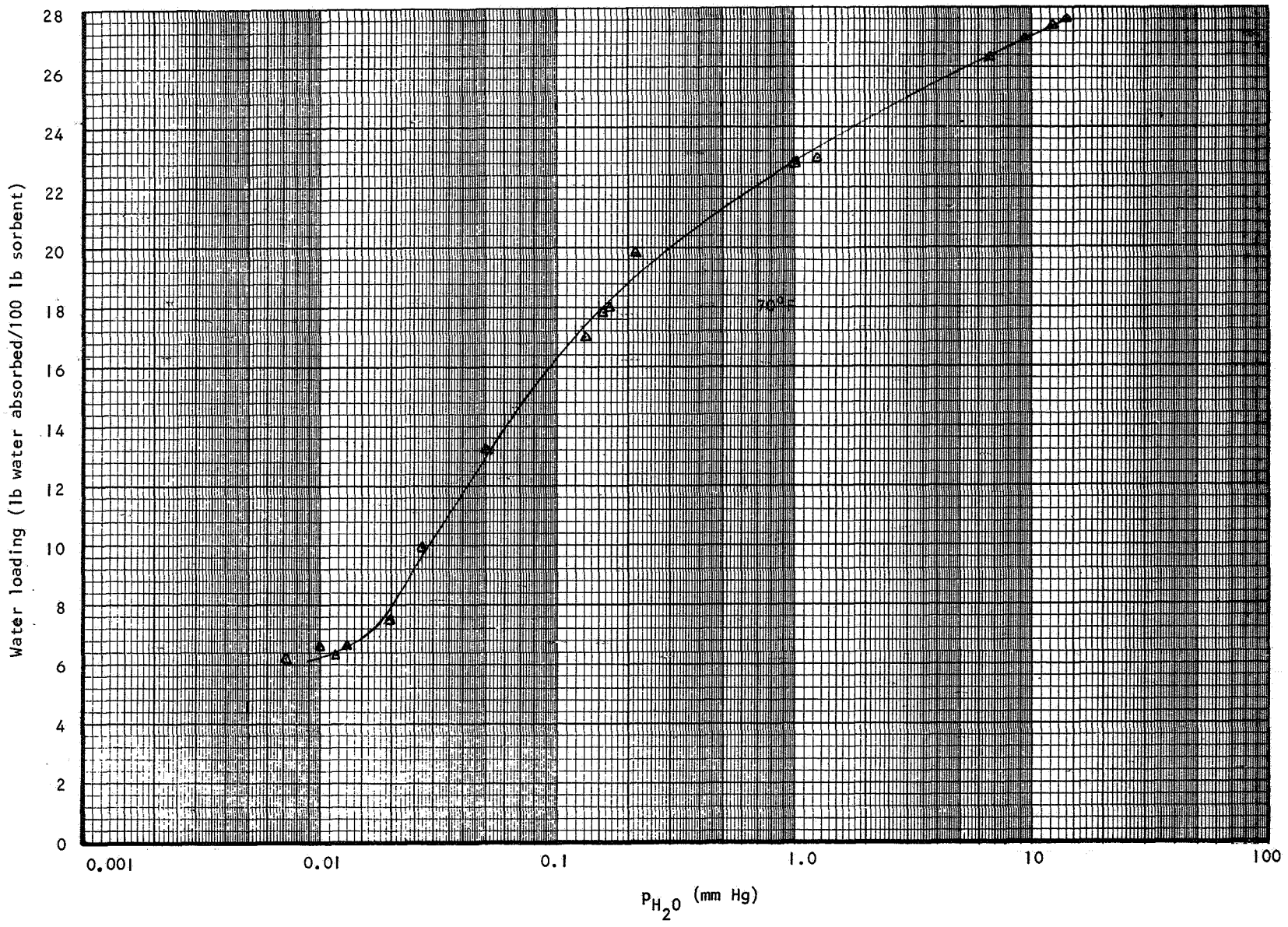

Figure 3-12. Water Vapor Equilibrium Data for Linde 10X Sorbent

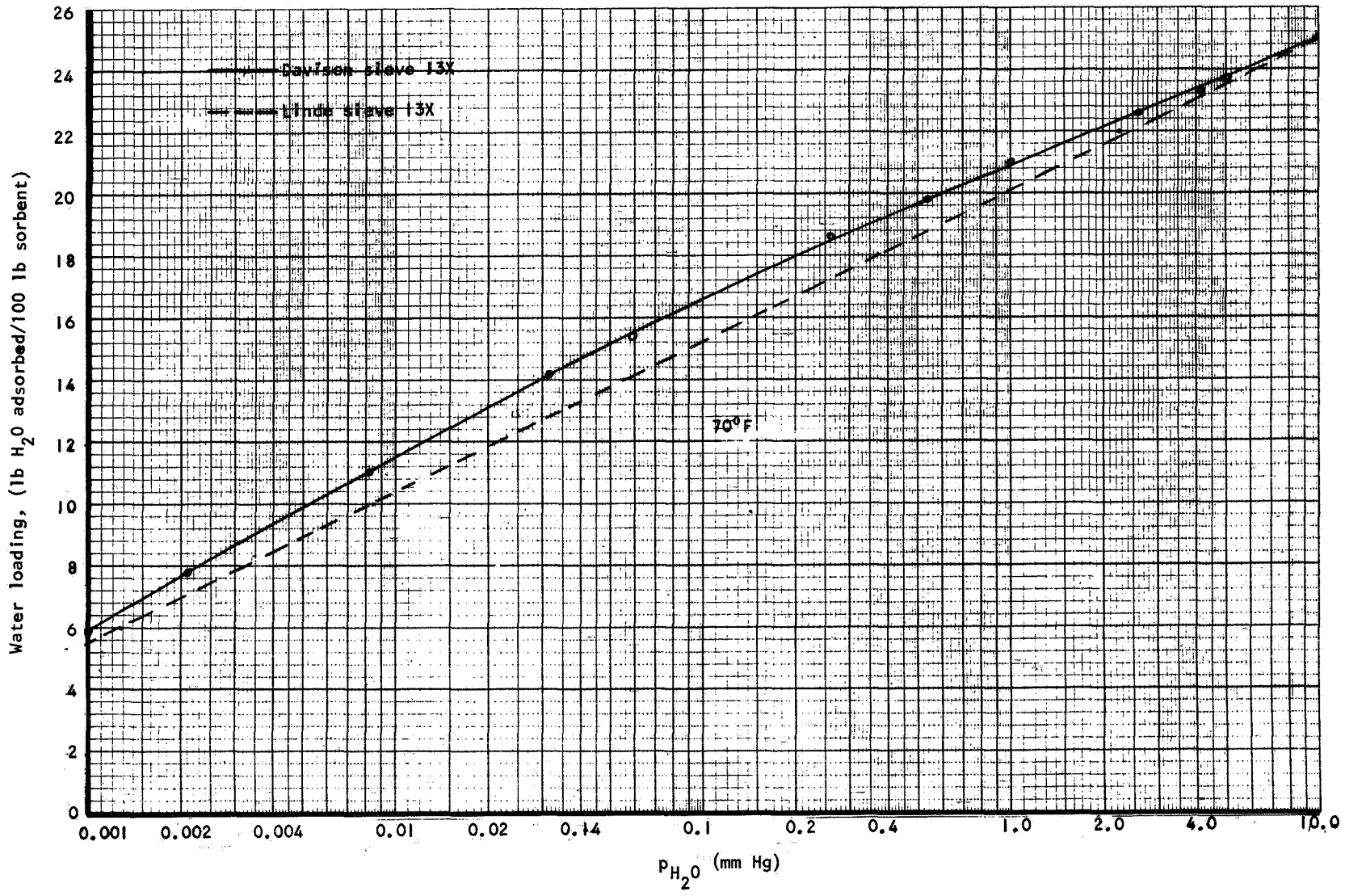

Figure 3-13. Water Vapor Equilibrium Data for Linde and Davison 13X Sorbents

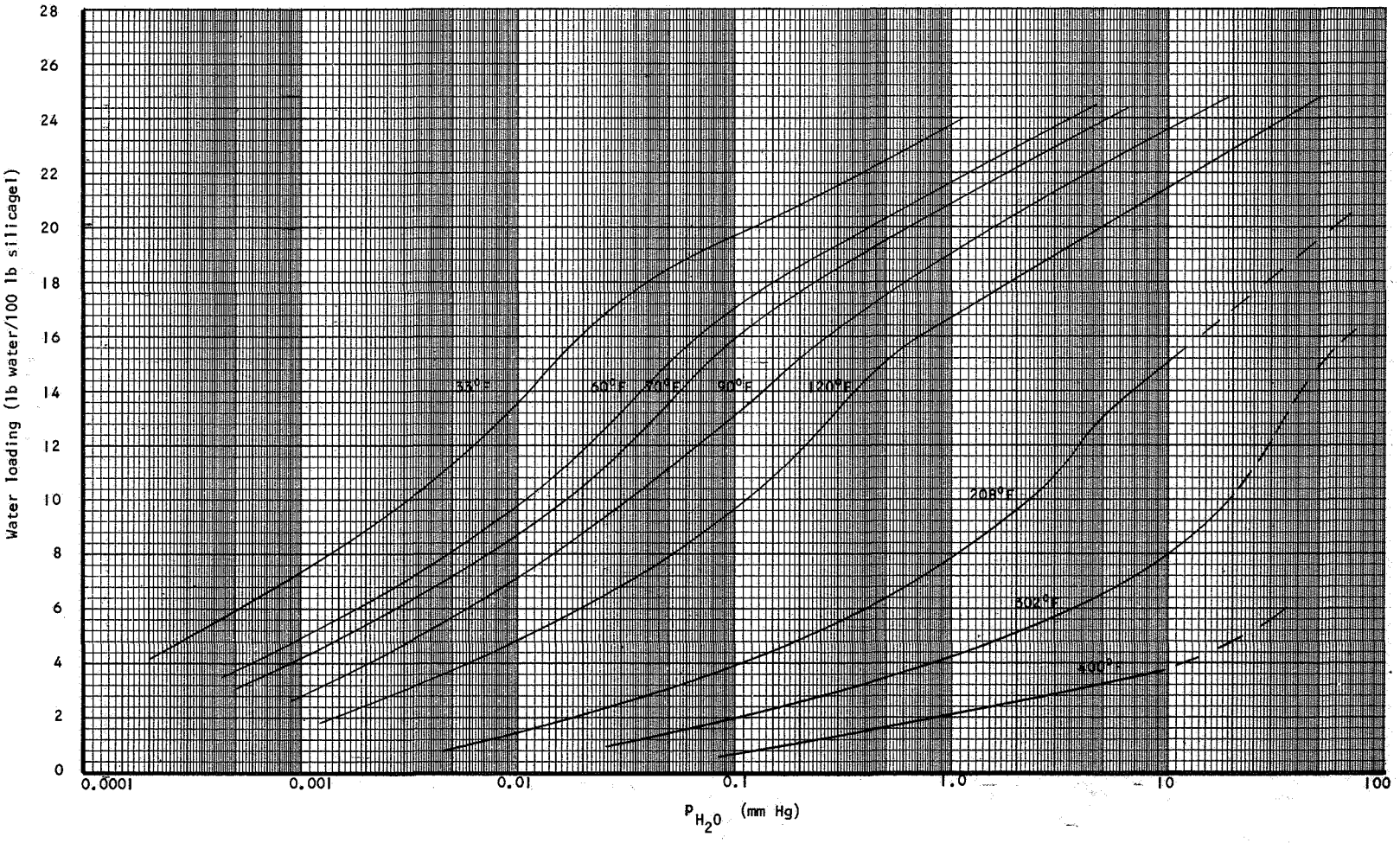

Figure 3-14. Water Vapor Equilibrium Data for Linde 13X Sorbent (Summary)

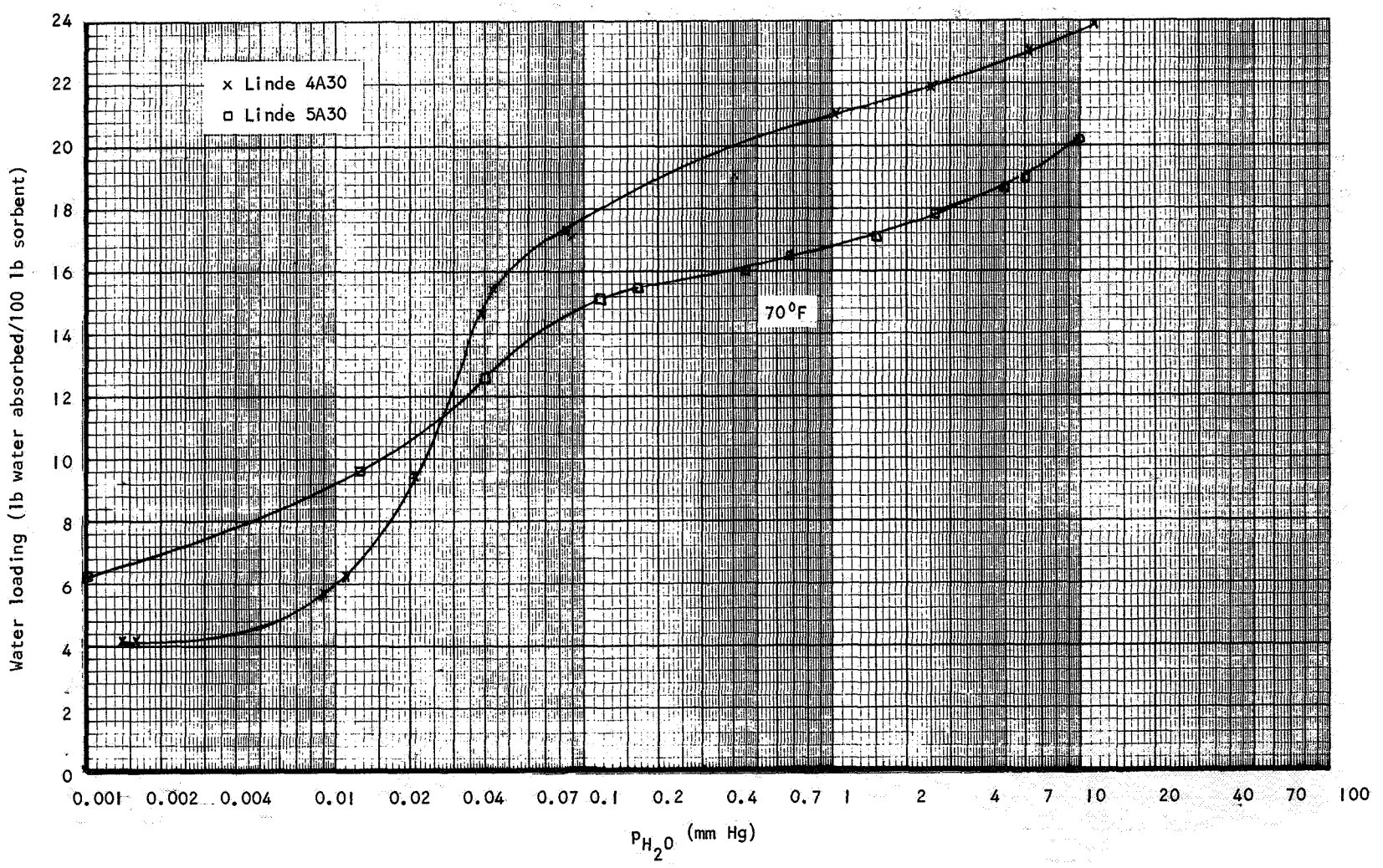

Figure 3-15. Water Vapor Equilibrium Data for Linde 4A30 and 5A30 Sorbents

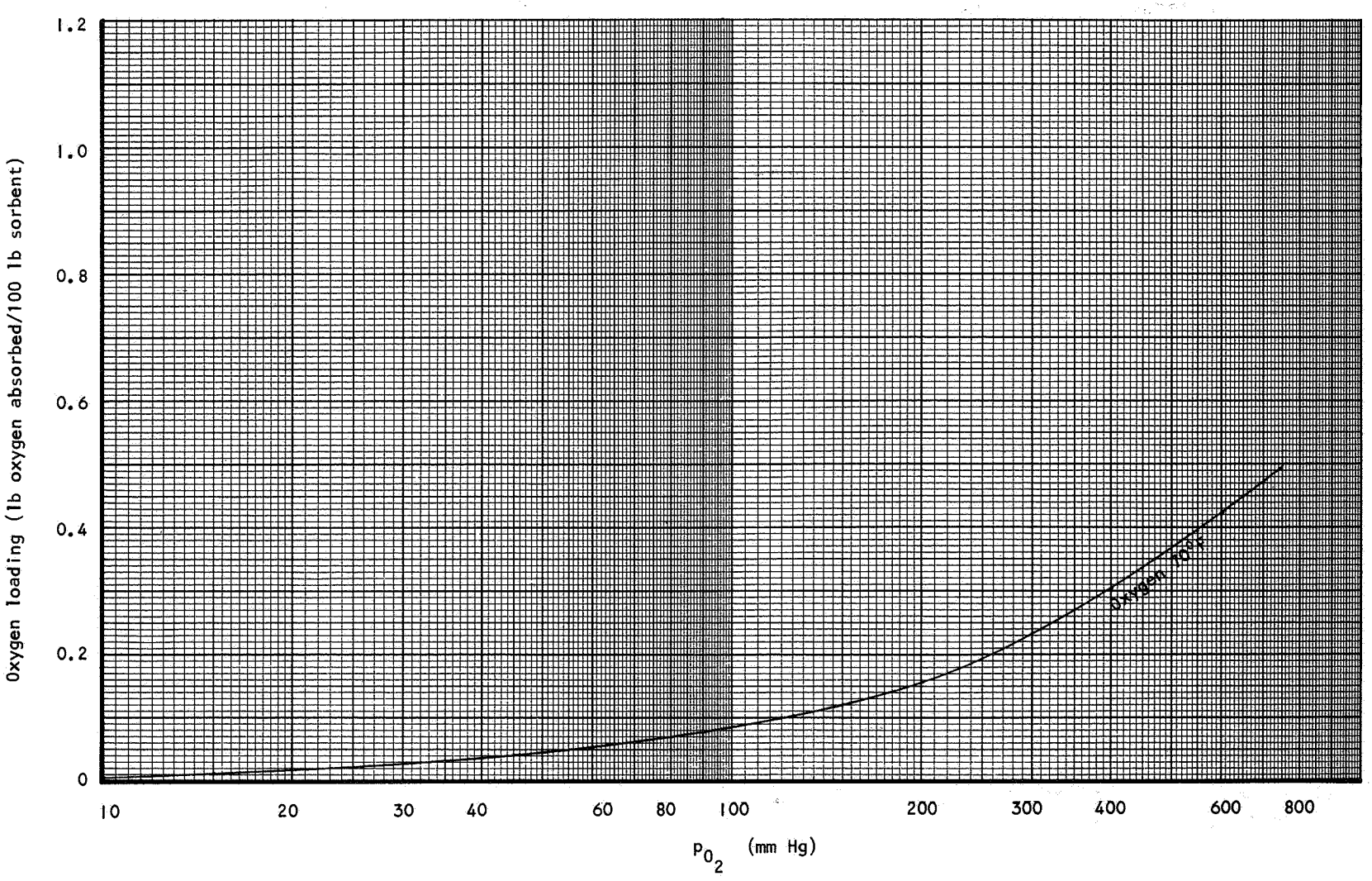

Figure 3-16. Oxygen Equilibrium Data for Linde 4A Sorbent

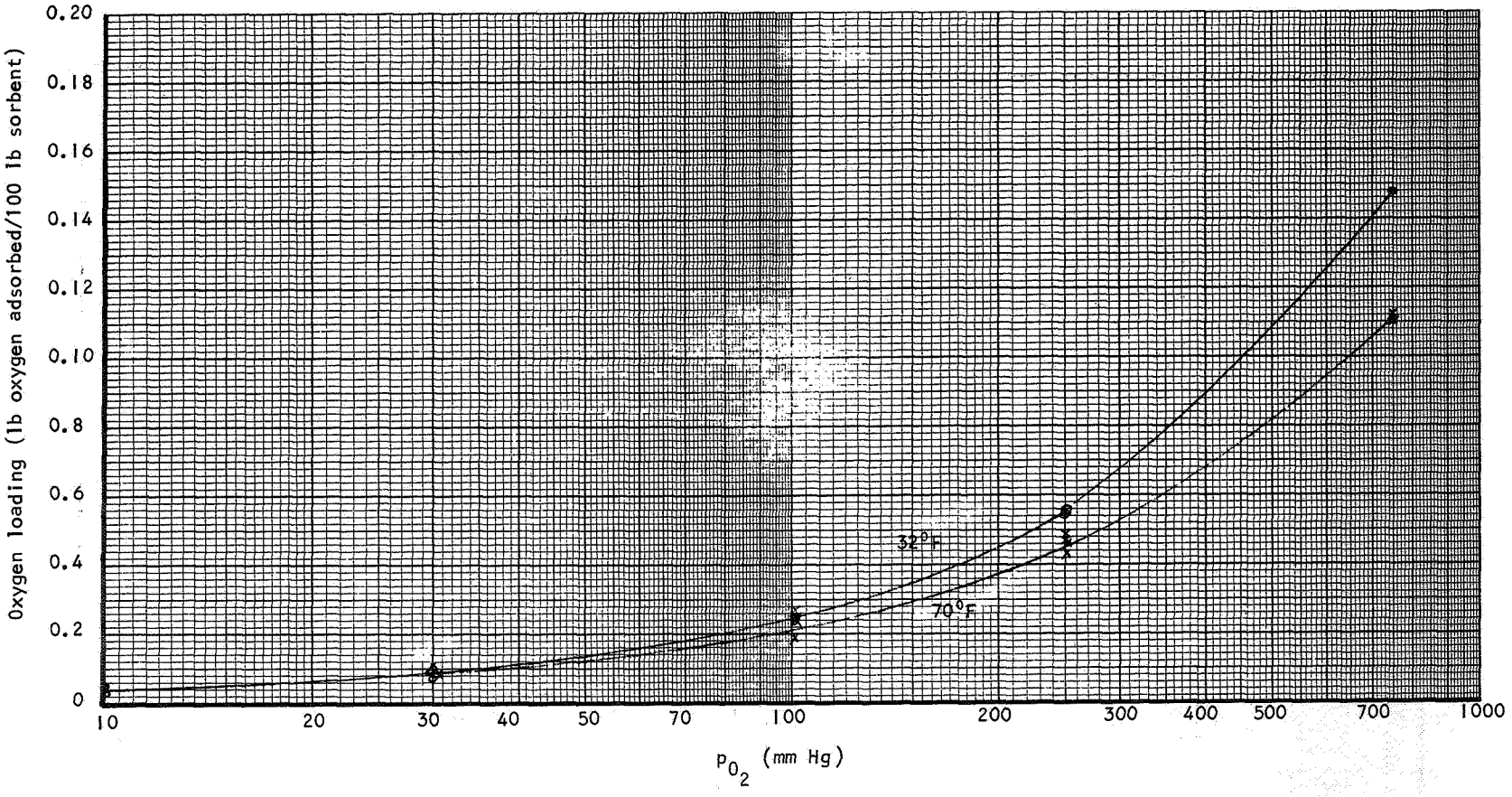

Figure 3-17. Oxygen Equilibrium Data for Linde 5A Sorbent

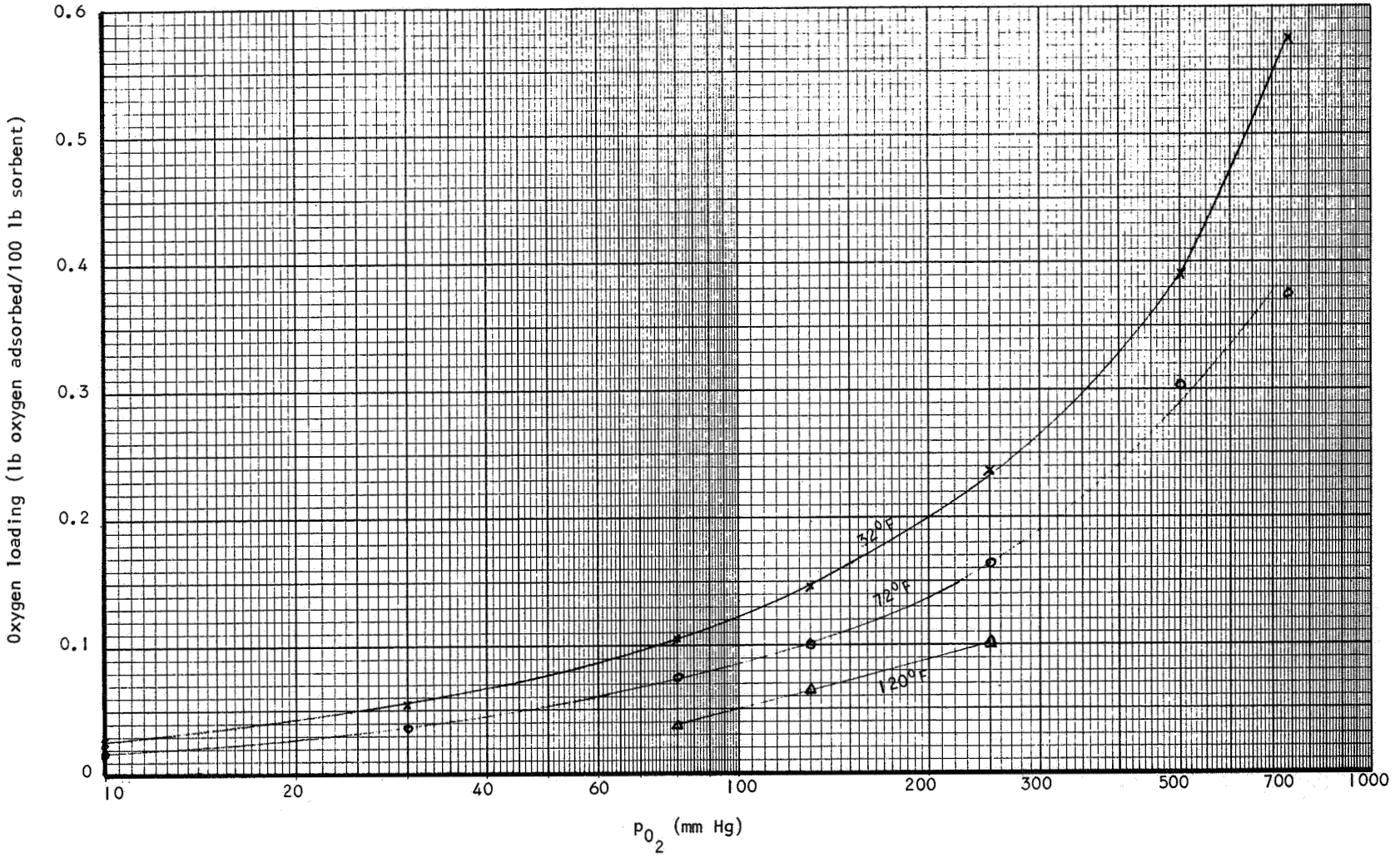

Figure 3-18. Oxygen Equilibrium Data for Linde 13X Sorbent

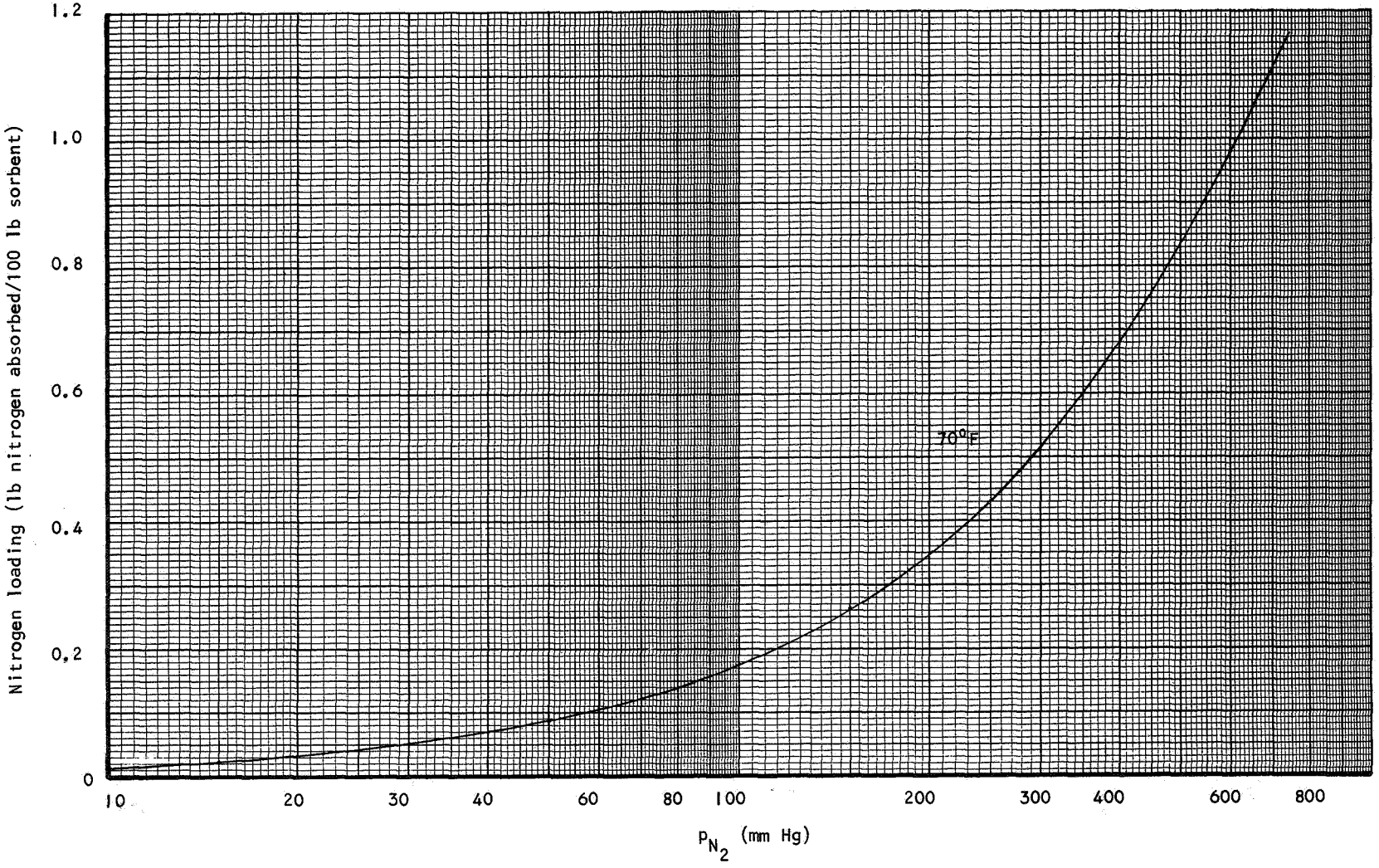

Figure 3-19. Nitrogen Equilibrium Data for Linde 4A Sorbent

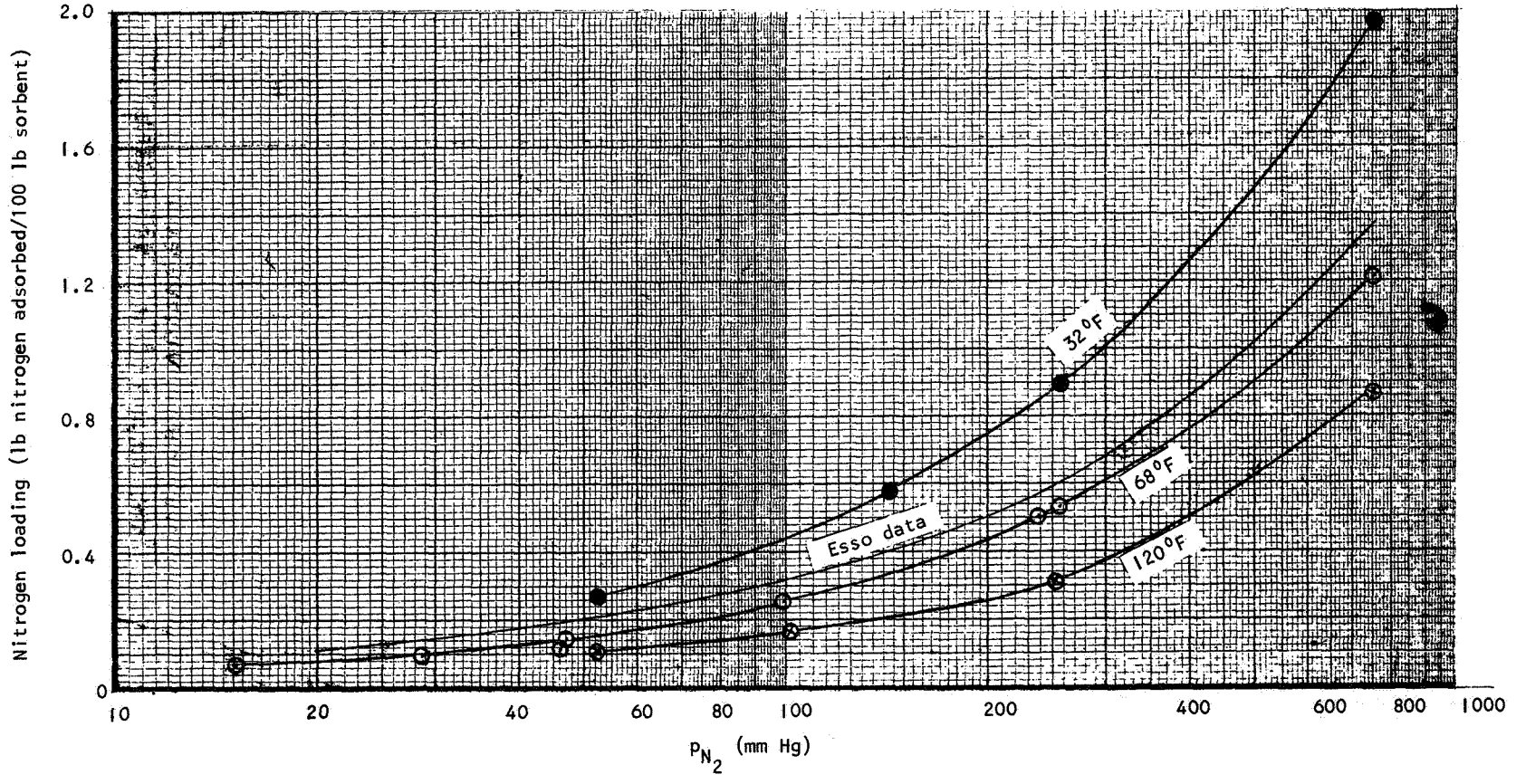

Figure 3-20. Nitrogen Equilibrium Data for Linde 5A Sorbent

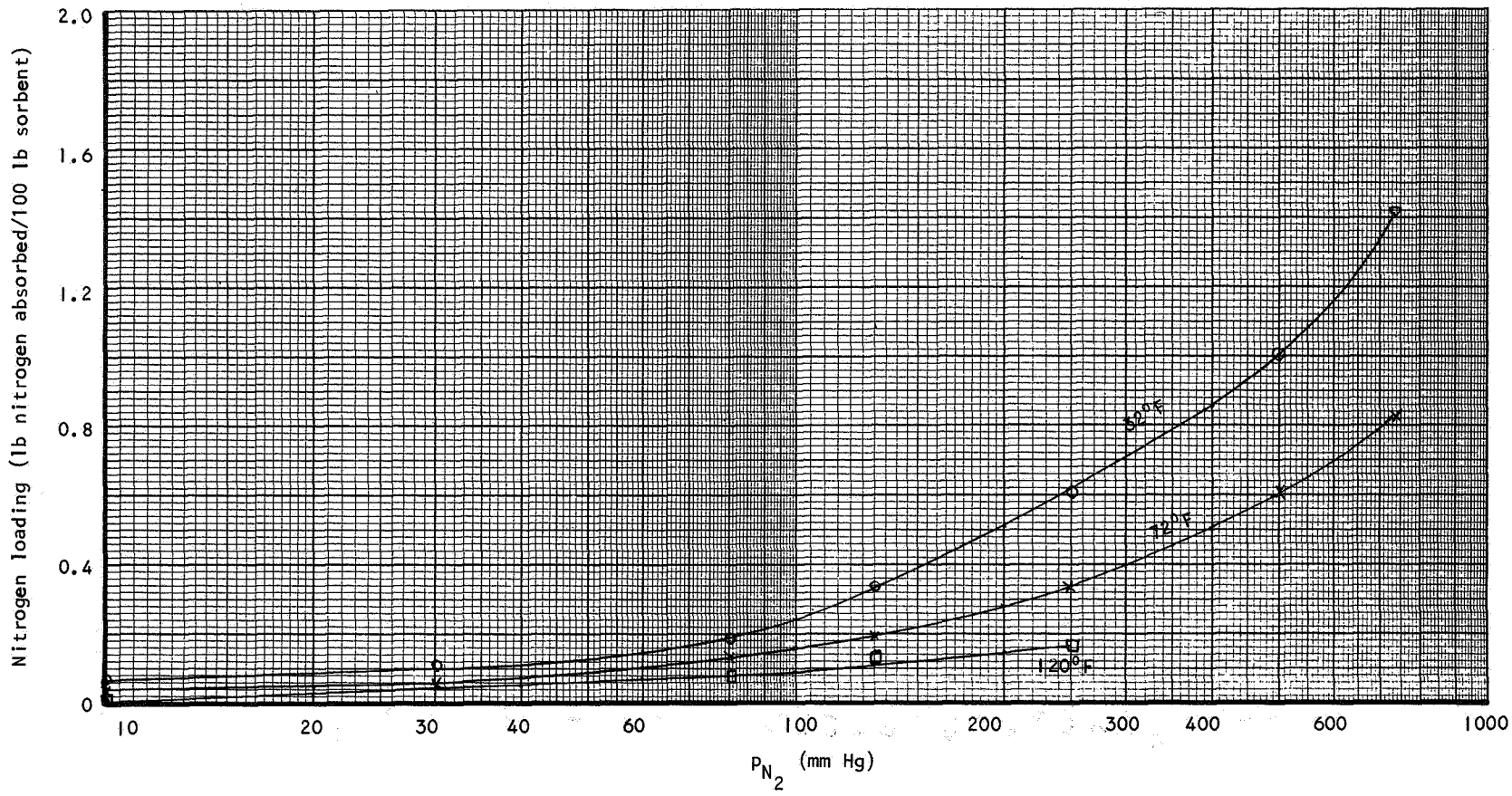

Figure 3-21. Nitrogen Equilibrium Data for Linde 5A Sorbent

observation is based on an approximated 70°F isotherm. The 4A and 13X are essentially identical, within experimental repeatibility, at low pressure levels; however the 4A has an increasingly higher load capacity from approximately 200 mm Hg on up to 760 mm Hg.

Water Vapor Equilibrium on Silica Gel

A test series was performed on Silica gel to determine the water vapor adsorption characteristics. Two isotherms were plotted and are included in Figure 3-22.

The silica gel used on the test was Davison Grade 05 in the form of a 6-15 mesh irregularly-shaped particles. The isotherms were plotted from test data at 60°F and 120°F. A 90°F isotherm was then interpolated from the test data and is also included on the figure. Prior Davison data for 60°F and 120°F are also included in phantom lines in the figure. Major differences are obvious in the low-pressure-range isotherm slopes, as well as in the high pressure termination slopes. Because of this discrepancy the Davison Chemical Division of W. R. Grace and Company was contacted. Apparently the Davison data are almost 15 years old and the silica gel manufacturing process has been continuously improved. An important characteristic of the silica gel adsorption characteristics can be observed on the 60°F isotherm where the slope of the loading curve decreases rapidly above 6 mm Hg pressure. At 11 mm Hg the loading is 41.6 percent. This compares with the calculated maximum loading for silica gel of 43 percent assuming that the maximum loading occurs when intra-crystalline voids are full of liquid water.

The 60°F and 120°F isotherms generated for this program provide very close correlation with the associated dynamic test data.

COADSORPTION TEST DATA FOR MOLECULAR SIEVES

It is common in the mass transfer field to consider adsorption processes on the basis of one primary sorbate, and to ignore the simultaneous sorption of other gases. Primarily this is done for simplicity; to do otherwise might possibly involve considerable complications. In many instances the actual process can be characterized well on the basis of one sorbate; i.e., the drying of a gas stream by molecular sieves. Here, the water equilibrium data, which was taken without the carrier gas being present, is considered to be valid, with no effect due to the presence of the large amount of carrier gas. The mass-transfer dymanics are similarly characterized without considering the sorption of the carrier gas. If the carrier gas sorption is considered, the assumption is usually made that it has no effect on the sorption of water.

There are, however, many cases where there is appreciable adsorption of more than one material, and as a consequence, interactions take place which alter both the dynamic and the equilibrium character of the process. Spacecraft CO_2 removal systems using molecular sieves certainly fall into this

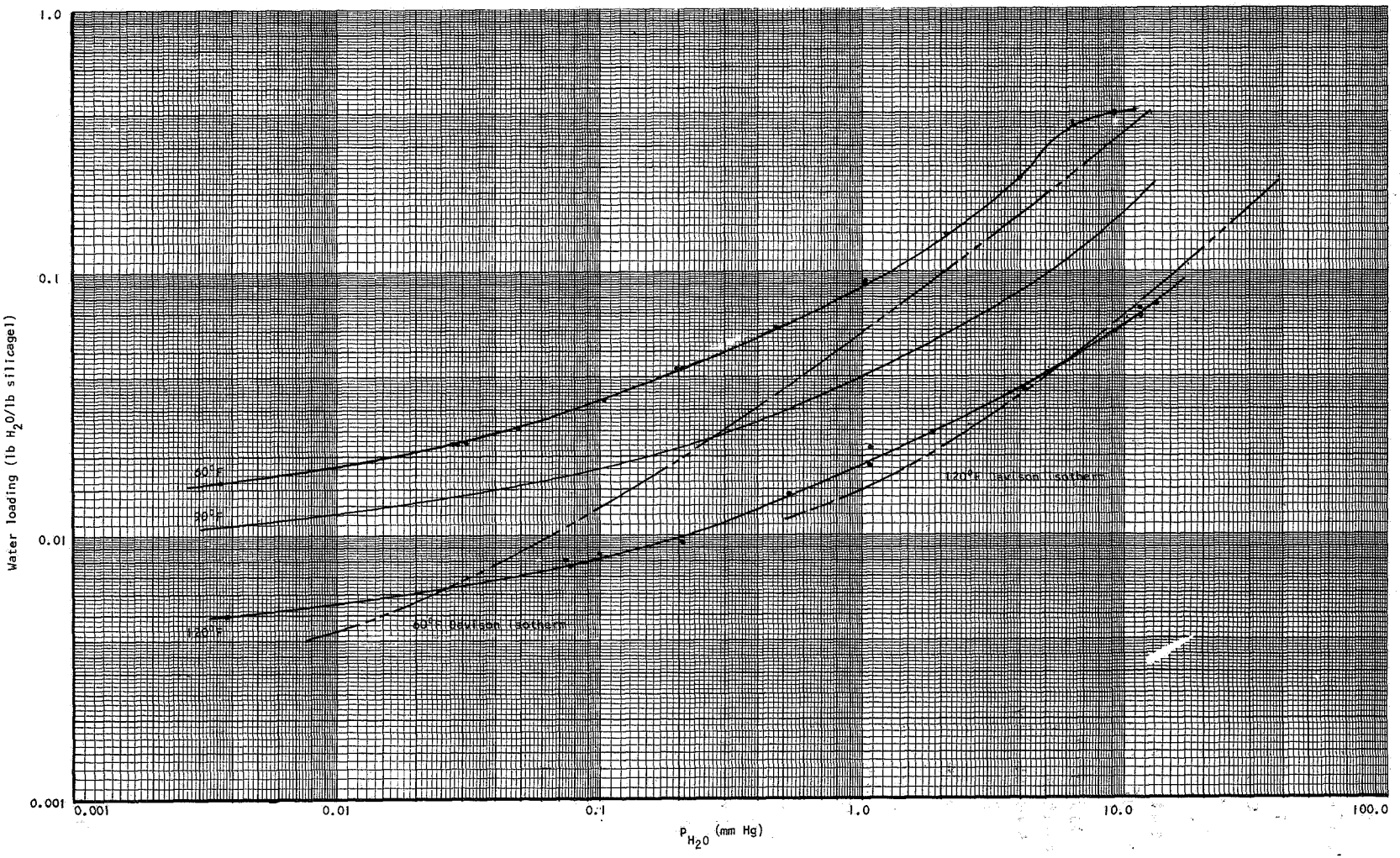

Figure 3-22. Water Vapor Equilibrium Data for Silica Gel

category. The poisoning effect of coadsorbed water on the CO_2 capacity of molecular sieves has been well known for some time. However, until lately, little quantitative information was available.

In this program it was desired to produce quantitative data on the equilibrium capacity of molecular sieves for a particular sorbate in the face of the coadsorption of another sorbate. Obviously, the most important coadsorption sorbate pair for which data were sought is CO_2 and water, i.e., the poisoning effect due to water. This was not the only coadsorption pair considered. Other pairs of interest can be seen in Table 3-3.

The coadsorption pairs involving either nitrogen or oxygen were of interest for two reasons. First, in most instances where these gases are adsorbed, they will eventually be lost from the vehicle. Therefore they represent a definite weight penalty to the CO_2 removal system; and of course provisions would have to be made within the spacecraft to store makeup gases. It was desired, in this program, to ascertain any possible coadsorption effect, especially with water, which might appreciably alter the loss of atmosphere gases. The second reason for the oxygen and nitrogen equilibrium data is to observe if the large volumetric preponderance of these gases has an effect on the equilibrium capacity for CO_2 and water. To a great extent, the answer to this latter inquiry can be obtained from the single-sorbate dynamic tests contained in Section 4. From these tests it is concluded that the equilibrium capacity data as taken with only the sorbate (either CO_2 or water) in contact with the molecular sieve is not noticeably affected by the presence of the nitrogen carrier gas.

The following figures present the results of equilibrium sorbent capacity testing for conditions where a preload of one sorbate is produced followed by adsorption of another gas. The sorbate pairs for which tests were conducted, are shown in Table 3-3. Also included in the table are the sorbant temperature and pressure range.

Coadsorption of CO_2 with H_2O Preload

The figures 3-23 through 3-26 present the coadsorption test data for carbon dioxide and water vapor. It can readily be observed that for coadsorption of CO_2 with a H_2O preload the CO_2 capacity is significantly reduced, however, even for a water load of 11.9 percent, some carbon dioxide was still adsorbed. Figure 3-23 presents a family of 70°F isotherms at various water vapor preload percentages, 0, 1.89, 4.02, 6.43, and 12 percent. The 12 percent curve was run twice to verify repeatibility; excellent agreement was obtained. Figure 3-24 presents a family of curves for constant water preload (approximately 6.1 percent) at different temperatures, 32°, 70°, 120°, and 200°F. It is obvious that as the sorbent temperature is increased less and less adsorption sites for CO_2 adsorption are available. Figure 3-25 presents the coadsorption

TABLE 3-3

COADSORPTION TEST MATRIX

Sorbent	Manufacturer	CO_2 on H_2O		N_2 on H_2O		N_2 on CO_2		O_2 on H_2O	
		Isotherms °F	Percent H_2O	Isotherms °F	Per cent H_2O	Isotherms °F	Percent H_2O	Isotherms °F	Percent H_2O
5A	Linde	70	0	70	0	70	0	70	0
			1.89		3.0		3.0		3.1
			4.02		5.1		5.0		5.0
					8.1		8.0		8.0
			6.43						
			12.0						
		32	6.1						
		120	6.1						
		200	6.1						
13X	Linde	32	6			70	0		
			12				3.0		
			18				5.0		
		70	2.07						
			3.99						
			11.9						
			12.1						
			17.9						
		72	0						
			5.9						
			11.9						
		120	5.5						
			12.0						
		200	6.0						
		300	6.1						

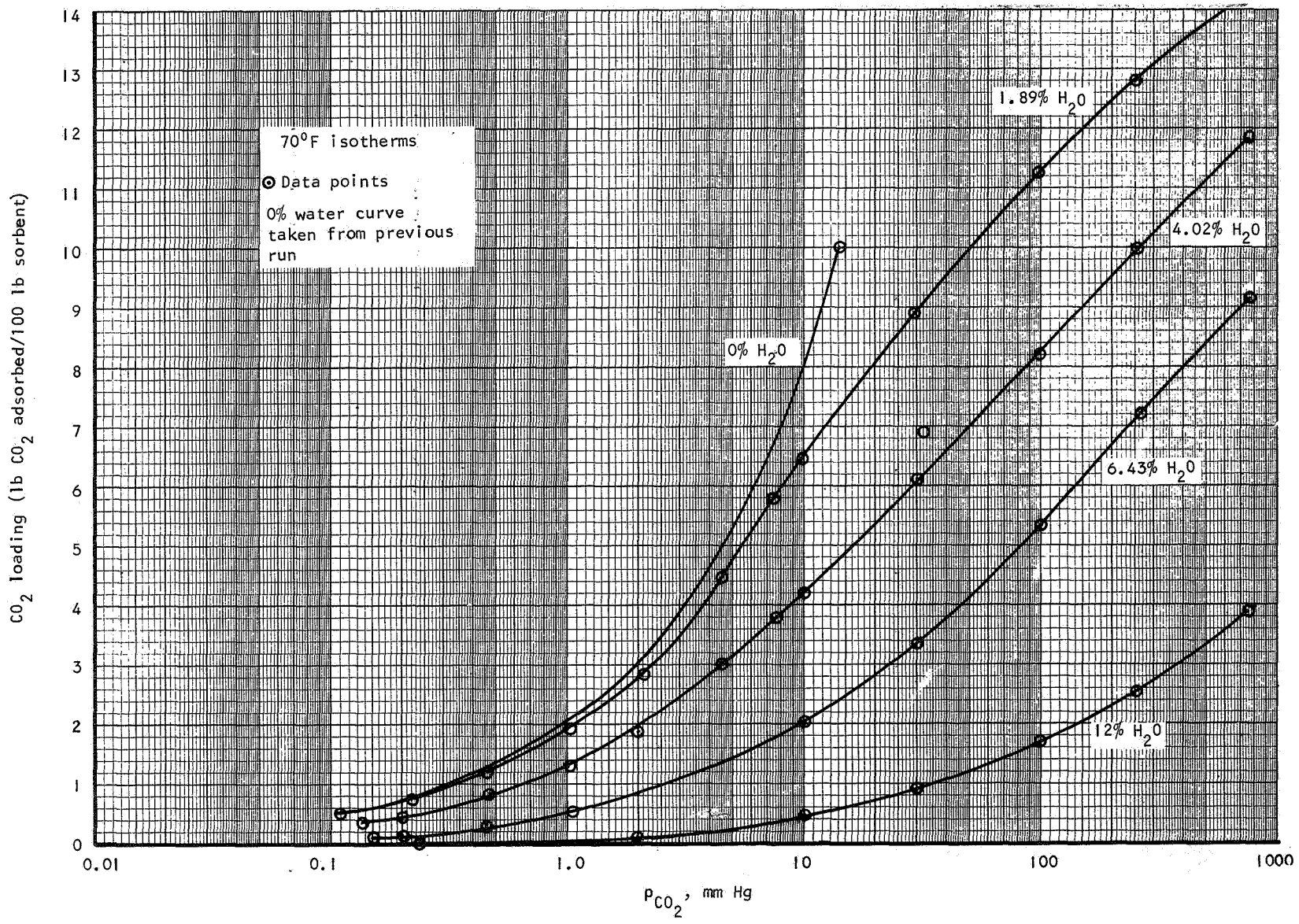

Figure 3-23. Coadsorption Equilibrium Data for Water Vapor and Carbon Dioxide on Linde 5A Sorbent

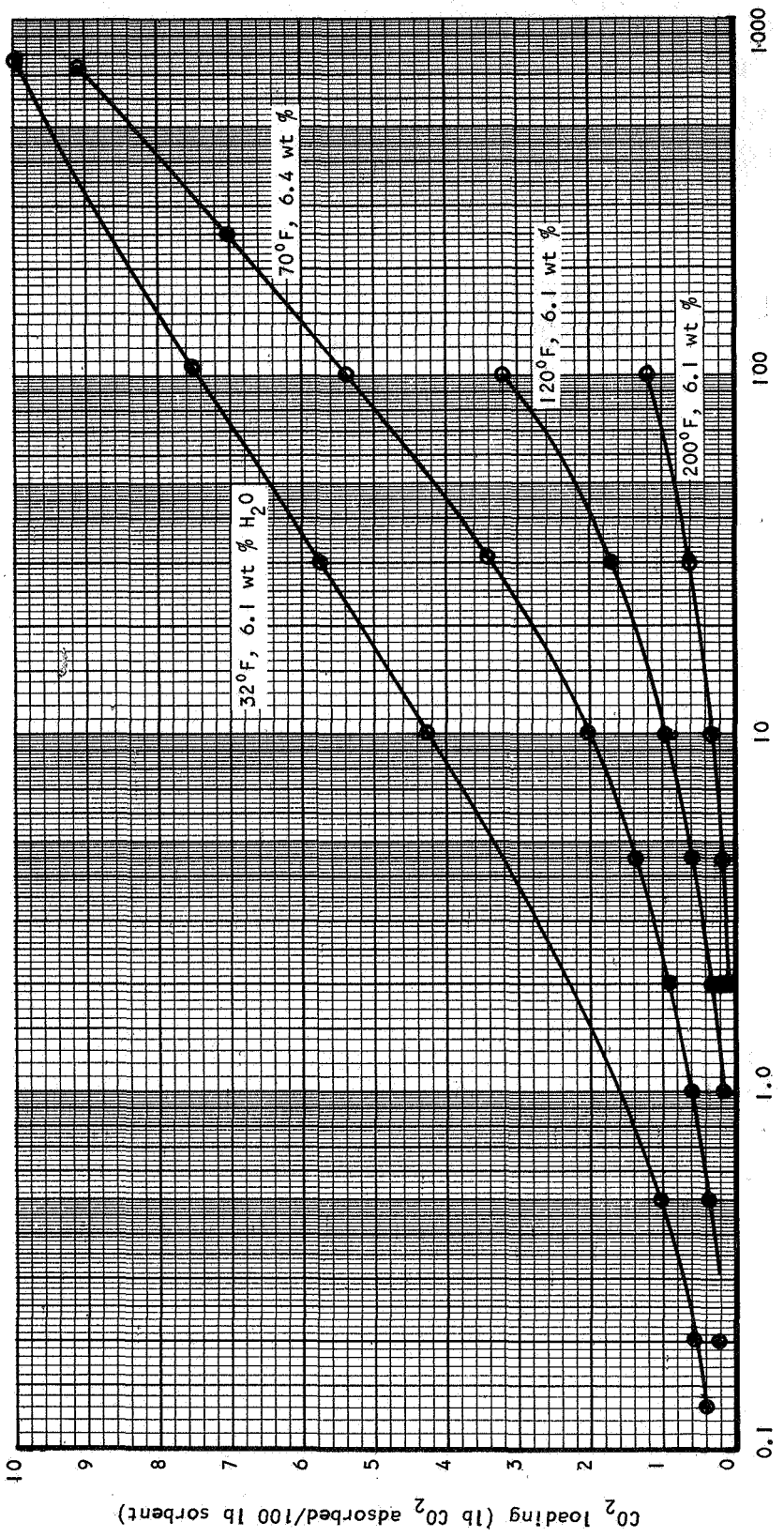

Figure 3-24. Coadsorption Equilibrium Data for Water Vapor and Carbon Dioxide on Linde 5A Sorbent

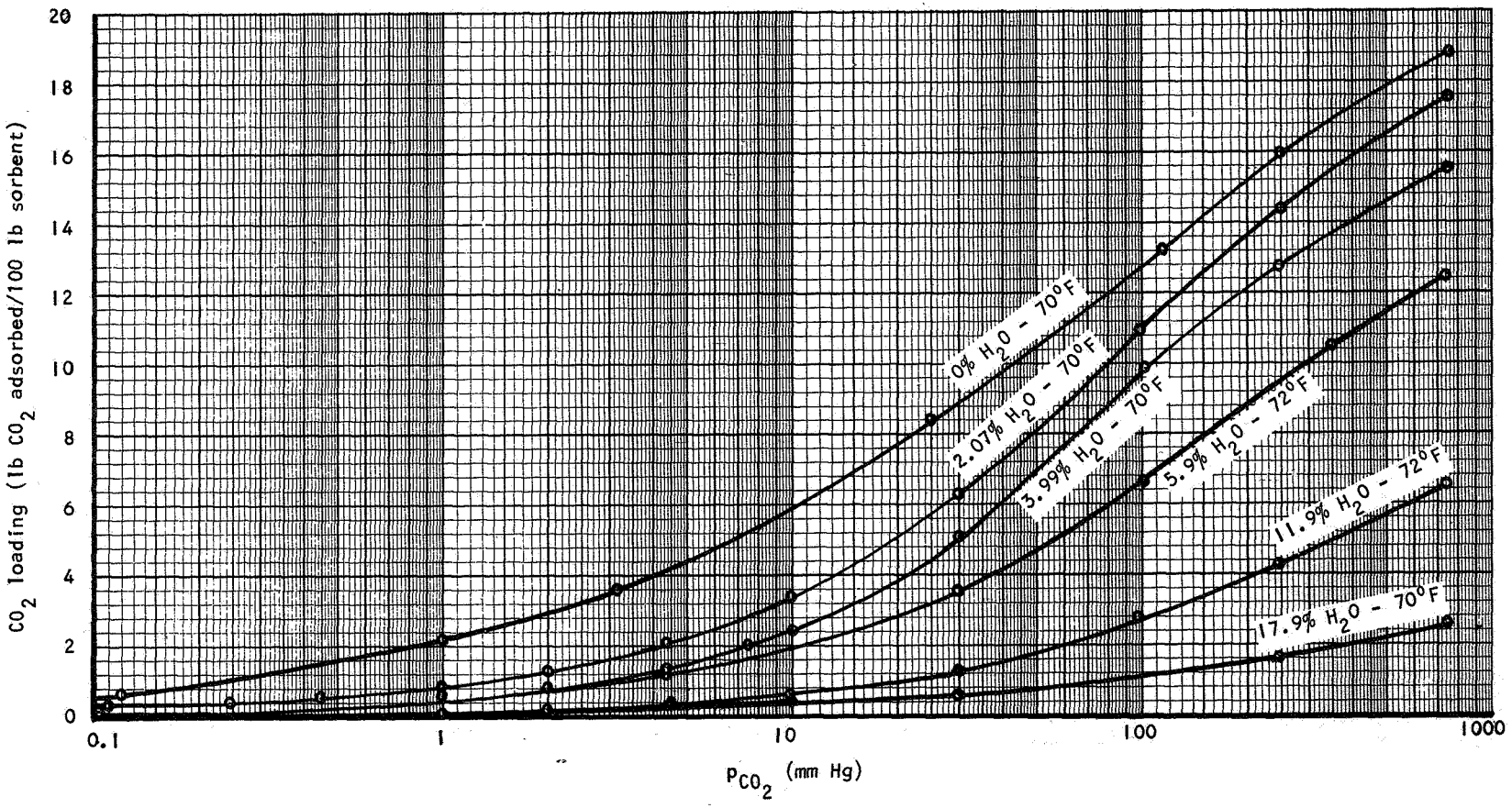

Figure 3-25. Coadsorption Equilibrium Data for Water Vapor and Carbon Dioxide on Linde 13X Sorbent

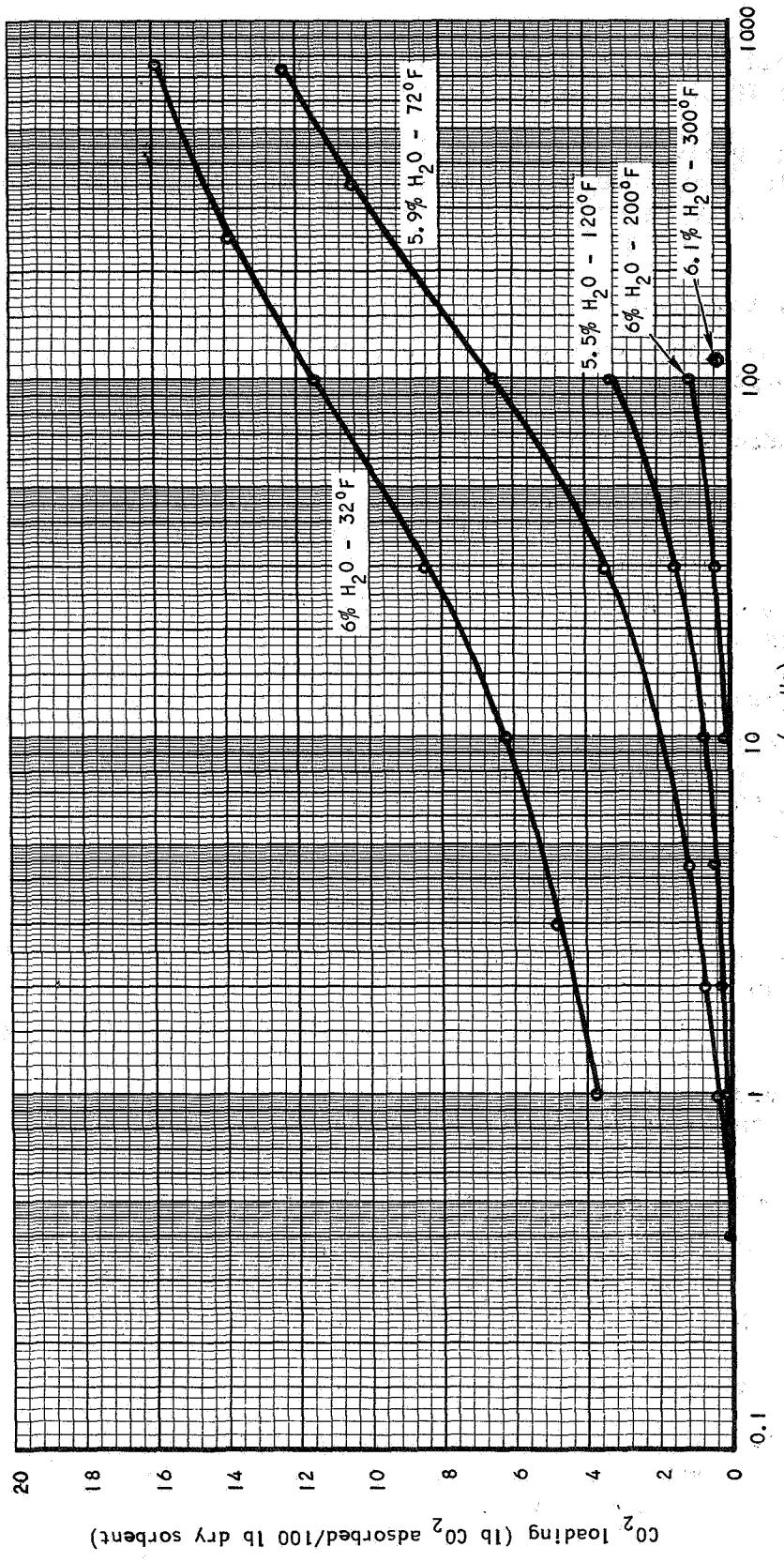

Figure 3-26. Coadsorption Equilibrium Data for Water Vapor and Carbon Dioxide on Linde 13X Sorbent

data obtained with Linde 13X sorbent. This figure contains coadsorption data at different water vapor preloads of 0, 2.07, 3.99, 5.9, 11.9, and 17.0 percent for the 70 or 72°F temperatures.

Figure 3-26 presents a family of isotherms at approximately the same water vapor preload for the Linde 13X sorbent. The water vapor preload is approximately 6 percent and the isotherms are 32°, 72°, 120°, 200°F, and a single point at 300°F.

It appears that even though the Linde 5A sorbent has a greater CO_2 capacity than 13X, with no water vapor present the converse is true when a water vapor preload is incorporated.

Coadsorption of Nitrogen With Carbon Dioxide Preload

Figure 3-27 and 3-28 present the test data for the Linde 5A and 13X sorbent, respectively, when subjected to nitrogen gas after preloading with carbon dioxide. Isotherms at 70°F was taken at different CO_2 preloadings. The 13X data taken was not acceptably repeatable, however the basic curves and the re-runs are presented.

For the Linde 5A sorbent, with a 3 percent CO_2 preload, the nitrogen adsorption was slightly higher than that obtained without a preload. The tests results indicate that the reduction in nitrogen adsorption is negligible up to 3 percent CO_2 preload. Above 3 percent CO_2 preload, negligible adsorption occurs until the nitrogen partial pressure exceeds 100 mm Hg.

In previous tests, the introduction of CO_2 to a water preload molecular sieve caused the weight to continuously increase until an equilibrium weight was achieved. In these tests, the introduction of nitrogen on a CO_2 preload sieve caused the weight to quickly increase above the final equilibrium value and then slowly decrease to the ultimate value. The initial increase was greater than that observed for pure nitrogen adsorption on the sorbent. This initial increase is due to local increase in CO_2 partial pressure in the vicinity of the sorbent, due to the imperfect mixing of the two gases as the nitrogen is introduced. Since the partial pressure of CO_2 for these tests is several mm of Hg, the rate of adsorption is quite high, and the initial additional CO_2 adsorption is greater than the final nitrogen adsorption. The weight indication drops slowly as the gases mix and finally reach an equilibrium value.

Coadsorption of Oxygen With Water Vapor Preload

Figure 3-29 presents the data obtained for Linde 5A molecular sieve preload with water and subjected to oxygen at various pressures. A family of 70°F isotherms presented at various water vapor preloads, 0, 3.1, 5, and 8 percent.

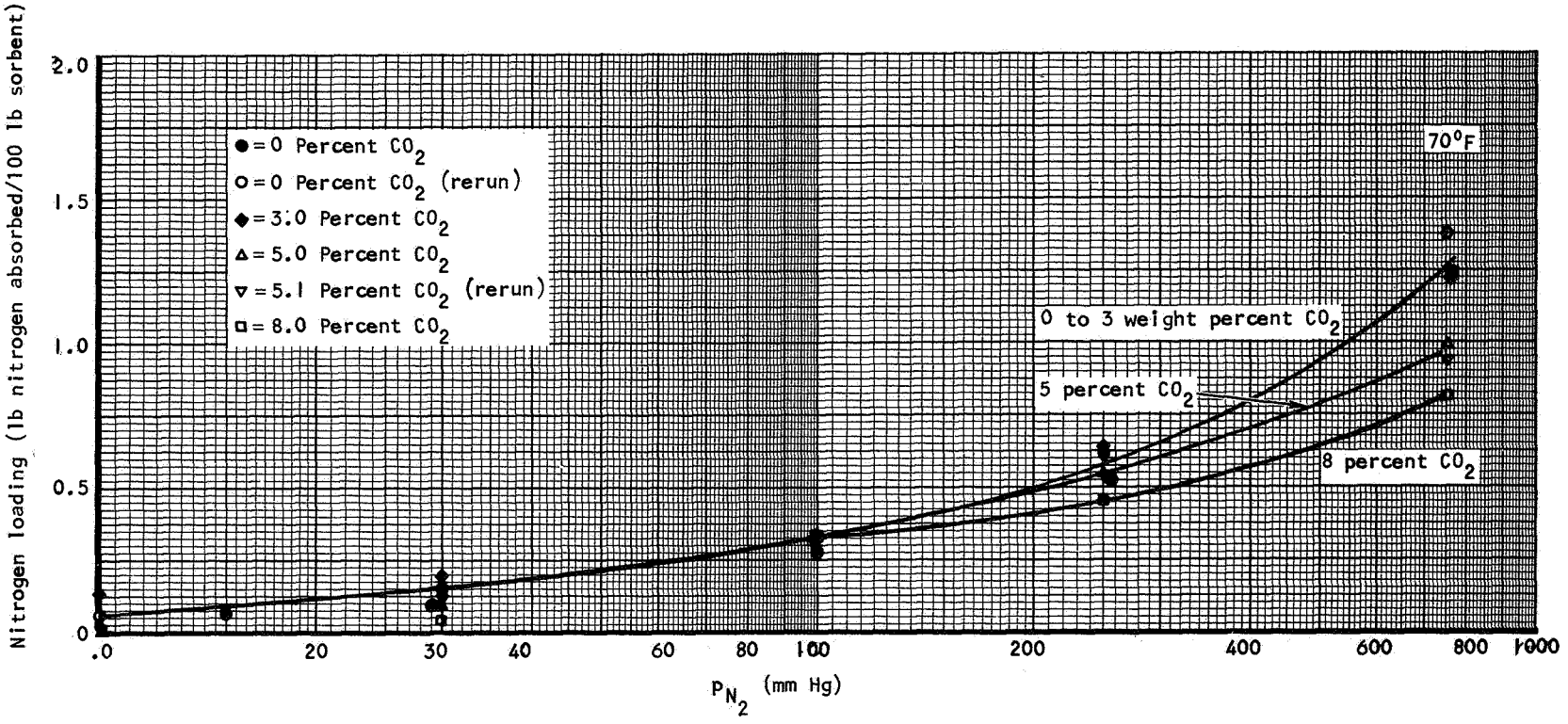

Figure 3-27. Coadsorption Equilibrium Data for Carbon Dioxide and Nitrogen on Linde 5A Sorbent

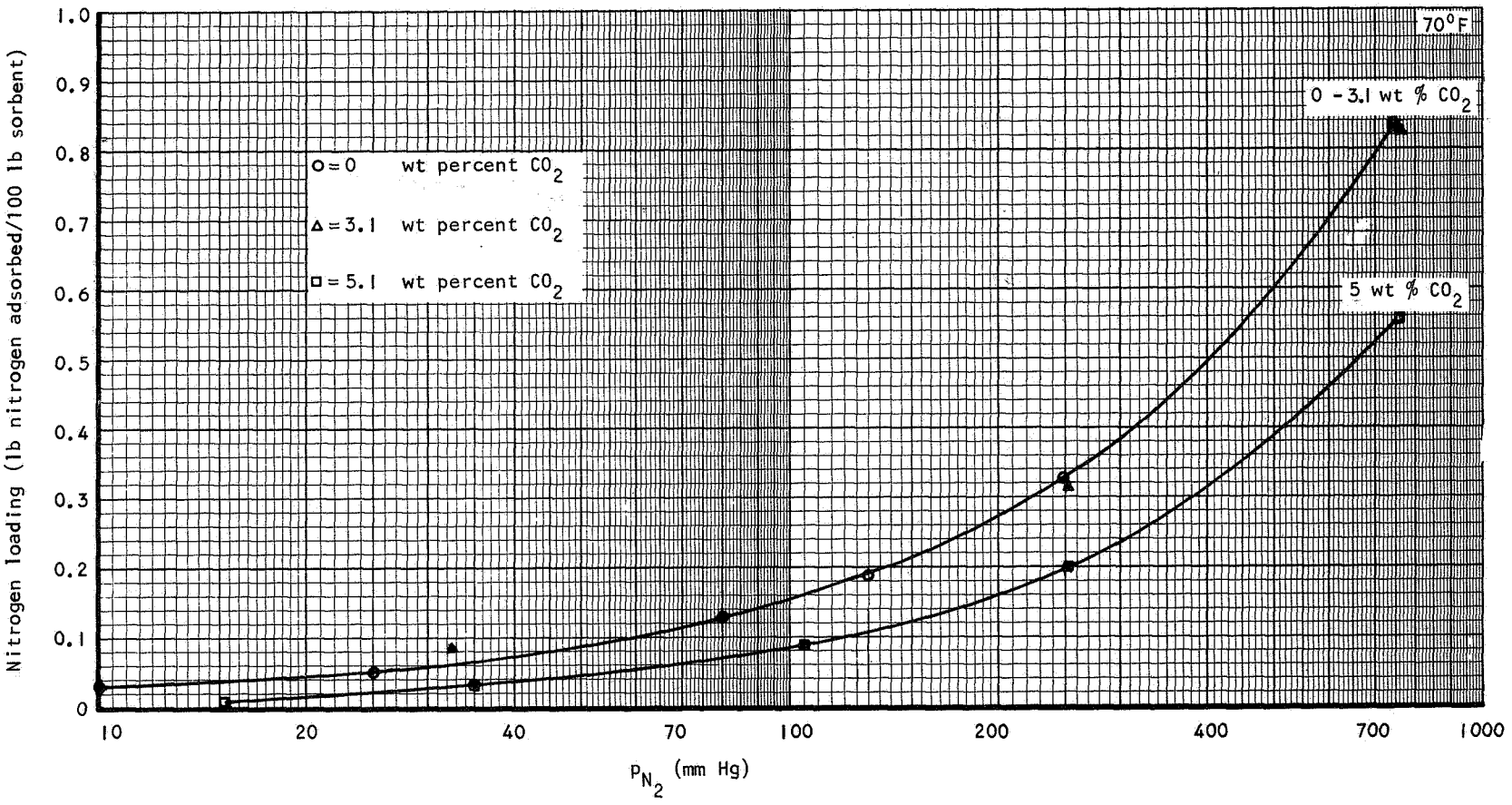

Figure 3-28. Coadsorption Equilibrium Data for Carbon Dioxide and Nitrogen on Linde 13X Sorbent

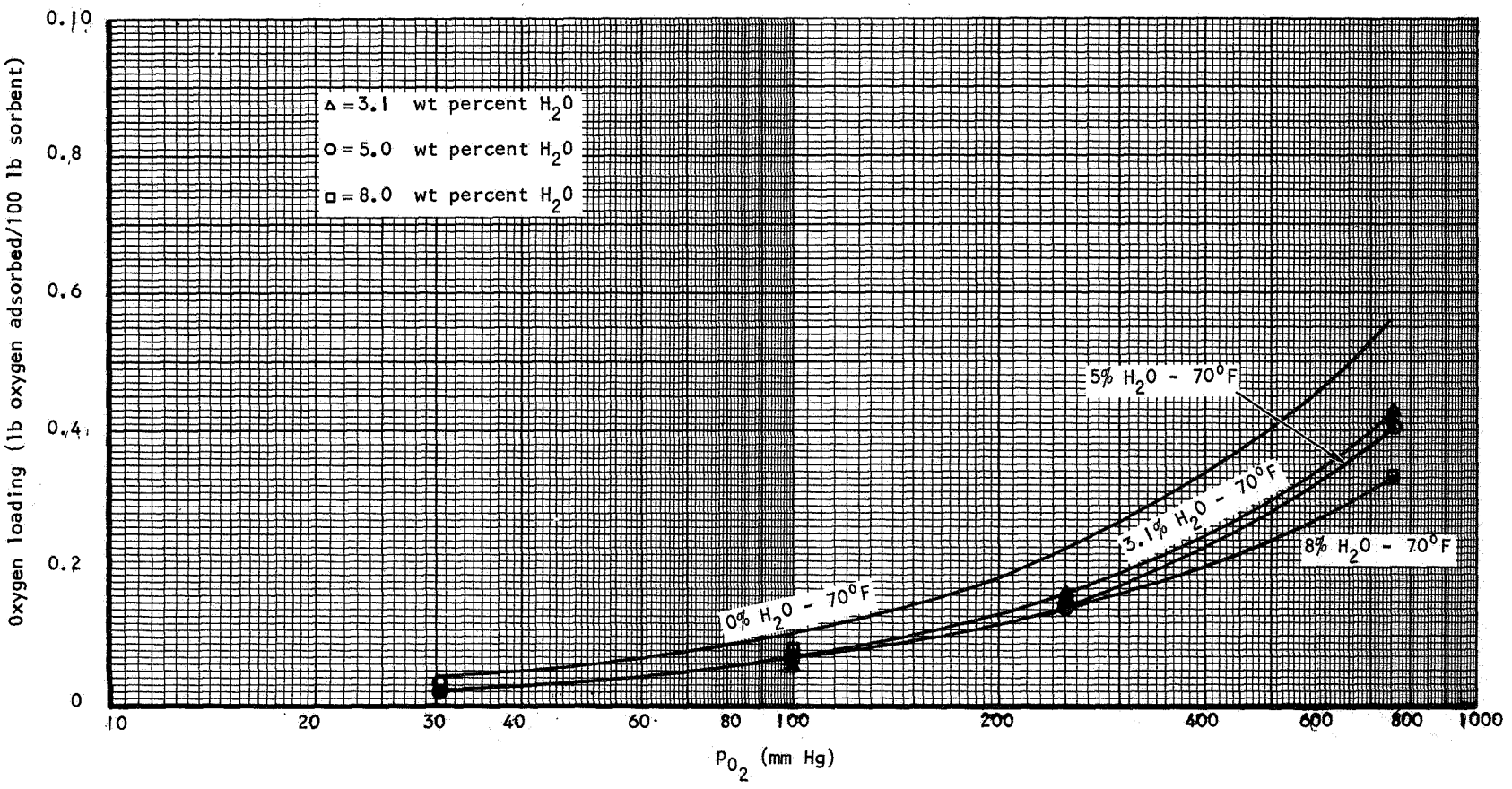

Figure 3-29. Coadsorption Equilibrium Data for Water Vapor and Oxygen on Linde 5A Sorbent

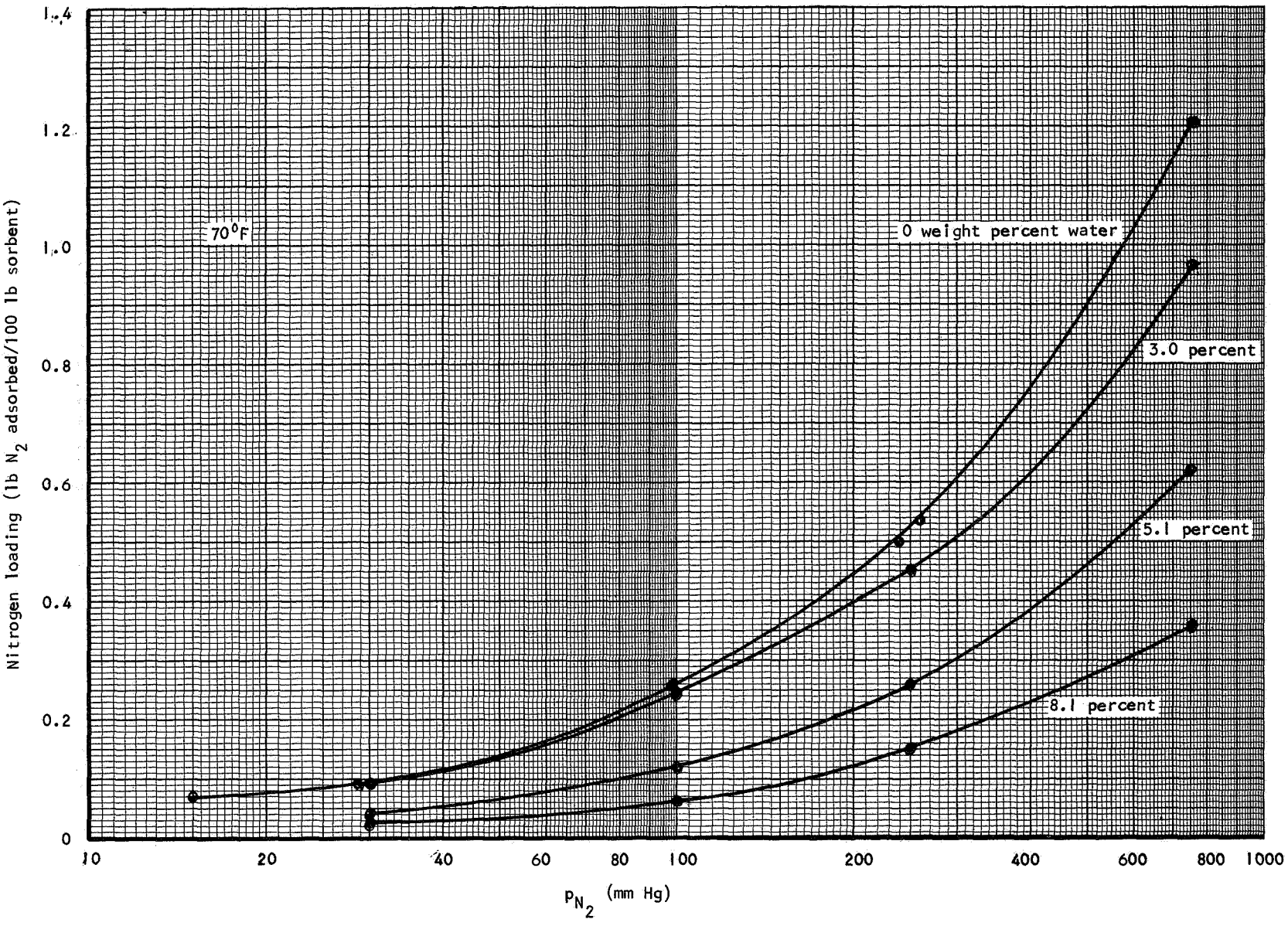

Figure 3-30. Coadsorption Equilibrium Data for Water Vapor and Nitrogen on Linde 5A Sorbent

Coadsorption of Nitrogen With Water Vapor Preload

Figure 3-30 presents the data obtained on the Linde 5A molecular sieve preload with water vapor and subjected to nitrogen at various pressures. A family of 70°F isotherms are presented at various water vapor preloads, 0, 3, 5.1, and 8.1 percent.

HEAT OF ADSORPTION

The adsorption of gases on solids is accomplished with the evolution of heat, which varies with the quantity of gas adsorbed, the characteristics of the solid, and the adsorption temperature. The heat given off is called the heat of adsorption. This heat varies with the amount of material adsorbed; when evaluated for an infinitesimally small sorbent loading change, it is called the differential heat of adsoprtion. As a lower limit, as the amount of gas adsorbed increases the differential heat of adsorption approaches the heat of liquefaction. Differential heats of adsorption can be calculated from the Clausius-Clapeyron equation. Usually this involves obtaining isotherms (equilibrium pressure versus temperature for constant adsorption weight loadings) by plotting the natural logarithm of the pressure against the reciprocal of the sorbent temperature. The slope of the isotherms is the heat of adsorption divided by the universal gas constant.

Figure 3-31 represents several isotherms plotted on semi-log coordinates for CO_2 on Linde 13X sieve (the data for this plot are from Figure 3-8). The differential heats of adsorption obtained by this procedure are plotted in Figure 3-32. It should be noted that at zero loading the maximum exothermic energy release occurs and as adsorption takes place the energy decreases. The equation used for this calculation is obtained from the Clausius-Clapeyron equation:

$$\Delta H = \ln \frac{P_2}{P_1} \left(\frac{R}{W}\right) \frac{1}{\frac{1}{T_2} - \frac{1}{T_1}}$$

where ΔH = differential heat of adsorption, Btu/lb

P_1 = equilibrium pressure at specific weight loading for low temperature isotherm, mm Hg

P_2 = equilibrium pressure at specific weight loading for high temperature isotherm, mm Hg

R = Universal gas constant, 1.987 Btu/lb-mole x °R

W = Molecular weight

T_1 = Temperature at P_1, °R

T_2 = Temperature at P_2, °R

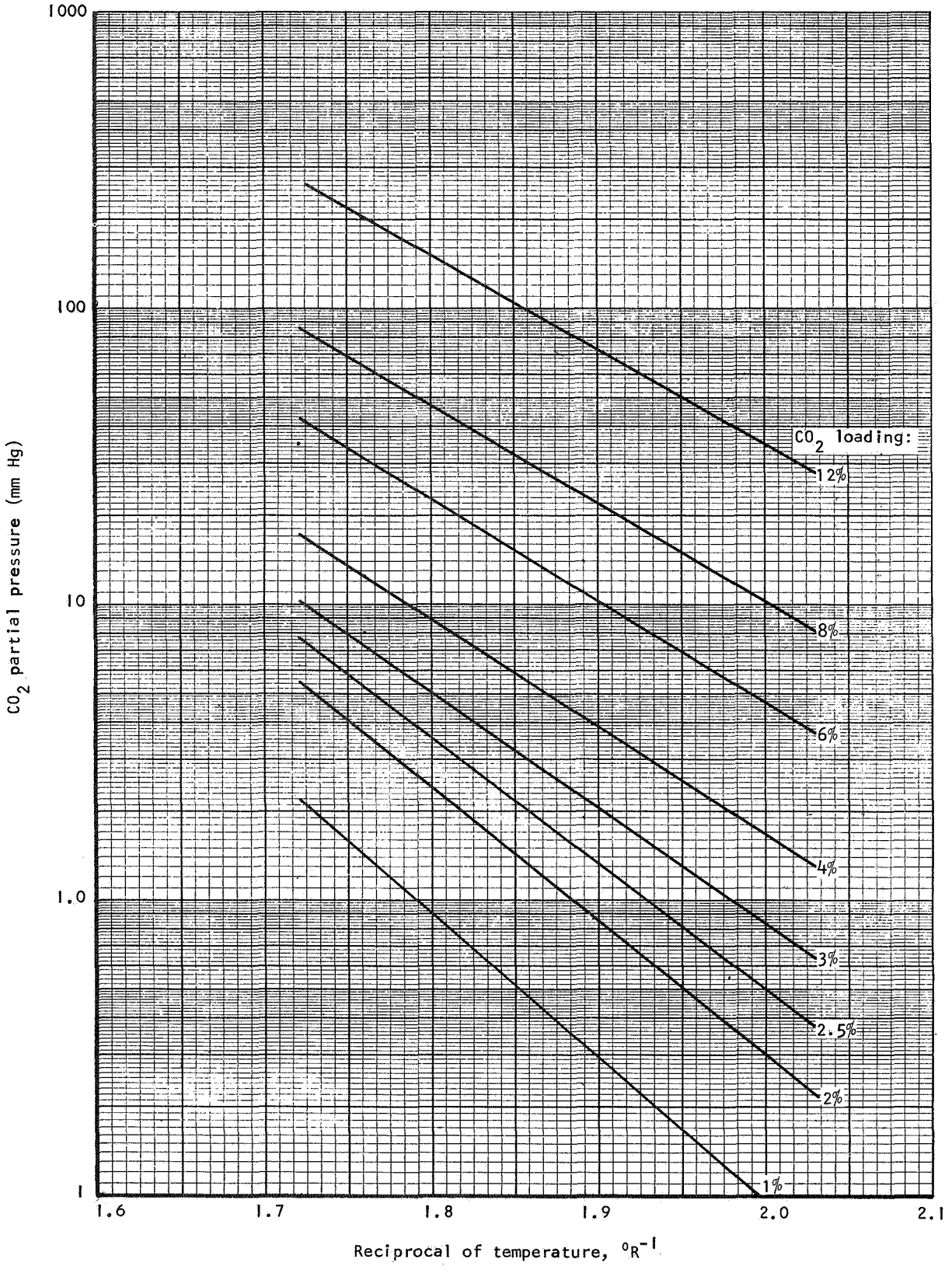

Figure 3-31. Determination of Differential Heat of Adsorption for CO_2 on Linde 13X

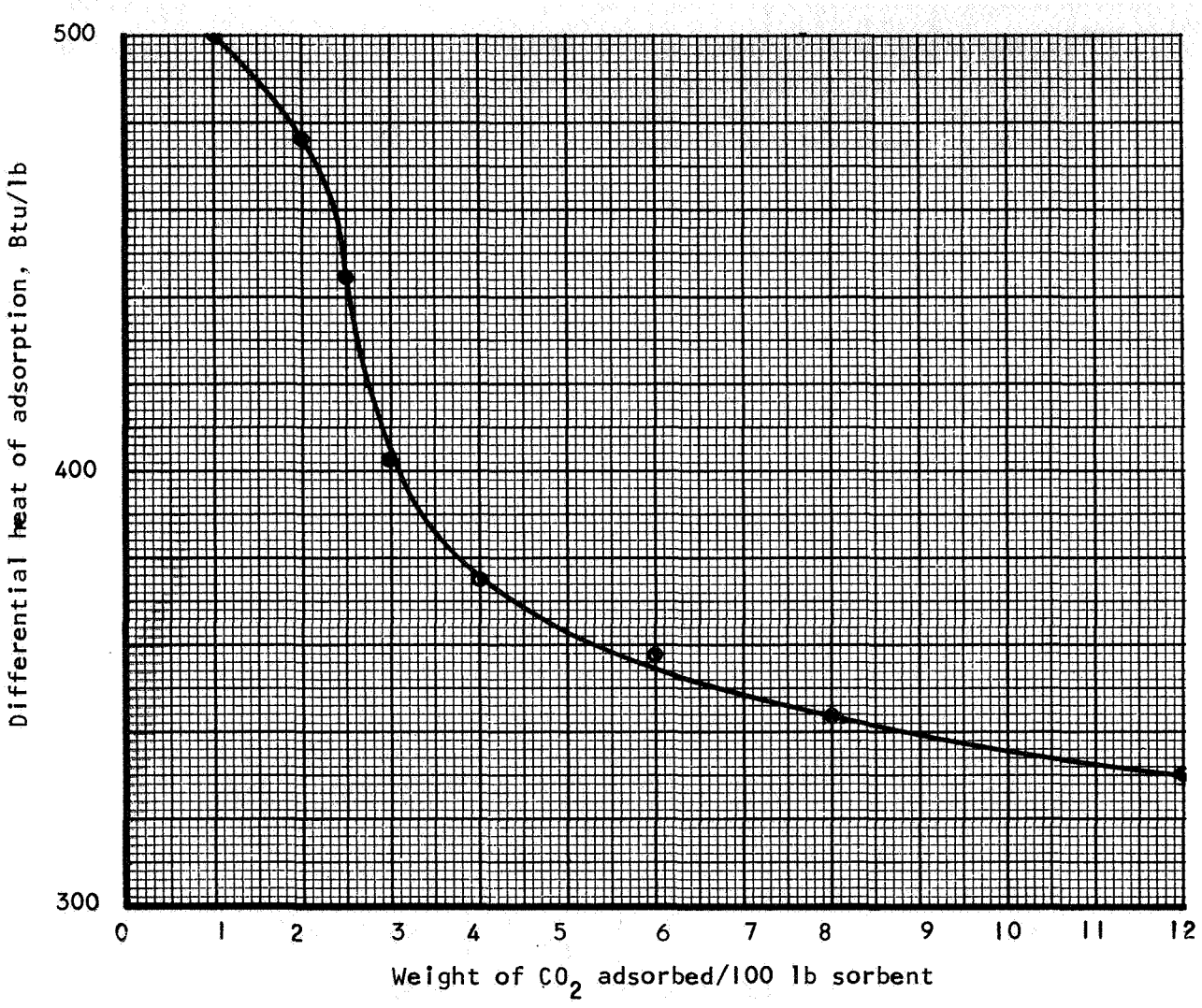

Figure 3-32. Differential Heat of Adsorption for Carbon Dioxide on Linde 13X Sorbent as a Function of Loading

Table 3-4 presents some typical heat adsorption values calculated at nominal loadings of the sieve. The expanded data points shown for CO_2 at various loadings indicate the physical trend of the heat of adsorption. Where only two isotherms are available calculations were made because the slope's could not be sufficiently guarenteed.

TABLE 3-4

DIFFERENTIAL HEATS OF ADSORPTION

Gas	Molecular Sieve Type	Weight Loading, %	Differential Heat of Adsorption, Btu/lb
CO_2	LI3X	1	500
		2	476
		2.5	445
		3	403
		4	375
		6	358
		8	344
		12	330
CO_2	L5A	4	416
H_2O	LI3X	10	1111
O_2	LI3X	.1	245

SECTION 4

SINGLE-SORBATE DYNAMIC MASS-TRANSFER DATA

OBJECTIVES AND SCOPE

The general objective of the single-sorbate dynamic mass-transfer test series was to produce information that would allow a better understanding and characterization of molecular-sieve sorbents under dynamic sorption conditions typical of spacecraft systems. The method used to produce this information was to conduct single-sorbate breakthrough runs under controlled, constant conditions. Such testing is a standard tool in evaluating the performance of packed beds. The testing is carried out in two steps. The first step is the establishment of initial bed conditions of temperature and sorbent loading which are uniform and can be accurately determined numerically. For example, the usual bed conditioning prior to an adsorption run is a vacuum bakeout to remove all traces of sorbates, followed by cooling to the desired adsorption temperature. In the second step, a gas stream containing the sorbate of interest is passed through the bed until the bed has adsorbed as much of the sorbate as is possible under the test conditions; that is, until the bed is saturated or equilibrated. During the transient sorption period, all inlet and boundary conditions (flow rate, pressure levels, inlet concentrations, bed temperature) are held constant and all parameters are monitored, especially inlet and outlet sorbate concentrations.

Several specific objectives and goals were defined for the breakthrough tests:

- The most important goal was the evaluation of mass-transfer coefficients and intraparticle diffusivities for various representative operating conditions. These basic parameters were obtained from the breakthrough data with the help of the performance-prediction programs. With this data properly correlated, the programs can be used with confidence for a wide variety of bed geometries and process conditions.

- Qualitatively, from the shape of the plotted breakthrough curve (the outlet concentration plotted vs time), it was desired to compare the performance of various sorbents under similar operating conditions, and to compare the performance of a single sorbent under various adsorption conditions.

- Also in a qualitative sense, it was desired to compare the thermal performance of the different heat-transfer surfaces which were incorporated into the test beds. This was to be accomplished by observing the ability of the heat-transfer surfaces to maintain an isothermal bed during the exothermic adsorption period.

- By integration techniques to yield the amount of sorbate left on the bed, an equilibrium datum point, corresponding to the final bed temperature and inlet partial pressure, can be obtained. This was desired as a check on the data produced from the equilibrium testing, or obtained from the literature.

- From the breakthrough data, removal efficiency of the sorbent bed (cumulative fraction of entering sorbate which is retained by the bed) as a function of time can be obtained. This is desired to properly size spacecraft beds and to set cycle times.

Table 4-1 presents the sorbent/sorbate combinations for which dynamic adsorption breakthrough tests were made. For the potential predrier-bed sorbents, Linde 13X and silica gel, both adsorption breakthrough tests and gas strips were performed. Table 4-2 presents conditions and ranges for which breakthrough tests were performed. Dry nitrogen was used as the carrier gas in all dynamic tests. Obviously, tests could not be run for all possible test conditions; however, it is believed that sufficient ranges were included to identify trends and to permit mass-transfer parameter evaluations.

TABLE 4-1

SORBENT/SORBATE COMBINATIONS USED IN SINGLE-SORBATE DYNAMIC MASS-TRANSFER TESTS

Sorbent Type	Sorbent Manufacturer	Form and Size	Sorbate in Nitrogen Carrier Gas
Silica gel (Grade 05)	Davison	Granules, 6 to 16 mesh	Water
13X	Linde	Pellets, 1/16-inch	Water CO_2
5A	Linde	Pellets, 1/16-inch	CO_2
5A	Davison	Spherical beads, 8 to 12 mesh	CO_2

TABLE 4-2

CONDITIONS FOR WHICH SINGLE/SORBATE BREAKTHROUGH TESTS WERE PERFORMED

Sorbate	Inlet Partial Pressure (and Dew Point)	Total Pressure	Inlet Concentration	Bed Temperature	Flowrate
Water	9.2 mm Hg (50°F dew point)	5 psia (258 mm Hg) for silica gel 7 psia (363 mm Hg)	0.024 gm water/ gm N_2 0.018 gm water/ gm N_2	60°F 70°F 90°F 120°F	1.3 to 5.4 lb/hr
CO_2	7 mm Hg 1.75 mm Hg	7 psia (363 mm Hg)	0.031 gm CO_2/ gm N_2 (1.9 vol % CO_2) 0.0075 gm CO_2/ gm N_2 (0.45 vol % CO_2)	50°F 70°F	1.3 to 5.4 lb/hr

EQUIPMENT AND PROCEDURES

Bed Designs and Heat-Transfer Surfaces

One of the objectives of this program has been to compare the effectiveness of various size heat-transfer surfaces placed within packed sorbent beds. This information is desired for those cases where bed cooling and heating is to be provided by the spacecraft heat-transport system. It is not obvious what type of surface will produce the optimum bed performance, due to a number of counteracting effects. For example, from only a heat-transfer point of view, it is desired to produce as nearly isothermal a bed as possible; thus, small, close-packed heat-transfer surfaces would be desired. However, with very dense heat-transfer matrices, a great deal of "wall effect" is to be expected. The wall effect is due to the fact that sorbent pellets do not pack closely in the region of the walls created by the plethora of fin surfaces. This results in lower overall packing density (greater void fraction in the wall region), and lesser contact between gas and sorbent, often described by the names "channelling", "bypassing", or "fingering".

Prior to this contract, AiResearch had developed a number of research and development sorbent systems which involved high-density heat-transfer surfaces placed within packed beds. Basically, these beds were cross-flow plate-fin heat exchangers, with sorbent material packed into one set of

passages. Most of the previous experience was with rectangular straight fins, 1/4 in. in height and spaced 1/4 in. apart. The results of tests with such heat-transfer surfaces showed less-than-desired packed bed densities, and a tendency of premature breakthrough due to channeling. For this contract, three specially designed beds were fabricated, each with a different size rectangular, offset plate-fin surface. The sizes were 1/4 in., 1/2 in., and 1 in. In any bed, the fin height and spacing were the same. In addition, for these special beds the fin surfaces were all offset (or interrupted) in the flow direction by a dimension equal to the fin height. Thus, in the 1/2-in.-fin bed, the continuous fin length in the flow direction is only 1/2 in. At this point, the downstream fins are placed midway between the previous fin positions. Figure 4-1 gives a comparison of plain and offset rectangular fin surfaces. The fins are shown in their original form, before stacking into a heat-exchanger configuration and brazing. The offset fin was adopted because of the expectation of reduced wall effects (channeling) afforded by the interruptions of the fins. No effect on packed-bed density was expected.

Figure 4-2 is an outline drawing typical of the beds used in this program. Figure 4-3 is a photograph of the 1/2-in.-fin bed. To promote uniform distribution of coolant in the liquid passages of the beds, the fin surfaces were turned sideways to the normal flow direction. This forces the coolant to flow in and out around the fins. This coolant fin arrangement is shown in Figure 4-2.

A few points should be noted concerning the choice of plate-fin surfaces for use in sorbent beds when bed cooling and heating are desired. First, the manufacturing technology for the plate-fin heat-exchanger sorbent beds is well developed, and is essentially qualified for use in space. Such sorbent bed designs are only slightly different from many heat exchangers used in Mercury, Gemini, and Apollo environmental control systems. Second, as in many heat-exchanger applications, plate-fin designs offer tremendous flexibility in tailoring the ratio of heat-transfer surface area on one side to that on the other side. With heat exchangers, optimum designs are usually characterized by having the product, hA, of heat-transfer coefficient and area on one side approximately equal to that on the other side. With a fluid stream, such as a low-velocity gas, where low heat-transfer coefficients are developed, it is easily possible to provide considerably more plate-fin surface area for the gas and to tailor the ratio of areas so that the hA products of the exchanger are nearly equal. With packed sorbent beds, since the sorbents are very poor conductors of heat, it is almost mandatory to provide much more heat-transfer area on the gas/sorbent side than on the coolant side. With plate-fin designs, it is quite easy to accomplish this, no matter what the desired bed area and length values may be. In addition, the plate-fin concept provides both very low coolant-side pressure drop (when desired), and very low liquid holdup within the bed. Further, the large amount of surface area can be incorporated uniformly throughout the packed sorbent particles, and the presence of these surfaces has very little effect on the gas-side pressure drop. Other means of providing bed cooling, such as cooling coils with external fins, cannot compete with plate-fin surfaces in the several areas of concern as discussed above. For small beds like those for spacecraft applications, the additional cost of plate-fin sorbent beds is far outweighed by their many advantages.

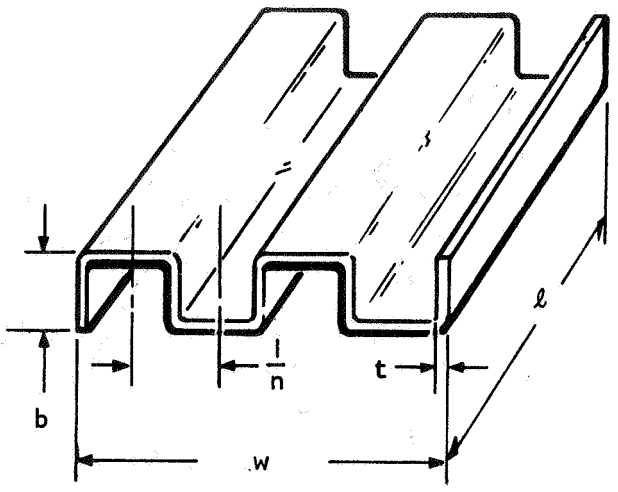

a. Plain Or Straight Rectangular Plate-Fin Surface

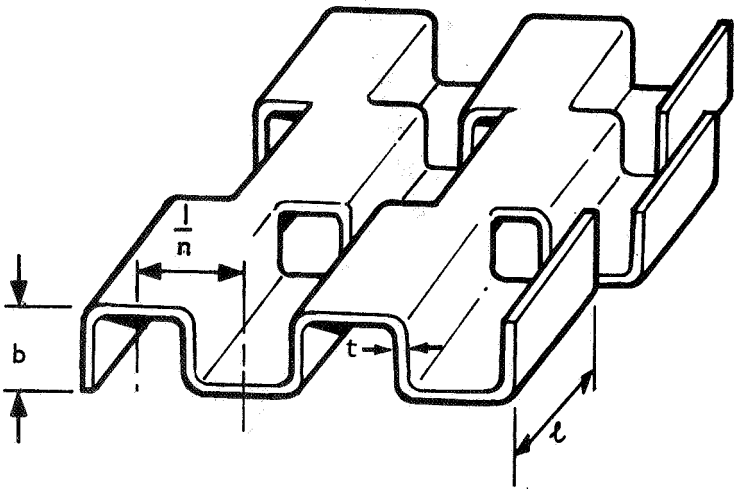

b. Rectangular Offset Plate-Fin Surface As Used In Test Beds

S-41922 -A

Figure 4-1. Rectangular Plate-Fin Heat-Transfer Surfaces for Packed Beds

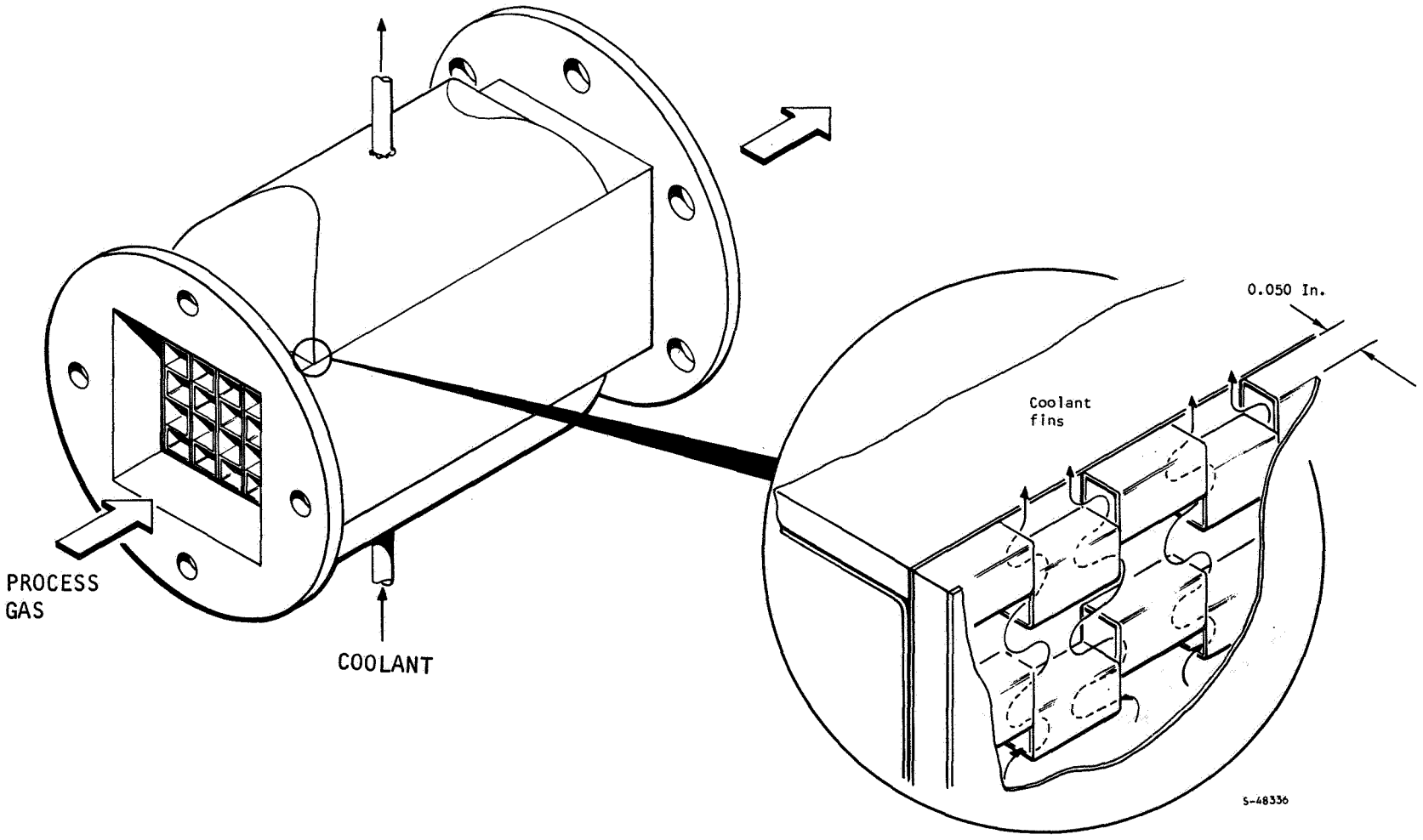

Figure 4-2. Test Bed for Dynamic Adsorption Tests

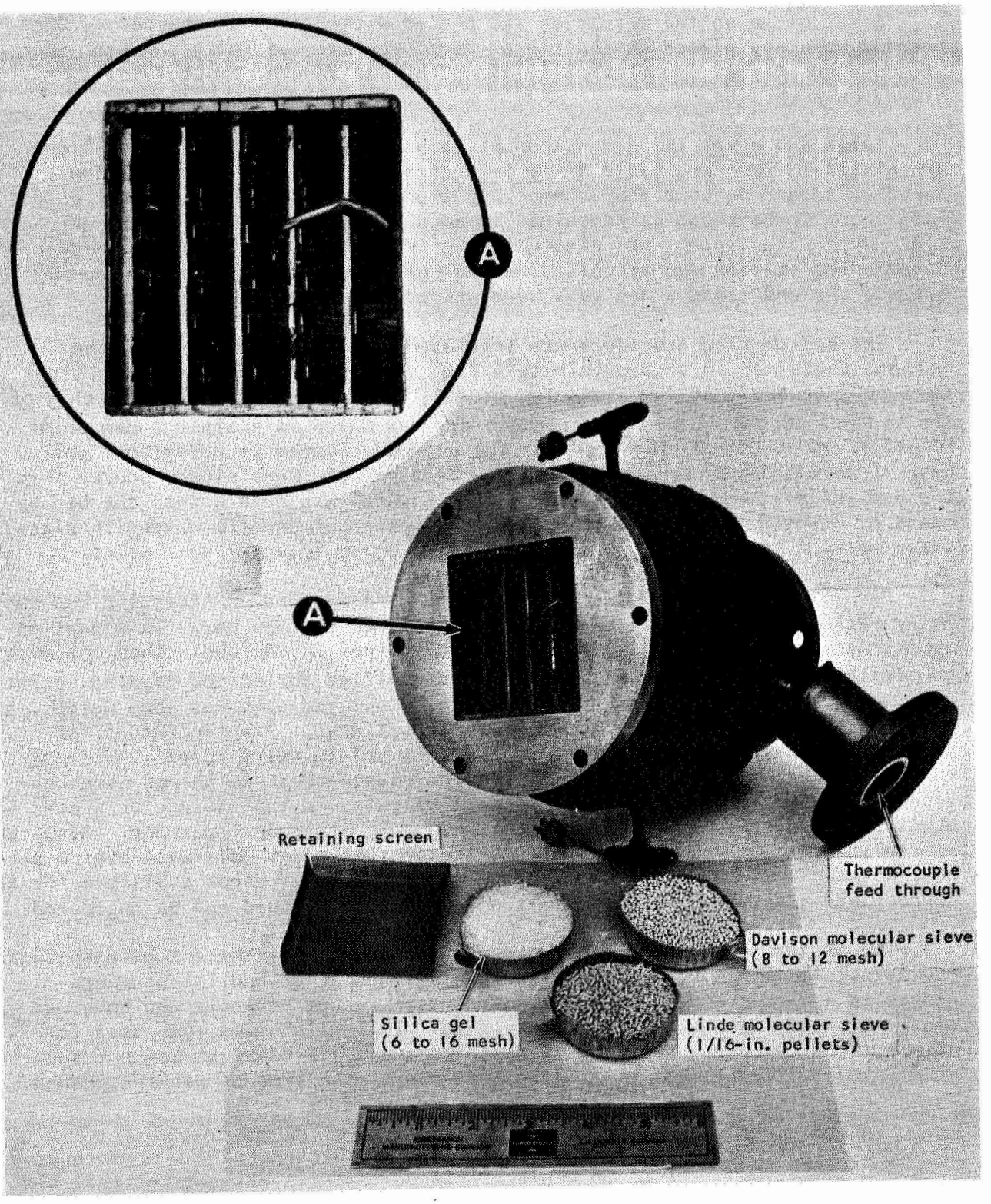

Figure 4-3. 1/2-in.-Fin Adsorption Bed

A set of seven thermocouples was placed within each of the beds. One thermocouple was placed on the fin surface near the bed inlet and the other six were positioned longitudinally along the bed length, about 1 in. apart, midway between fins.

Table 4-3 gives the dimensions of each bed and pertinent physical characteristics. Each bed had a 3- by 3-in. frontal face with a 6-in. flow length. Depending upon the sorbent and the method of packing, from 1.0 to 1.25 lb of sorbent can be contained by each bed. Except for the packed-bed fins, which are copper, and the coolant fins, which are nickel, the beds are constructed of stainless steel. The bed heat exchanger core was vacuum brazed; the end flanges and pans were welded to the core.

The bed packing procedure was initiated by a vacuum-bakeout of the sorbent contained in an approximately 2-qt sample bomb. Bakeout conditions were 500° to 600°F at low pressure, usually approaching 10 μ Hg. Packing of the bed was accomplished in a nitrogen dry box which maintained a dew point of -40°F or lower. During packing, the bed was clamped in a vertical position to an electric vibrator table. Sorbent pellets were slowly poured into the bed while it was being vibrated. The sorbent was held within the bed by means of 24-mesh screens. The bottom screen was permanently welded in place; after packing, the top screen was secured in place by small tack welds.

Prior to packing, the bed and the bomb were weighed. After the bed was fully packed, it was again weighed while still in the dry box. This gave an approximation of the mass of dry sorbent contained in the bed. Then, as much as possible of the excess sorbent which was spilled during the packing operation was swept up and placed back in the sample bomb. The bomb was then weighed to obtain another approximation of the dry sorbent mass. The two values for bed mass were usually in close agreement, but not in every case. The reason for the deviation between readings, and the reason these weighings were considered to yield only approximate sorbate weights, is that molecular sieves have equilibrium capacities for nitrogen at 760 mm Hg of about 1 percent. Also, even at the dry box humidity conditions, molecular sieves can hold well over 6 percent water. It is doubtful that there was enough water vapor available for any appreciable adsorption; however, nitrogen adsorption could not be neglected.

The packed bed mass was more accurately measured at the end of a sequence of tests. At that time, the bed was carefully unpacked and its contents placed in a sample bomb. After a considerable vacuum bakeout, the bomb was closed off and, after cooling, was weighed. This weight was then used to obtain the dry sorbent weight. In most instances, this weight was not substantially different from the values obtained at the time of packing. When there was a difference, the latter weight was used.

During the program in some cases where a bed was packed two or more times with the same type of Linde molecular-sieve pellets, it was noticed that bed weights could be substantially different. It is considered that the primary reason for the differences lies in the method of packing. During packing, moderate vibration of the bed was employed. High levels of vibration were

TABLE 4-3

TEST BED DIMENSIONS

Physical Item	Nominal Packed-Bed Fin Height, (in.) Bed Designation		
	1	1/2	1/4
PACKED-BED/GAS SIDE:			
Bed width (in.)	3.00	2.98	3.00
Bed height (in.)	3.25	2.93	2.95
Bed length (in.)	6.10	6.02	6.02
Number of passages	3	5	5
Number of sandwiches per passage	1	1	2
Fin thickness (in.)	0.008	0.008	0.008
Fins per in. ($in.^{-1}$)	1	2	4
Splitter thickness (in.)	--	--	0.010
Plate thickness (in.)	0.010	0.010	0.010
Fin cross-section area to gas ($in.^2$)	0.155	0.237	0.382
Coolant passage cross-section area to gas ($in.^2$)	0.780	1.192	1.200
Free flow area ($in.^2$)	8.82	7.29	7.27
Plate area ($in.^2$)	145.5	207.8	205.5
Fin area ($in.^2$)	89.6	176.8	524.5
Total heat-transfer area ($in.^2$)	235.1	384.6	730.0
Plate volume ($in.^3$)	5.67	5.59	5.64
Fin volume ($in.^3$)	0.95	1.43	2.30
Free bed volume ($in.^3$)	53.95	43.66	43.75
COOLANT SIDE:			
Passage width (in.)	5.80	5.80	5.80
Passage length (in.)	3.25	3.25	3.25
Number of passages	4	6	6
Fin height (in.)	0.050	0.050	0.050
Fins per in. ($in.^{-1}$)	20	20	20
Fin thickness (in.)	0.002	0.002	0.002
Plate area ($in.^2$)	144.8	217.2	217.2
Fin area ($in.^2$)	144.8	217.2	217.2
Total heat transfer area ($in.^2$)	289.6	434.4	434.4
Coolant volume ($in.^3$)	3.47	5.21	5.21

avoided as this tended to eject a large fraction of the sorbent bellets that were being poured onto the face of the bed. As the program continued, it was found that after the initial filling, some additional settling could be accomplished by a sustained vibration at very high levels and more sorbent could be added. Thus, later packings tended to yield higher bed weights.

There are other factors involved in the final bed weight. The length of the Linde pellets is of importance. Some batches of material seemed to have larger amounts of fairly long pellets (about 1/4 in.). It is suspected that these longer pellets do not pack as well as shorter pellets; at least not without considerable vibration. There can also be variation in the density of the basic material produced by the manufacturer.

Packed bed density is discussed separately in Section 8. Packed densities of the test beds are presented, along with densities obtained in special containers constructed to determine the effect of fin size on packing density.

Dynamic Mass-Transfer Apparatus

Figure 4-4 is a simplified schematic of the dynamic mass-transfer apparatus. Figure 4-5 is a photograph of the test equipment. The heart of the apparatus, the dynamic test bed, is located in the lower left side of the photograph of Figure 4-5. The apparatus was so constructed as to allow flow in either direction through the bed, and also to be able to vacuum desorb from either or both ends of the bed. Consequently, there are dual sets of inlet and outlet valves on both sides of the bed. The two large vacuum gate valves flanking the bed are clearly visible in the photograph. Three valves are attached to the inlet manifold above the bed. Two of the valves are used to direct flow to the desired inlet of the bed. The other valve, mounted between the inlet valves, is a bypass valve. The back-pressure valves on the bed exits, and their connections to the large vacuum duct, are obscured in the photograph.

Referring to the simplified schematic of Figure 4-4, the flow path in the apparatus is as follows. First, laboratory dry nitrogen, derived from large-scale cryogenic storage (<-80^{0}F dew point), passes through a pressure regulator. This regulator outlet is maintained at 20 psia. The flow is directed through a bank of rotameters, each being calibrated at 20 psia. To introduce water vapor into the stream, all or a portion of the nitrogen flow can be directed through a water-filled bubbler. To enhance the humidification process, the bubbler is contained in a hot water bath. Next, the humidified nitrogen steam is directed to a condenser. In some of the experiments, the condenser was used to adjust the dew point of the gas stream. In other cases, the condenser was dormant.

The gas emerging from the humidity-control condenser enters the bed inlet manifold, where flow can be diverted around the bed directly through a back-pressure valve to the vacuum system. This was the case while experimental conditions were being established. For adsorption tests, the flow is directed through the bed, then through a back-pressure valve to the vacuum

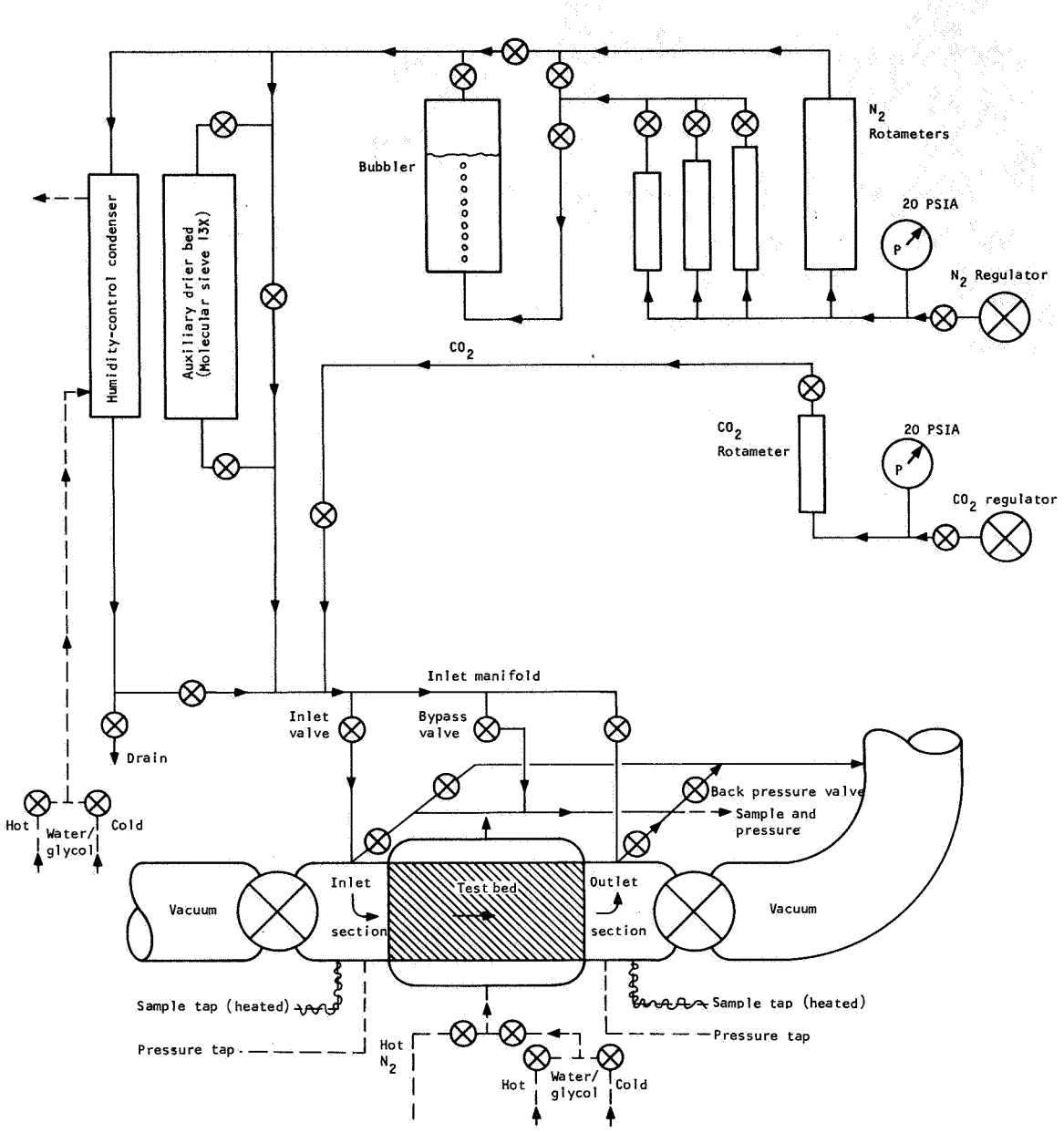

Figure 4-4. Schematic of Dynamic Mass-Transfer Apparatus

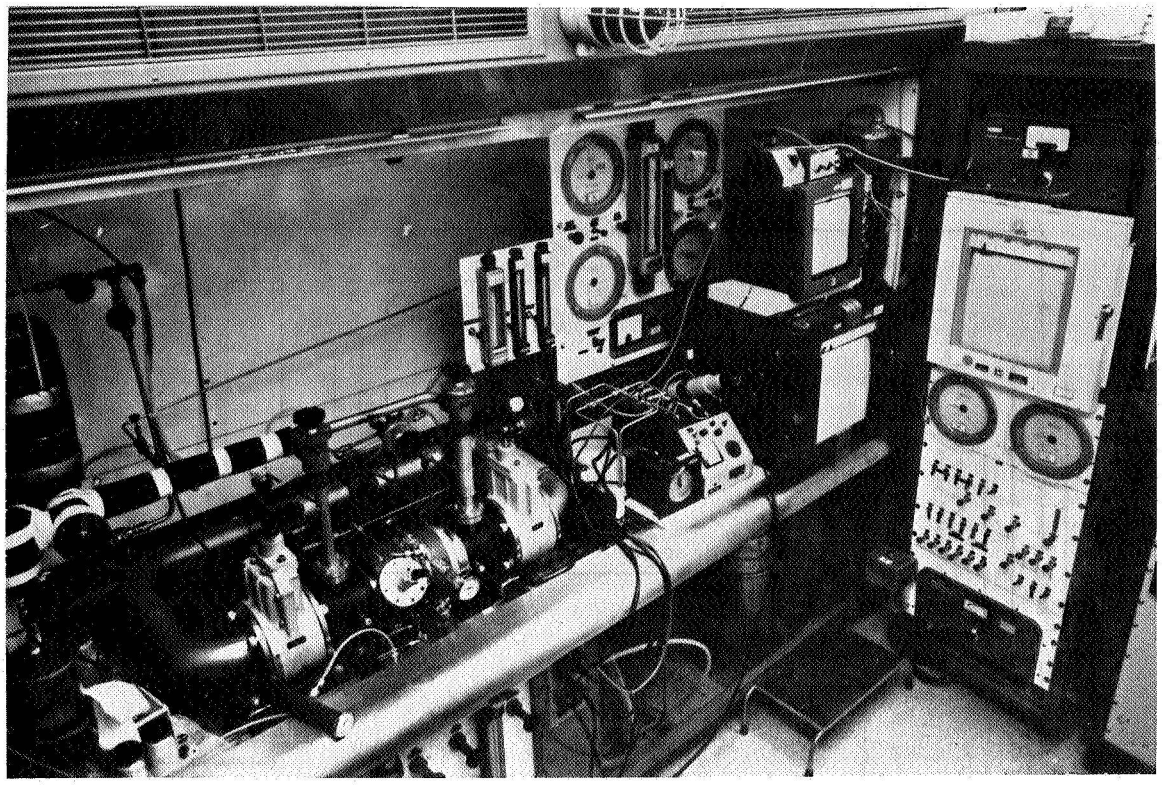

Figure 4-5. Dynamic Mass-Transfer Apparatus

system. Vacuum is provided by two large pumps. One pump is used when high flow rates and moderate vacuums are required, as in adsorption runs. The other vacuum pump is used when very low pressures are desired; for example, during vacuum bakeouts.

Thermal control of the bed and of the humidity-control condenser is provided by a heat-transport circuit using 62.5-percent ethylene-glycol/water mixture. The water-glycol emerging from the reservoir-pump system is split into two separate streams. One stream is directed through temperature-controlled electric heaters. The other stream is cooled by a Freon refrigeration system. By selective mixing of these streams at the bed, and also at the condenser, the desired temperatures can be obtained. Thus, a bed can be heated to 120°F for an adsorption run, while the condenser can be held at 50°F for humidity control. The water-glycol system is capable of temperatures from 20°F up to approximately 200°F. Water-glycol effluents from the bed and the condenser are returned to the pump reservoir.

Above 200°F, bed heating can be accomplished by use of an open-loop nitrogen heating circuit. Separate electric heaters were installed for this purpose. To use the nitrogen heating circuit, the bed is first drained of water-glycol and then isolated from the liquid circuit. By use of appropriate valving and lines, the hot nitrogen can be directed into the heat-transfer passages of the bed. This system was actually used in only a few adsorption runs. Its main use is for vacuum bakeouts of the bed. In these instances, the nitrogen is heated to approximately 500°F. For bakeouts, both of the large gate valves are opened to the vacuum system.

The source for carbon dioxide used in the experiments is a high pressure bottle of very dry CO_2 gas. Through a dual stage regulator, CO_2 is supplied to a precision rotameter operating at 20 psia. CO_2 flow rate is controlled by a valve downstream of this rotameter. The CO_2 is mixed into the main nitrogen stream downstream of the humidity-control condenser.

Humidification is provided by the heated bubbler. Two methods of humidity control are available. One of these methods has already been mentioned: the condensation of excess moisture in the humidity-control condenser. As experience was gained with the test apparatus, it was found that the inlet dew point was sometimes hard to control in this manner. This is because the condenser and the bed both use the same hot and cold water-glycol streams. During the period of time when the adsorption rate in the bed was nearly constant, conditions could be maintained fairly steadily. However, as the desorption process subsided, the water-glycol stream returning to the reservoir from the bed became cooler and cooler. This had the effect of gradually cooling the water-glycol flow to the condenser. Without continual adjustment, bed inlet dew point tended to decline. In addition, over humidification at the bubbler caused the rate of extraction of water from it to be relatively large, requiring frequent adjustments to the water level.

A second more stable method of humidification was devised. In this method, the flow rate of gas flowing to the bubbler is carefully controlled so that precisely the desired amount of humidification will be obtained at the bubbler. The condenser is isolated from the coolant system. In this method, the means of humidity control is independent of the bed coolant system and does not drift with the adsorption rate. The bubbler water level is also easier to control. For low levels of the humidification, for example, humidifying the laboratory dry nitrogen to $-40^{\circ}F$ dew point, the apparatus can operate unattended for a period of several days without the dew point drifting more than 1° or $2^{\circ}F$. Whenever humidification to a higher level (usually $50^{\circ}F$ dew point) is desired, some supervision and control of the bubbler is required; that is, small adjustments might be required as often as every 30 minutes.

Instrumentation

Pressures are measured at all critical points in the flow system with precision Wallace and Tiernan gages. For unattended operation, critical pressures can be measured and recorded by Baraton pressure transducers. Temperatures are measured throughout the system and in the beds by copper constantan thermocouples. All temperatures are continuously monitored and recorded during test periods. As noted earlier, all flow rates are measured by rotameters calibrated at 20 psia.

Water concentrations are measured by means of dew point hygrometers.* Sample lines to the hygrometer system are provided at the bed inlet, at the

---

* In such instruments, dew points are measured above $32^{\circ}F$ and frost points below $32^{\circ}F$. For simplicity, the term dew point is used throughout this report. Below $32^{\circ}F$ proper conversion to water vapor pressures was made by use of tables based on water vapor equilibrium with ice.

outlet, and in the bypasss system. For those runs dealing with dew points above room temperature, the entire sample line system can be heated with electric strip heaters. During the first series of tests, dew point measurements were taken with a Cambridge Model 992 automatic hygrometer and with an AiResearch manual hygrometer. The Cambridge hygrometer, at that time, had the capability to measure and continuously record dew points from about $+10^{0}$ to 120^{0}F. The manual AiResearch instrument can be used from room temperature down to -100^{0}F; but as a manual instrument, it could produce only instantaneous readings. Generally such readings were taken about every 15 to 20 minutes.

Later in the program, the Cambridge hygrometer was modified to allow it to read over an extended range, from -100^{0} to $+120^{0}$F. During the early part of adsorption breakthroughs, the Cambridge hygrometer was set to read the inlet dew point to the test bed. Once it was confirmed that conditions had settled down, the instrument was switched to the outlet stream. In this manner almost the entire breakthrough curve was recorded by this instrument. During the rest of the breakthrough, the inlet dew point was monitored with the manual AiResearch hygrometer. Later on in the test series, a second Cambridge hygrometer was purchased and installed in the apparatus. In the final configuration, inlet and outlet humidities are continuously monitored and recorded. Finer control of the adsorption conditions is afforded by this setup. Also, with no need for manual readings, the test procedure is greatly simplified.

The hygrometers were subjected to a rigorous calibration procedure. It was found that the accuracy of the Cambridge instruments was good, usually within $\pm 1^{0}$F, and no corrections were employed. However, the AiResearch hygrometers were found to read considerably low in the low dew-point range. Where possible, corrections were made to these readings. Because the region where these corrections were made represents very low water concentrations, the shape of breakthrough curves is not greatly affected by the inaccuracy of the manual unit.

In early experiments, CO_2 concentrations were measured by a Beckman IR 15A infrared analyzer. Later a wider range, more stable, instrument, the Beckman IR 315B, was procured. This infrared analyzer was capable of much greater accuracy in lower CO_2 concentration regions, and is thus more valuable for those experiments dealing with CO_2 partial pressures below 7 mm Hg. The infrared analyzers were calibrated by means of pre-mixed and analyzed gases; five different gas mixtures ranging from 0.5 to 3.0 volume percent CO_2 in nitrogen were available. At all times when taking readings with the infrared CO_2 analyzers, the pressure at the instrument's detecting cell was held precisely at 7.0 psia. This pressure was read on a precision Wallace and Tiernan gage. To facilitate the sampling of the various test and calibration gases by the one CO_2 analyzer, a special sample manifold was installed in the apparatus. The flow rate of all sample flows was measured by rotameters.

For those experiments in which appreciable quantities of both water vapor and CO_2 were mixed into the nitrogen stream, water traps containing magnesium perchlorate (trade name Anhydrone) were included in the sample lines leading to the CO_2 analyzer. Calibrations verified that these dryers produced accurate CO_2 readings.

Test Procedure

Each test in this program was preceded by a prolonged vacuum bakeout of the sorbent bed. Usually 450° to 500°F was attained within the bed at a pressure of approximately 10 to 20 μ Hg. The objective of the vacuum bakeout was to reduce the water content of the bed to about 0.1 percent or less.

The actual adsorption run was preceded by a period of usually about 2 hr in which the proper test conditions were established. These included bed temperature, bed pressure, flow rate, inlet dew point, and inlet CO_2 partial pressure. During this period, the bed was closed off and the flowstream was directed around the bed through the bypass system. When all conditions were satisfactory, the timer clock was initiated, and the flow was directed through the bed. During the first minute or two of the adsorption run, flow rates, pressures, temperatures, and inlet concentrations were given final adjustments to compensate for the slightly different conditions of the bypass system and the bed system. Throughout the adsorption breakthrough, inlet and bed conditions were continually monitored and, when necessary, small adjustments were made. At regulator intervals, all items of data were recorded on data sheets. This was in addition to the temperatures, dew points, and CO_2 concentrations which were continually recorded.

Normally, breakthroughs were carried out in one continuous run, until inlet and outlet conditions were verified to be the same. For some of the runs dealing with the adsorptions of water on molecular sieve 13X or silica gel, it was not possible to man the equipment during the full period of the breakthrough. In these instances, with the 1/2-in.-fin bed, it was decided to suspend the test, and shut off the bed and cool it below its adsorption temperature. The adsorption run was then restarted on the next day. The results of these long tests seem to be quite reasonable, and very little effect was evident from the interruption in the test procedure. With the 1/2-in.-fin bed, the temperature profiles were usually fairly uniform; that is, temperature excursions at the adsorbing front were not large. Thus, the restart of the bed at nearly uniform temperature was not a large departure from the conditions at the time of shut down. The continual cooling of the bed during the idle period tended to maintain the sorbate loading distribution on the bed. On the other hand, the 1-in.-fin bed tests were characterized by large temperature excursions at the adsorption front. For these tests, it was undesirable to interrupt the adsorption procedure. Therefore, as much as possible, continual coverage of the adsorption runs was afforded. Even then, there were some conditions where test suspension and restart were necessary. These runs did show appreciable effects of the interruption.

For CO_2 adsorption runs, the infrared analyzers were calibrated at regular intervals by means of the special bottled gases. In some instances, several calibrations were made during a run. For shorter runs, the calibrations of the infrared analyzer were done at the beginning and at the end of the test. It was usually found that the calibration drift was very slight during the runs. This was especially true for the newer infrared analyzer.

One goal of the test program was to obtain information on gas-stripping of water from silica gel and 13X molecular-sieve beds. Thus, after some of the water breakthroughs were completed, a gas-stripping test was conducted. These tests usually involved just the turning off and isolating of both the bubbler and the humidity-control condenser, and allowing dry nitrogen to pass through the bed. Other than dispensing with the humidity-control functions, the test procedures were the same as during absorption breakthroughs.

In some instances, however, it was desired to run the gas-stripping operation at a different temperature than the adsorption run. As discussed earlier, one goal of the dynamic tests was to produce data on mass-transfer parameters while eliminating heat-transfer effects from the evaluations. Accordingly, for these particular gas-strip operations, a transition desorption sequence was introduced, altering bed temperature to the conditions at which the gas strip was to be run. Usual conditions for this type of test were a 60°F adsorption to be followed by a 90°F gas strip. To accomplish this, after complete breakthrough at 60°F had been ascertained, the bed temperature was brought up to 90°F without changing any of the other test parameters. Normal data monitoring and recording continued. During the transition period, because of the increase in bed temperature, the outlet humidity rose above that of the inlet and stayed above it for a period of time. Finally, enough water was removed from the bed and, again, the inlet and outlet conditions became equal. Then the bubbler and humidity control condensers were turned off and isolated, and dry nitrogen was allowed to pass through the bed.

The data from the transition period was of no real use in the evaluation of mass-transfer parameters because of the changing bed temperature. However, the recording of inlet and outlet concentrations allowed calculation of the amount of water removed from the bed. Similarly, the calculated amounts of water left on or removed from the bed during the adsorption period and the following gas strip allows a complete material balance to be obtained. This material balance compares total sorbate influx to total efflux. It does not relate to equilibrium conditions, and is thus independent of bed temperature measurements. In effect, it is a direct check on the concentration measurements.

In some rare cases, the laboratory nitrogen contained much more water vapor than usual (normally -80°F dew point or less). To properly run gas strips and other low humidity tests when this occurred, an auxiliary drying bed was installed in the system. Molecular sieve 13X was the sorbent used in this bed.

CHARACTERISTICS OF BREAKTHROUGH CURVES

Data Reduction and Presentation

The raw data taken from the mass-transfer apparatus was subjected to a data reduction procedure to smooth out experimental upsets and to provide information in more meaningful terms. The data reduction was initiated by checks of instrument calibrations. Then, on the strip charts of the hygrometer and CO_2 analyzer outputs, short-term discrepancies due to pressure and temperature fluctuations, adjustments in flow rate, and adjustments in inlet conditions were smoothed. (In some instances, where the fluctuations were large, the data was judged to be of such poor quality that the run was rejected and set aside for a rerun.) This was followed by the transformation of dew-point and CO_2-volume-percent readings into concentration readings. From published tables, the dew-point readings were transformed into water vapor pressures; water vapor concentrations were then obtained

$$C_{H_2O} = \frac{P_{H_2O}}{P_{N_2}} \frac{18}{28} = \frac{P_{H_2O}}{P_{Total} - P_{CO_2} - P_{H_2O}} \frac{18}{28} \qquad (4\text{-}1)$$

This concentration unit has the units of mass of water per mass of nitrogen.

From the calibration curve produced at the time of the test, the CO_2 analyzer output trace was transformed into CO_2 concentration values (in the units of volume-percent CO_2). These values were then used to obtain mass concentration units

$$C_{CO_2} = \frac{(\text{Vol \% } CO_2)}{(100 - \text{Vol \% } CO_2)} \frac{44}{28} \qquad (4\text{-}2)$$

Since water traps were included in the sample lines to the CO_2 analyzer, this formula was valid regardless of whether water was involved in the test. The units of this concentration are mass of CO_2 per mass of nitrogen.

The inlet and outlet concentrations were plotted against test time to produce the desired breakthrough curve. The unit of concentration (mass of sorbate material per unit mass of nitrogen) selected for the presentation of breakthrough curves may not allow one to easily obtain a feel for the mass-transfer operation by mere inspection of the breakthrough curves. That is, one might have a greater inherent feeling for the adsorption process if partial pressures of water or CO_2 were plotted versus time. However, the mass concentration units are much more useful when detailed design and performance predictions are considered. First of all, by integrating either graphically or numerically between the inlet and the outlet traces, one is able to obtain the amount of sorbate left on the bed at any particular time. This calculation can then be used to obtain removal efficiency vs time. In system designs, this information is used to set cycle times.

When the integration is carried out for the entire breakthrough, the result is the ultimate sorption capacity of the sorbent bed. Dividing by the dry sorbent mass yields, by definition, the equilibrium loading of the sorbent with respect to bed temperature and inlet sorbate partial pressure. A direct comparison with published equilibrium data, or that data taken from a static test, is then possible.

As a goal, it was desired that the experimentally derived bed loading would be within ±5 percent of that obtained from equilibrium data. In those cases where the comparison (usually called a material balance check) was considerably larger than ±5 percent, there was usually something wrong with the experimental run in question. Thus, the derived loading and the resulting material balance check were used as indicators of the quality of the adsorption runs.

There are several different ways in which the material balance check was used to improve, or at least to certify, the quality of the data taken in the program. For example, in the first runs conducted in the program concerning water adsorption on silica gel, it was consistently found that the bed adsorbed considerably more water than predicted by equilibrium. Detailed checks of the experimental equipment and instrumentation revealed no reason for this deviation. Data reduction procedures were carefully checked without finding any errors. Even selected test reruns did not shed light on the problem. Finally, suspicion was cast upon the silica gel equilibria as published by the manufacturer. Up to that time no silica gel equilibrium data had been taken in this program; therefore, it was decided to obtain 60^0 and 120^0F of isotherms. (These have already been discussed and presented in Section 3.) The effect was to show that the silica gel as presently manufactured by the Davison Company is much better than would be expected from published information. In fact, in a personal communication, it was related that the manufacturing process had been altered in the hope of improving the sorbent capacity. However, no new equilibrium capacity data had been available.

Whenever a material balance check was decidedly negative (that is, the derived bed loading was much less than the predicted equilibrium loading), either a leak into the bed system from the ambient, or a poor vacuum bakeout was suspected. Invariably, negative material balances of as much as 20 to 30 percent were narrowed down to one of these two causes.

Large positive discrepancies in the material balance checks (that is, the bed picking up considerably more than equilibrium), were invariably connected to an undesired and unknown bypass of the gas stream around the adsorption bed. In one situation concerning several runs, upon checking for just this sort of a bypass around the bed, a failed (leaking) valve was discovered. Other cases involving single runs usually involved the inadvertent opening of a valve; in one instance, the failure of a differential pressure gage was suspected.

In some cases, there were material balance checks of about 10 percent which could not be attributed to poor bakeouts, to leaks into the system, etc. It is suspected that the reason these material balance checks were not

better is a shift in the output of the temperature recorder. That is, the actual bed temperature was somewhat higher or lower than that desired and indicated. This situation is discussed later with the presentation of the pertinent breakthrough curves.

There was always some uncertainty as to what the effective bed temperature actually was during a run. There were seven thermocouples within the packed bed, one thermocouple each on the inlet and outlet process gas streams, and one thermocouple each on the inlet and outlet water/glycol coolant streams. During adsorption conditions, there was always a variation in the readings. It was considered that the inlet and outlet temperatures of the gas stream or the water/glycol stream were not representative of bed temperature. This left the bed interior thermocouples for the determination. One of these seven thermocouples was attached to a copper fin, and therefore would not be representative of the sorbent temperature. The other thermocouples were distributed along the bed length. As the mass-transfer zone proceded along the bed, the thermocouples within this zone would read higher than the others. The difference could be 3° to $10^{\circ}F$, sometimes more. It was decided that effective bed temperature was most properly determined by the temperature readings outside of the mass-transfer zone.

There were still variations in these readings, due to transverse temperature gradients in the bed packing between fins and uncertainty in thermocouple location. The thermocouples were attached to a thin wire which was stretched longitudinally down the bed length. Even though thermocouple position could be determined accurately in the empty bed, there was no guarantee that during packing, the thermocouples had not been displaced laterally. Moreover, due to the offset nature of the fins, and the normal waviness of the thin copper fins, not all thermocouples could be placed initially in the center of a passage. Therefore those thermocouples located closer to fin surfaces would be cooler than mean bed temperature. The best that could be done was to average those readings for thermocouples not in the mass-transfer zone. Temperature recorder calibration shifts, evidenced in a few instances, also caused some uncertainty in bed temperature readings.

In the foregoing discussions concerning material balance checks, it has been assumed that the equilibrium loading of CO_2 or water is not affected by the presence of the nitrogen carrier gas. It is noted that the CO_2 and water equilibrium data as presented in Section 3 is taken with only the sorbate in contact with molecular sieve. That is, the total pressure and the sorbate partial pressure are synonomous. In the dynamic tests, the calculated sorbate loadings are those developed in the presence of considerable nitrogen gas. From the well-controlled single-sorbate dynamic tests, it is concluded that the above assumption is correct; there is negligible effect of the carrier gas.

Characteristics of Dimensional and Dimensionless Breakthrough Curves

Figure 4-6 shows a number of possible breakthrough curves. Curve A is a hypothetically perfect breakthrough curve. It represents conditions whereby all sorbent material that enters the bed is held on it up until the time that the equilibrium loading capacity has been reached. Then the breakthrough is instantaneous, and the inlet and outlet streams become equal. Curve B represents a realistically attainable, good breakthrough curve. With this type of curve, very little sorbate passes through the bed until quite late in the breakthrough period. Then the breakthrough is reasonably steep and the outlet concentration reaches that of the inlet fairly quickly. Curve B is representative of almost all of the single-sorbate breakthrough curves obtained under this program. Curve C represents a much poorer breakthrough curve. It does show a period of time where very little sorbate passes through the bed; then an initial period of steep breakthrough is followed by a rather slow approach of the outlet concentration to that of the inlet. Curve D represents conditions of adsorption so poor that the breakthrough of sorbate is immediate. Subsequently, a very long time is required for the outlet concentration to reach that of the inlet.

Curve B represents conditions in which the mass-transfer resistances in the convective gas stream outside of the pellets, and in the diffusive flow of sorbate within the pellets pores, are low. Curve C represents a situation in which there is considerable resistance within the sorbent particle, or the equilibrium curve shape is somewhat unfavorable to adsorption. That is, high

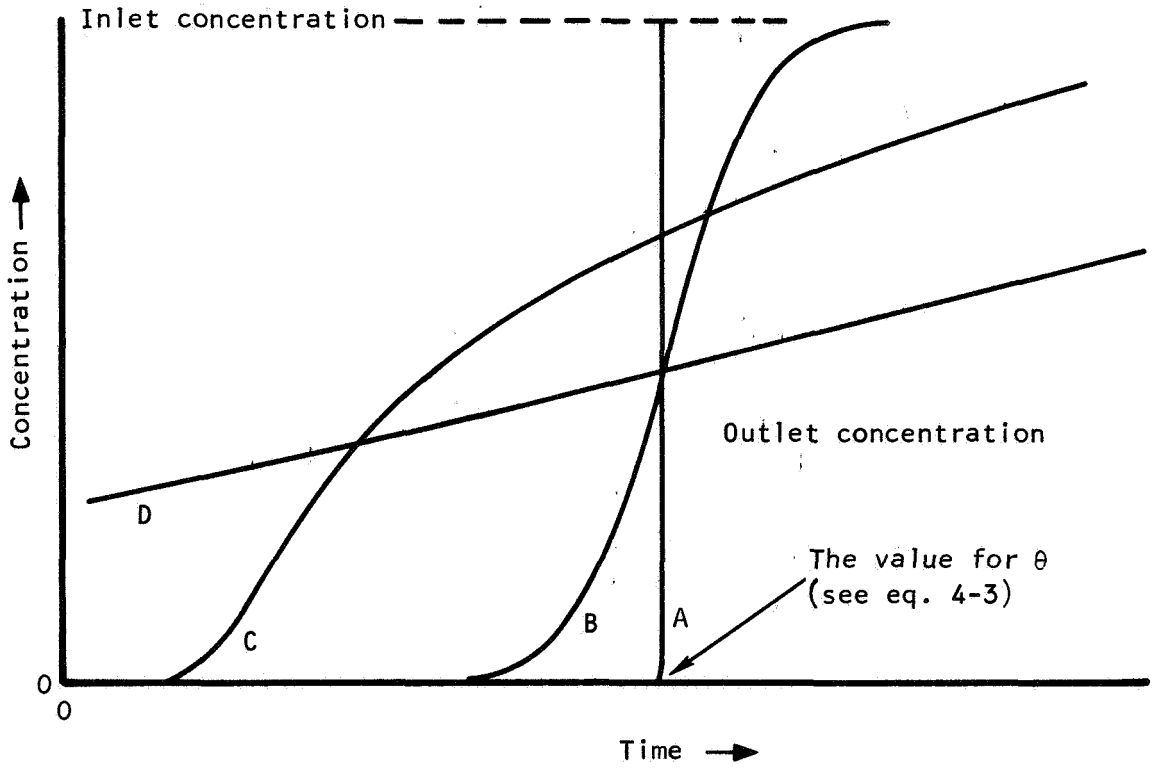

Figure 4-6. Typical Breakthrough Curves

loadings are only attained at higher partial pressures, and the equilibrium curve is pronouncedly convex upward. Curve D represents a condition of high convective mass-transfer resistance, possibly coupled with high internal diffusive resistance, or conditions where the equilibrium is definitely not favorable.

As discussed previously, the breakthrough curve can furnish data on the equilibrium sorption capacity, and the shape of the curve tells something of the mass-transfer process. However, from the dimensional breakthrough curves it is often difficult to make critical comparisons of one sorbent with another, or of one sorption condition with another. One of the reasons for this is that the breakthrough curves will lie in differing time positions on the dimensional breakthrough graph. Without some sort of time scaling, the curve shapes will be distorted and comparisons will be difficult. To facilitate critical comparisons of sorbents and sorbent conditions, it is useful to express the dimensional breakthrough curves in terms of dimensionless quantities. From the concept of the perfect sorbent bed, a representative dimensional time parameter may be designated. This quantity is the time required to introduce just enough sorbent into the bed to saturate it. For the hypothetical perfect bed, this is the time at which breakthrough occurs. This time, θ, is expressed mathematically as (written for CO_2 as the sorbate)

$$\theta = \frac{\text{Bed Capacity}}{\text{Rate of Sorbent Introduction}} = \frac{w_\infty M_{Bed}}{W_{N_2} C_{CO_2,inlet}} \quad (hr) \qquad (4\text{-}3)$$

where w_∞ = the bed loading at infinite time; or in other terms, the equilibrium loading capacity with respect to the bed temperature and inlet partial pressure (mass of CO_2/ mass of dry sorbent)

M_{Bed} = bed mass (mass of dry sorbent)

W_{N_2} = flow rate of the carrier gas (mass of N_2/hr)

$C_{CO_2,inlet}$ = inlet concentration of CO_2 (mass of CO_2/mass of N_2)

If one wants to consider that the bed may have had a preload of sorbate at time zero, the definition can be restructured (shifted in concentration)

$$\theta = \frac{\left(w_\infty - w_{t=0}\right) M_{Bed}}{W_{N_2}\left(C_{CO_2,inlet} - C^*_{CO_2,t=0}\right)} \qquad (4\text{-}4)$$

where $w_{t=0}$ = the bed preload at time t=0 (mass of CO_2/mass of dry sorbent)

$C^*_{CO_2, t=0}$ = the equilibrium concentration over the bed at time t=0 and corresponding to the loading $w_{t=0}$ (mass of CO_2/ mass of N_2); can be converted to $p^*_{CO_2, t=0}$ by knowing P_{total}

Gas stripping may also be considered in the same manner as adsorption. The perfect-bed breakthrough time, θ, is given by Equation (4-4) in the rearranged form

$$\theta = \frac{\left(w_{t=0} - w_\infty\right) M_{Bed}}{W_{N_2}\left(C^*_{CO_2, t=0} - C_{CO_2, inlet}\right)}$$

The dimensionless time is simply obtained by dividing the actual test time by parameter θ

$$\tau = \frac{t}{\theta} = \frac{W_{N_2}\left(C_{CO_2, inlet} - C^*_{CO_2, t=0}\right)}{M_{Bed}\left(w_\infty - w_{t=0}\right)} t \qquad (4\text{-}5)$$

A dimensionless concentration Ψ is chosen in a simple, classical manner

$$\Psi = \frac{C_{CO_2, t} - C^*_{CO_2, t=0}}{C_{CO_2, inlet} - C^*_{CO_2, t=0}} \qquad (4\text{-}6)$$

In the discussions that follow, it was found that the dimensionless breakthrough curves provided the best means of visual comparison of sorption conditions and the performance of beds. It should be stressed again, that the primary purpose of the single-sorbate breakthrough tests was for the evaluations of mass-transfer coefficients and intraparticle diffusivities. Rigorous comparisons of sorbents and sorption conditions can then be made using the performance-prediction programs applied to actual bed designs and systems of interest.

PRESENTATION OF BREAKTHROUGH CURVES

Range of Parameters Covered

Table 4-2 presented earlier has given the range of test conditions covered in this program. Table 4-4 relates these test conditions to the bed size and volume, and further relates the test conditions to those of use in a spacecraft system. For the breakthrough curves presented in the balance of this section, a run number designation has been devised as follows:

TABLE 4-4

FLOW PARAMETERS RELATED TO TEST CONDITIONS

Based upon 1.25 lb of Linde 5A in the 1/2-in.-Fin Bed.
P_T = 363 mm Hg, p_{CO_2} = 7 mm Hg, T_{Bed} = 70°F

Parameter Related to Bed Size and Flow Rate	Flow Rate (lb/hr)		
	1.4	2.8	5.6
Superficial Velocity (ft/sec)	0.22	0.45	0.89
Residence Time (sec)	2.3	1.1	0.56
Space Velocity (Bed Volumes/sec)	0.45	0.89	1.8
Reynolds No.	3.3	6.7	13.4
CO_2 Removal Rate, at 100 percent CO_2 Removal Efficiency (lb CO_2/hr)	0.043	0.087	0.173
"Perfect Bed" Breakthrough Time, θ, at 100 percent CO_2 Removal Efficiency (hr)	1.94	0.97	0.48
Man Rating at 100 percent CO_2 Removal Efficiency (No. of Men)	0.47	0.94	1.89

Individual run designation

Sorbent/Sorbates (Fin Size) - Xs,p

Sorbent abbreviations are

SG - Silica gel, Davison (Grade 05), 6 to 16 mesh

5A - Linde 5A molecular sieve, 1/16-in. pellets

5AD - Davison 5A molecular sieve, 8 to 12 mesh spheres

13X - Linde 13X molecular sieve, 1/16-in. pellets

Sorbate designations were W for water and CO_2 for carbon dioxide. The fin sizes used in the tests were 1/2-in. and 1-in. The X in the run designation is the serial number of test run. The s or the p which follows the serial number denotes the test was either a gas strip, or a water preloading sequence. An example of the run designation is SG/W(1/2)-1. This represents run number one with water adsorbing on silica gel in the 1/2-in.-fin bed.

Adsorption of Water by Silica Gel

Figures 4-7* through 4-16 are breakthrough curves for the adsorption of water by and the gas stripping of water from silica gel contained in the 1/2-in.-fin bed. Figures 4-17 and 4-18 are water adsorption breakthroughs for silica gel packed in the 1-in.-fin bed.

For the 1/2-in.-fin bed, the calculated sorbent loadings compare acceptably with equilibrium data--generally within 10 percent. Originally, when the data was first reduced, the tests showed 20 to 30 percent more sorption capacity than the equilibrium data published by the manufacturers. As discussed earlier, new data was then taken which yielded much higher capacities. This brought the dynamic and equilibrium capacities into general agreement. The remaining deviations are considered to result from errors in temperature measurement and control--possibly as much as $3^{\circ}F$. Later in the program, refinements were made in the bed temperature instrumentation.

The basic dew-point and concentration measurements are considered to be of good quality. This is evidenced by the closeness of the material balances between gas stripping runs and the preceding adsorption runs: -2.5 percent between Runs 3 and 4s; +6.4 percent for Runs 6 and 7s; +0.8 percent for Runs 8 (plus the transition adsorption) and 9s. These balances are not dependent on equilibrium data or bed temperature measurements; they relate to only the concentration (dew point) and flow rate measurements. They are even independent of flow rate if it is held truly constant.

The shapes of the breakthrough curves for the 1/2-in.-fin bed vary from fair to good. The best breakthrough curve shape is given by Run SG/W(1/2)-1 (Figure 4-7) for the low flow rate of 1.37 lb/hr at $60^{\circ}F$. Silica gel performs quite satisfactorily under the conditions of this run, which are the most representative of those that the sorbent would undergo in a spacecraft system. There is a fairly long period of time where removal efficiency is over 99 percent--5 to 7 hr. For higher flow rates at $60^{\circ}F$, the breakthrough begins disproportionately earlier. This is shown for 2.87 lb/hr in Run SG/W(1/2)-5 Figure 4-11), where 99 percent removal efficiency is attained for only 1 to 2 hr.** For 5.37 lb/hr, Run SG/W(1/2)-8 (Figure 4-14), the breakthrough is almost immediate.

All of the adsorptions at $120^{\circ}F$ evidence early breakthroughs, which would not be acceptable for predrier applications. However, there was never any intent to have predrier beds function isothermally at $120^{\circ}F$; the purpose of these runs was to obtain information on the temperature dependence of K_g and

---

* Due to the large number of pages required for Figures 4-7 through 4-52, these figures are presented at the end of this section.

**Due to equipment malfunction, inlet dewpoint was nearly uncontrollable during this run. The earlier portion of breakthrough should not have been affected and this portion of the data is considered satisfactory. However, the entire breakthrough was not used in the subsequent evaluation of mass-transfer parameters.

D_{H_2O}. This is desired as gas strips could be conducted in a spacecraft system at 120°F; also, in adiabatic beds, local temperatures in the adsorption zone could approach 100° to 120°F.

Two gas stripping runs at 90°F are included; Runs SG/W(1/2)-2s and SG/W(1/2)-9s. These runs followed adsorptions at 60°F, which, in turn, were followed by transition adsorption periods whereby bed temperature was raised from 60° to 90°F. For illustration, Figure 4-15 shows the transition adsorption following Run SG/W(1/2)-8. The 120°F gas strips (SG/W(1-2)-4s and 7s) were all conducted immediately after the preceding adsorption breakthrough was completed.

From the dimensional breakthrough curves, some tentative conclusions can be drawn. First, at low enough flow rates, good performance with silica gel can be attained at 60°F. At higher flows, breakthroughs are not as good--possibly this is an effect of channeling within the bed becoming more important. Second, silica gel desorption by gas stripping at 90° and 120°F proceeds reasonably well, but not in the same time period as adsorption. With -80°F dew-point nitrogen, the desorption is essentially quantitative.

With respect to use as a predrier desiccant, it should be noted that breakthrough curves like that of Figure 4-7 represent the best possible performance. This is because the adsorption followed a vacuum bakeout, which left the sorbent completely dry. In actual use in a spacecraft, after a large number of cycles, a repeating steady-state water loading would be retained by the bed. In the face of this resident loading, the bed would have to achieve 99.5 percent removal efficiency. Certainly the bed of Run SG/W(1/2)-1 would not operate nearly as long (5 hr) under cyclic steady-state conditions. Detailed computer computations would be needed to obtain the exact allowable cycle time.

The adsorptions carried out in the 1-in.-fin beds are not as good as those for the 1/2-in.-fin bed. This is due to the poorer heat-transfer performance of the 1-in. fins. These tests and comparisons of fins are discussed in more detail later in this section.

Figures 4-19 and 4-20 present the dimensionless breakthrough curves for the 1/2-in.-fin bed silica-gel/water runs. Figure 4-19 contains breakthrough curves for adsorption runs. Here, the effect of flow rate and sorbent temperature on the quality of the breakthrough is demonstrated. At 60°F, the 1.37 lb/hr breakthrough is far better than that for 5.37 lb/hr. Although not shown, the early portion of the curve for 2.87 lb/hr (from Run SG/W(1/2)-5; Figure 4-11 is very close to that for the 5.37 lb/hr, showing a quite early breakthrough. The data of Curve A, 1.37 lb/hr, is well substantiated as two additional runs were taken at this condition, each showing nearly the same behavior.

All of the 120°F breakthroughs show performance similar to Curve C of Figure 4-19. That is, much earlier breakthrough than the low flow run at 60°F.

The dimensionless representations of the gas stripping runs are contained in Figure 4-20. These curves all show that the stripping desorption is carried out with some difficulty. There seems to be little flow-rate dependence. To emphasize this, the high flow run (5.37 lb/hr) at 120°F was not plotted, as it fell almost precisely on Curve B (1.37 lb/hr).

Adsorption of Water by Molecular Sieve 13X

Adsorption and gas-stripping breakthroughs for water vapor on Linde molecular sieve 13X are shown in Figures 4-21 through 4-29. Four adsorptions and two gas strips are presented for the 1/2-in.-fin bed; and two adsorptions are presented for the 1-in.-fin bed. For comparison, the four adsorptions for the 1/2-in.-fin bed are shown on one graph, Figure 4-27.

The first general observation is that all adsorption breakthroughs are reasonably well shaped, regardless of flow-rate, temperature, or fin size. For example, Run 13X/W(1/2)-5 for 2.36 lb/hr at 120°F shows an excellent breakthrough (Figure 4-25). This can be contrasted to that of silica gel for the same conditions, Figure 4-12. From these tests it appears that molecular sieve 13X has much more latitude in adsorption than silica gel. This is substantiated by comparing equilibrium data for the two sorbents (as contained in Section 3). It is noticed that the sorption capacity of 13X is greater for low vapor pressures and does not vary nearly as much with temperature. Thus, from the basic equilibrium data, one would conclude the same as these tests show, that 13X has more favorable adsorption characteristics than silica gel.

On the other hand, the 13X equilibria is not as favorable for gas stripping. This is substantiated by the gas strips presented here. For the tests of Figures 4-24 and 4-26, only a small fraction of the water originally present is stripped off during the rather lengthy tests. There are two reasons for this. First, the sorbent has a substantial equilibrium water capacity with respect to the inlet vapor pressure of the stripping gas. For -100°F dew-point nitrogen (water vapor pressure of approximately 0.0007 mm Hg), molecular sieve 13X has water capacities of about 5.6 and 3.3 percent at 90° and 120°F, respectively. That is, a substantial fraction of the original water could not be removed at all, even at infinite time. Still, additional water could have been removed with more test time. For the 90°F gas strip, it was estimated that 0.120 lb of water could still have been removed from the bed. For the 120°F gas strip the estimate is 0.115 lb.

The second reason for the poor gas strips is due to a rate phenomenon. The rate is low because of a very low driving force for mass transfer. This driving force is the difference between the equilibrium partial pressure and the actual free stream partial pressure. It is believed that convective or diffusional resistances are not appreciable enough to cause the slow desorption rate. If they were, the adsorptions would be similarly affected, which of course they are not.

The calculated sorbent capacities for the adsorption breakthroughs are all very close to those obtained from the equilibrium data presented in Section 5. These tests indicate capability of the apparatus to produce quality data. The 1-in.-fin bed tests show calculated capacities less than equilibrium values. This is due to non-isothermal sorbent conditions, as a result of the poor heat transfer of the larger fins. This situation is discussed in detail later in this section.

Figure 4-30 presents typical dimensionless breakthrough curves for the adsorptions. The curve shapes are all quite similar and there is not clear cut dependence of temperature or flow rate. It should be noted that Run 13X/W(1/2)-5, plotted as curve C, was done on a different packing of the bed than the other two runs shown on this figure. Also, Run 13X/W(1/2)-3, for 2.26 lb/hr and 60°F, was not plotted as its breakthrough curve was very close to curves A and B.

Figure 4-31 shows dimensionless breakthrough curves for the gas strips. It is again evident from these curves that such gas strips are carried out with difficulty. There is little difference in the curve shapes for the two temperatures.

Adsorption of CO_2 by Molecular Sieve 5A

Adsorption breakthroughs were made for CO_2 on both Linde 5A molecular sieve (1/16-in. pellets) and Davison 5A molecular sieve (8 to 12 mesh spherical beads). A good deal of experience had been obtained in previous programs with the pelleted Linde 5A sorbent. Some of this experience was in 1/4-in.-fin beds, which were suspected of excessive channeling. That is, the pelleted material did not seem to pack well into the 1/4-in. fins. To gain some experience with Davidson 5A molecular sieve to evaluate channeling effects with the beaded material, the test program included both 5A sorbents.

Figures 4-32 through 4-39 present adsorption breakthroughs for CO_2 on molecular sieve 5A. Figure 4-40 is a gas strip of CO_2 from 5A. Gas stripping of CO_2 from 5A has little practical application, but one such gas strip was made for comparative purposes.

Figures 4-32 and 4-33 show comparisons of the Linde and Davison materials for essentially similar conditions. The first observation from these two figures is that the Linde material provides better breakthroughs at both flow rates. Even though both materials show good breakthroughs, Davison 5A might be rejected on the basis of these tests. This decision is tempered however when one considers the somewhat poorer Linde 5A breakthroughs which were obtained later in the experimental program with another packing of the bed, Figures 4-38 and 4-39. There is no apparent reason for the difference in quality between the breakthroughs of the two packings. In fact, a rerun of the 2.4 lb/hr condition (Figure 4-39) was made in an attempt to determine a reason for the difference. The rerun was virtually the same.

The only explanation at present is that the sorbent used in the two packings (from different production batches) were manufactured with different quality. Possibly, there are variations in the blending and extruding process which result in pellets with more constricted pore structure. There are a number of instances in the literature where dynamic performance variations are thought to be caused by differences in the manufacturing process. It is possible that moisture, temperature, pressure, and other process variables could have pronounced effects on the developed pore structure. On the other hand, it is not expected that equilibrium values would be altered significantly by the manufacturing process. The basic molecular-sieve crystal structure should be easily reproduced; the equilibrium behavior would then depend upon only the proportion and the inertness of the clay binder. It seems these too could be easily controlled. Thus, differences in batches would not be detectable from equilibrium tests.

As a result of these tests, no conclusion can be made with regard to which 5A material, Davison or Linde, is preferred. In fact, with either, it is possible that dynamic performance differences between batches might exist. It might be desirable to run small-scale dynamic tests on samples before using a particular sorbent batch.

The gas strip shown in Figure 4-40 indicates a process carried out with some difficulty. This is probably due to the unfavorable equilibrium characteristics for gas stripping. The stripping of CO_2 is much more complete than that observed for water from molecular sieve 13X.

The dimensionless breakthrough curves shown in Figure 4-41 show variations due to process conditions and due to the different sorbent batches. Curves A, B, and D show a slight dependence on flow rate. This variation with flow rate is overshadowed by the variation between sorbent batches, curves B and E. The variation with bed temperature, curves B and C, is slight and may be due to experimental inaccuracies. The curve for Run $5A/CO_2(1/2)$-4 for 50°F sorbent temperature was not plotted as it was quite close to the 70°F curves, A and B.

Adsorption of CO_2 by Molecular Sieve 13X

The primary interest in molecular sieve 13X is as a desiccant or sorbent for the predrier beds of a spacecraft CO_2 removal system. In this use, its adsorption of CO_2 is negligible due to the poisoning effect of the resident water loading. However, there is the possibility that 13X might be considered as a candidate for the CO_2 removal sorbent. Above approximately 2 mm Hg p_{CO_2}, it does not have the equilibrium capacity of 5A. For example, at 7 mm Hg and 70°F, 5A has 33 percent greater capacity. However, below 2 mm Hg, 13X is nearly equivalent to 5A. Since spacecraft beds operate predominantly in the low loading range, 13X might not compare too unfavorably to 5A. In addition, its much larger pore (or window) structure potentially can produce better dynamic performance than 5A.

Therefore, a series of CO_2 adsorption tests on Linde 13X were included in the dynamic test series. The breakthrough curves for both the 1/2-in.-fin and the 1-in.-fin beds are shown in Figures 4-42 through 4-48. Except for the high flowrate run with the 1-in.-fin bed (Figure 4-48), all of the breakthroughs are of good shape. As expected from equilibrium data the developed loadings are not as large as those obtained with 5A.

The high flow rate run (5.31 lb/hr) with the 1-in.-fin bed, represents conditions of bed geometry and sorption conditions which are generally unacceptable. The heat-transfer aspects of the 1-in. fin are discussed in detail in the following paragraphs. It should be noticed that breakthrough is relatively soon and requires a relatively long time to complete.

COMPARISON OF 1/2-INCH AND 1-INCH FINS

Of the three beds constructed for the dynamic tests, the bed containing the 1/2-inch rectangular offset fin was selected as the primary test article, to which the other beds would be compared. In earlier development programs considerable data had been obtained with 1/4-inch fins. Heat-transfer performance was shown to be good, but packing density was not as high as desired, and there seemed to be a tendency to channeling. It was reasoned that the 1/2- and 1-inch fins, especially of the offset variety, would allow less channeling, but their heat transfer adequacy was questioned. To obtain at least a rough idea of the heat-transfer performance of the larger fins, a hand, relaxation finite-difference computation was performed for the 1-inch fin. Silica gel was chosen as the sorbent; the calculation was made for steady-state conditions representative of vacuum desorption. It was expected these conditions would produce the largest temperature drop in the packed bed.

Figure 4-49 shows the results of the finite-difference computation. Due to symmetry, the calculation was performed, for a quarter of one channel formed by the 1-in. fin matrix. The maximum temperature difference of 46^0F is much higher than desired, and would not allow efficient vacuum desorption. It should be noted that the fin effectiveness is not limiting; that is, the fin is nearly isothermal. The limiting factor is the low bed thermal conductivity. Under adsorption conditions with a flowing gas, a slightly lower temperature drop would be expected. However the limiting factor would still be the low bed conductance.

It was concluded that the 1-inch fin would probably have poor heat-transfer performance. Therefore, the 1/2-inch-fin test bed was used for the bulk of the experimental runs. Several runs were conducted with the 1-inch-fin bed for comparative purposes. The dimensional breakthrough curves for these runs have already been presented. The following paragraphs present comparisons of the performance of the two beds, and some observations of their heat-transfer performance.

Figure 4-50 shows the comparison of dimensionless breakthrough curves obtained for water on Linde 13X molecular-sieve pellets with the 1/2-inch-fin bed and the 1-inch-fin bed. The poorer breakthrough performance of the 1-inch-fin bed is due strictly to heat-transfer deficiencies of this bed. In both cases water/glycol heat-transport fluid was fed to the bed coolant passages at 59° to 60°F, at such a rate that the temperature rise of the coolant was less than 1°F. From the thermocouples placed within the bed it was easy to conclude which bed had the better heat-transfer characteristics. For the 1/2-inch-fin bed the traveling mass-transfer zone was evidenced by temperature readings of about 18°F above the coolant temperature. For the 1-inch-fin bed the temperature excursions were 35° to 40°F above the coolant temperature. The resulting shift with temperature in the sorbent's equilibrium capacity causes the breakthrough curve for the 1-inch-fin bed to be less steep and more prolonged than that for the bed with the closer-spaced heat-transfer matrix.

Figure 4-51 shows the same general behavior for the adsorption of water on silica gel. Here the temperature excursions from 60°F are not as noticeable--4° to 5°F for the 1/2-inch-fin bed and 8° to 10°F for the 1-inch-fin bed. However, since silica gel's sorption capacity for water is much more temperature dependent than molecular sieve 13X, the early portion of the breakthrough curve (which is the important consideration for actual spacecraft systems) is much poorer for the 1-inch-fin bed.

One other point can be made to show the poorer performance of the larger fin. All runs with the 1-inch-fin bed were made with no control on the bed inlet gas temperature. Thus, the temperature at the bed inlet was generally the same as the laboratory ambient, about 75°F. Because of poor bed heat transfer, the first 10 to 15 percent of the bed operated above 60°F. In contrast, with no inlet temperature control with the 1/2-inch-fin bed, usually a negligibly small portion of the bed was above 60°F.* The result of this higher temperature region in the entrance of the 1-inch-fin bed is a lower overall bed sorption capacity. Indeed, most water adsorption runs with the 1-inch-fin bed show material balance checks some 10 to 15 percent below that predicted by the 60°F sorbent equilibrium capacity.

It should be noted that it is quite conceivable that some spacecraft systems would not include precoolers for the airstream flowing to a sorption bed. In such cases, if isothermal bed operation were desired, the 1-inch fin would be downrated with respect to cooling the airstream in the entrance region of the bed.

Figure 4-52 for CO_2 adsorption by Linde 13X shows again the same general comparison between the two beds. This was not entirely expected as the heat effects of CO_2 adsorption are not as much as that for water vapor. However, excursions of temperature in the mass-transfer zone were noted as high as 16°F for the 1-inch-fin bed.

---

* For very high flow rates, for example, 5.37 lb/hr for Run SG/W(1/2)-8, Figure 4-14, even in the 1/2-inch-fin bed an appreciable entrance region was above the 60°F coolant temperature. This led to less sorbent loading than expected if the bed were truly isothermal.

The conclusion can be made that when internal fins are desired, the 1-inch size fin should not be used. In the test series, it showed only 1.7 percent greater packing density than the 1/2-inch-fin bed, and the adsorption performance was significantly and repeatably poorer. Based upon these tests, it is considered that 3/8-inch offset fins would also produce very good thermal performance. The packed bed density would be a little less than 1/2-inch fins, but temperature excursions in the mass-transfer zone would be even less.

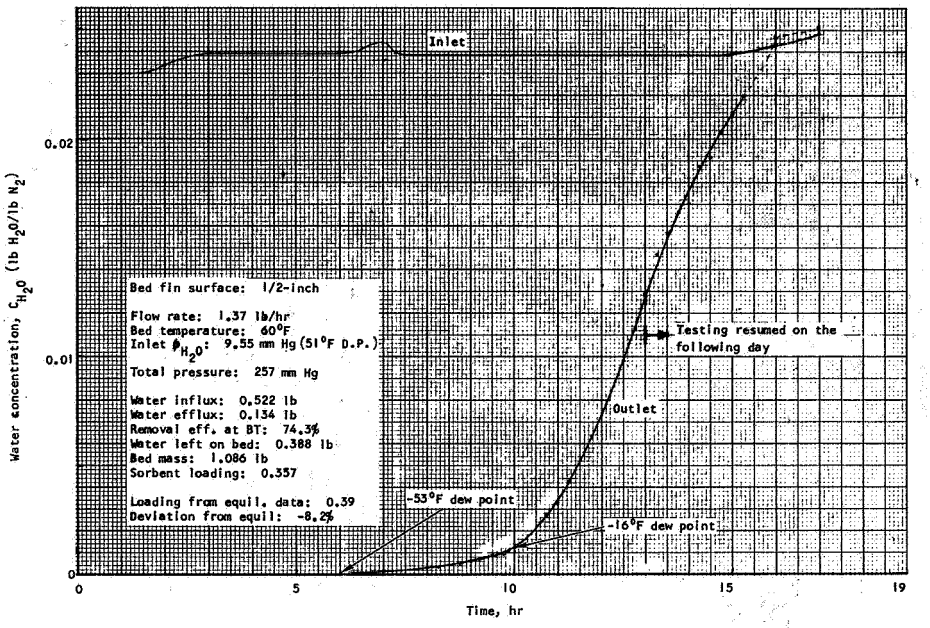

Figure 4-7. Water Vapor Adsorption Breakthrough on Silica Gel, Run No. SG/W(1/2)-1

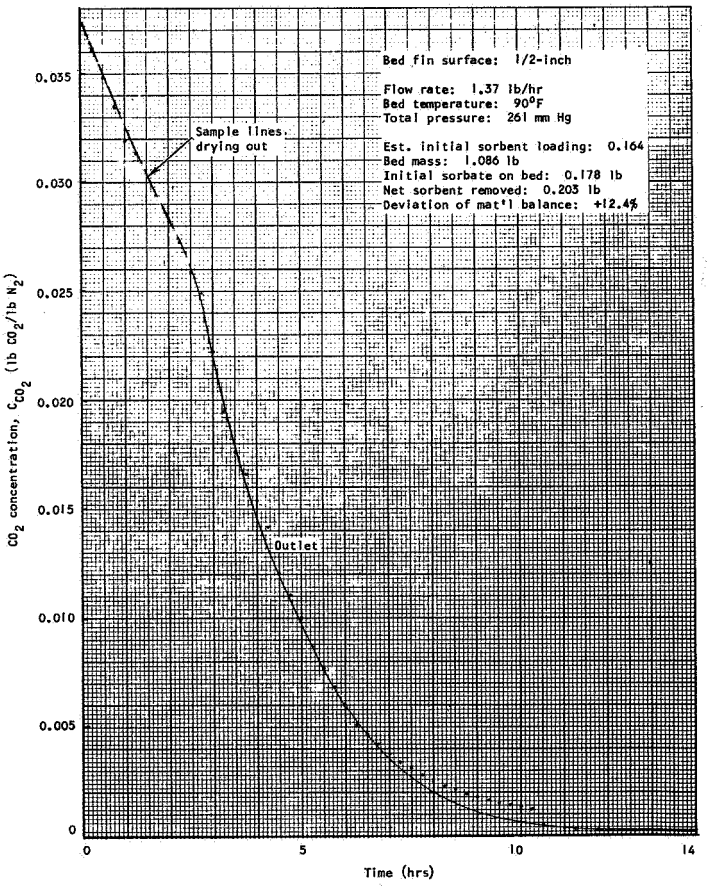

Figure 4-8. Gas Strip of Water from Silica Gel, Run No. SG/W(1/2)-2s

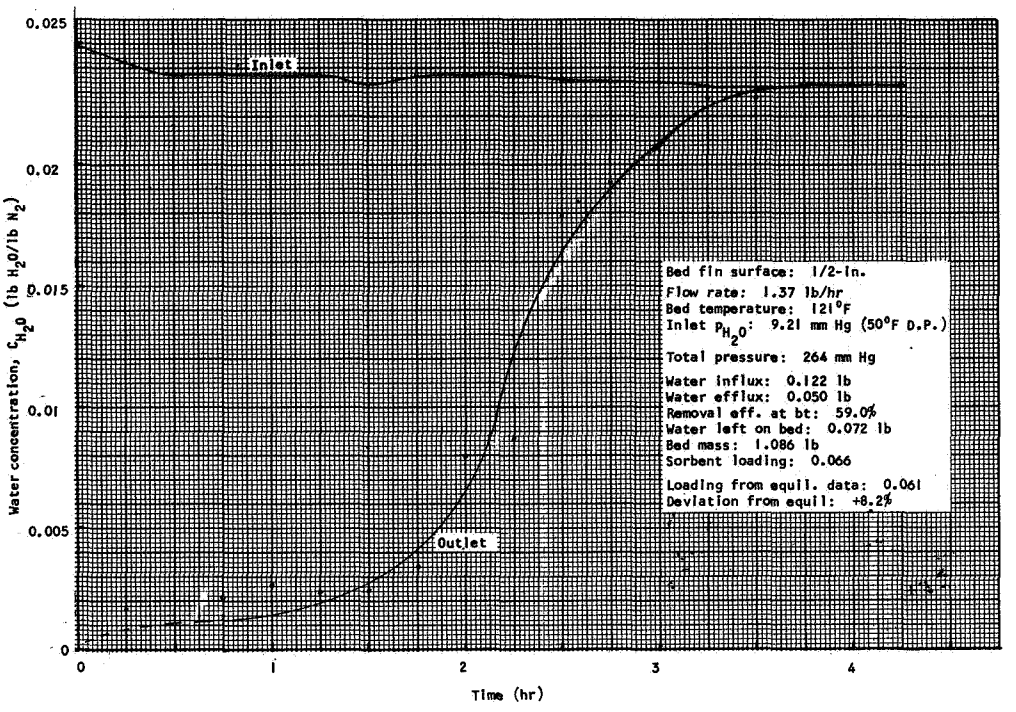

Figure 4-9. Water Vapor Adsorption Breakthrough on Silica Gel, Run No. SG/W(1/2)-3

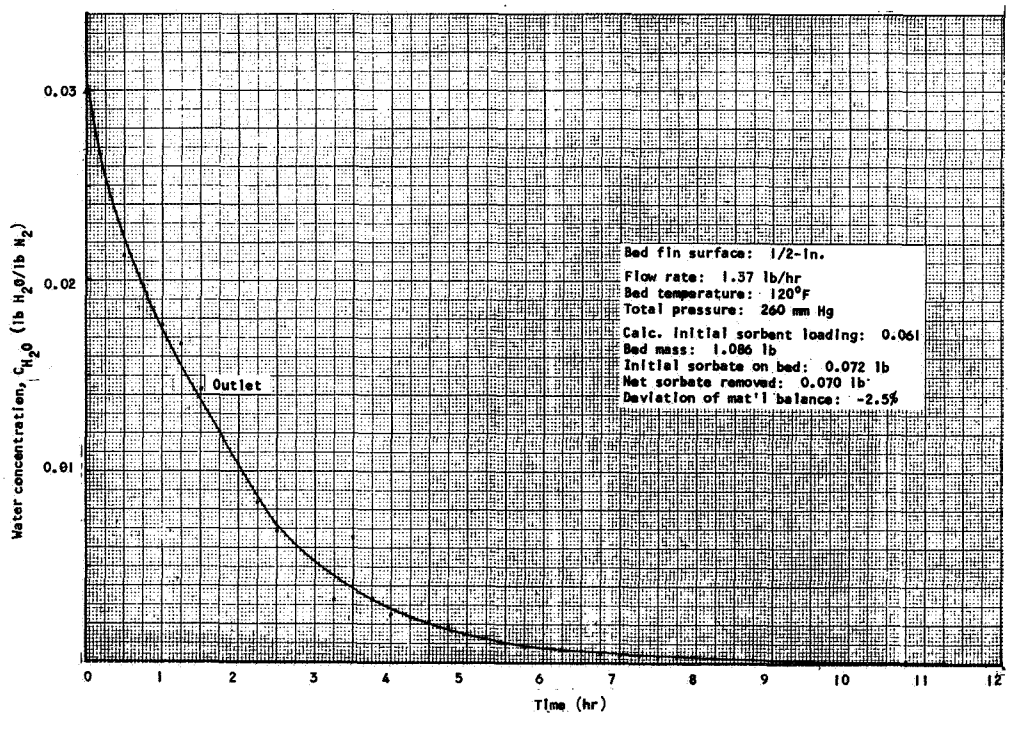

Figure 4-10. Gas Strip of Water from Silica Gel, Run No. SG/W(1/2)-4s

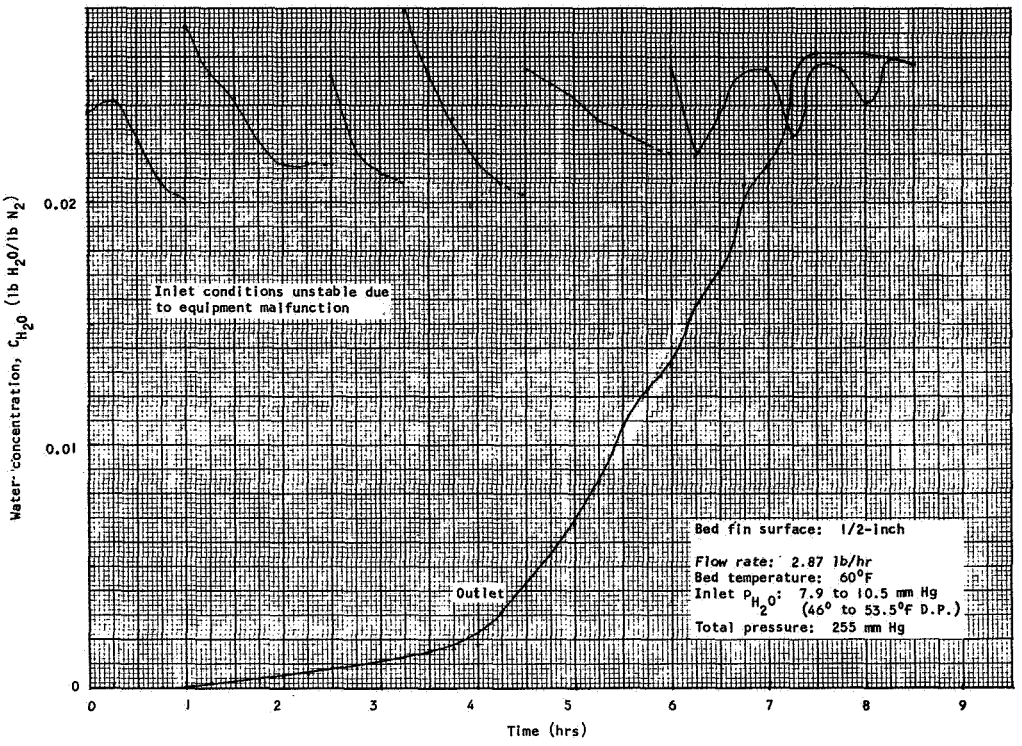

Figure 4-11. Water Vapor Adsorption Breakthrough on Silica Gel, Run No. SG/W(1/2)-5

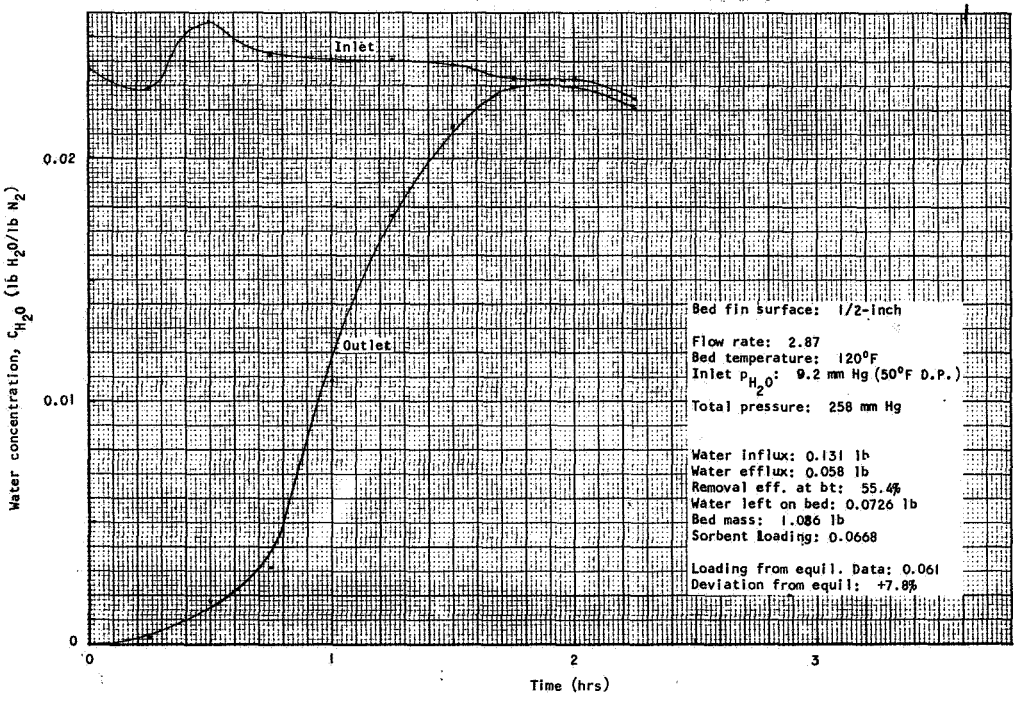

Figure 4-12. Water Vapor Adsorption Breakthrough on Silica Gel, Run No. SG/W(1/2)-6

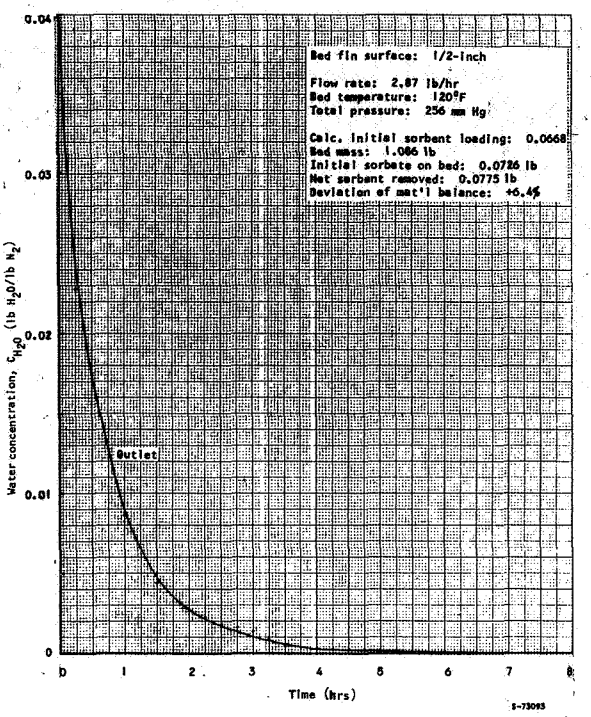

Figure 4-13. Gas Strip of Water from Silica Gel, Run No. SG/W(1/2)-7s

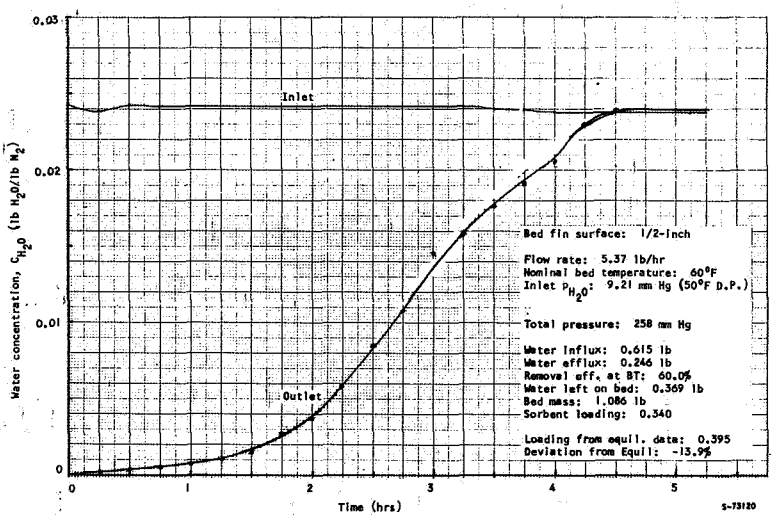

Figure 4-14. Water Vapor Adsorption Breakthrough on Silica Gel, Run No. SG/W(1/2)-8

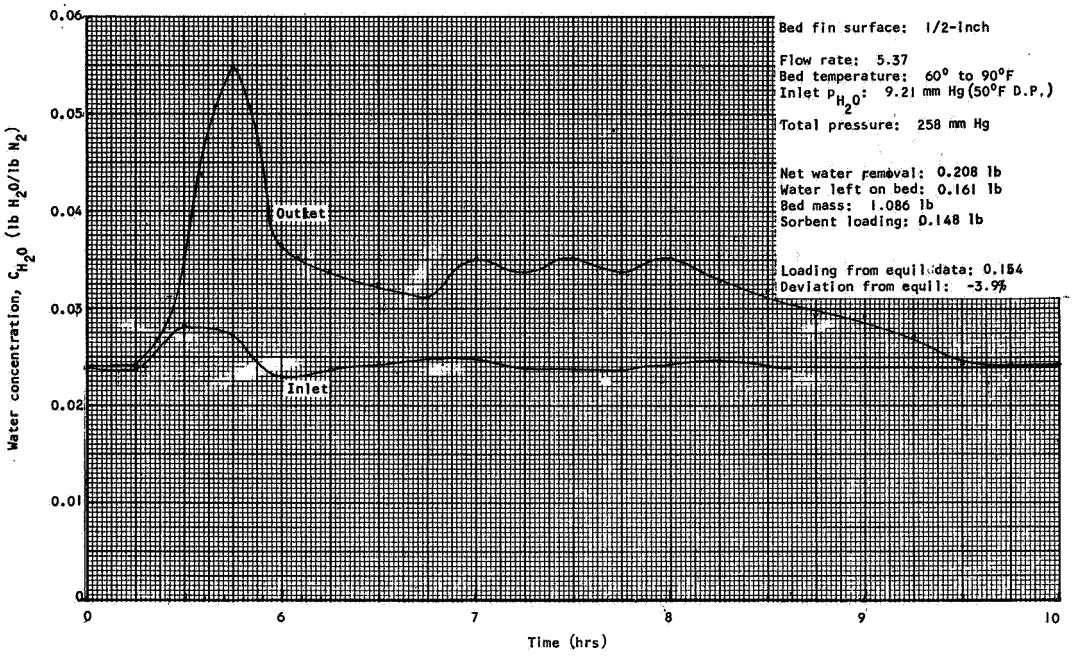

Figure 4-15. Water Vapor Adsorption Transition on Silica Gel, Run No. SG/W(1/2)-8

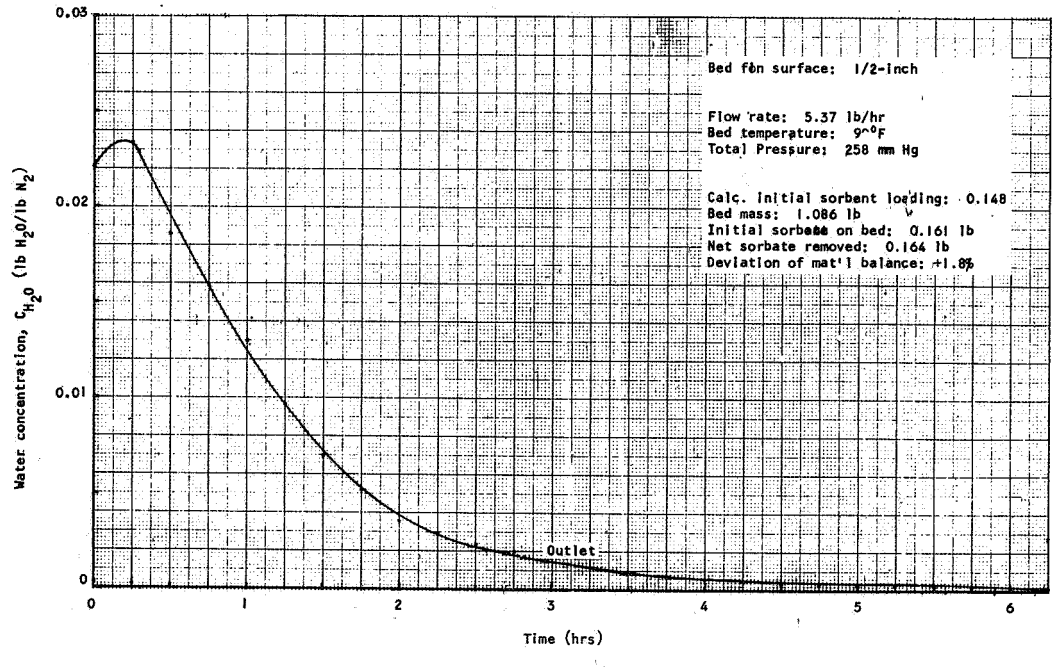

Figure 4-16. Gas Strip of Water From Silica Gel, Run No. SG/W(1/2)-9s

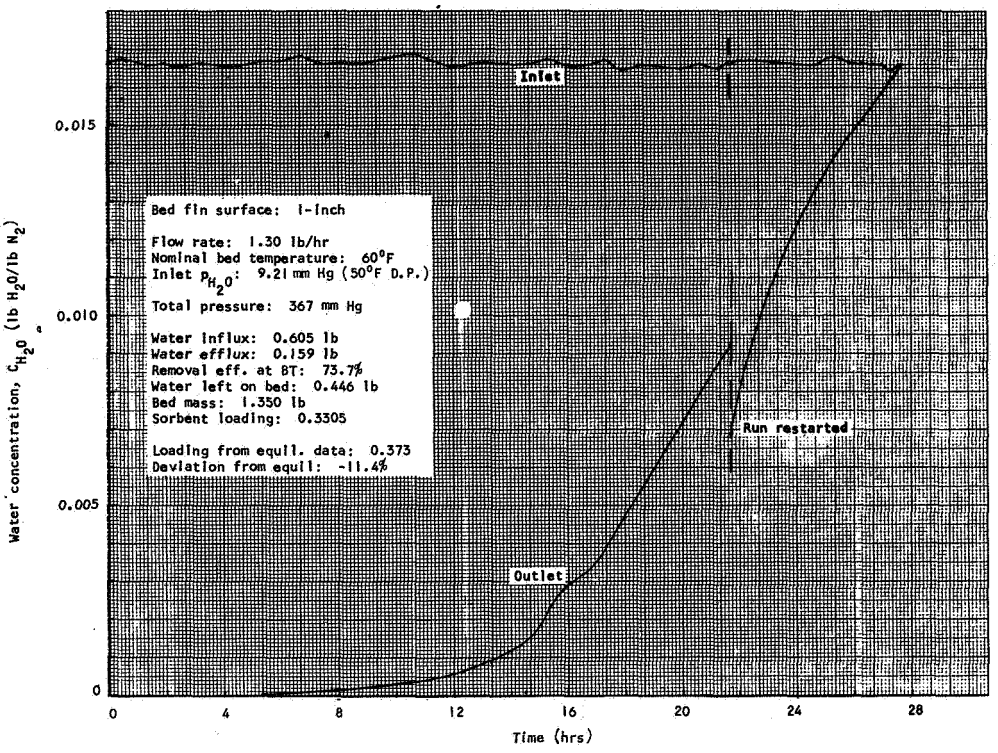

Figure 4-17. Water Vapor Adsorption Breakthrough on Silica Gel, Run No. SG/W(1)-1

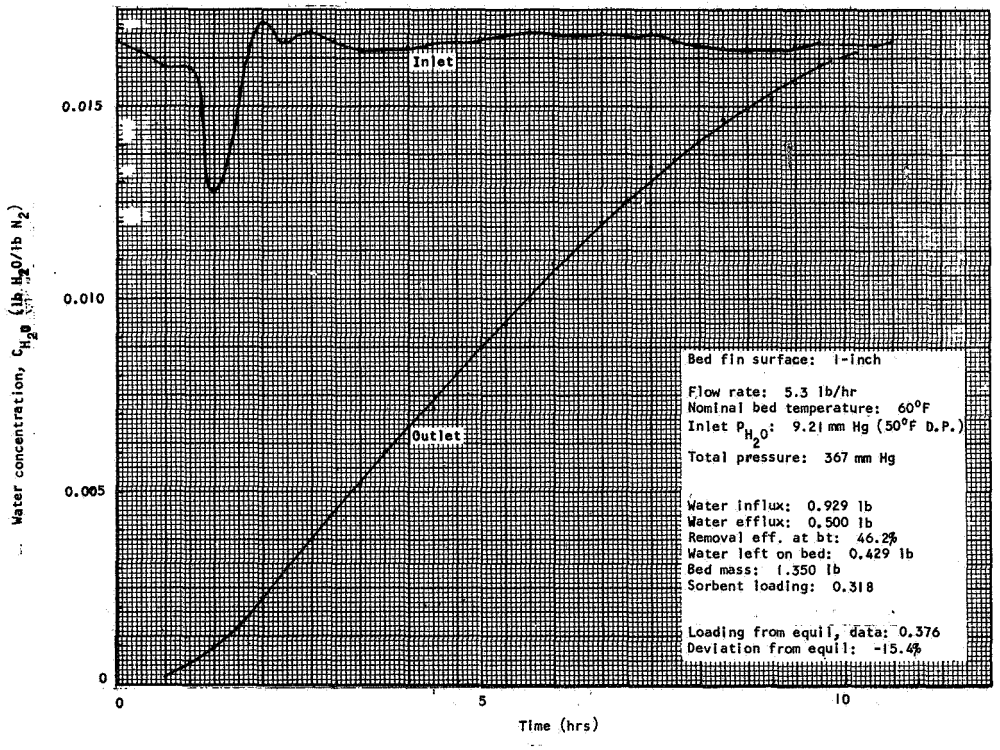

Figure 4-18. Water Vapor Adsorption Breakthrough on Silica Gel, Run No. SG/W(1)-2

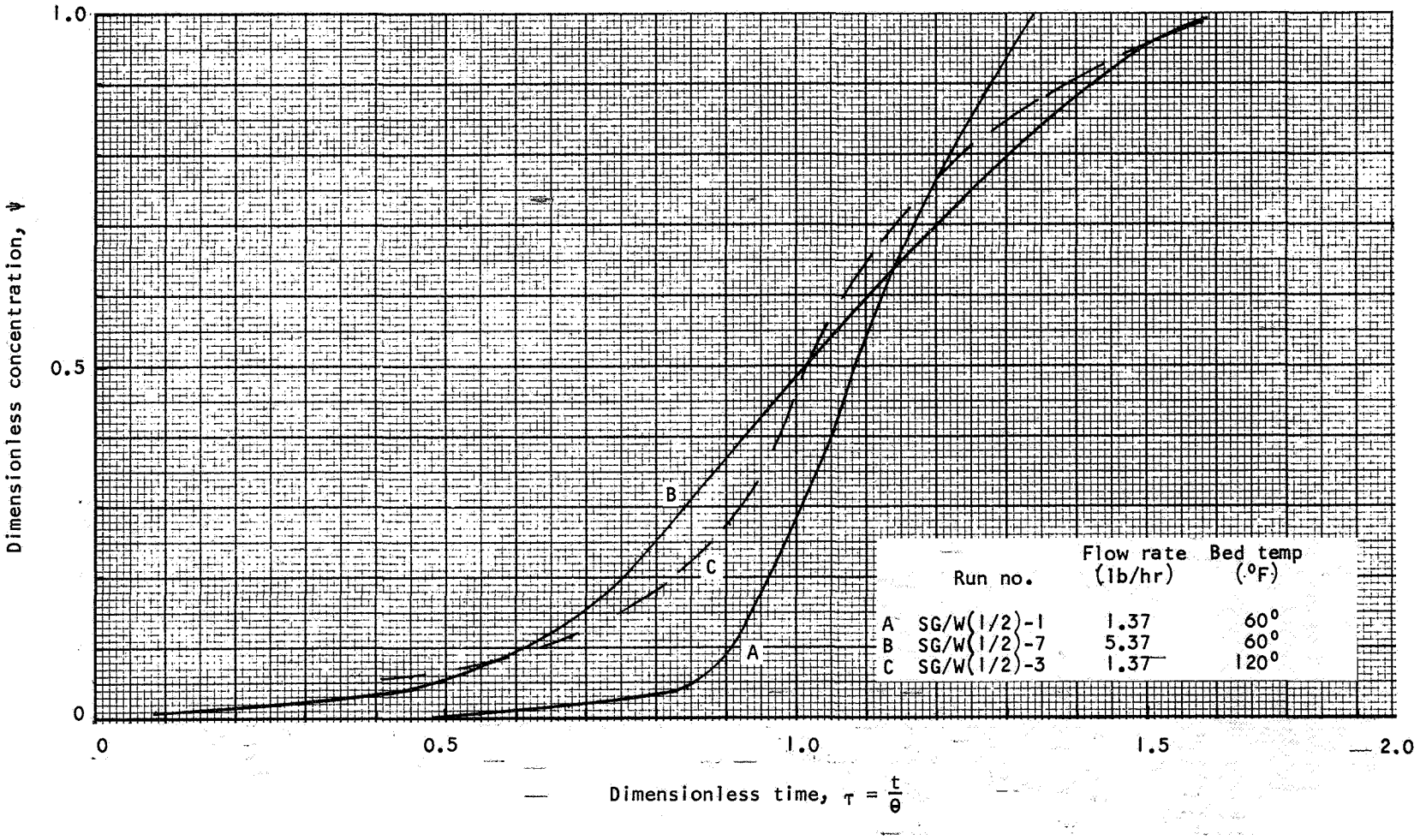

Figure 4-19. Dimensionless Breakthrough Curves, Adsorption of Water by Silica Gel

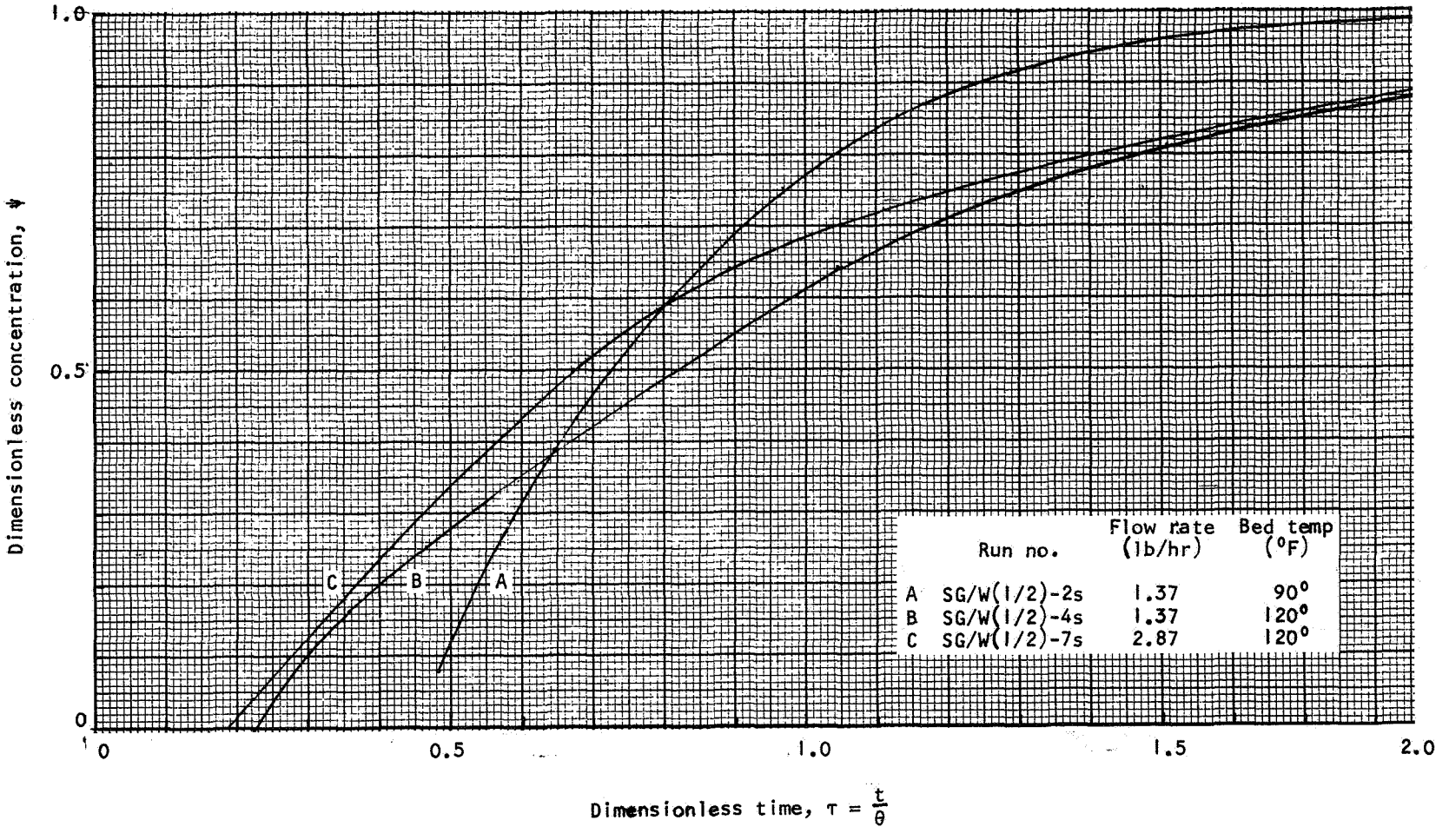

Figure 4-20. Dimensionless Breakthrough Curves, Gas Stripping of Water From Silica Gel

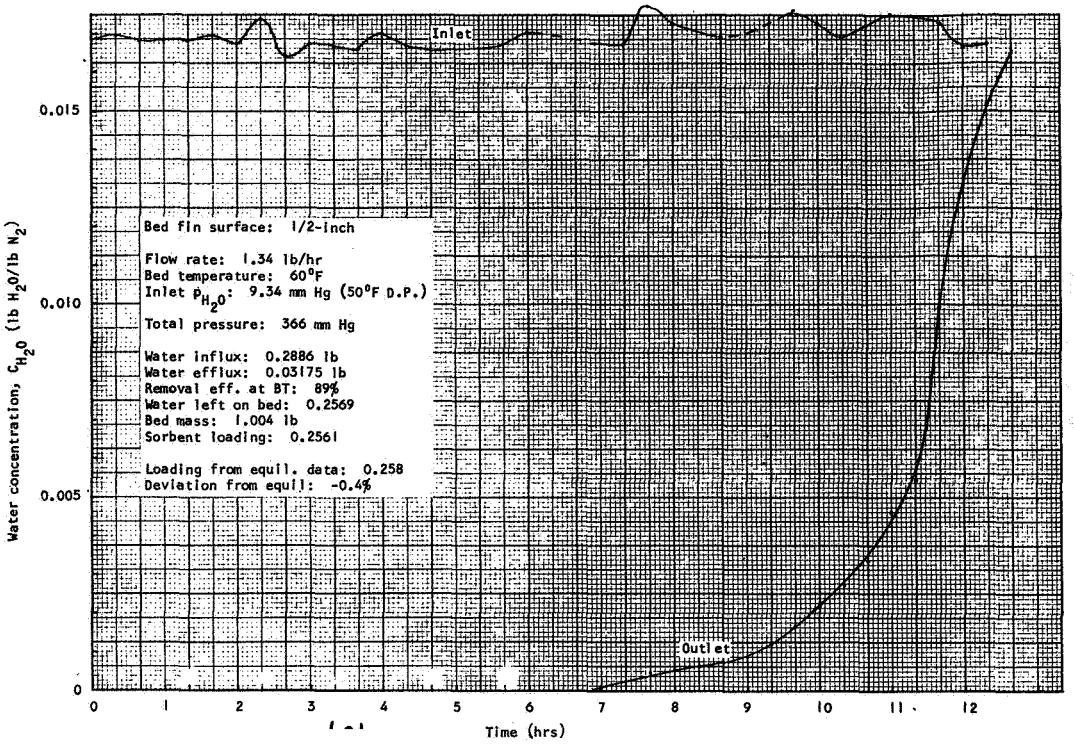

Figure 4-21. Water Vapor Adsorption Breakthrough on Linde 13X, Run No. 13X/W(1/2)-1

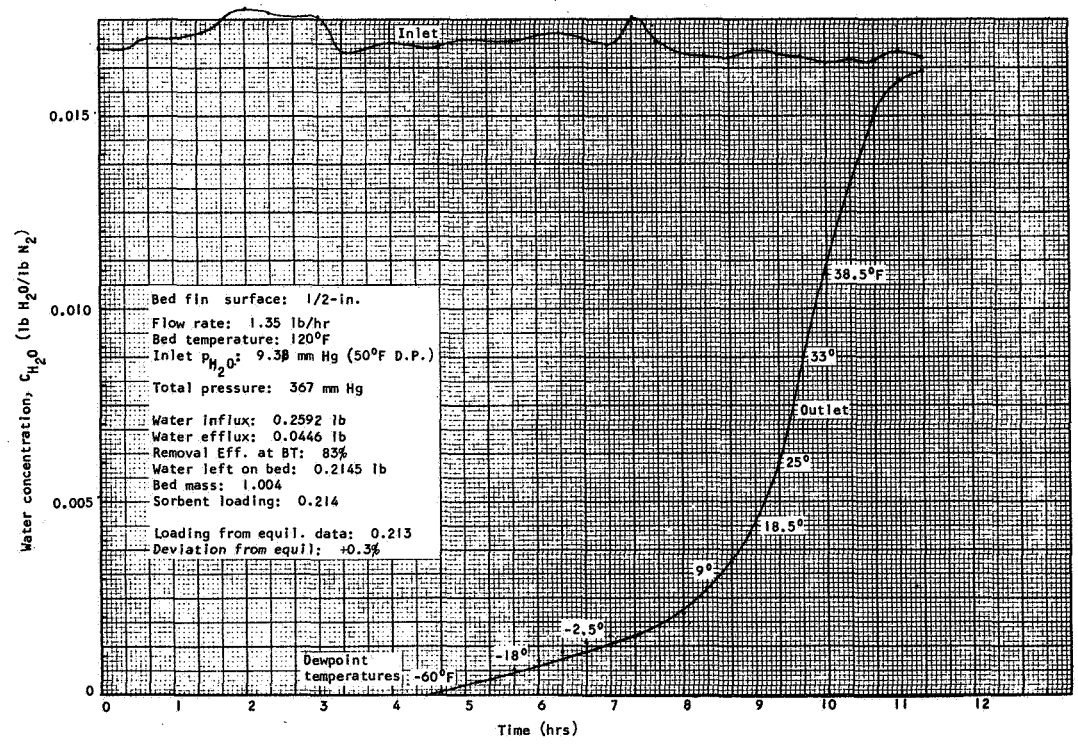

Figure 4-22. Water Vapor Adsorption Breakthrough on Linde 13X, Run No. 13X/W(1/2)-2

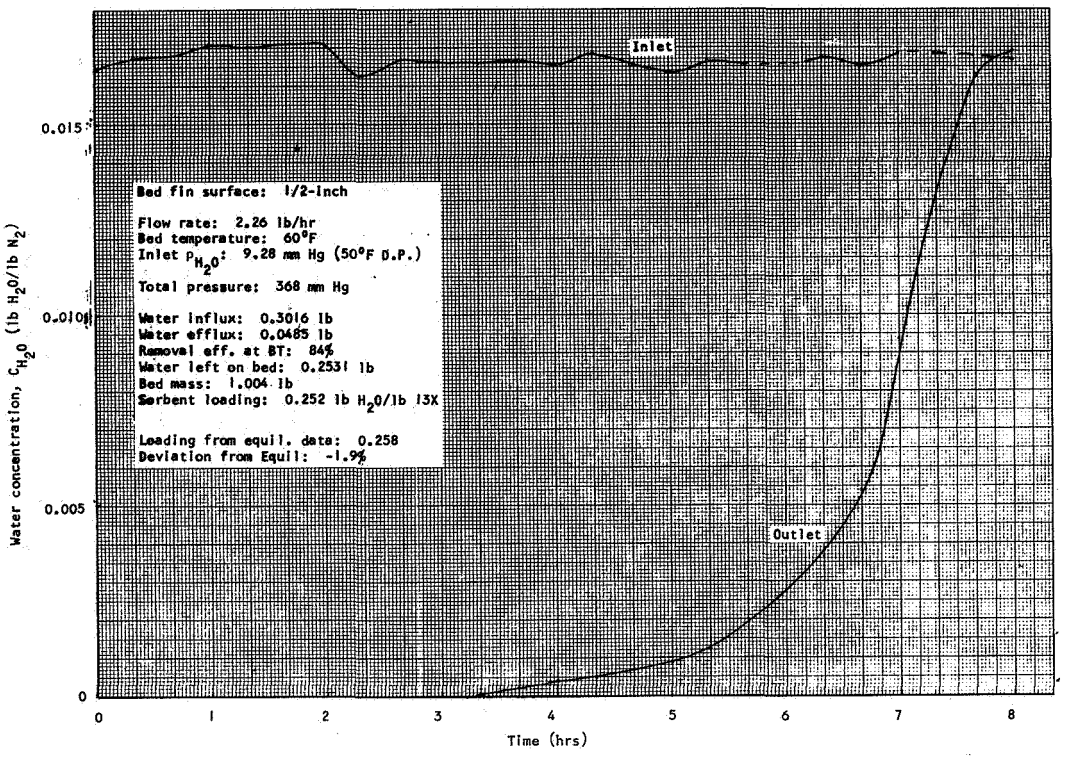

Figure 4-23. Water Vapor Adsorption Breakthrough on Linde 13X, Run No. 13X/W(1/2)-3

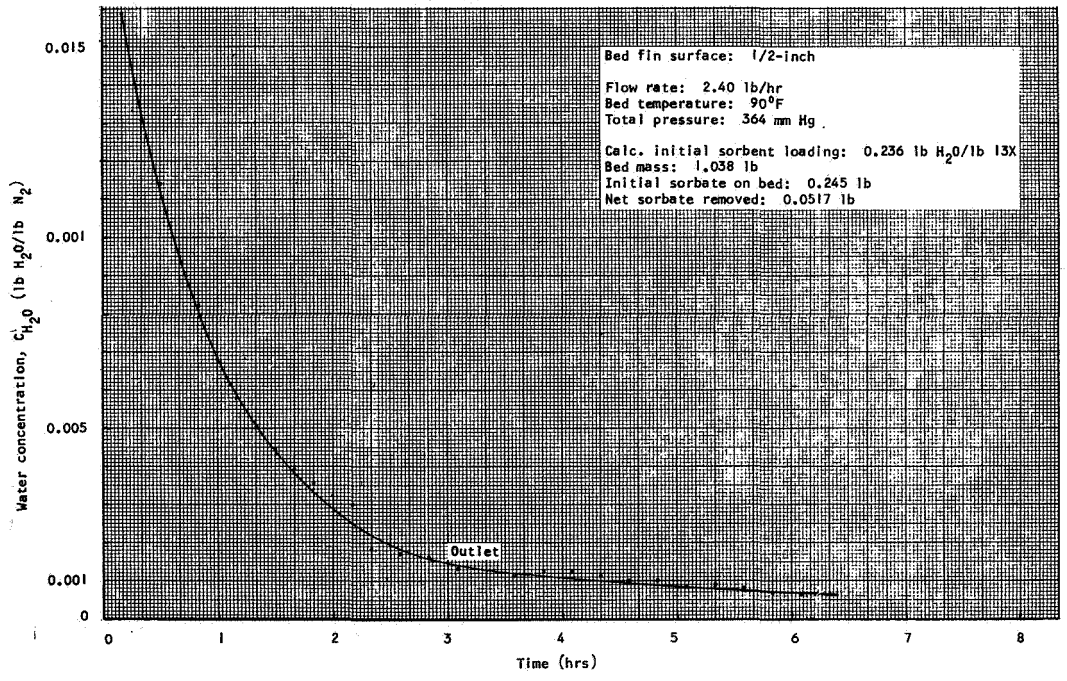

Figure 4-24. Gas Strip of Water from Linde 13X, Run No. 13X/W(1/2)-4s

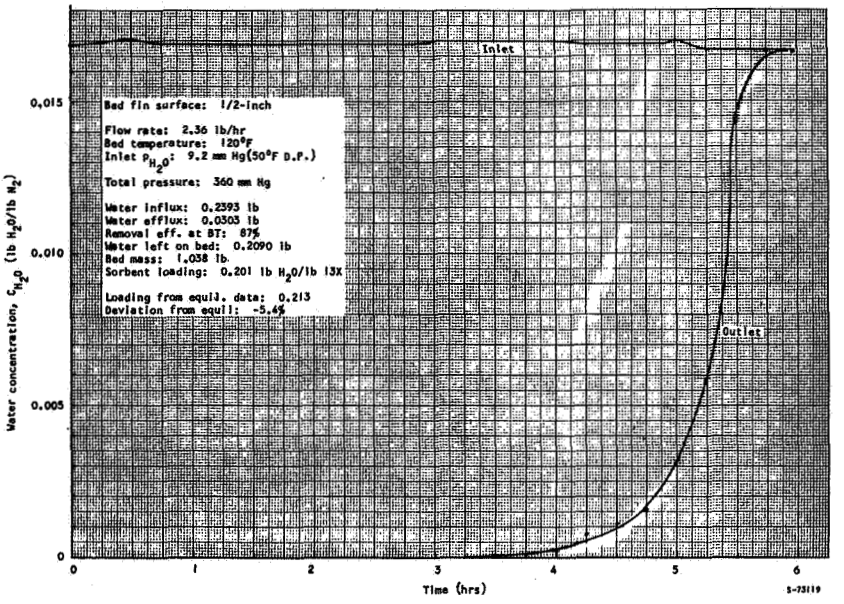

Figure 4-25. Water Vapor Adsorption Breakthrough on Linde 13X, Run No. 13X/W(1/2)-5

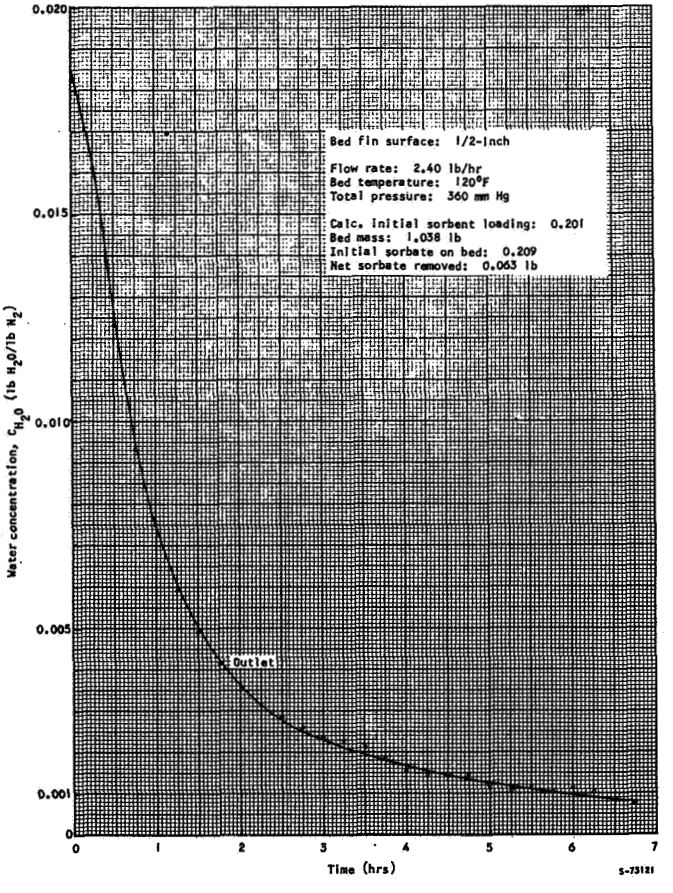

Figure 4-26. Gas Strip of Water From Linde 13X, Run No. 13X/W(1/2)-6s

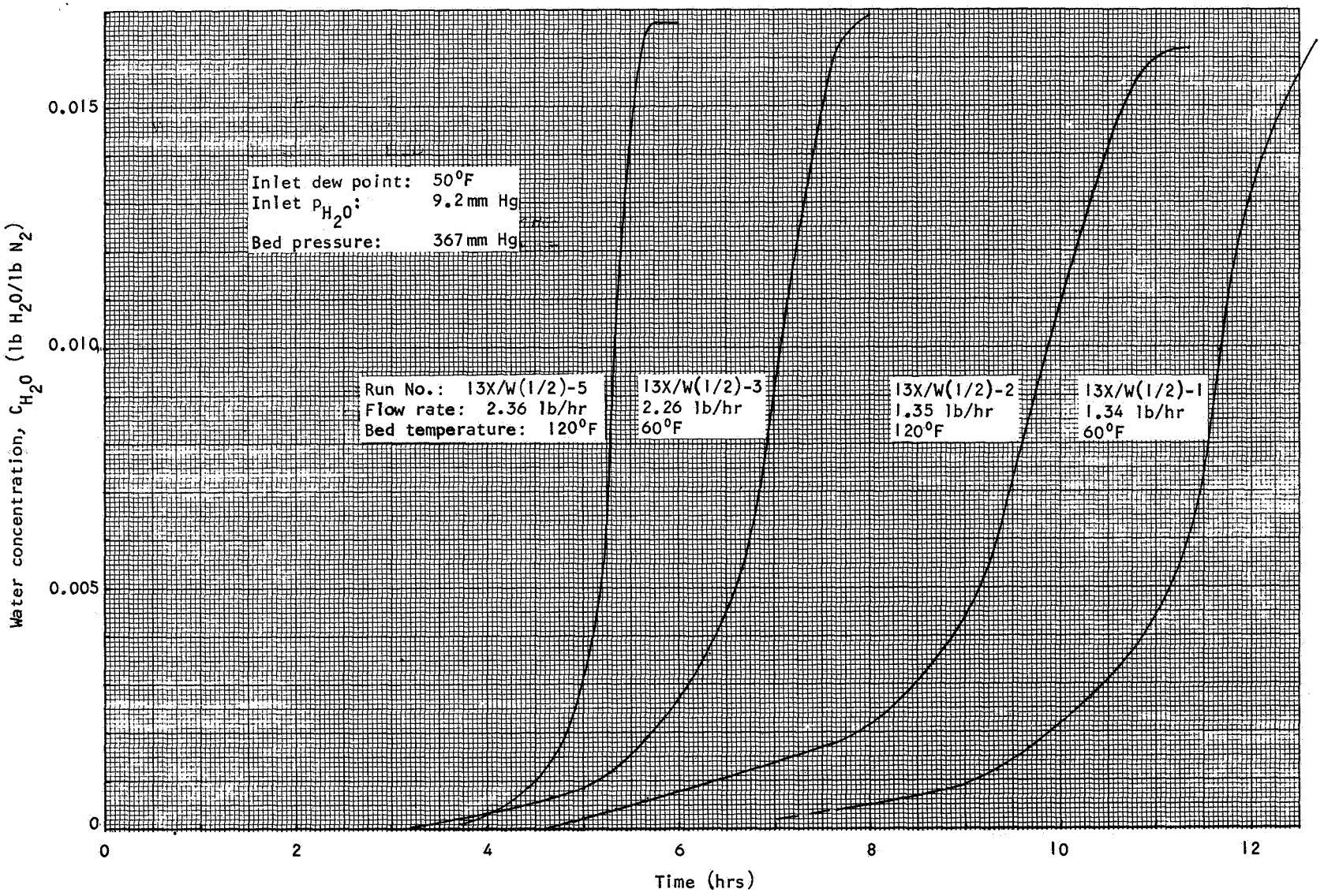

Figure 4-27. Water Vapor Adsorption Breakthrough Curves for Linde 13X

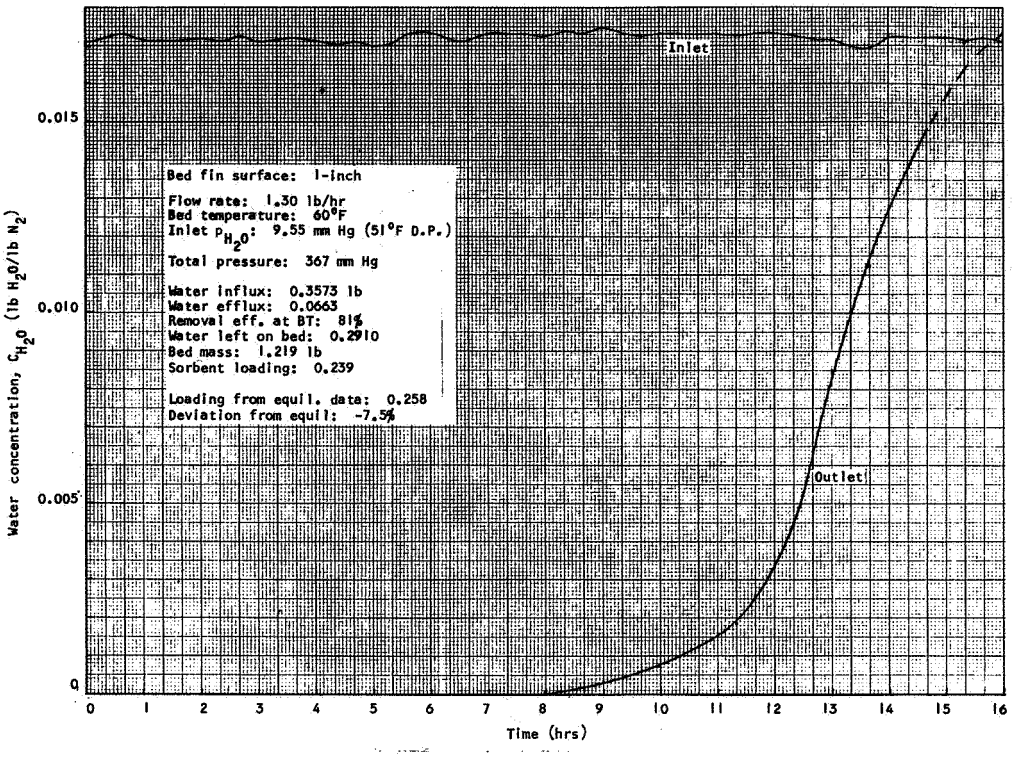

Figure 4-28. Water Vapor Adsorption Breakthrough on Linde 13X, Run No. 13X/W(1)-1

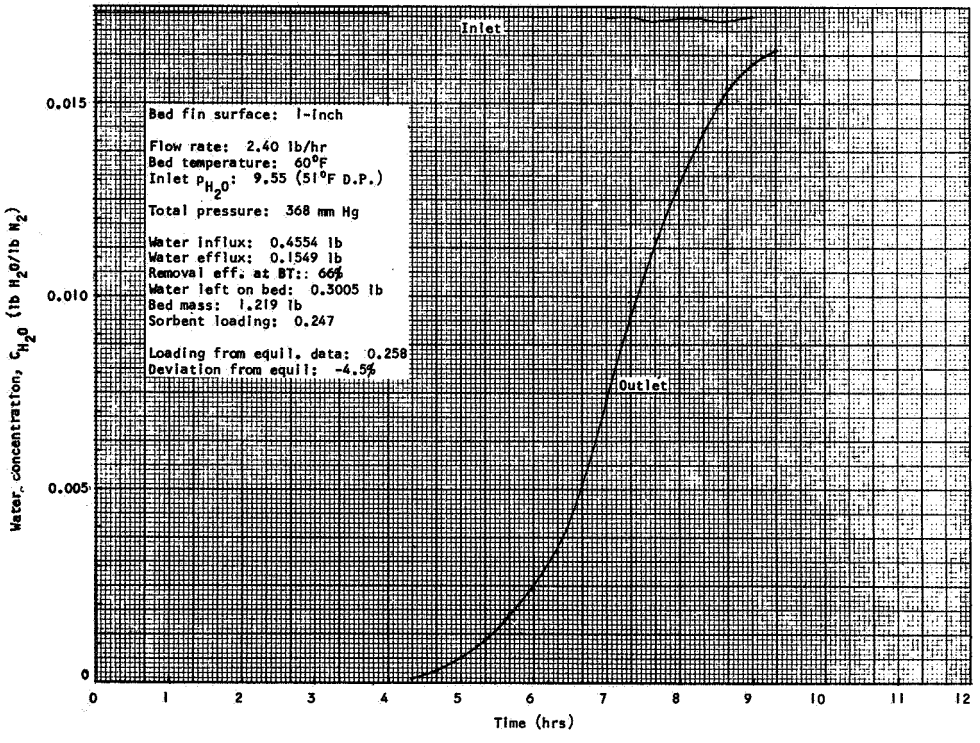

Figure 4-29. Water Vapor Adsorption Breakthrough on Linde 13X, Run No. 13X/W(1)-2

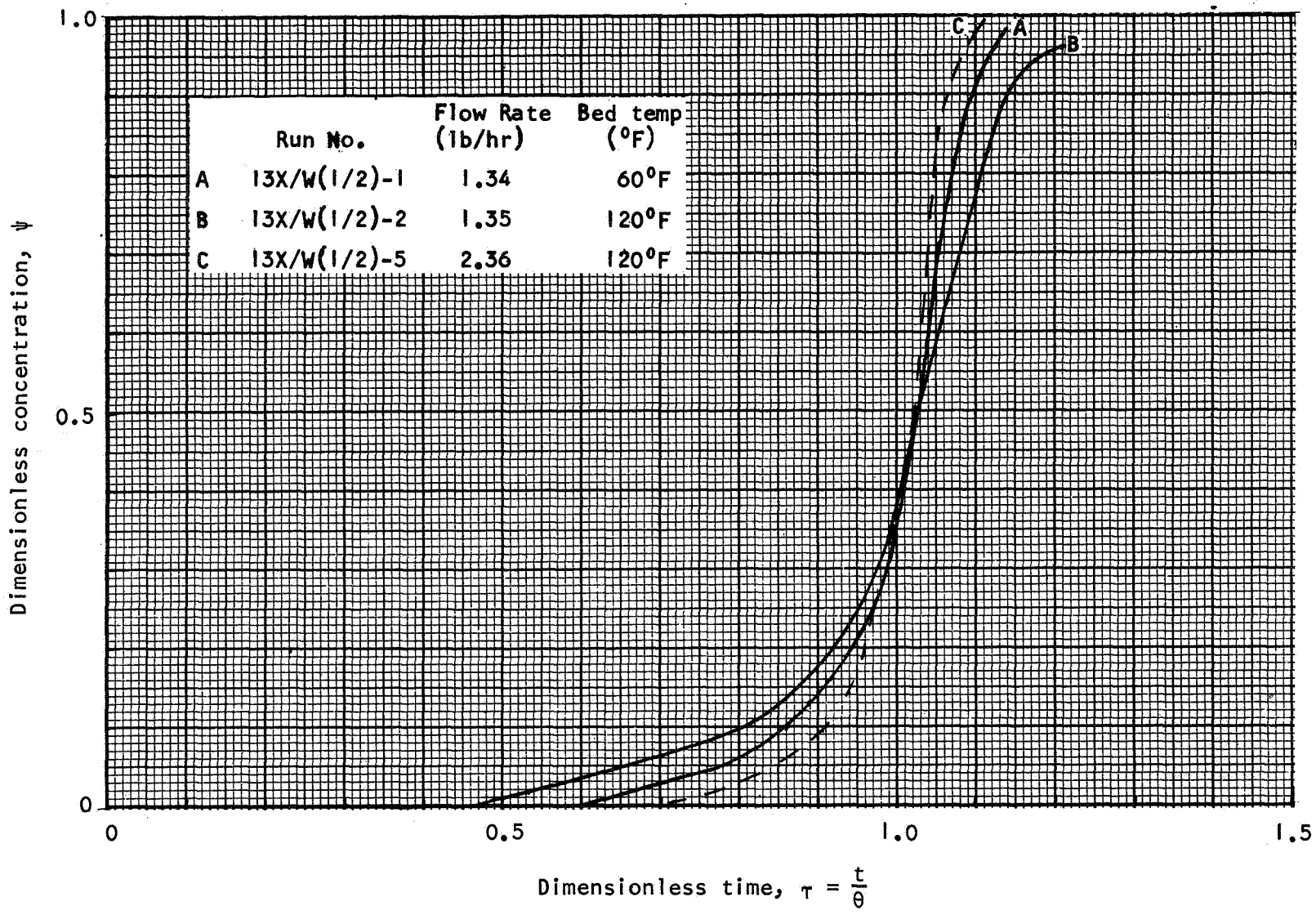

Figure 4-30. Dimensionless Breakthrough Curves, Adsorption of Water by Linde 13X

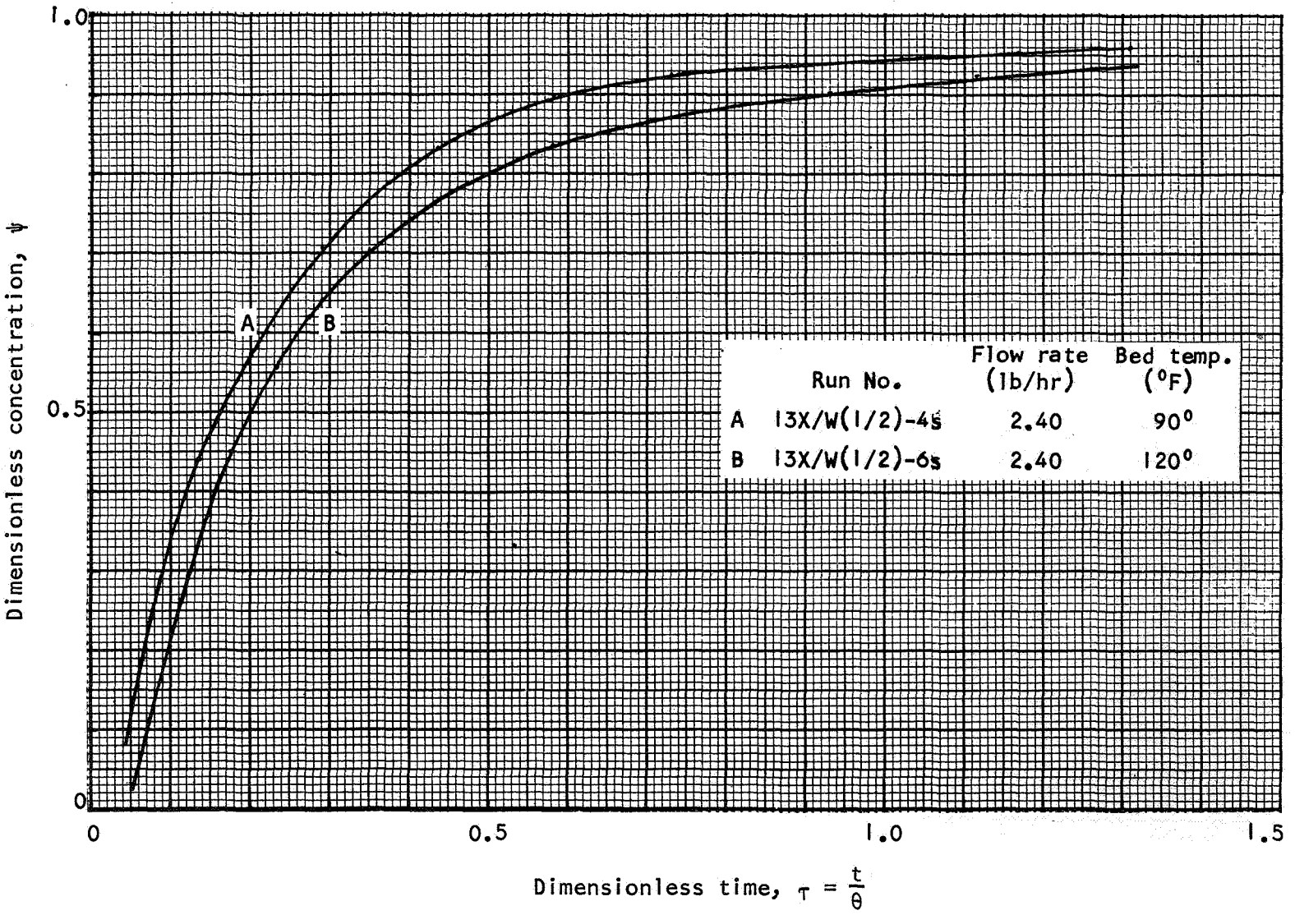

Figure 4-31. Dimensionless Breakthrough Curves, Gas Stripping of Water From Linde 13X

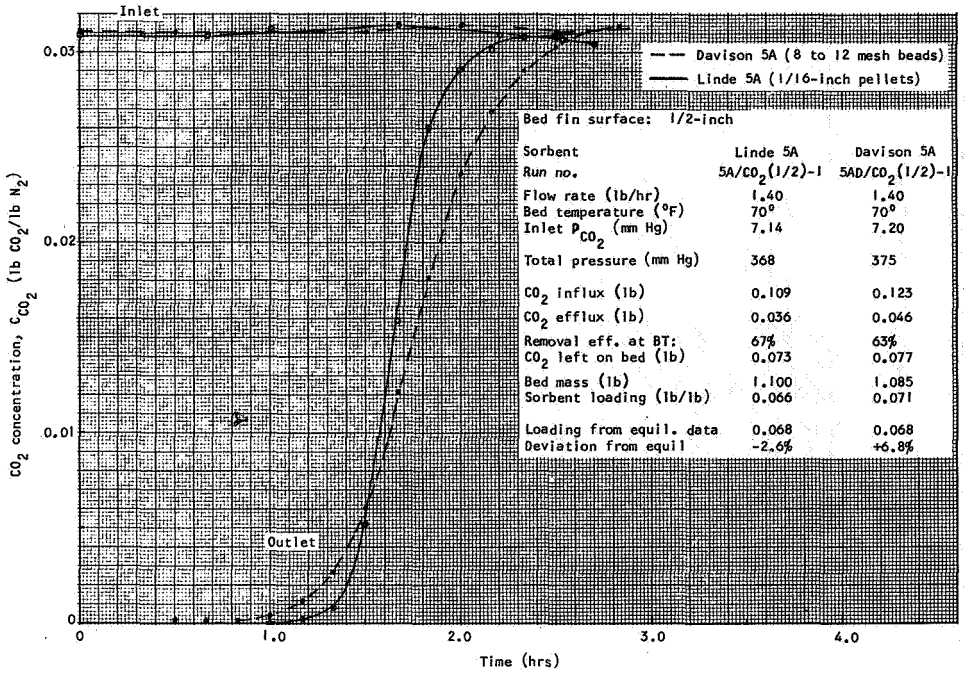

Figure 4-32. CO_2 Adsorption Breakthroughs on Type 5A Molecular Sieves (1.4 lb/hr)

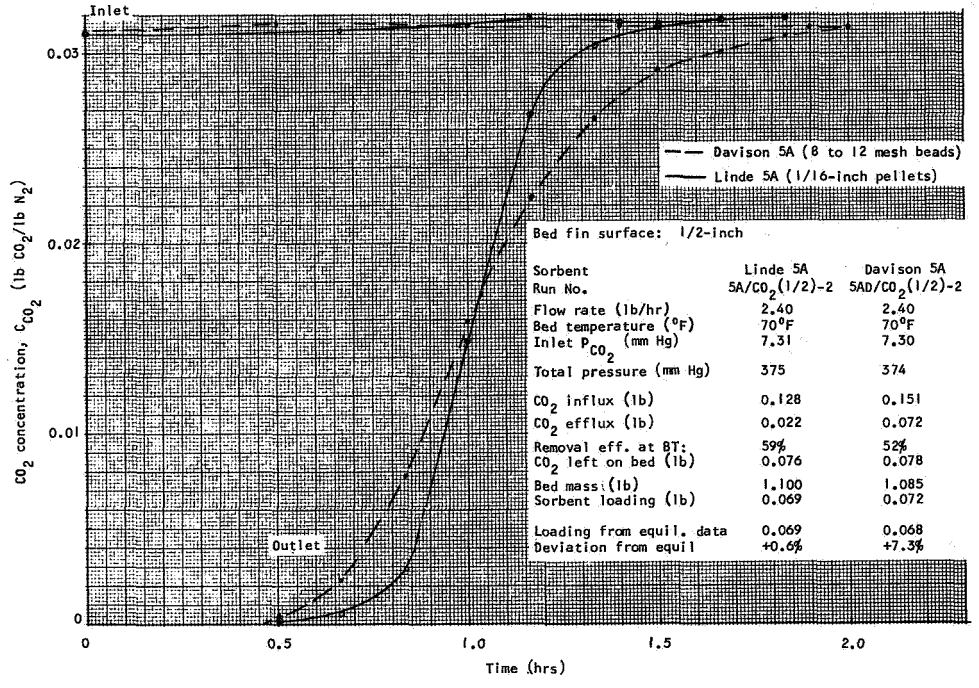

Figure 4-33. CO_2 Adsorption Breakthroughs on Type 5A Molecular Sieves (2.40 lb/hr)

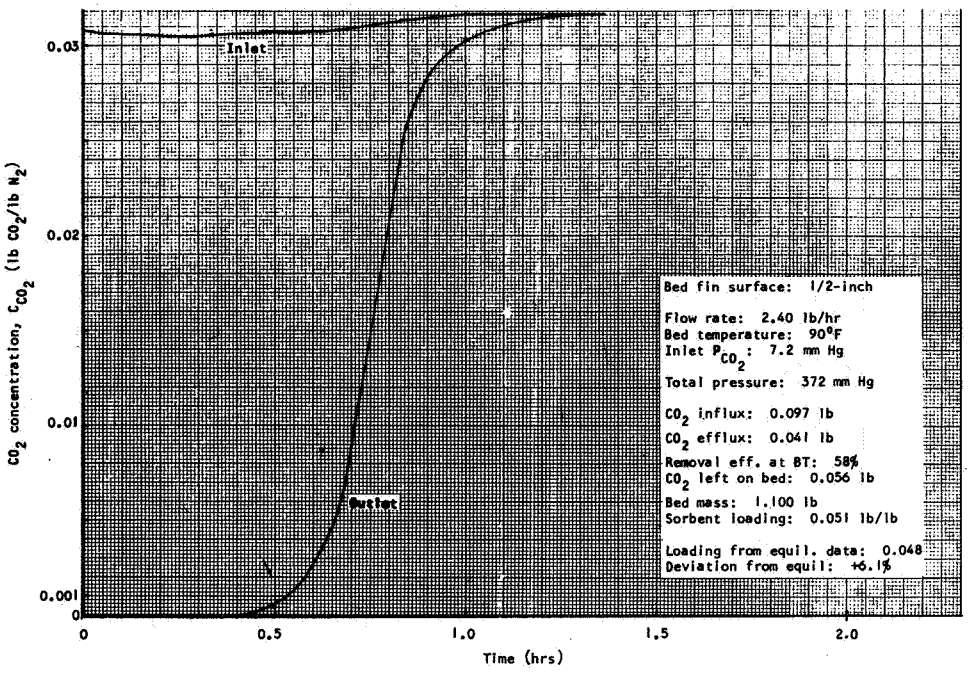

Figure 4-34. CO_2 Adsorption Breakthrough on Linde 5A, Run No. 5A/CO_2(1/2)-3

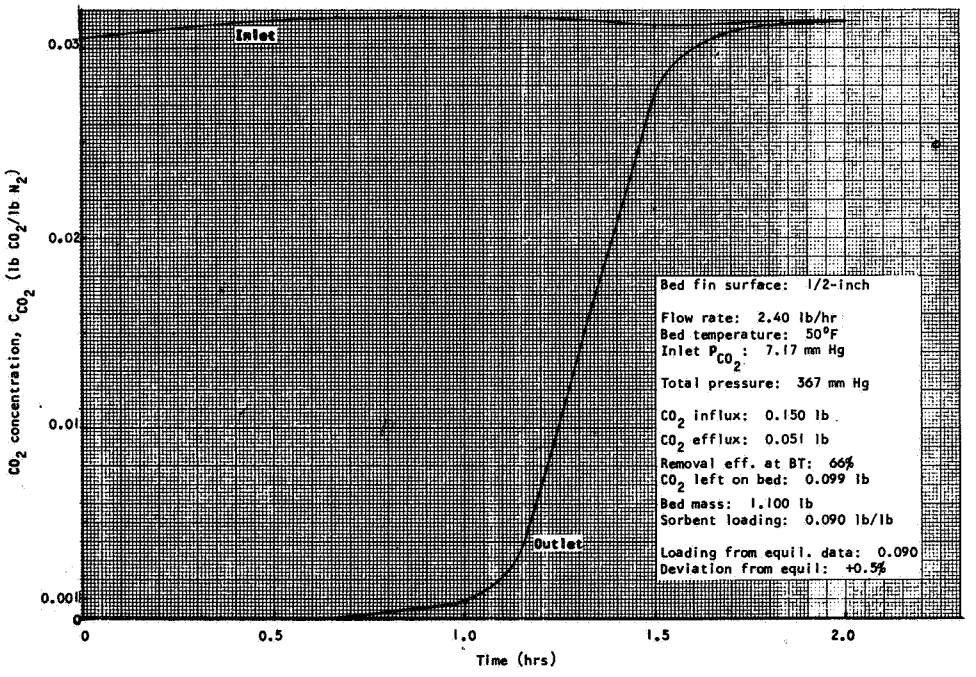

Figure 4-35. CO_2 Adsorption Breakthrough on Linde 5A, Run No. 5A/CO_2(1/2)-4

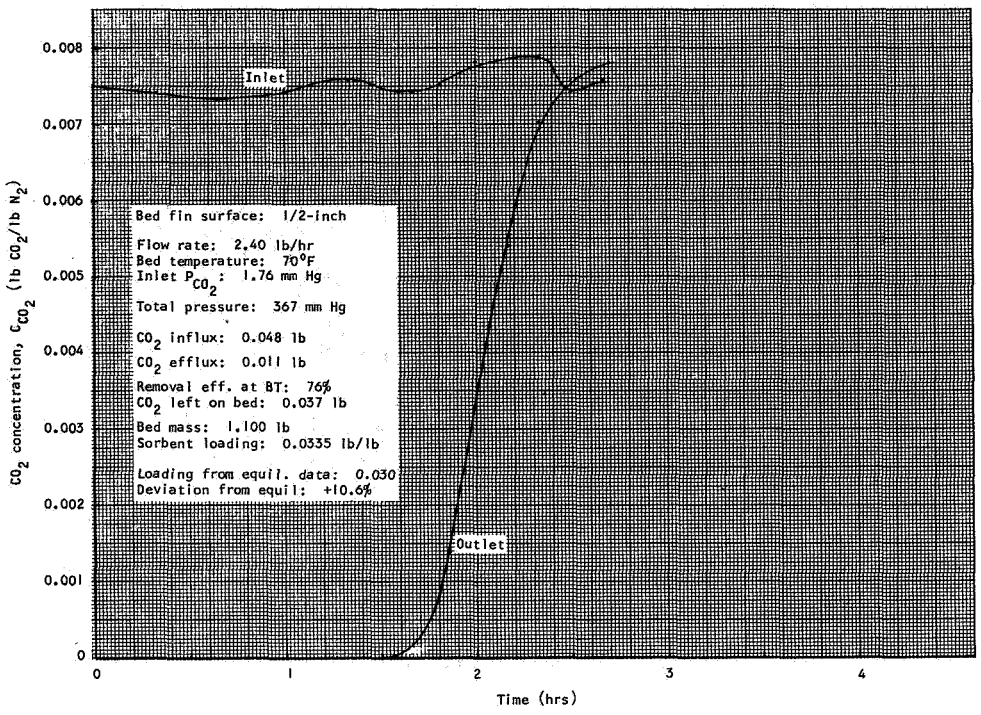

Figure 4-36. CO_2 Adsorption Breakthrough on Linde 5A, Run No. 5A/CO_2(1/2)-5

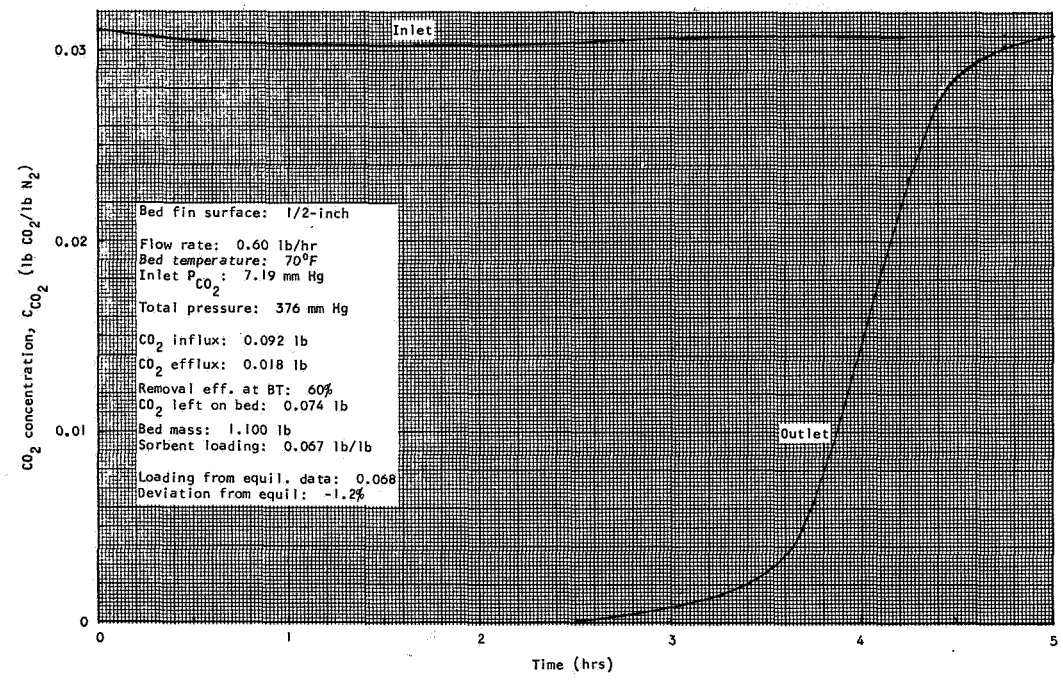

Figure 4-37. CO_2 Adsorption Breakthrough on Linde 5A, Run No. 5A/CO_2(1/2)-6

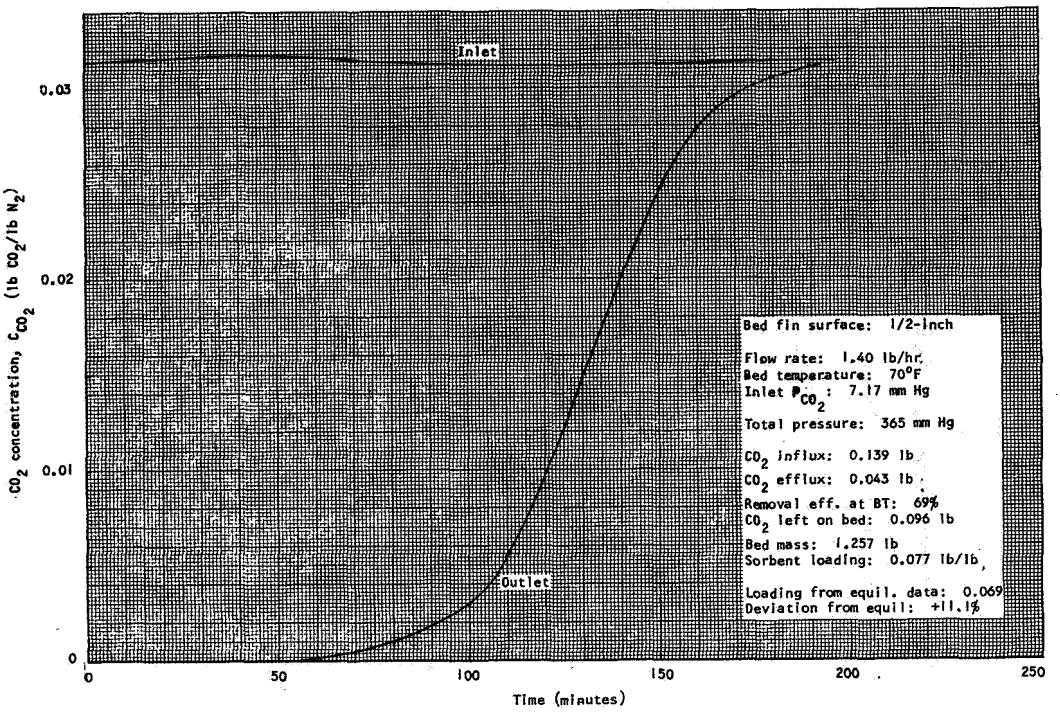

Figure 4-38. CO_2 Adsorption Breakthrough on Linde 5A, Run No. 5A/CO_2(1/2)-7

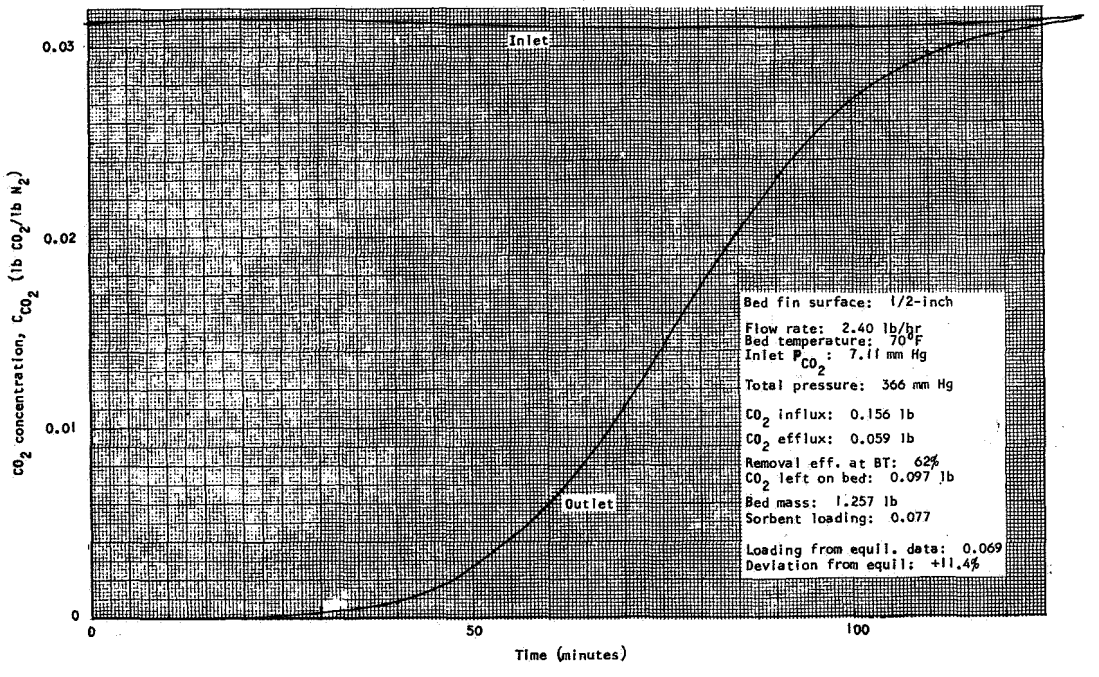

Figure 4-39. CO_2 Adsorption Breakthrough on Linde 5A, Run No. 5A/CO_2(1/2)-8

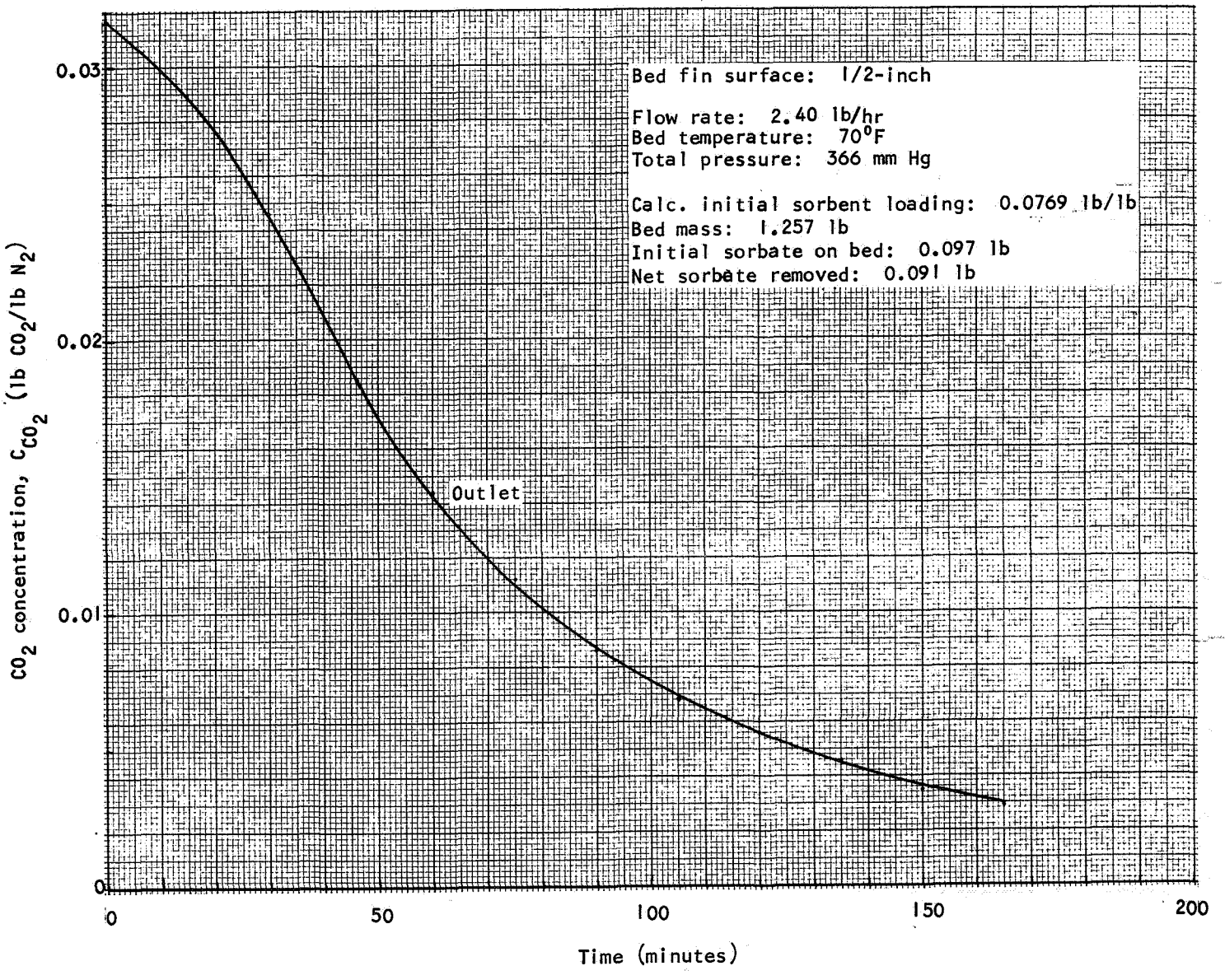

Figure 4-40. Gas Strip of CO_2 From Linde 5A, Run No. 5A/CO_2(1/2)-9s

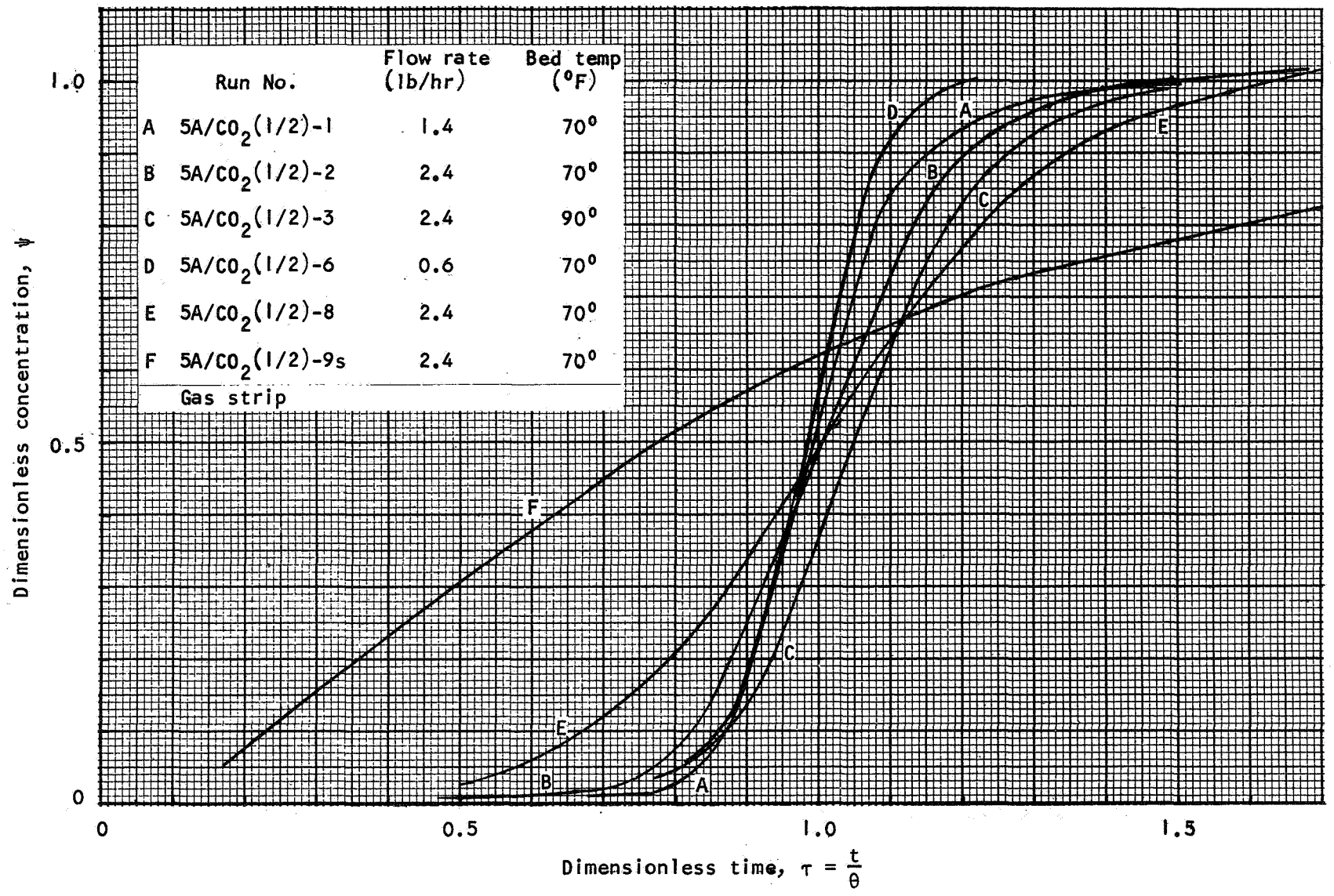

Figure 4-41. Dimensionless Breakthrough Curves, Adsorption of CO_2 by Linde 5A

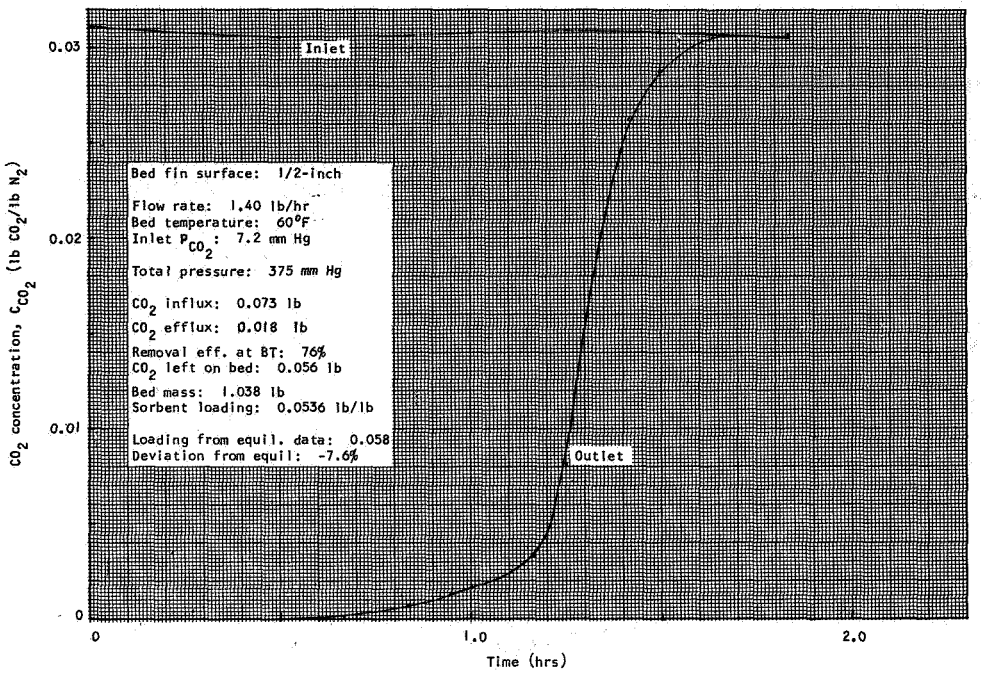

Figure 4-42. CO_2 Adsorption Breakthrough on Linde 13X, Run No. 13X/CO_2(1/2)-1

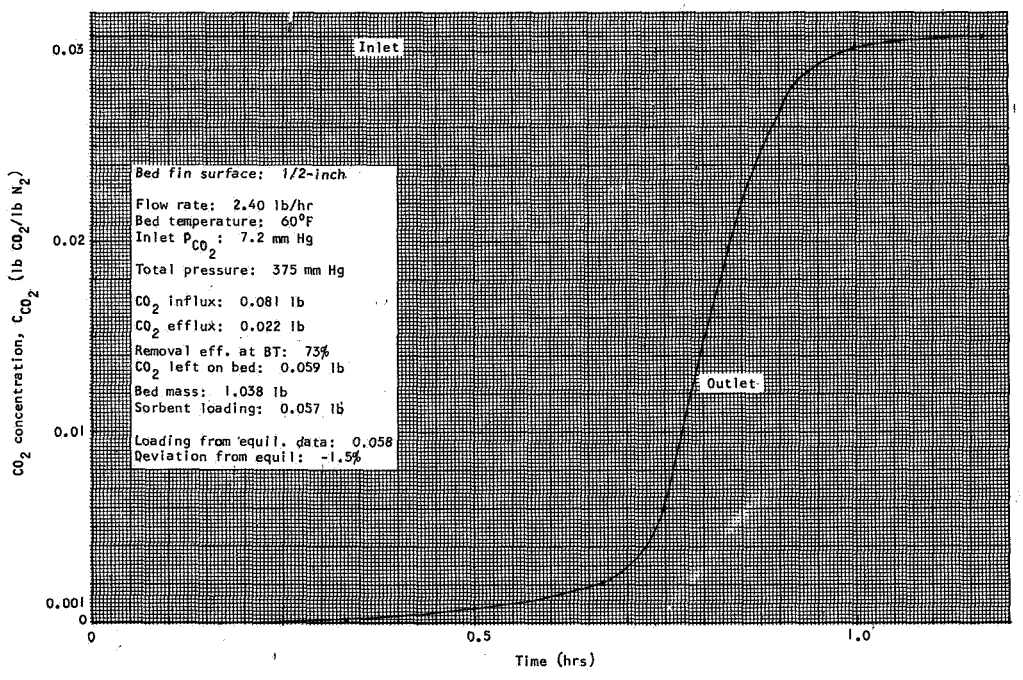

Figure 4-43. CO_2 Adsorption Breakthrough on Linde 13X, Run No. 13X/CO_2(1/2)-2

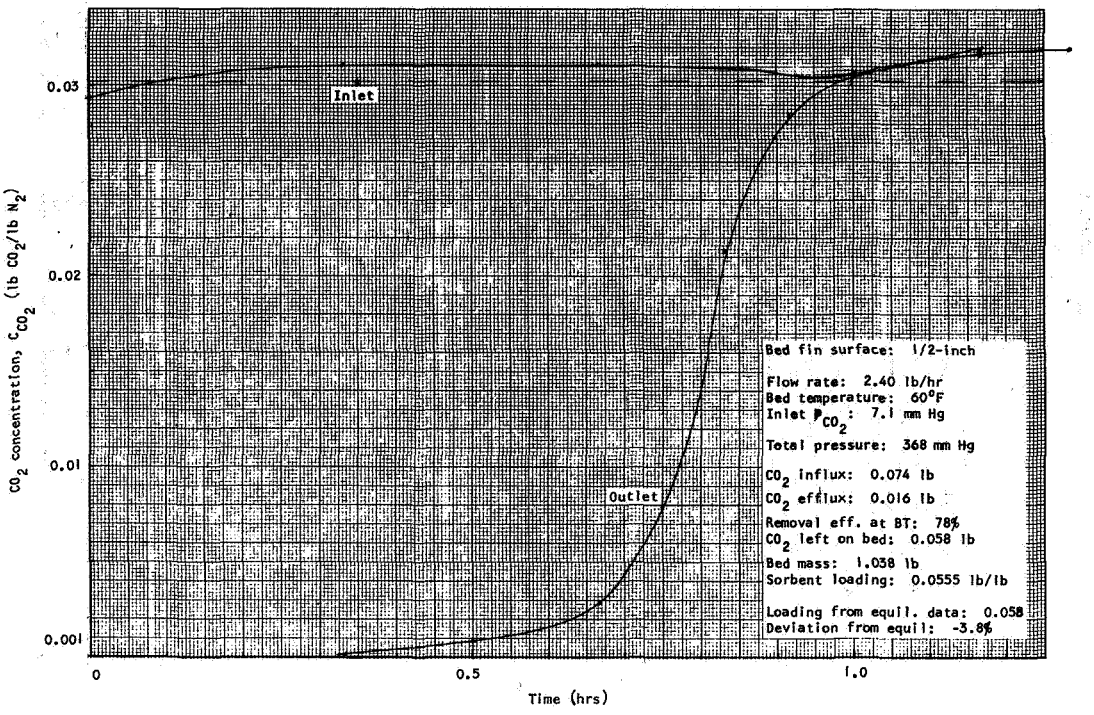

Figure 4-44. CO_2 Adsorption Breakthrough on Linde 13X, Run No. 13X/CO_2(1/2)-3

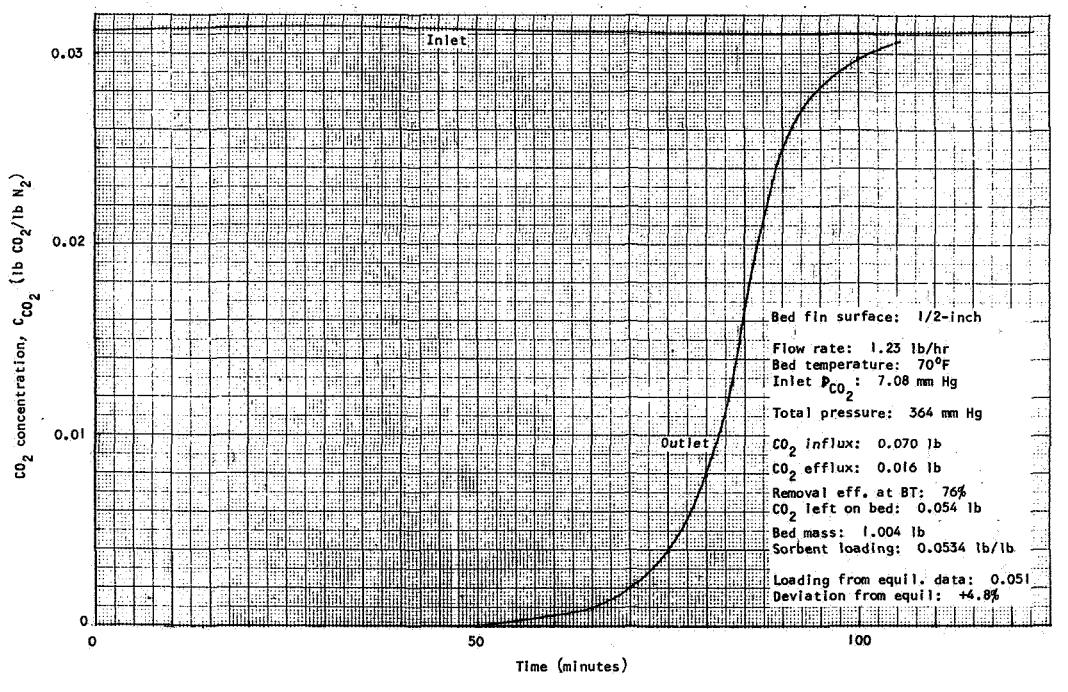

Figure 4-45. CO_2 Adsorption Breakthrough on Linde 13X, Run No. 13X/CO_2(1/2)-4

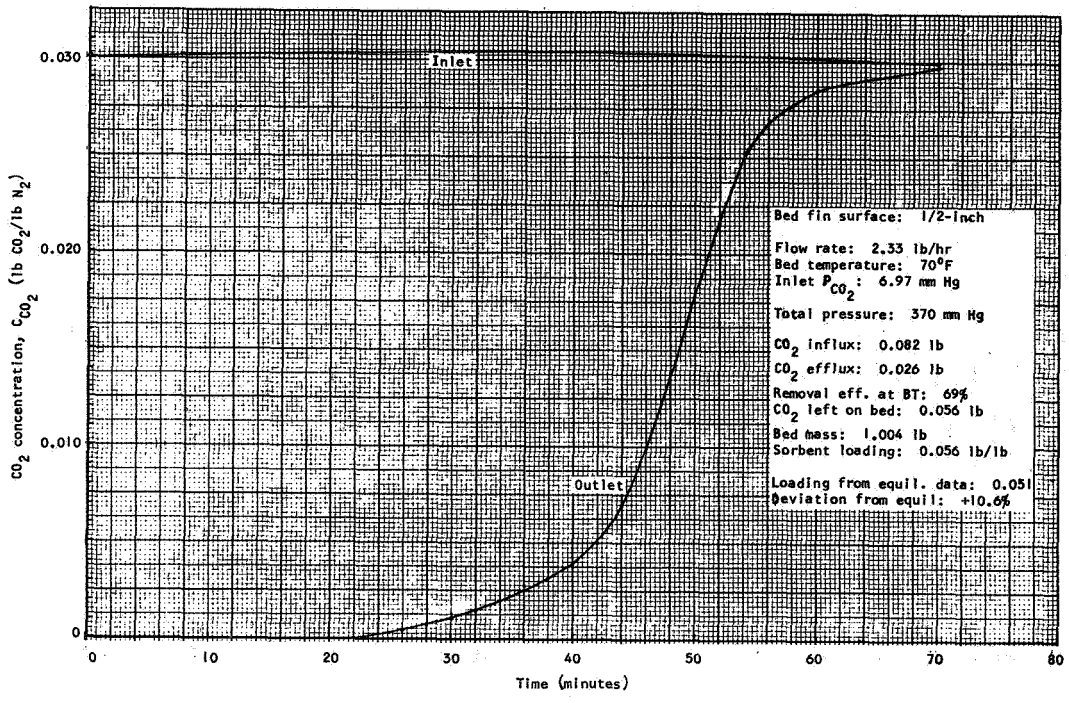

Figure 4-46. CO_2 Adsorption Breakthrough on Linde 13X, Run No. 13X/CO_2(1/2)-5

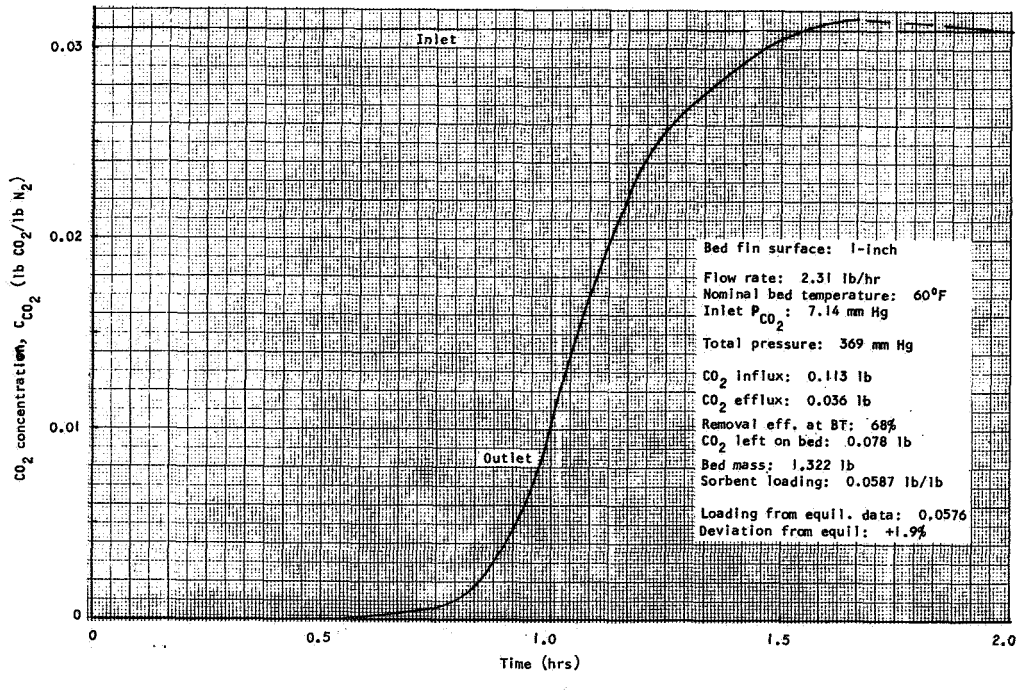

Figure 4-47. CO_2 Adsorption Breakthrough on Linde 13X, Run No. 13X/CO_2(1)-1

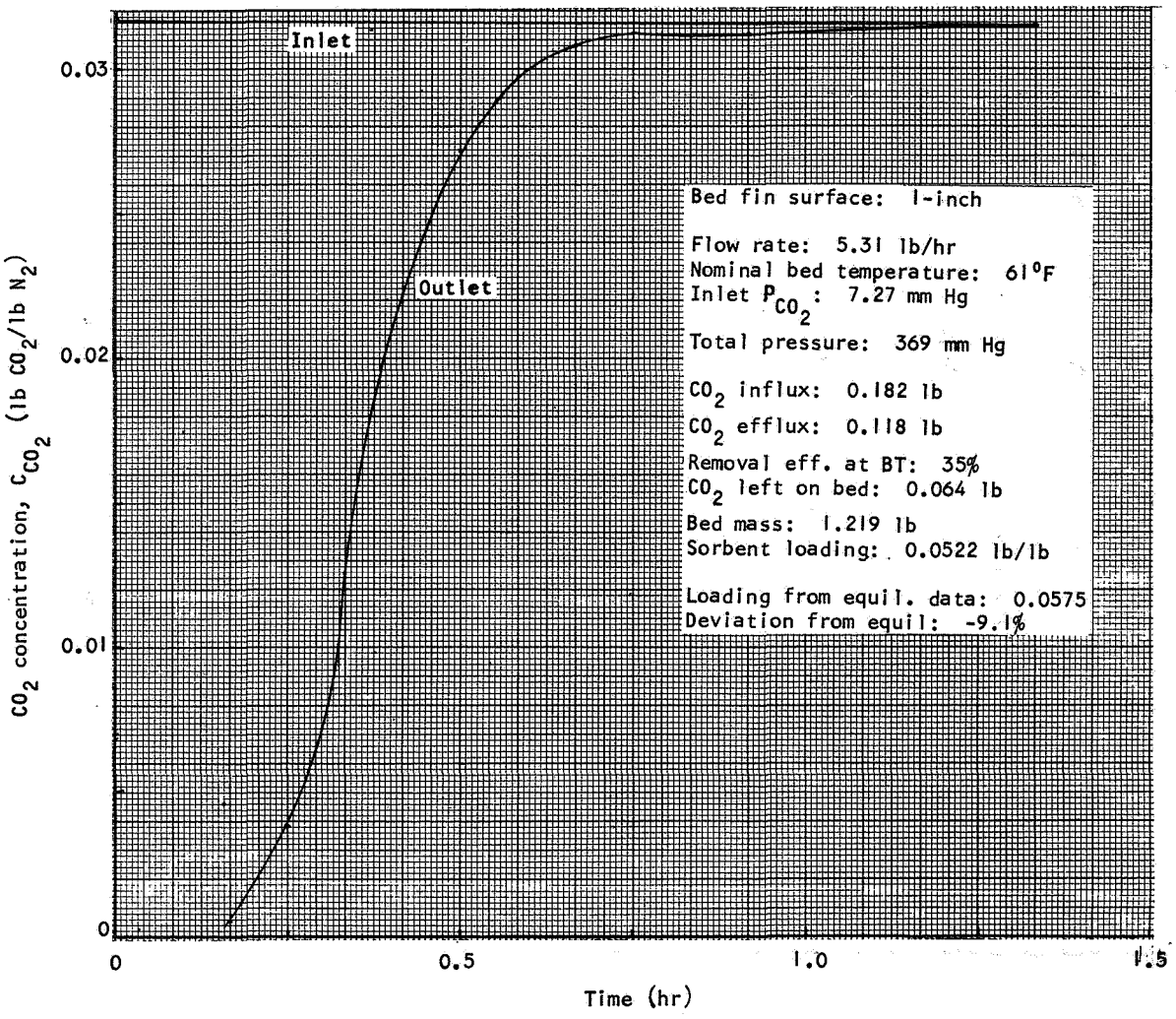

Figure 4-48. CO_2 Adsorption Breakthrough on Linde 13X, Run No. 13X/CO_2(1)-2

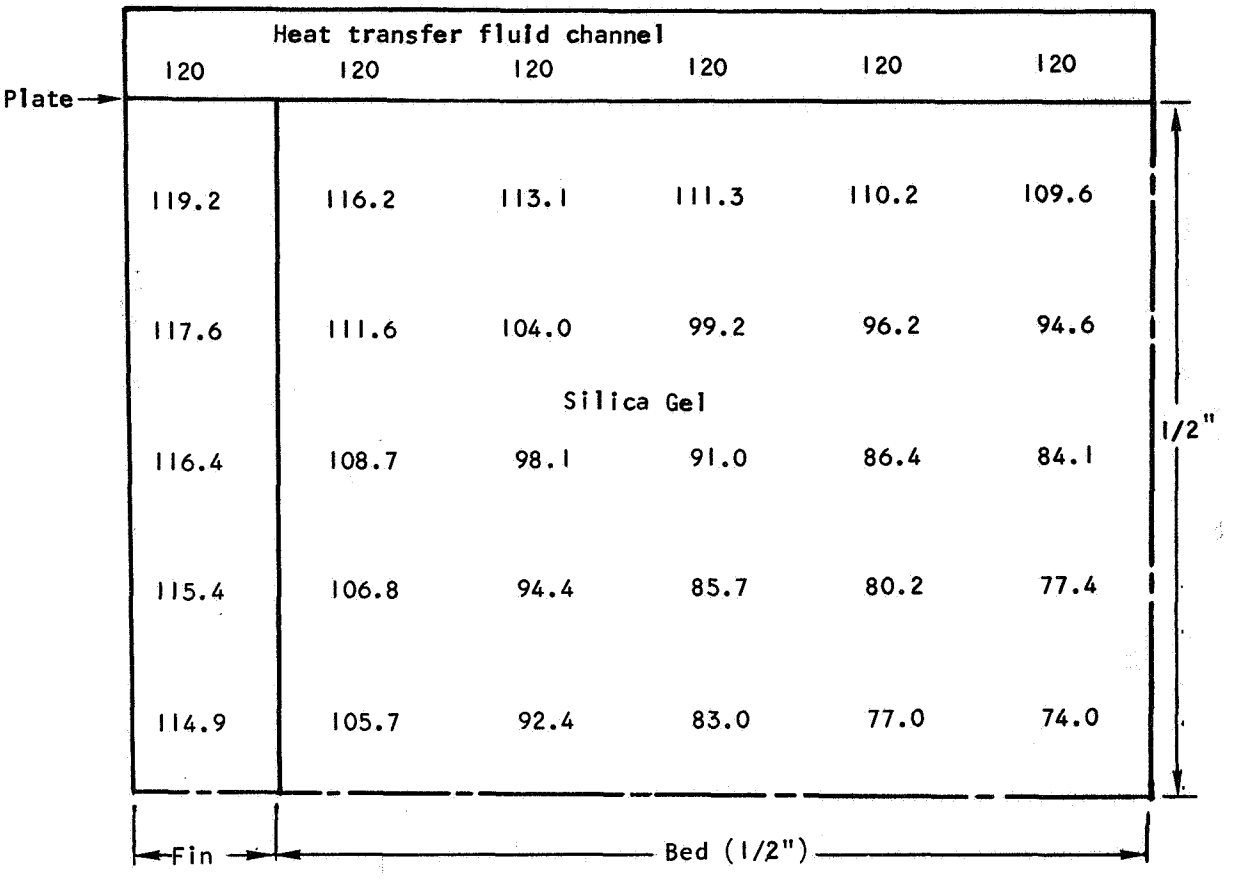

Assumptions:

Desorption rate, 250 Btu/hr-lb silica gel

Bed effective conductivity, 0.1 Btu/hr-ft^2-^{0}F/ft

Aluminum fins, 1 in. high by 1 in. spacing, 0.006 in. thick

Figure 4-49. Temperature Distribution (^{0}F) in a Desorbing 1-in. Channel of Silica Gel

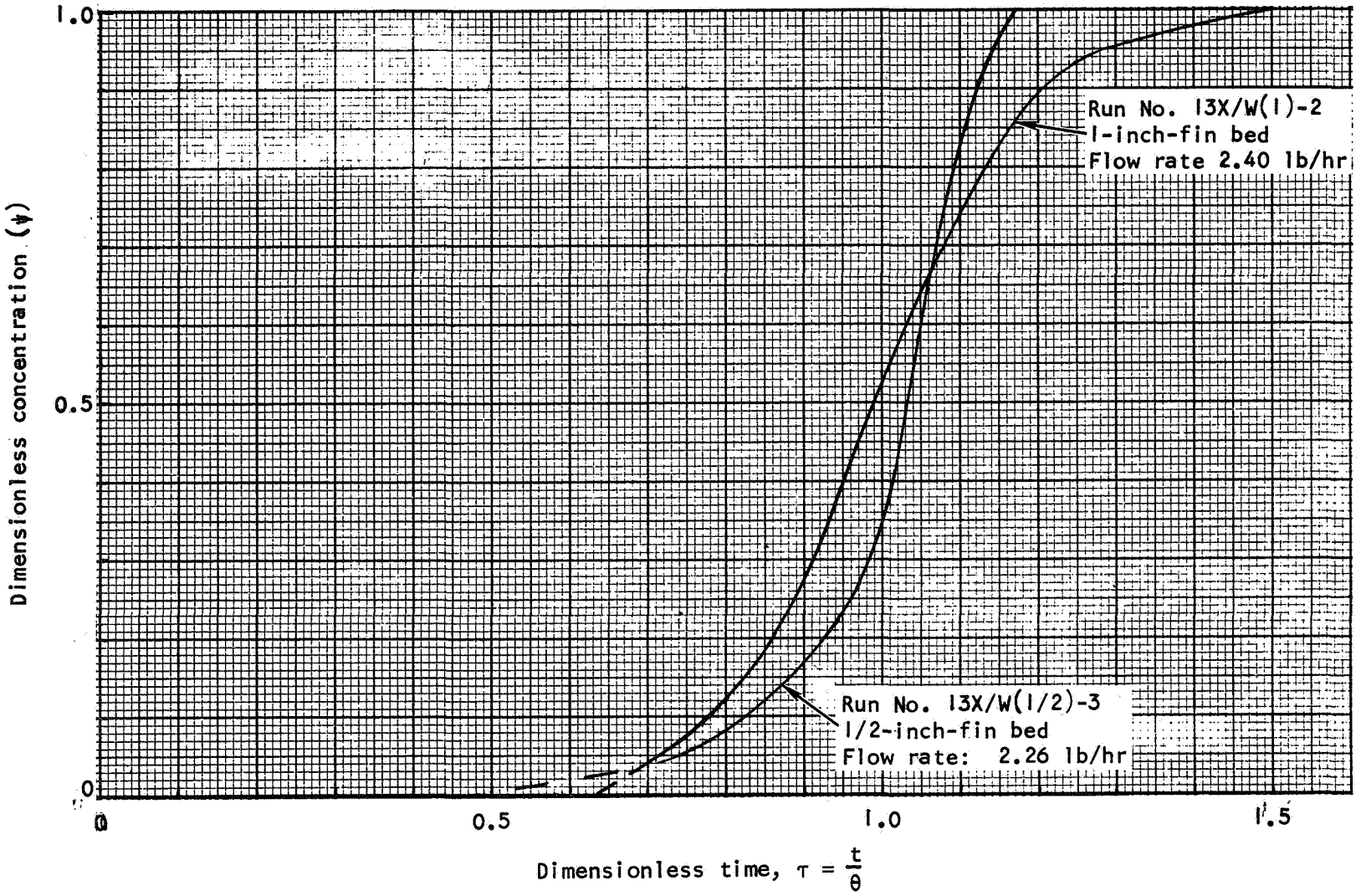

Figure 4-50. Comparison of 1/2-Inch and 1-Inch Heat-Transfer Surfaces, Water on Molecular Sieve 13X

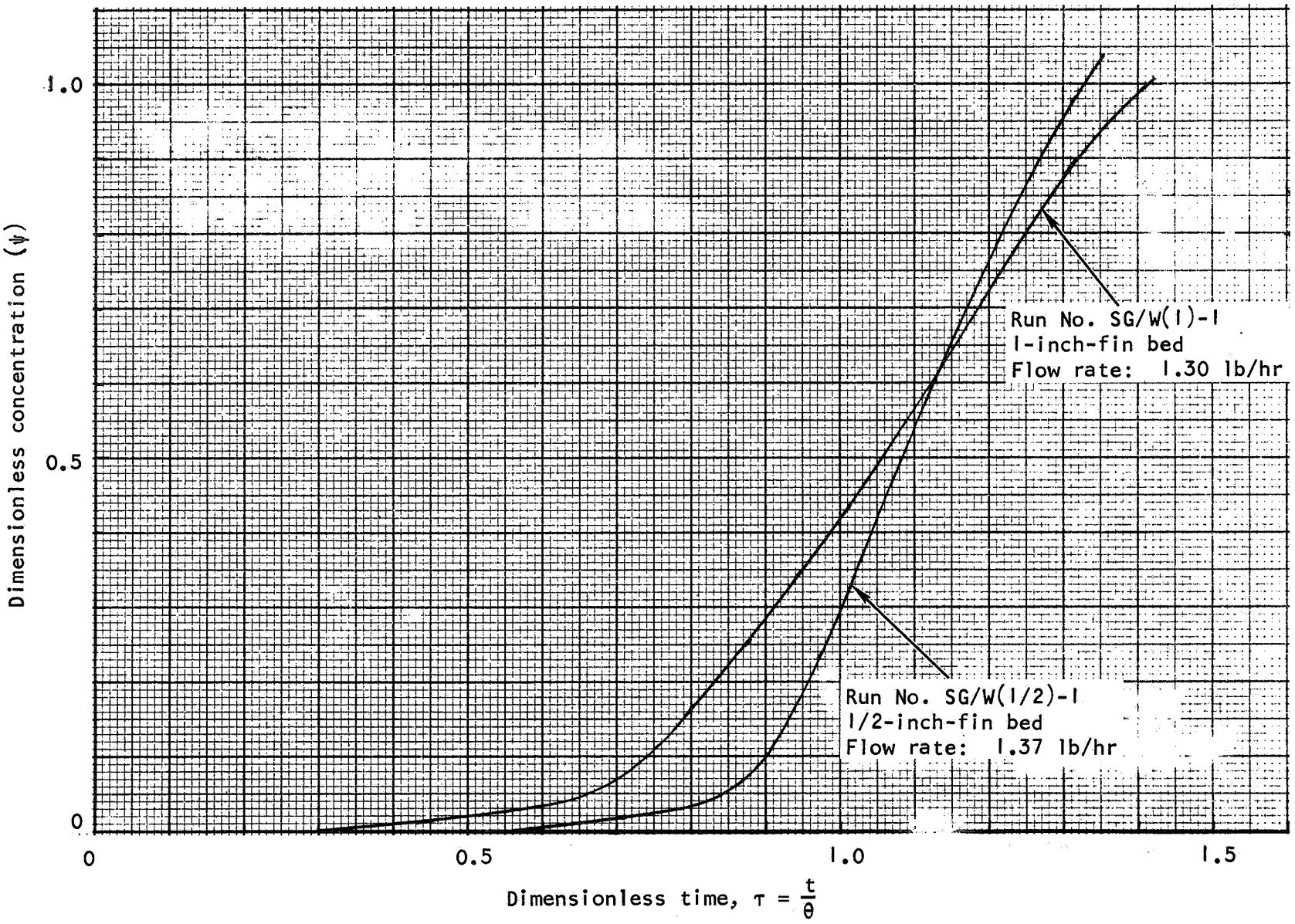

Figure 4-51. Comparison of 1/2-Inch and 1-Inch Heat-Transfer Surfaces Water on Silica Gel

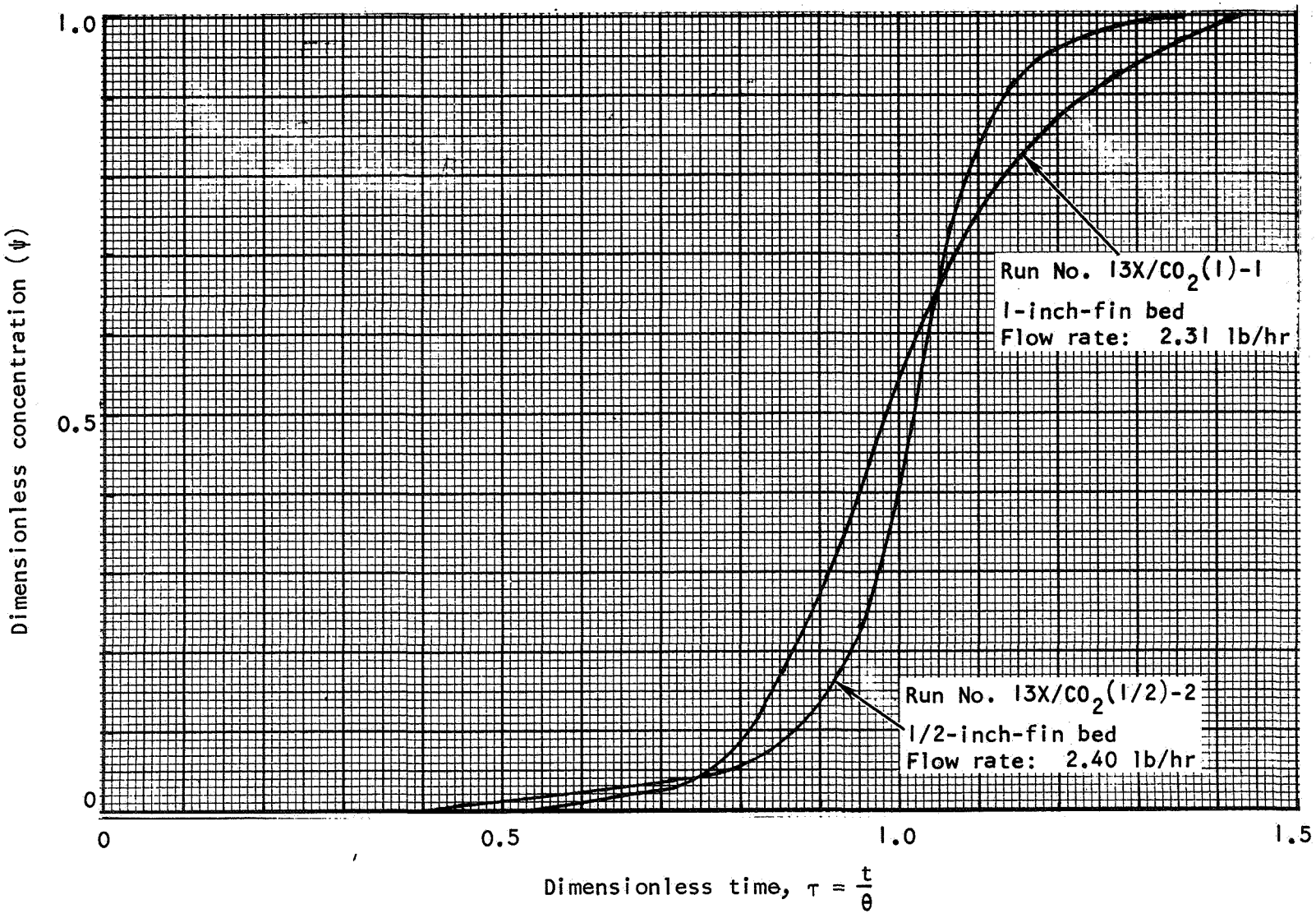

Figure 4-52. Comparison of 1/2-Inch and 1-Inch Heat-Transfer Surfaces CO_2 on Molecular Sieve 13X

SECTION 5

EVALUATION OF MASS-TRANSFER COEFFICIENTS AND INTRAPARTICLE DIFFUSIVITIES

DEFINITIONS

In this section, values of gas-phase mass-transfer coefficient K_g and intraparticle diffusivity D are determined for the single-sorbate breakthrough tests presented in Section 4.

From Reference 1, the intraparticle diffusivity for sorbate k is defined by the diffusion equation for the interior of a sorbent pellet:

$$\frac{\partial w_k}{\partial t} = \frac{D_k}{\rho_s} \frac{1}{r^2} \frac{\partial}{\partial r} r^2 \frac{\partial w_k}{\partial r} \qquad (5\text{-}1)$$

D_k has the units ft^2/hr; the local sorbent loading w_k is in the units mass of sorbate k per mass of sorbent. Time t is in hr; r in ft is the effective distance from the spherical pellet center. Sorbent particle density ρ_s is in the units of $lb\text{-}mass/ft^3$.

The gas-phase mass transfer coefficient K_g is defined by the following relation expressing the sorbate flux at the sorbent pellet boundary:

$$-\rho_s D_k \frac{\partial w_k}{M_k \partial r} = K_g (p_{ks} - P X_k) \qquad (5\text{-}2)$$

The mass-transfer coefficient has the units of $lb\text{-}moles/hr\text{-}ft^2\text{-}mm\ Hg$; M_k is the molecular weight of sorbate k. The total pressure P is in mm Hg; p_{ks} is the sorbate partial pressure at the sorbent boundary, mm Hg; X_k is the molefraction of sorbate k in the free stream. Note $P \cdot X_k = p_k$ the sorbate partial pressure in the free stream, mm Hg.

The mass-transfer coefficient is also used in the gas phase material balance in the x- or longitudinal flow direction:

$$\frac{dp_k}{dx} = \frac{P M_g}{f \rho_g u_g} a_{sg} K_g (p_{ks} - p_k) \qquad (5\text{-}3)$$

Here a_{sg} is the sorbent specific external surface area, sq ft per unit volume of packed bed. M_g is the average molecular weight of the process gas; f is the bed void fraction, ρ_g is the gas density, $lb\text{-}mass/ft^3$; u_g is the interstitial or true gas velocity, ft/hr.

It should be noted from Equation 5-3, that K_g and a_{sg} must both be known. In any evaluation of K_g, the corresponding value of a_{sg} must be given. Table 5-I presents several pertinent values, including a_{sg}, used in the evaluations.

TABLE 5-I

PARAMETERS USED IN MASS-TRANSFER COEFFICIENT EVALUATIONS

Parameters	Silica Gel (6 to 16 Mesh)	Linde 5A (1/16-in. Pellets)	Davison 5A (8 to 12 Mesh)	Linde 13X (1/16-in. Pellets)
Particle density, ρ_s, lb/ft^3	75.0	64.0	66.4	64.0
Packed density, ρ_{sb}, lb/ft^3	42.96	43.55 49.73	42.97	41.06 39.73
Surface area per unit volume, a_{sg}, ft^2/ft^3	575.0	636.0	653.7	636.0

METHOD OF DETERMINATION

The method used for the determination of the coefficients K_g and D involves the use of the performance-prediction program, S9960, discussed in Section 7 of this report. If this program is considered to be a valid mathematical simulation of the actual bed mass-transfer phenomena, and if the true values of K_g and D are included in the program input data, the predicted performance should match that observed. Conversely, if a prediction matches the experimental performance, then the values of K_g and D used by the program must be the true values. Stated in simple terms, after producing a number of performance predictions for various pairs of values of K_g and D, the adopted values were those which produced the best fit of the predicted performance to that of the experimental test. The judgment of the best fit was by a visual comparison of predicted and actual breakthrough curves.

In order to aid the visual comparisons, which at times were difficult, a systematic computation and graphing procedure was set up. Table 5-2 shows the values of mass-transfer coefficient and diffusivity for which performance predictions were usually obtained. It should be noted from the table that the performance predictions were in groupings of constant diffusivity. For each grouping (that is, for a constant value of diffusivity) the various performance predictions were plotted on one graph with mass-transfer coefficient as a parameter. For convenience, all predictions were plotted on xerographic copies of the experimental breakthrough curve. For each plot, or for each

TABLE 5-2

VALUES OF MASS-TRANSFER COEFFICIENT K_g AND DIFFUSIVITY D USED IN EVALUATIONS

Mass-Transfer Coefficient, K_g (lb-mole/hr-ft^2-mmHg)	Diffusivity, D (ft^2/hr)
0.00025 0.0005 0.001 0.005	0.000004
0.0001 0.00025 0.0005 0.001 0.005	0.00001
0.0001 0.00025 0.0005 0.001 0.005	0.00004
0.0001 0.00025 0.0005 0.001 0.005	0.0001
0.0001 0.00025 0.0005 0.001 0.005	0.001

grouping, the best value of mass-transfer coefficient was selected and a representative curve drawn. Sometimes this curve was drawn precisely through the predicted points. In other cases, the best curve was drawn by visual interpolation between predicted curves, interpolating with respect to K_g. Finally, for all five values of diffusivity, the best breakthrough curves were compared, and a tentative selection of mass-transfer coefficient and diffusivity was made.

For all evaluations presented here, the bed was broken into 20 finite-difference elements in the flow direction. For early computations, as many as 6 internal-particle finite-difference elements, that is, up to six radial layers, were considered for calculation of diffusion in the pellet. However, it became evident that the best predictions occurred for large values of diffusivity which produce very small loading gradients within the sorbent particle. Therefore, the number of sorbent finite-difference elements was reduced to two. This produced distinct savings in computer time. For most of the adsorption or gas strips, about 4-1/2 minutes of computer time was required on a Univac 1108 system to process the K_g/D sets given in Table 5-2. In some cases, computations for lower or intermediate values of K_g were made in addition to those of Table 5-2.

DISCUSSION OF EVALUATION RESULTS

Sample Evaluation

Figure 5-1 shows predicted points for Run No. 13X/CO_2(1/2)-2. The predictions for this run are typical in many aspects to all of the other evaluations for adsorptions. First, at low diffusivities (0.000004 and 0.00001 ft^2/hr) no value of K_g gives a good prediction. As diffusivity increases, so does the accuracy of the prediction. Usually the best prediction is obtained for $D = 0.001$ ft^2/hr. With this diffusivity, the computed sorbent loadings (part of the printed output of the program) show essentially no radial variation; that is, the calculated resistance to diffusional sorbate transfer within the pellet is so small that no concentration or loading gradient is developed. The same is essentially true for $D = 0.0001$ ft^2/hr.

One might conclude at this point that diffusion within the sorbent is negligible and all of the mass-transfer resistance is in the convective transfer from the free stream to the sorbent surface. This will be discussed in more detail later.

A second observation is that K_g does have a definite influence on curve shape. The dependence of K_g is not, however, linear. For example, using the $D = 0.001$ ft^2/hr plot of Figure 5-1, there is a marked difference between the $K_g = 0.0001$ curve and the $K_g = 0.00025$ curve. On the other hand, the difference between $K_g = 0.0005$ and $K_g = 0.001$ is not as great. This should be remembered when considering the tabled results presented later in this section. In effect, there is a range of K_g that will give a good prediction. For Figure 5-1, $D = 0.001$, the best curve was estimated to be for $K_g = 0.00037$

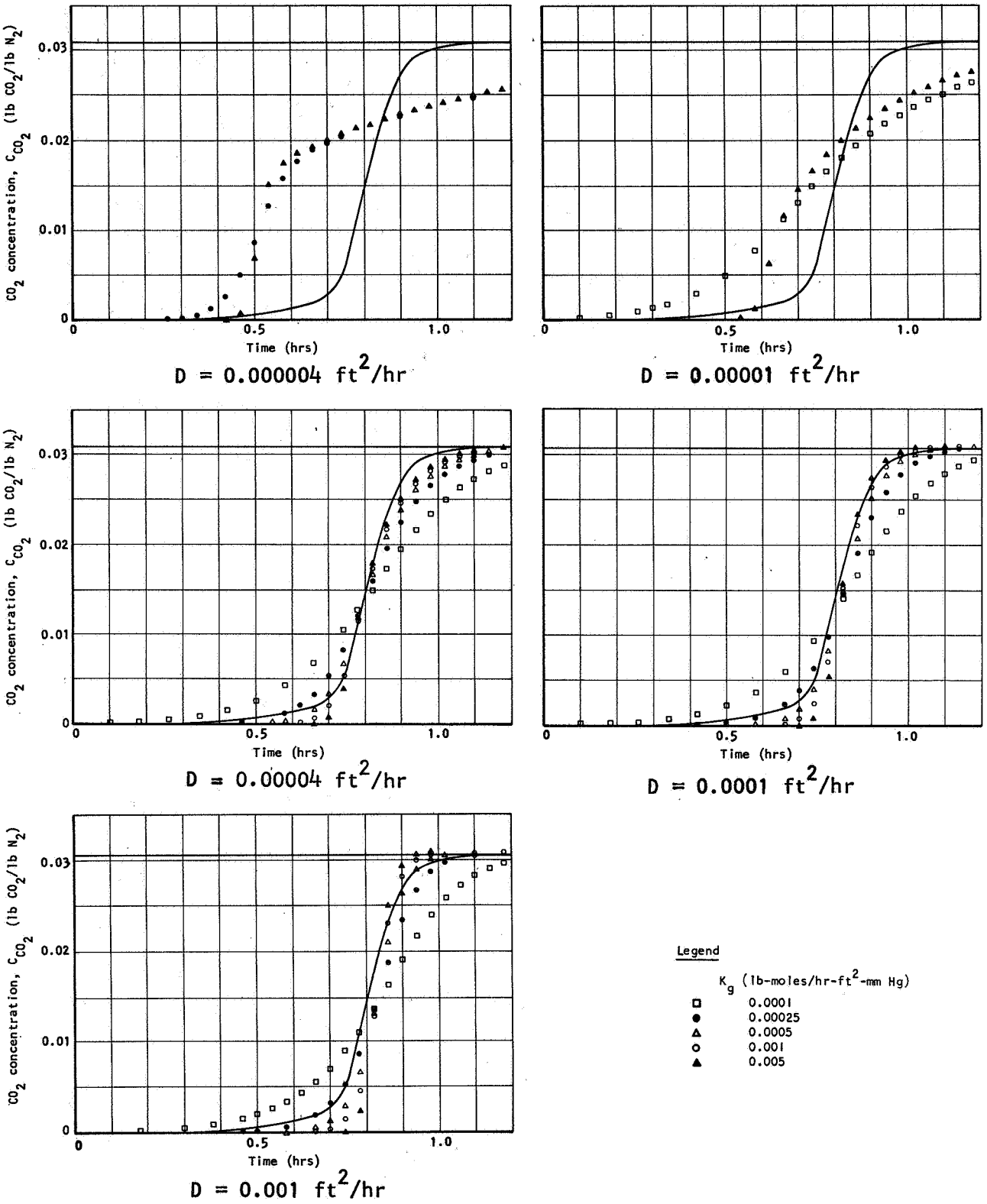

Figure 5-1. Performance Prediction for Run No. 13X/CO_2(1/2)-1 as a Function of Mass-Transfer Coefficient K_g and Diffusivity D

(midway between 0.00025 and 0.0005). However, considering experimental accuracies in both the dynamic data, and in the equilibrium data which the programs use, the range of K_g from 0.00015 to 0.0007, or possibly higher, would produce satisfactory predictions.

A third observation typical of almost all cases, is that the value of K_g that fits the early breakthrough test does not fit the entire breakthrough shape as well. Because of this, two pairs of K_g/D values were determined for each run: one pair for the best curve shape and another pair for the best approximation of the early breakthrough performance.

A fourth observation was usually made, although the illustrated run does not show this well. In several cases, no matter what value of K_g was used, the predicted curves were displaced in time from the experimental curve. That is, the predicted breakthroughs were earlier or later than the experimental. In most cases, the offset in time was in accord with the material balance error between calculated (from experiment) and equilibrium sorbent capacities. If the calculations for a dynamic test showed greater sorbate pickup than equilibrium, the predicted breakthrough curves would be earlier than the experimental; if less capacity than equilibrium, predictions would appear later. Since it was usually considered that error in the measurement of the temperature level of the bed was the cause of the problem, giving more or less capacity than expected, but not appreciably altering the real values of K_g or D, it was decided that curve shape was the most important evaluation criterion for determining K_g.

It would be possible to eliminate the offset between predicted curves and experimental by appropriately choosing effective bed temperature and using the equilibrium isotherm corresponding to it. This was not done, however, as it was considered unjustified.

The predictions for gas strips showed little variation with diffusivity and only slight variation with K_g. The variation with K_g occurred in the very early portion of the stripping procedure; later in the gas strip, curves for all values of K_g tended to coincide. Most of the predictions tended to show more ultimate desorption (higher outlet concentration) than the experiments. It is believed this is due to the inaccuracies in the equilibrium data for very low partial pressures.

Accuracy of the Procedure

There are a number of areas where this method of mass-transfer coefficient evaluation is vulnerable to inaccuracies in data and technique. Obviously, any inaccuracy in the dynamic tests will lead to scatter in resulting values of K_g and D. These inaccuracies have been discussed before, bed temperature determination being a key parameter.

Accuracy of the entire equilibrium isotherm is important. The predicted performance depends on the entire isotherm, not just the value corresponding to bed inlet conditions. In this regard, several runs were subjected to the

evaluation procedure with differing equilibrium isotherm shapes, but with essentially the same total bed capacity. The results showed that predicted breakthrough offset and curve shape are significantly changed by isotherm shape. The values of K_g and D given here are based upon the currently available equilibrium data, most of which is given in Section 3.

The numerical procedure used by the program can also introduce inaccuracy into the evaluation procedure. Investigations showed that by varying the finite-difference size, that is, varying the number of finite-difference elements into which the bed is divided, slightly different predicted breakthrough curves could be obtained. Furthermore, these different breakthrough curves did not always result in the same amount of sorbate material being left on the bed. In some instances, the material balance comparison between equilibrium data and the capacity obtained from the predicted curve was not as good as the comparison made with the experimental data. As noted earlier 20 longitudinal finite-difference elements were used for all computations. The magnitude of the time step was also important. Small time steps tend to produce more accurate predictions; but consume more computer time. For the evaluations, the time step in the range of 0.01 hr to 0.025 hr, was chosen to be as large as possible while still giving good accuracy.

Presentation of Results

Tables 5-3 through 5-6 present the results and observations of the mass-transfer coefficient evaluations conducted for the single-sorbate tests on the 1/2-inch-fin bed presented in Section 4. Because of the large temperature variations noted in all of the 1-inch-fin bed tests, no evaluations were performed on the dynamic tests conducted with this bed. Run conditions are noted in the evaluation tables to help in the assessment of trends, if any.

It is not difficult to see that the best predictions are almost always obtained for a very high value of diffusivity (0.001 or 0.0001 ft^2/hr). With such diffusivity values, there is effectively no resistance to diffusional mass transfer in the sorbent particle, and thus no loading gradient is developed within the sorbent. It should be noted that the value of D = 0.001 ft^2/hr was not used for silica-gel evaluations. But as can be seen from the other tables, the results for D = 0.001 and 0.0001 ft^2/hr are usually nearly identical.

In no system does there seem to be a clear relationship of K_g upon flow rates. Even though the dimensionless curves seem to indicate weak flow-rate dependency, the scatter of the mass-transfer coefficients is large enough to mask the effect. In the $13X/CO_2$ runs there seems to be a slight flow rate dependence, but the number of runs and the flow rate variation is not large enough to substantiate this.

For the $5A/CO_2$ runs, the best K_g values are not consistent with flow rate either. Ignoring Runs $5A/CO_2(1/2)$-7 and -8, for the second packing of the bed, one might conclude that Run 6, for the very low flow of 0.5 lb/hr, does show a lower value of K_g which is due to a flow rate effect. However, noting the K_g values for Runs 7 and 8, as well as the two Davison 5A runs, the flow rate dependence is uncertain.

TABLE 5-3

EVALUATION OF K_g AND D FOR SILICA-GEL/WATER ADSORPTIONS

Run No.	Flow Rate (lb/hr)	Bed Temp. (°F)	Sorbate Partial Press. (mm Hg)	Total Press. (mm Hg)	Material Balance Error (%)	Offset of Best Predicted Breakthrough Curve		Breakthrough Time θ (hr)	Best Values by Curve Shape		Remarks	Best Values to Fit Early Portion of BT Curve	
						Description	Magnitude (hr)		K_g lb-mole/hr-ft²-mm Hg	$\mathcal{D}$ Ft²/hr		K_g (lb-mole/hr-ft²-mm Hg)	D_2 (ft²/hr)
SG/W(1/2)-1	1.37	60°	9.55	257	-8.2%	Late, moderate	+0.6	11.85	0.0004	0.0001	Reasonably good approximation	0.0003	0.0001
									0.0004	0.0004	Not quite so good		
									0.0005	0.0001	Somewhat poorer		
-2s	1.37	90°	-	261	+12.4	Very little	-	-	0.005	0.00001	Good except for first portion of run	0.001	0.0001
									0.0005	0.0001	Both about equal; not quite as good as above.		
									0.001	0.00004			
-3	1.31	121°	9.21	264	+8.2	Early, moderate	-0.15	2.31	0.0002	0.0001	Good shapes, about equal	0.0002	0.0001
									0.00015	0.00004			
-4s	1.37	120°	-	260	-2.5	Early, moderate	-	-	0.0004	0.0001	Middle portion of prediction is early; both about equal	0.00025	0.0001
									0.0005	0.00004			
-6	2.87	120°	9.2	258	+7.8%	Essentially none	-	-	0.0002	0.0001	Very good fit, Not quite as good	0.0002	0.0001
									0.0002	0.00004			
-7s	2.87	120°	-	256	+6.4%	Early, moderate	-		0.0005	0.0001	Middle portion of prediction is early; D = 0.0001 is better	0.0005	0.0001
									0.001	0.00004			
-8	5.37	60°	9.21	258	-13.9%	Late in mid portion of BT	+0.175	2.85	0.0004	0.0001	Good at early and late portion of BT	0.00037 0.0006	0.0001 0.0001
									0.0006	0.00001	Not quite as good		
-9s	5.37	90°	-	258	+1.8	Essentially none	-	-	0.0004	0.0001	Very good fit throughout	0.0004	0.0001
									0.0004	0.00004	Both about equal, not quite as good as above		
									0.001	0.00001			

TABLE 5-4

EVALUATION OF K_g AND D FOR MOLECULAR-SIEVE 13X/WATER ADSORPTIONS

Run No.	Flow Rate (lb/hr)	Bed Temp. (°F)	Sorbate Partial Press. (mm Hg)	Total Press. (mm Hg)	Material Balance Error (%)	Offset of Best Predicted Breakthrough Curve		Break-through Time θ (hr)	Best Values by Curve Shape		Remarks	Best Values to Fit Early Portion of BT Curves	
						Description	Magnitude (hr)		K_g (lb-mole/hr-ft^2-mm Hg)	D (ft^2/hr)		K_g (lb-mole/hr-ft^2-mm Hg)	D (ft^2/hr)
13X/W(1/2)-1	1.34	60°	9.34	366	-0.4%	Late, moderate	+0.47	11.3	0.00018 0.00018 0.00018	0.001 0.0001 0.00004	All about equal, independent of D. Curve shapes are good; but late in time.	0.00009 0.00009 0.00009	0.001 0.0001 0.00001
-2	1.35	120°	9.38	367	+0.3%	Late, slight	+0.33	9.38	0.000075 0.000075 0.000075 0.000075	0.001 0.0001 0.00004 0.00001	All about equal, independent of D. Curve shapes are good; offset, late in time, is slight. Early fit is good.	0.00006 0.00006 0.00006 0.00006	0.001 0.0001 0.00001 0.00004
-3	2.26	60°	9.28	368	-1.9%	Late, moderate	+0.33	6.72	0.0002 0.00022 0.00022	0.001 0.0001 0.00004	All about equal. Curve shapes good; but offset, late, is moderate	0.00013 0.00013 0.00013	0.001 0.0001 0.00004
-4s	2.40	90°	-	364	-	Late, considerable at large times; predictions never reach as low concentrations as observed.			0.0001 0.00015 0.0002 0.005	0.001 0.0001 0.00004 0.00001	Slightly better than other curves. Both about equl, not quite as good as above. This fit is not as good	0.0001	0.001
-5	2.36	120°	9.20	360	-5.4%	Late, moderate	+0.33	5.24	0.0005 0.0005 0.0005	0.001 0.0001 0.00004	Curve shapes good, independent of D. Offset, late, is moderate to large.	0.0002 0.0002 0.0002	0.001 0.0001 0.00004
-6s	2.40	120°	-	360	-	Late, moderate; predictions do not reach the low concentrations observed.			0.00035 0.0005 0.001	0.001 0.0001 0.00004	Best shape. Not quite as good as above. Slightly poorer fit than above two. Not greatly dependent on K_g.	0.00035	0.001

TABLE 5-5

EVALUATION OF K_g AND D FOR MOLECULAR-SIEVE 5A/CO_2 ADSORPTIONS

Run No.	Flow Rate (lb/hr)	Bed Temp. (°F)	Sorbate Partial Press. (mm Hg)	Total Press. (mm Hg)	Material Balance Error (%)	Offset of Best Predicted BT Curve		Breakthrough Time θ (hr)	Best Values by Curve Shape		Remarks	Best Values to Fit Early Portion of BT Curves	
						Description	Magnitude (hr)		K_g (lb-mole/hr-ft^2-mm Hg)	D (ft^2/hr)		K_g (lb-mole/hr-ft^2-mm Hg)	D (ft^2/hr)
Linde 5A 5A/CO_2(1/2)-1	1.4	70°	7.14	368	-2.6%	Late; slight to moderate	+0.055	1.67	0.0004 0.0005 0.001	0.001 0.0001 0.00004	Both about equal; Curve shapes good. Nearly as good as above.	0.00025	0.001
-2	2.4	70°	7.31	375	+0.6%	None	-	-	0.00035 0.0005 0.001	0.001 0.0001 0.00004	Excellent fit everywhere. Early portion not quite as good as above. Slightly poorer prediction.	0.00035	0.001
-3	2.4	90°	7.20	372	+6.1%	Early, very slight	0.03	0.71	0.0004 0.0005 0.001 0.005	0.001 0.0001 0.00004 0.00004	Excellent prediction. Almost as good as above. Poor fit.	0.0004	0.001
-4	2.4	50°	7.17	367	+0.5	Late, slight	0.04	1.32	0.0004 0.0005 0.001	0.001 0.0001 0.00004	Fits total curve well. Both about equal; early performance somewhat poorer than above.	0.0004	0.001
-5	2.4	70°	1.76	367	+10.6%	Early, considerable	-0.2	1.84	0.00075 0.001 0.005	0.001 0.001 0.00004	All about the same; curve shape good, but too early	0.005	0.001

TABLE 5-5 (CONTINUED)

EVALUATION OF K_g AND D FOR MOLECULAR-SIEVE 5A/CO_2 ADSORPTIONS

Run No.	Flow Rate (lb/hr)	Bed Temp. (°F)	Sorbate Partial Press. (mm Hg)	Total Press. (mm Hg)	Material Balance Error (%)	Offset of Best Predicted BT Curve: Description	Offset of Best Predicted BT Curve: Magnitude (hr)	Breakthrough Time θ (hr)	Best Values by Curve Shape: K_g (lb-mole/hr-ft^2-mm Hg)	Best Values by Curve Shape: D (ft^2/hr)	Remarks	Best Values to Fit Early Portion of BT Curves: K_g (lb-mole/hr-ft^2-mm Hg)	Best Values to Fit Early Portion of BT Curves: D (ft^2/hr)
-6	0.60	70°	7.19	376	-1.2%	Late, moderate	0.16	4.08	0.00025 0.00035	0.001 0.0001	Curve shapes good, but late	0.0001	0.001
-7	1.4	70°	7.17	365	+11.1%	Early, considerable	0.18	2.02	0.00015 0.00017 0.00025	0.001 0.0001 0.0004	About same, reasonable shape but quite early prediction. Slightly poorer prediction.	0.0002 0.0002	0.001 0.0001
-8	2.4	70°	7.11	366	+11.4%	Early, considerable	0.12	1.19	0.0002 0.00015 0.00018	0.0004 0.001 0.0001	Slightly better shape, but all curve shapes reasonable; all curves early.	0.00022	0.001
Davison 5A 5AD/CO_2 (1/2)-1	1.4	70°	7.22	375	+6.8%	Very slight	-	-	0.00013 0.00015 0.00018	0.001 0.0001 0.00004	All very good predictions.	0.00015	0.001
-2	2.4	70°	7.30	374	+7.3%	None	-	-	0.0002 0.0002 0.00015	0.00004 0.0001 0.001	Best shape. Almost as good as above. Also good.	0.0002 0.00015	0.00004 0.001

TABLE 5-6

EVALUATION OF K_g AND D FOR MOLECULAR-SIEVE 13X/CO_2 ADSORPTIONS

Run No.	Flow Rate (lb/hr)	Bed Temp. (°F)	Sorbate Partial Press. (mm Hg)	Total Press. (mm Hg)	Material Balance Error (%)	Offset at Best Predicted BT Curve		Break-through Time θ (hr)	Best Value by Curve Shape		Remarks	Best Values to Fit Early Portion of BT Curve	
						Description	Magnitude (hr)		K_g (lbmole/hr-ft^2-mm Hg)	D (ft^2/hr)		K_g (lb-mole/hr-ft^2-mm Hg)	D (ft^2/hr)
13X/CO_2 (/12)-1	1.40	60°	7.2	375	-7.6%	Late, considerable	0.14	1.29	0.00025 0.00037 0.0006	0.001 0.0001 0.00004	Both about the same; good shape but quite late. Slightly poorer shape.	0.0001 0.0001	0.001 0.0001
-2	2.40	60°	7.2	375	-1.5%	Late, slight	0.03	0.80	0.00037 0.00045	0.001 0.0001	Good prediction; only slightly poorer than above	0.00022 This would give good overall fit also.	0.001
-3	2.40	60°	7.1	368	-3.8-	Late, slight	0.025	0.78	0.00035 0.00042	0.001 0.0001	Good shape, but slightly late. Almost as good shape.	0.0002 0.00022	0.001 0.0001
-4	1.23	70°	7.08	364	+4.8%	Early, very slight	0.025	1.40	0.0002 0.00025 0.00037	0.001 0.0001 0.00004	Very good prediction. Reasonable fit, better a high end than above. Poorer fit, but good at both ends.	0.0002	0.001
-5	2.33	70°	6.97	370	+10.6%	Early, moderate	0.053	0.80	0.0002 0.00025 0.0003	0.001 0.0001 0.00004	Best shape, but early. Reasonable shape. Poorer shape.	0.00025 0.00025	0.001 0.0001

For the water adsorptions on silica gel and molecular sieve 13X, using diffusivity D = 0.001 ft^2/hr, one value of K_g can be chosen for each sorbent that will give good performance predictions. These values are 0.0004 lb-mole/hr-ft^2-mm Hg for silica gel and 0.0002 for molecular sieve 13X.

For the CO_2 adsorptions on Linde 5A and 13X, the scatter of K_g values is large enough that it appears from the evaluation tables that no one single value can be used to produce acceptable predictions. To help in visualizing the results of the mass-transfer coefficient evaluations, Figures 5-2 and 5-3 were prepared showing the range of K_g, for D = 0.001 ft^2/hr, which give acceptable predictions for the CO_2 adsorptions. For 13X/CO_2 adsorptions Figure 5-3 indicates that there is a single value of K_g (= 0.00025 lb-mole/hr-ft^2-mm Hg) which can be used to produce good predictions over the range of experimental conditions. However, for the 5A/CO_2 adsorptions no one value seems sufficient.

The problem lies in the second set of Linde 5A runs (Runs 7 and 8) and the two Davison 5A tests, The sorbent materials used in these runs may have had restricted pore networks, hindering internal diffusion. To test this assumption, a number of predictions were made for K_g = 0.0004, while varying diffusivity over a considerable range. That is, using a mass-transfer coefficient that in combination with a high diffusivity seemed to give good results for other tests, it was questioned whether a low diffusivity value existed which could give good predictions for the runs in questions. It was found that no diffusivity value coupled with K_g = 0.0004 gave really good predictions; the curve shapes were definitely distorted. If shape is ignored, the combination K_g = 0.0004, D = 0.000015 gives a reasonable prediction of the breakthrough end points for the Linde 5A/CO_2 Run No. 7.

The possibility of channeling in these tests was considered. If this were the cause of the poorer breakthroughs, lower effective K_g values would indeed have to be used in the predictions. However, there is no evidence to show that channeling caused the poorer breakthroughs in either of these tests or the substantiating, nearly identical, reruns made for each system. The second packing of Linde 5A material in the 1/2-inch-fin bed resulted in a larger quantity of sorbent being held in the bed than in the first set of runs. Thus, it would be expected there would be less channeling, rather than more. With regard to the runs with Davison 5A, it was observed that the sorbent beads packed very well in the bed. Here too channeling was expected to be insignificant.

It was concluded that for the 5A/CO_2 tests no one mass-transfer coefficient value could produce acceptable predictions over the entire range of experimental conditions. Therefore, a range of K_g from 0.0002 to 0.0004 lb-mole/hr-ft^2-mm Hg must be considered. Possibly, individual tests on sorbent samples might be required to pinpoint the value of K_g to be used. Table 5-7 contains recommended values of mass-transfer coefficient and intraparticle diffusivity for all of the systems studied in this program.

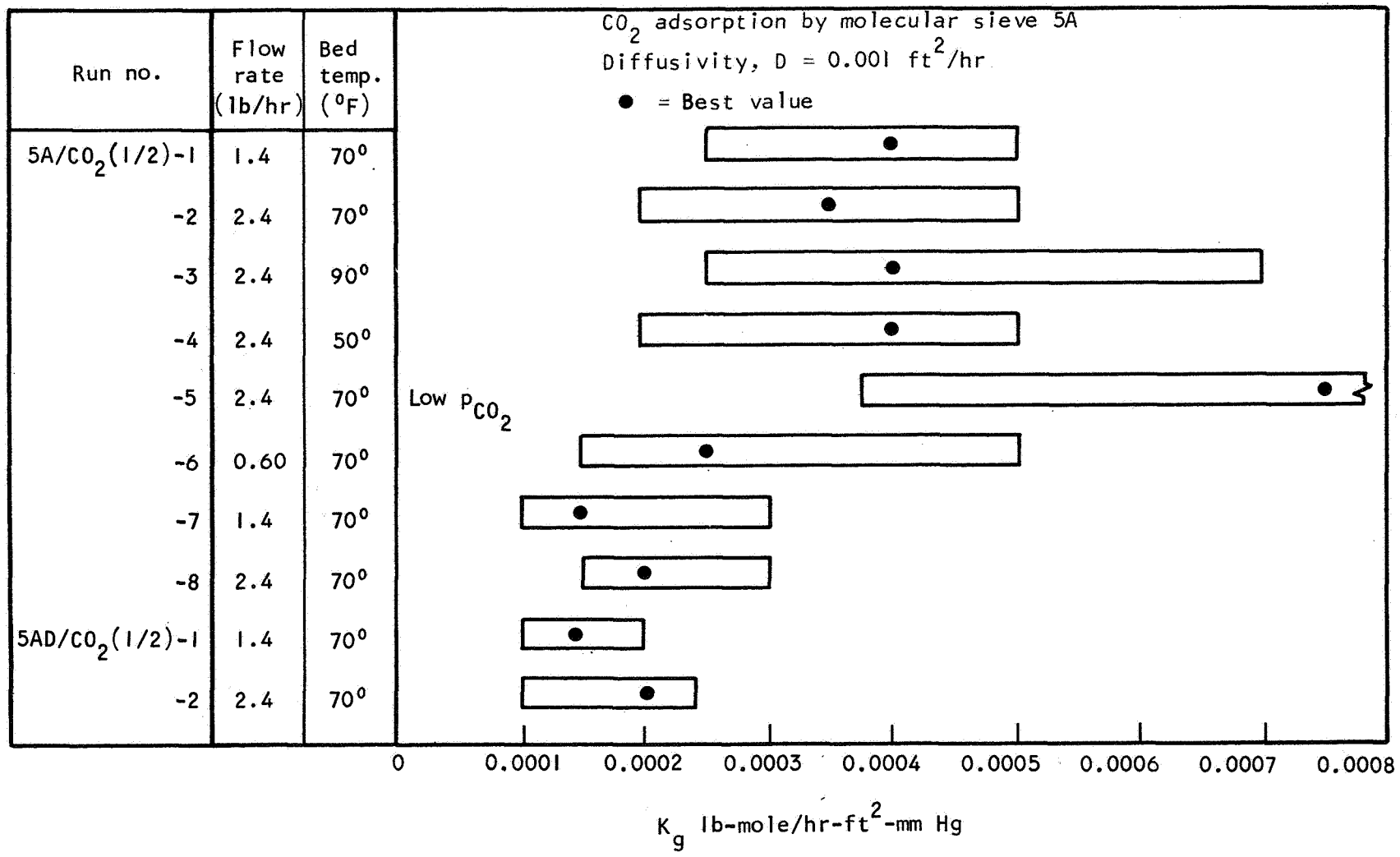

Figure 5-2. Range of Mass-Transfer Coefficient K_g, for D = 0.001 ft^2/hr, Which Give Acceptable Predictions for $5A/CO_2$ Adsorptions

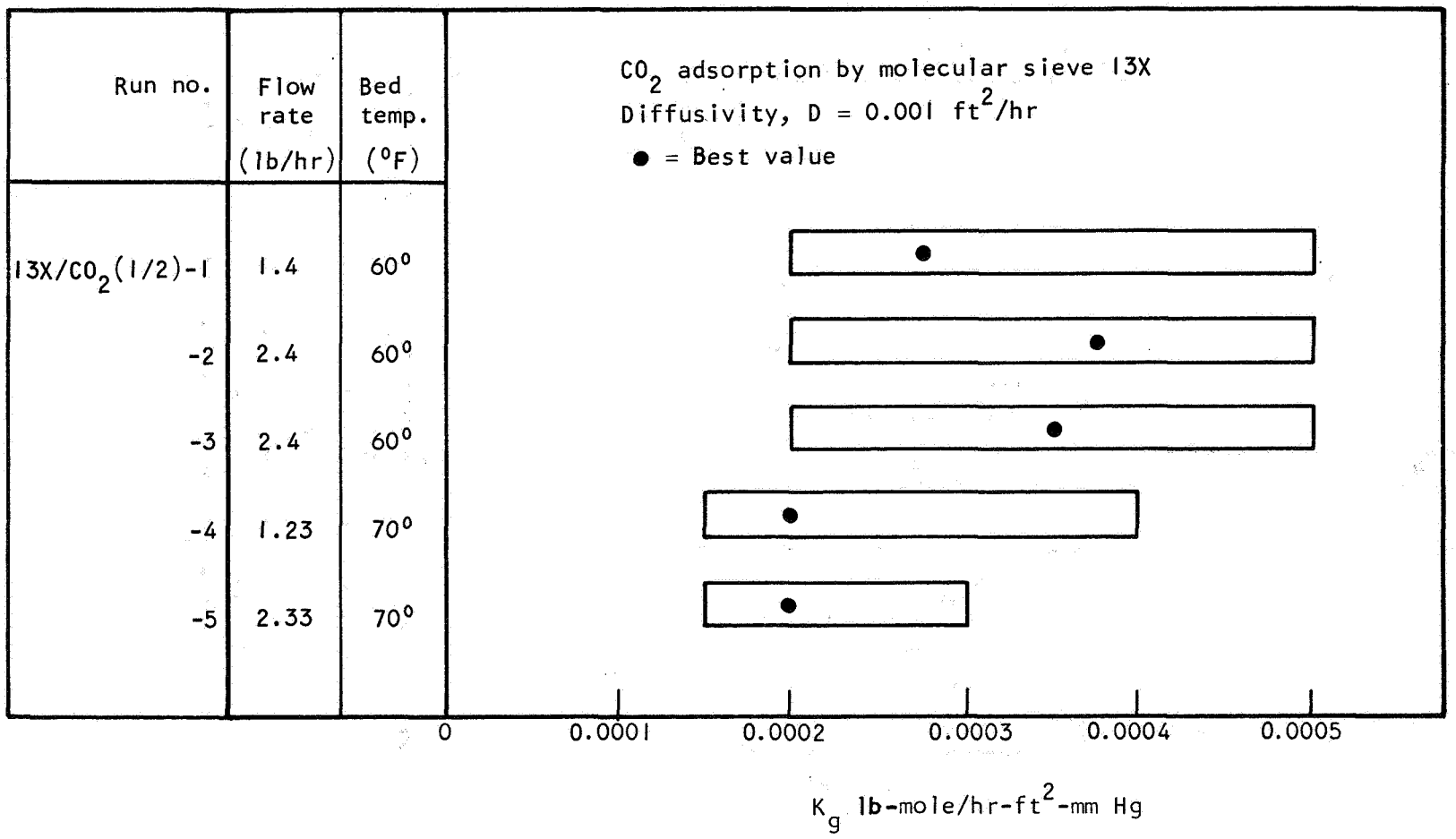

Figure 5-3. Range of Mass-Transfer Coefficient K_g, for D = 0.001 ft^2/hr, Which Give Acceptable Predictions for 13X/CO_2 Adsorptions

TABLE 5-7

RECOMMENDED VALUES OF MASS-TRANSFER COEFFICIENT K_g AND DIFFUSIVITY D TO BE USED IN PERFORMANCE PREDICTION PROGRAMS

System	K_g (lb-moles/hr-ft^2-mm Hg)	D (ft^2/hr)
Silica-Gel/water (Davison Grade 05)	0.0004	0.001 or 0.0001
	0.0003 for some conservatism	0.001 or 0.0001
Linde 13X/Water (1/16-inch pellets)	0.0002	0.001
Linde 5A (1/16-inch pellets)	0.0002 to 0.0004	0.001
Davison 5A (8 to 12 mesh beads)		
Linde 13X/CO_2 (1/16-inch pellets)	0.00025	0.001

Mass-Transfer Coefficients and Diffusivities Predicted from Published Correlations

In order to offer some justification of the values obtained in this study, mass-transfer coefficients K_g were calculated from two published correlations: one recommended by Vermeulen (Reference 7) and the other due to Lightfoot (Reference 5) as used by Lee and Cummings (Reference 6). Using a mean spherical particle diameter of 0.008 ft for 1/16-in. Linde molecular sieve pellets, and conditions for 2.4 lb/hr CO_2 adsorptions in the 1/2-inch-fin bed, both correlations gave values in the range 0.0015 to 0.0025 lb-mole/hr-ft^2-mm Hg. These values are somewhat higher than the recommended values given in Table 5-7. However, as can be seen from Figure 5-1, the effect on the breakthrough of using the higher K_g values in this range is not as great as might be expected. It should be noted, that the recommended values inherently include the effects of any channeling in the finned bed, and the non-isothermal conditions in the mass-transfer zone. Both of these nonideal conditions tend to be detrimental to the breakthrough performance; it is considered that the temperature variations in the mass-transfer zone are by far the most important. With the program computations, the only way to compensate for these effects on the breakthrough curve is to use a lower effective value of K_g.

From a recent adsorption NTU (number of transfer units) correlation by Vermeulen (Reference 7), it appears that the adsorptions of this program are characterized as being controlled by a combination of axial dispersion and external transport. That is, from the flow Peclet number and the dimensionless NTU parameter, data points for the experiments of this program fall on the correlation plot generally between the regions of axial dispersion controlling and external transport controlling.*

This brings up a topic not yet discussed, that of axial dispersion. The mathematical model in the performance-prediction programs does not include the effects of axial dispersion, i.e., the diffusional flow of sorbate from the front of the bed toward the rear which is caused by the concentration gradient developed across the bed due to the adsorption onto the solid sorbent. For those familiar with heat-exchanger design, axial dispersion diffusional effects can be considered analogous to axial or longitudinal conduction effects on high effectiveness (high NTU) exchangers. If one were to test a heat exchanger controlled by longitudinal conduction effects, and were to subsequently calculate from these tests heat-transfer coefficients using simple heat-exchanger theory which ignores these important effects, the effective coefficient values would be lower than those predicted by well-known correlations. This would also be the case--as evidenced here--with adsorption bed experiments where axial dispersion is important. Again, there seems to be justification for the K_g values being evaluated lower than published correlations.

With regard to effective intraparticle diffusivity for molecular sieves, there is physical reasoning to believe that high D values and low loading gradients would result from the performance-prediction evaluations. This contention relates to the makeup of molecular-sieve pellets, where 3 μ crystallites (the active sorbent particles) are suspended in a porous clay matrix. Ideally, the matrix will have negligible diffusion resistance; therefore, the only resistance would be in the very small crystallites. Since the program computes pore diffusion on the basis of effective spherical sorbent granules which have a mean diameter of the same magnitude as the actual pellet dimensions, the diffusion resistance of the crystallites would not be handled properly. It would then be expected that on the basis of the pellet diameter, the intraparticle diffusion resistance would appear to be negligible. Therefore, high diffusivity values would result.

In actuality, both the clay binder matrix and the molecular sieve crystallites have some finite resistance to intraparticle diffusion. At the present time, little has been done in the adsorption field in the area of modeling the diffusion phenomena in sorbents, such as molecular sieves, which possess bi-modal pore-size distributions. Previous experimental work conducted at AiResearch (Reference 8), has shown an effect of gross-particle size, comparing the performance of 1/8-inch to 1/16-inch pellets. This work would then indicate that there is at least some diffusional resistance in the clay matrix of

---

* The NTU is calculated according to the relations given in Reference 7. It involves the mid-height slope of the dimensionless breakthrough curve. A typical NTU value is 52.

the larger particles. This is essentially the reason, that for spacecraft uses, the 1/16-in. pellets have been chosen; from the data presented here, it seems the diffusional resistance within the smaller pellets is negligible.

In summary, it appears that the 1/16-in. molecular sieve pellets and the 6 to 16 mesh silica gel particles have only slight intraparticle diffusion resistance, and high values of diffusivity should be used in performance prediction programs. The recommended mass-transfer coefficient values in Table 5-7 should provide good predictions for spacecraft sorbent beds. The recommended mass-transfer coefficient values appear somewhat low compared to published correlations; however, nonuniform bed temperature, and axial dispersion effects, as well as channeling effects, if any, are not considered in the performance-prediction program's mathematical model and therefore cause effective K_g values to be lower than the correlations.

SECTION 6

COADSORPTION DYNAMIC MASS-TRANSFER TESTS

GOALS

The effect on the equilibrium capacity of molecular sieves for coadsorbed gases and vapors has been discussed in Section 3. Although the coadsorption equilibrium data presented in that section is certainly not all inclusive, this information provides a quantitative basis for more detailed analyses than were previously possible. However, this data does not provide insight as to possible dynamic effects accompanying the coadsorption of two or more sorbates. One of the goals of the program was to provide information on the dynamic behavior of molecular sieves when CO_2 and water sorbates are both involved.

For spacecraft molecular-sieve CO_2-removal systems, two modes of coadsorption of CO_2 and water are of interest. One mode involves the predrier bed where appreciable quantities of both CO_2 and water are contained in the gas stream. The second mode concerns the CO_2-removal bed; it involves very small water-vapor concentrations in the gas stream, but with appreciable resident loadings of water. The first coadsorption mode is not considered to be very important. Usually the assumption is made that the presence of CO_2 has no effect on the predrier bed. There already is a reasonable amount of data to support this assumption, at least for design purposes. Consequently only a few dynamic runs of this test series involve this coadsorption mode.

Of much greater importance, is the effect of a resident load of water on the CO_2 adsorption process. Therefore, a good deal of test time in this program was devoted to dynamic tests involving this coadsorption mode.

SIMULTANEOUS COADSORPTION OF CO_2 AND WATER ON MOLECULAR SIEVE 13X

Two dynamic tests were conducted which represent the first adsorption half-cycle of a predrier bed with both CO_2 and water vapor in the nitrogen carrier gas. The CO_2 partial pressure was 7 mm Hg; the water partial pressure was 9.2 mm Hg ($50^{\circ}F$ dew point); and the total pressure was essentially 7.0 psia. The sorbent in both cases was Linde 13X in the form of 1/16-in. pellets. Two runs were conducted; one in the 1/2-inch-fin bed, and one in the 1-inch-fin bed. Both runs were preceded by a vacuum bakeout reducing CO_2 and water loadings on the sorbent to negligible values. Both runs were continued until the breakthrough of both sorbates was complete.

Figures 6-1* through 6-4 show the water and CO_2 breakthroughs. The poisoning of the bed is dramatically illustrated by the CO_2 breakthroughs. Immediately after the CO_2 breakthrough is complete, CO_2 removal from the bed commences and continues until it is all stripped off. For the test with the

---

* Due to the large number of figures, they are included for convenient reference at the end of this section.

1/2-inch-fin bed, the CO_2 efflux (as determined by an integration over the test period) matches the influx within 1.2 percent; for the 1-inch-fin bed, CO_2 efflux and influx matched within 1 percent. Thus, there is no net CO_2 retention by the bed. On the other hand, the water capacity is unhindered by the presence of CO_2. In the 1/2-inch-fin bed test, the calculated sorbent loading is 0.257 lb H_2O/lb sorbent, which is within 2.2 percent of that predicted by equilibrium data.

To emphasize the contention that there is little effect on the water adsorption due to the presence of CO_2, data from similar single-sorbate tests (water on 13X from Section 4) have been superimposed on the water breakthrough curves. For the 1/2-inch-fin bed test, where temperatures were relatively easily controlled, the two water breakthroughs are quite close together. The deviation between the two 1-inch-fin water breakthroughs is felt to be due to temperature control. It is doubtful that the temperature control variations are due to the CO_2, as the CO_2 adsorption period was long past when significant water breakthrough was noticed. Before water breakthrough at roughly four hours, the exit dew points for both tests with the 1/2-inch-fin bed were below -87°F (0.000006 lb H_2O/lb N_2). For the 1-inch-fin bed runs, lowest dew points were -82° and -76°F. From these data, there is no discernable effect of the CO_2.

ADSORPTION OF CO_2 BY MOLECULAR SIEVE BEDS WITH PRELOADS OF WATER

General Description of the Poisoning Phenomena in CO_2-Removal Beds

Even though predrier beds for spacecraft CO_2-removal systems can reduce the water concentration of the process gas stream to very low levels (-100° to -60°F dew point, approximately 2 to 45 ppm by weight), inevitably some of the water that does reach the CO_2-removal bed will be retained there. This of course is due to the tremendous affinity of molecular sieves for water. In a spacecraft system, with its cyclic sorption/desorption operation, the buildup of water on the CO_2-removal bed is very slow. This is as expected since much of the water adsorbed in one half cycle would be desorbed in the following half cycle. But over a long period of continual operation, a significant water load would be attained. Eventually, a cyclic, steady-state condition would be reached and no further net water retention would occur.

As the water load increases, the CO_2-removal performance of the system declines. Depending upon the actual design and performance requirements, a point can be reached where CO_2-removal performance is unsatisfactory. If this does occur, provisions would have to be made to discontinue operation with the system, and to remove the water load by a vacuum bakeout.

Ideally, it would be desired to produce a system where CO_2 performance would be acceptable even with the presence of a steady-state water load. This may not be possible; it would probably not produce a practical system with respect to size and weight. In any case, it is most desirable to know quantitatively how long a given system design will provide satisfactory

performance. Up to present, there has been sufficient uncertainty in this regard, that all spacecraft systems have been designed very conservatively and with provisions for vacuum bakeouts.

The prediction of the deviation of acceptable performance is very difficult. This is due to two circumstances. First, the rate and equilibrium data required for such computations are generally insufficient in breadth and usually questionable in accuracy. Second, the computation must involve the transient adsorption/desorption performance of the system over many, many cycles, possibly hundreds of cycles. This requires an extremely accurate numerical procedure; and computer costs can be very large.

Experimentally, of course, the duration of acceptable performance can be determined. However, the procedure is complicated and expensive, as controlled conditions must be maintained continuously for very long periods of time, up to several months. Even if an experiment does determine system performance lifetime, little basic information is gained, due to difficulty in relating the observed performance conditions to the existing bed water loading distribution and to general mass-transfer rates.

As an example of the current state-of-the-art, long duration tests indicate that the Skylab RCRS would perform satisfactorily for a period in excess of 120 days without interruption for a vacuum bakeout. Because of mission durations, and to allow a margin of safety, vacuum bakeouts for the RCRS are scheduled for every 28 days. The original RCRS design computations were based on the most conservative assumptions. One of these was that all water entering the CO_2-removal bed (containing molecular sieve 5A) would be retained by it. Similarly, conservative assumptions were made as to the poisoning effect of the retained water. With these assumptions it was relatively easy to produce a design that would meet the 28-day performance requirement; and the cost of the design process was held to a reasonable level. As indicated by tests mentioned above, the actual performance duration far exceeds the requirement. Fortunately, as can be seen by the basic bed sizes (7.5 and 9.9 lb) compared to total system weight (195 lb), little penalty is paid for the over design. However, as mission durations and crew sizes increase, it will be more important to produce more accurate designs. This will require considerably more and better information than that available for the Skylab RCRS design.

Test Concept

In order to produce refined data on the dynamic performance of beds with resident water loads, a series of controlled tests were devised. The test concept and conditions were compiled jointly between personnel of NASA Manned Spacecraft Center, NASA Langley Research Center, and AiResearch. Specific test procedures were implemented by AiResearch. Basically, the test concept was to place a known preload of water on the sorbent bed (either 5A or 13X) then to run a CO_2 adsorption breakthrough. The amount of the preload in all cases was to be that which would be in equilibrium with -80°F dew point (at 0.006 mm Hg p_{H_2O}). Baseline tests were to be run with the preloads placed

uniformly on the beds. Then, nonuniform preloads, but of the same total magnitude, were to be placed on the bed from flow streams of -40°F dew point and also of -20°F dew point. CO_2 breakthroughs were then to be run on these preloaded beds. Table 6-I presents summaries of the test conditions for which data is reported.

CO_2 Adsorption on Linde 5A Beds Containing Water Preloads

Procedure for Producing -80°F Dew Point Uniform Preload. - From Linde data, it was determined that the water loading on molecular sieve 5A corresponding to -80°F dew point, 0.006 mm Hg p_{H_2O}, and 70°F was 8.5 percent. At 7.0 psia total pressure, the water concentration in nitrogen for 0.006 mm Hg p_{H_2O} is only 7.7 ppm by weight. In order to load the 1/2-inch-fin bed containing about 1 lb of Linde 5A to 8.5 percent water, using the maximum flow rate possible in the apparatus (approximately 5 lb/hr), it would take nearly 100 days of continuous running if the process gas stream had a -80°F dew point. This was clearly an impractical situation. The procedure used involved operation of the bed at higher temperature and higher inlet dew point, such that the equilibrium loading was also 8.5 percent. From the equilibrium data, possible operating conditions lie on the line of constant 8.5 percent loading. It was desired to have as high water partial pressure as possible, in order to increase water concentration and decrease preloading time. However, very high sorbent temperatures were to be avoided due to limitations in the bed heating equipment. The conditions of 100°C (212°F) and 1.6 mm Hg p_{H_2O} (10°F dew point) were chosen as they would give the desired loading and were well within the capabilities of the equipment.

The procedure used is described as follows. The bed was first heated to essentially 212°F by the hot-nitrogen thermal loop, then opened to vacuum and pumped down to about 27 μ Hg. From equilibrium data, this operation would strip off all CO_2, but would leave a 2.5 percent water load on the bed. Then, with the bed still at 212°F, nitrogen with a 13°F dew point was passed through the bed at a flow rate of 4.0 lb/hr and pressure of 251 mm Hg. Flow was continued for a little over 9.5 hrs. At about 5 hrs into the test it was observed that inlet and outlet humidities were essentially equal. The additional test time was provided to insure bed saturation. According to equilibrium data with 13°F dew point (1.85 mm Hg p_{H_2O}) and 212°F isothermal bed, this operation would produce 8.9 percent loading. It was intended to produce a loading above the desired 8.5 percent and then gas strip back to the desired value. Calculations from the recorded inlet and outlet dew points indicated that the developed loading at that time was 8.76 percent. However, during the preloading procedure, mechanical problems were experienced with the manual dew-point instrument. Because of this, the full water breakthrough curve was not recorded and thus the 8.76 percent load value is only approximate. In view of the recorded temperatures in the bed, which varied from 163°F at the inlet

TABLE 6-I

TEST CONDITIONS FOR CO_2 ADSORPTIONS ON MOLECULAR-SIEVE BEDS WITH WATER PRELOADS

Run No.	Flow Rate (lb/hr)	Bed Temp. (°F)	P_{CO_2} (mm Hg)	Total Pressure (mm Hg)	Water Preload		CO_2 Adsorption (lb CO_2/lb MS)
					Percent	Preload Condition	
Linde 5A Molecular Sieve							
5A/W-CO_2 (1/2)-1	1.23	70°	7.22	365	8.76	Uniform	0.00443
-2s	1.23	70°	-	365	8.76	Uniform	0.00447
-3	1.23	70°	1.88	365	8.76	Uniform	0.00133
-4s	1.23	70°	-	365	8.76	Uniform	0.00105
-5	2.33	70°	7.14	365	8.76	Uniform	0.00152
-6s	2.23	70°	-	365	8.76	Uniform	0.00414
-7	1.23	70°	7.13	366	7.93	Derived from -20°F D.P. flow	0.0254
-8	1.23	71°	7.06	365	8.70	Derived from -20°F D.P. flow	0.0230
-9	2.23	72°	6.90	365	9.78	Derived from -20°F D.P. flow	0.0278
-10	1.23	70°	1.77	365	8.50	Derived from -20°F D.P. flow	0.0096
-11	1.23	70°	7.08	364	8.84	Derived from -40°F D.P. flow	0.0282
-12	2.23	70°	7.03	365	8.59	Derived from -40°F D.P. flow	0.0573
-13	1.23	70°	1.77	364	8.62	Derived from -40°F D.P. flow	0.0125
Linde 13X Molecular Sieve							
13X/W-CO_2(1/2)-1	1.23	70.5°	7.31	368	7.50	Uniform	0.00840
-2s	1.23	70°	-	368	7.50	Uniform	0.00898
-3	2.33	70.5°	7.02	366	7.50	Uniform	0.00855
-4s	2.33	70.5°	-	366	7.50	Uniform	0.00844
-5	2.33	70.5	7.00	368	7.50	Uniform	0.00844
-6s	2.33	70°	-	368	7.50	Uniform	0.00859
-7	2.33	70°	7.11	364	9.36	Derived from -20°F D.P. Flow	0.0294
-8	1.23	70°	7.10	364	9.58	Derived from -40°F D.P. flow	0.0224
-9	2.33	70°	7.07	364	9.42	Derived from -40°F D.P. flow	0.0233

to 230°F within the bed, an average of 220°F, the 8.9 percent theoretical loading would not be developed. The 8.76 percent value seemed reasonable.

The bed was then cooled to 70°F, inlet humidity adjusted to -80°F (±2°F), followed by several hours of gas stripping. During stripping it was evident that very little water was removed from the bed, and the procedure was discontinued. The slowness of the gas stripping is probably due to the extremely low partial-pressure driving forces involved.

The preload procedure was not as smooth as desired, especially with some data problems during breakthrough. However, the calculated 8.76 percent water loading is believed to be valid within about ±5 percent. This tolerance was considered acceptable for the test series.

CO_2 Adsorption by Linde 5A with a -80°F Dew Point Uniform Water Preload. - Immediately after the preloading sequence was finished CO_2 adsorption tests were conducted on the bed. In all such tests the water concentration in the nitrogen carrier gas was adjusted to -80°F dew point ±5°F. CO_2 adsorptions were conducted as in the single-sorbate test series. After complete CO_2 breakthrough was obtained, a gas stripping operation was performed to remove the CO_2 and prepare the bed for the next run. Calculations showed the gas strips quantitatively removed the CO_2 from the bed.

Figure 6-5 shows the CO_2 breakthrough and gas strip for the flow rate of 1.23 lb/hr. The curve shapes--when the gas strip curve is inverted--are almost identical. This is more clearly seen in the dimensionless curves of Figure 6-6. These curves show a much poorer breakthrough shape than noticed in the single-sorbate tests with CO_2 on dry Linde 5A.

Figure 6-7 presents the CO_2 adsorption and gas strip for the flow rate of 2.23 lb/hr. Altogether, 12 runs--adsorptions and gas strips--were run at 7 mm Hg p_{CO_2} and 70°F. Very good reproducibility was obtained. The average CO_2 loading obtained for the 12 runs was 0.00406 lb CO_2/lb sorbent; the standard deviation was 0.00026.

This CO_2 loading capacity compares reasonably well with coadsorption equilibrium data taken previously in the program, and shown in Figure 6-8. The loading does seem somewhat low with respect to the equilibrium data, and it might be speculated that the water preload on the bed was actually more than the calculated 8.76 percent. For example, if the water preload were 12 percent, the CO_2 loading derived from the dynamic tests would be more consistent with the equilibrium data taken earlier. However, according to Linde data, the partial pressure of water in equilibrium with 12 percent water loading is 0.025 mm Hg, which corresponds to a dew point of -60°F. The outlet dew point noted throughout the dynamic coadsorption tests was always much lower than this value, and there was virtually no change noted in later reruns after many hours of nearly continuous purging with -80°F dew-point flow. It is felt the CO_2 loading derived from the dynamic tests may be more reliable than that obtained in the equilibrium test apparatus.

CO_2 Adsorption by Linde 5A with Nonuniform Water Preloads. - The CO_2 adsorptions with uniform water preloads do not truly represent the phenomena expected in a spacecraft CO_2-removal bed. However, these tests can furnish basic data to help determine mass-transfer coefficients corresponding to the 8.76 percent water preload. A more realistic simulation would be with the resident water loading distributed predominantly at the front end of the bed. To accomplish this, a series of tests were conducted in which the preload was laid down by nitrogen flows which contained water to the level of -40° and -20°F dew points. The total water preloads were to be the same as that in the -80°F dew-point, uniform preload tests; that is, 8.8 percent. Each preload sequence was preceded by a vacuum-bakeout to remove all water and CO_2 from the bed. After each preload only one adsorption breakthrough was made as it was expected further testing would distribute the water preload. During each CO_2 adsorption, the flow stream dew point was adjusted to -80°F ±5°F.

Figure 6-9 shows the breakthrough curves derived for the flow rate of 1.23 lb/hr with nonuniform water preloads. Figure 6-10 shows the preload curves for the -40° and -20°F dew-point tests. Also shown on Figure 6-9 are the data points for a duplicate preload/CO_2-breakthrough of Run No. 5A/W-CO_2 (1/2)-8. This duplicate run (Run No. 5A/W-CO_2(1/2)-7) actually preceded the run that is plotted. Because of the circumstances of the duplicate run, the comparison between the two is of interest. The preloading sequence for each run required 24 hours continuous operation (see Figure 6-10a). The usual procedure was to bakeout the bed overnight, then to start the preload sequence by noon of the following day. Then in the afternoon on the day following this, the CO_2 breakthrough would be run. On this particular occasion, because of laboratory problems (-80°F dew point could not be attained due to anomalously high water content of the laboratory nitrogen), the CO_2 breakthrough could not be run. Since this was a Friday, it was decided to cool the closed bed at approximately 40°F during the weekend. The CO_2 breakthrough was then run on Monday. Because of doubts about the condition of the preload due to the 48-hr delay, the entire sequence was rerun. It seems obvious, because of the closeness of the breakthroughs, that there was not much migration of water within the bed during the idle period.

It is evident from Figure 6-9 that the distribution of the preload is quite important. For the -20° and -40°F dew-point preloads, it is expected that the water would be accumulated near the front of the bed, completely poisoning this region. However, the back end of the bed would be left relatively unpoisoned, capable of much more CO_2 adsorption than if the preload were uniform. It is noticed that the -40°F dew-point preload case picked up more CO_2 than that for -20°F dew-point preload. The proposed reason for this is that at the lower concentration, the bed would adsorb water more toward the front end of the bed and allow less to penetrate deeper into the bed. The net poisoning effect would thereby be somewhat less, and more CO_2 capacity would be retained.

Figure 6-11 presents CO_2 breakthroughs for nonuniform water preloads for the flow rate of 2.23 lb/hr. Figure 6-12 shows the water preload data for the -40° and -20°F dew-point sequences which preceded the CO_2 breakthroughs. In these tests there is a great difference in the CO_2 breakthroughs between the

-20° and -40°F dew-point preloads. It is not known why there is such a large difference here, and yet there was only a small difference for the low flow rate tests. The water preloading sequences were nearly identical, as can be seen from Figures 6-10 and 6-12. Possibly, with the longer CO_2 breakthrough for the low flow rate test, the preload could have migrated significantly, becoming more uniform and causing the breakthrough to be earlier, with less total CO_2 capacity.

However, the same general situation is felt to exist: that the -20° and -40°F dew-point preloads are concentrated at the front of the bed, leaving the rest of the bed relatively unpoisoned. Also, since the -40°F dew-point preload would be more concentrated toward the front of the bed, the CO_2 breakthrough would be longer and show higher loading.

Figure 6-13 presents CO_2 breakthrough curves on various water preloads for conditions of low CO_2 partial pressure, nominally 1.75 mm Hg. These curves exhibit the same effects as obtained with the 7 mm Hg p_{CO_2} tests. Figure 6-14 shows the water preload data for the -20° and -40°F dew-point sequences which preceded the tests shown in Figure 6-13.

Figures 6-15 and 6-16 present dimensionless CO_2 breakthrough curves for the test series with water-preloaded Linde 5A molecular sieves. Comparing the breakthroughs on preloaded beds to the dry breakthroughs, and also comparing the preloaded breakthroughs according to the type of preload, it seems that there is a definite mass-transfer rate effect due to the preadsorbed water. Since the flow rate and temperature in all CO_2 tests shown on each figure are the same, the gas-phase mass-transfer coefficient K_g would be essentially the same for all such tests. Therfore, increased intraparticle diffusional resistance due to the water preload is expected as the cause of the lower rates. It seems logical that partially filling the molecular sieve cages with water could impede the diffusional transfer of CO_2, or at least, produce a competition for adsorption sites that would impede the intraparticle adsorption process. On the other hand, it is possible that the poorer breakthrough shapes could be due to adverse or unfavorable equilibrium curve shapes. Data is not available to fully investigate this possibility. The possibility of greater intra-particle mass-transfer resistance seems much more likely.

CO_2 Adsorption on Linde 13X Beds Containing Water Preloads

Procedure for Producing the -80°F Dew Point Uniform Preload. - An improved procedure, over that used in the 5A series, was employed to produce the uniform water preload on the 13X molecular sieve beds. For -80°F dew point (0.006 mm Hg water partial pressure) and 70°F sorbent temperature, equilibrium data indicates a loading of 7.5 percent. As noted before, loading with -80°F dew-point flow stream is impractical; however, the same loading can be accomplished with higher dew points and higher bed temperatures. For this preload, -2°F dew-point (0.86 mm Hg p_{H_2O}) and 205°F bed temperature were chosen.

Two problem areas were encountered in the 5A procedure: nonuniform bed temperature and ineffectiveness of the gas strip procedure after loading. Nonuniform bed temperatures are due to the lack of a specifiec bed preheater and the rather high flow rate chosen for the preload sequence. It is noted that for 120°F adsorptions at normal flow rates, experience showed that the bed inlet section served as an adequate preheater. In the adopted procedure for preloading the 13X bed, it was decided to start with a high flow rate and produce the bulk of the preload, and then to reduce the flow until nearly uniform bed temperature was attained. Also, it was desired to load only to 7.5 percent and forego a gas strip afterward.

The 13X preload was preceded by a thorough vacuum-bakeout at 500°F. This was to remove all traces of water; thus producing a more well-defined starting point than in the 5A procedure. Final calculations of the water preload would then be more accurate.

The first portion of the preloading sequence used a relatively high flow rate of 4.0 lb/hr. The heating system was adjusted in an attempt to produce a bed temperature profile which averaged 205°F (the gradient actually produced was from 180° to 242°F). At these conditions, a water breakthrough was obtained in about 6-1/2 hours. This is shown clearly in Figure 6-17. After the initial breakthrough, the flow rate was reduced to 0.8 lb/hr in order to reduce the bed temperature gradient. The resulting temperature profile was from 190° to 209°F, with most of the bed at about 205°F. Immediately upon the adjustment of flow rate and temperature, the outlet dew point dropped to about -20°F, indicating the average bed temperature for the first breakthrough was considerably above the desired 205°F, and the bed was not yet saturated with respect to this sorbent temperature. Operation continued until the outlet dew point essentially reached the inlet at about -2°F. The total test time was over 17 hours. From a graphical integration of the data of Figure 6-17, the water loading derived in the operation was calculated as 7.5 percent, just as desired.

CO_2 Adsorption by Linde 13X with Uniform and Nonuniform Water Preloads. - Figures 6-18 and 6-19 show the CO_2 breakthrough curves obtained from the uniformly preloaded bed. Each CO_2 adsorption was followed by a gas stripping operation. The water preload was essentially unaffected by these operations as the dew point of the gas stream was maintained about -80°F. A rerun of the initial CO_2 breakthrough was made in order to check the condition of the preload. As shown in Figure 6-19, the rerun breakthrough was essentially identical to the first run. The CO_2 adsorption capacities for the three adsorptions and the three gas strips were all quite close, averaging 0.857 percent. From the coadsorption equilibrium data, the CO_2 loading for 7.5 percent water preload is interpolated to be 1.15 percent. No definite explanation for the difference between dynamic capacity and the equilibrium data is available. It is possible that the equilibrium data, which is rather difficult to obtain, is biased high.

Figures 6-20 and 6-22 show CO_2 breakthrough curves obtained for nonuniform water preloads. Figures 6-21 and 6-23 show the data from the water preload sequences involving -40° and -20°F dew-point flows. Those preload

sequences were essentially identical to those used in the 5A tests. There is one exception; for the preloading run 13X/W-CO_2(1/2)-7 (Figure 6-23) a lower carrier gas flow rate was used, 4.0 vs. 5.2 lb per hr.

The general trend of the data for 13X is the same as that for 5A. That is, the beds loaded uniformly with water in equilibrium with -80°F dew point show considerably less CO_2 capacity than dry beds. Beds loaded to the same extent (or more), but in such a manner as to concentrate the water at the front end of the bed, show CO_2 capacities intermediate between those of the uniformly preloaded beds and dry beds. One difference seems to be apparent. For 13X, the -20°F dew-point preloaded bed shows greater capacity than the -40°F dew-point preloaded bed. The opposite was true for 5A. The suspected cause of this difference lies in the -20°F dew-point preload on 13X being derived from the lower flow of 4.0 lb per hr. It is assumed that with the lower flow, in spite of the higher inlet concentration, the water was adsorbed more predominantly on the front end of the bed, with relatively less adsorption elsewhere in the bed.

Dimensionless CO_2 breakthrough curves are shown for all coadsorption tests on 13X in Figures 6-24 and 6-25. From the figures it is apparent that the water preload has a lowering effect on the mass-transfer rate. As noticed for the 5A tests, both the magnitude of the preload and the preload distribution are factors in how much the rate is affected.

It seems that 13X sorbent is less effected in rate by water preloads than 5A. This conclusion is based upon a comparison of Figure 6-24 and Figure 6-15. In Figure 6-15 for 5A sorbent, the curves for the preloaded beds are relatively less steep when compared to the dry-bed curves. As discussed earlier for the 5A tests, the general explanation for the lower mass-transfer rate is that the preloaded water significantly restricts movement of CO_2 molecules within the zeolite structure. Since 13X has a much more open crystal structure, it is expected that the preloaded water would indeed have less effect than with 5A.

Prediction of Water Preloads Derived from -20° and -40°F Dew-Point Flows

Performance-prediction program S9960 was used to predict the nonuniform water loading distributions for four of the preload sequences which involved -20° and -40°F dew-point flows. Two of the computations were for the Linde-5A series. Runs 5A/W-CO_2(1/2)-9p and -12p; the other two computations were for the Linde-13X series, Runs 13X/W-CO_2(1/2)-7p and -9p. The best predictions were obtained for K_g = 0.0004 lb-moles/hr-ft^2-°F and D = 0.001 ft^2/hr. Prediction accuracy was judged by comparing the total bed loadings from the computer predictions with that calculated from experimental data.

Figures 6-26 and 6-67 present the predicted water loading distributions (water loading vs axial position in the bed). As suggested earlier, the figures show that the preloads derived from -20° and -40°F dew-point flows are concentrated in the front of the bed, with the back of the bed relatively unloaded.

From Figure 6-26, showing the preloads on Linde 5A, it is difficult to see why the CO_2 breakthroughs conducted after the preload sequences (shown earlier in Figure 6-11) are so different (the -40°F dew-point preload breakthrough being much better). Possibly, the additional amount of water present migrated considerably during the CO_2 breakthrough for the -18°F dew-point-preload case, and caused considerable poisoning throughout the bed.

On the other hand, for the preloads on Linde 13X, shown in Figure 6-27, it seems that the -20°F dew-point preload would yield somewhat more CO_2 capacity than that for -40°F dew point. Figure 6-22 does show somewhat higher capacity for the -20°F dew-point run. The very small amount of loading in the rear of the bed is considered to give the greater observed capacity. It should be noted that at about 5 percent water loading, the CO_2 absorption capacity is a less than half of that of dry molecular sieve; at 7 percent it is about one quarter or less. Thus, it would seem that the front of the bed is completely poisoned and the loading in the rear of the bed determines the remaining capacity.

Prediction of Mass-Transfer Parameters on Uniformly Preloaded Beds

An attempt was made to evaluate mass-transfer parameters from the CO_2 breakthrough curve of Run No. 5A/W-CO_2(1/2)-5 on the uniformly water-preloaded Linde 5A bed. In order to do this, the equilibrium isotherm for the adsorption conditions had to be obtained. Experimental data was not available; therefore the isotherm was approximated. This was accomplished as follows: first, it was fairly certain from dynamic tests that at about 7.1 mm Hg p_{CO_2} the bed equilibrium loading was approximately 0.00406 lb CO_2/lb 5A. This was discussed earlier in this section. Then from the data contained in Figure 3-23 this equilibrium point was located and the slope for the isotherm was approximated. It was then estimated that the isotherm would pass through the point of w = 0.001 lb CO_2/lb 5A and p_{CO_2} = 0.4 mm Hg. On log-log paper a straight line was drawn through these two points; this straight line was the isotherm for which tabled values were included in the performance-prediction program.

The evaluation yielded one combination of K_g/D which gave a good fit of the experimental curve. The values were K_g = 0.0001 lb-mole/hr-ft^2-mm Hg and D = 0.0001 ft^2/hr. Figure 6-28 shows the prediction obtained with these values. From all of the predictions, it was fairly definite that diffusivity values of 0.00004 and 0.001 ft^2/hr were too low and too high, respectively. There seemed to be some latitude in the K_g value, possibly down to 0.00075 lb-mole/hr-ft^2-mm Hg.

Higher K_g values than shown in Figure 6-28 tended to predict later breakthroughs in the early portion of the run; however, predictions for all K_g values for a particular diffusivity seemed to merge into one line for the later part of the breakthrough.

No other evaluations were attempted due to the obvious approximate nature of the equilibrium data. This one evaluation does serve to point out that rate coefficients are reduced to some extent when the sorbent contains a water preload.

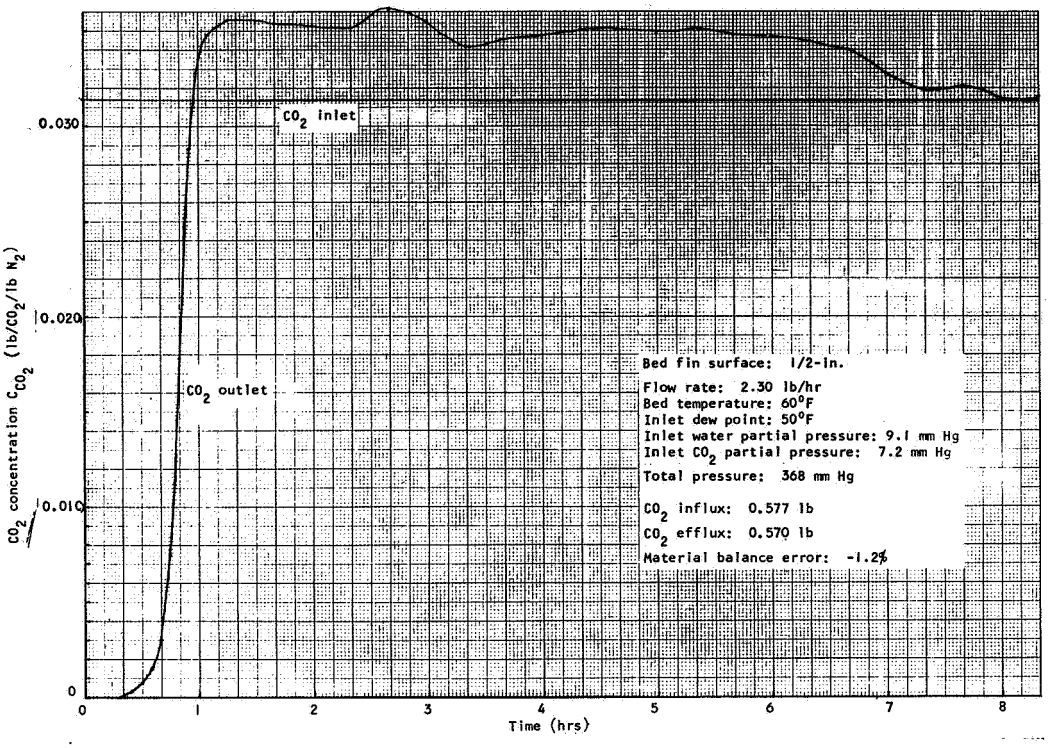

Figure 6-1. CO_2 Concentrations for Simultaneous Adsorption of CO_2 and Water on Linde 13X, Run No. 13X/CO_2-W(1/2)-1

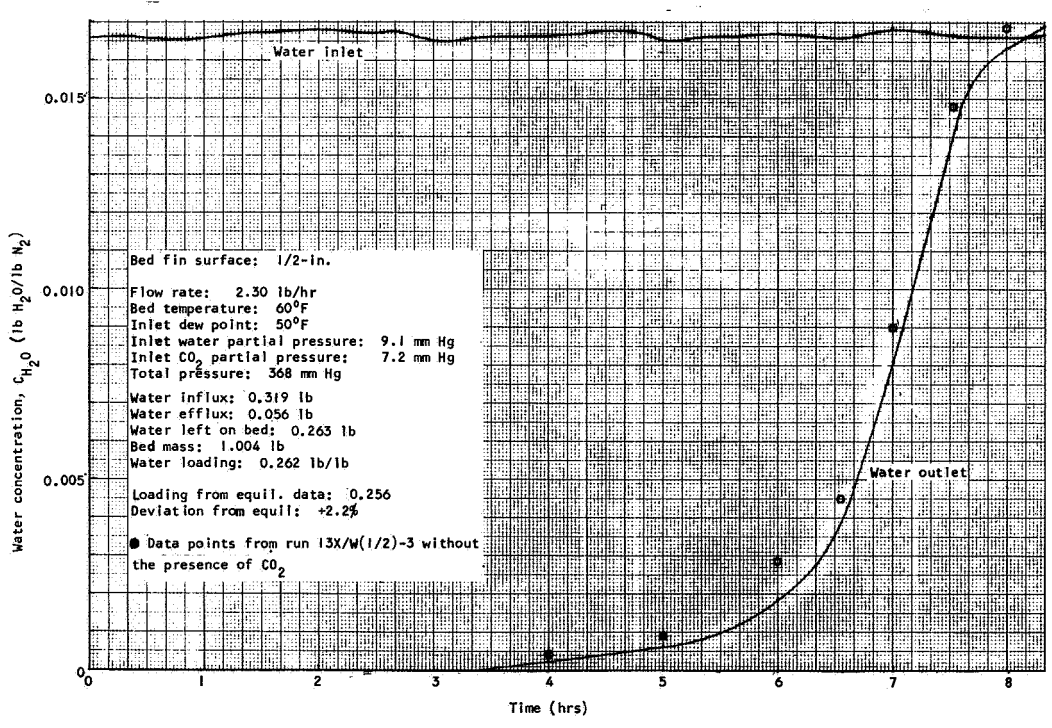

Figure 6-2. Water Concentrations for Simultaneous Adsorption of CO_2 and Water on Linde 13X, Run No. 13X/CO_2-W(1/2)-1

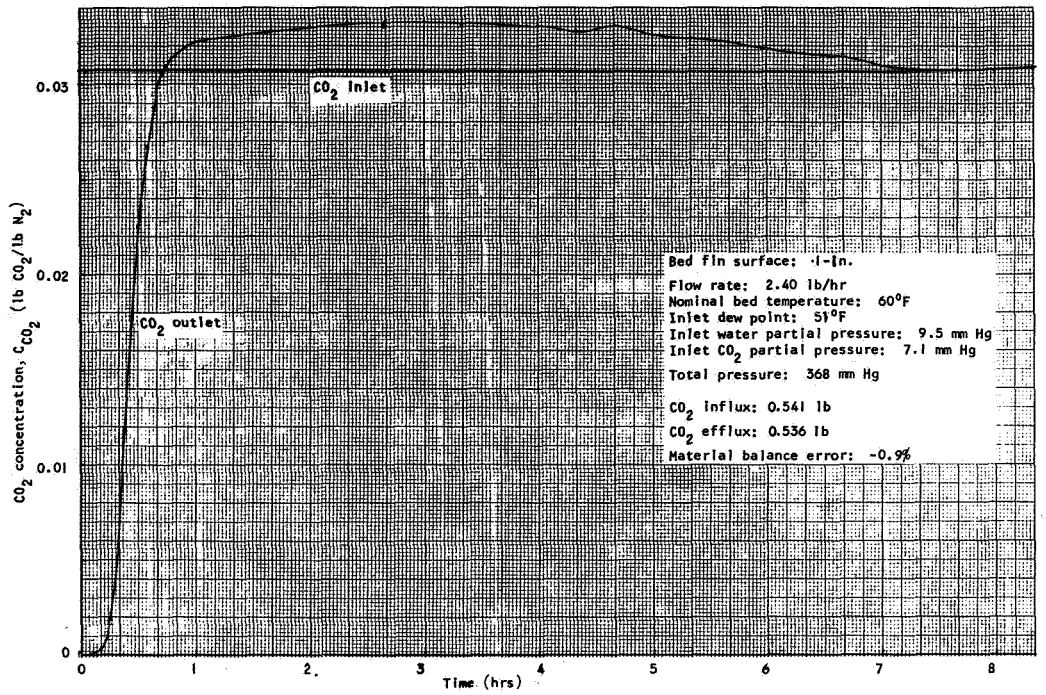

Figure 6-3. CO_2 Concentrations for Simultaneous Adsorption of CO_2 and Water on Linde 13X, Run No. 13X/CO_2-W(1)-1

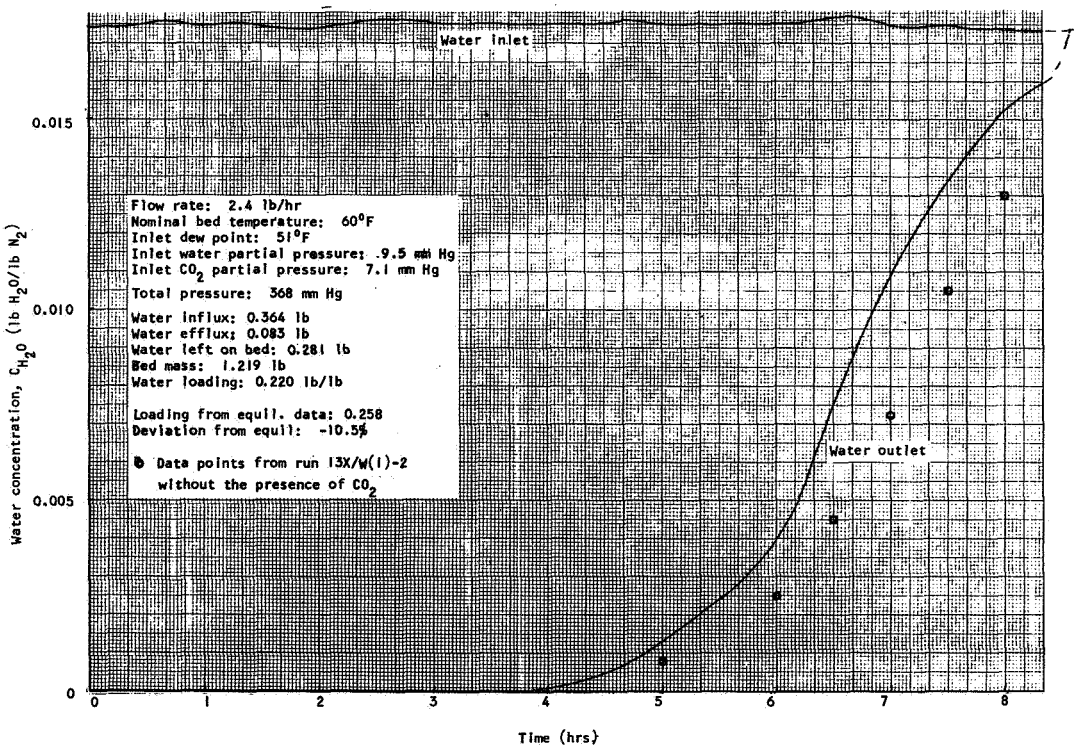

Figure 6-4. Water Concentrations for Simultaneous Adsorption of CO_2 and Water on Linde 13X, Run No. 13X/CO_2-W(1)-1

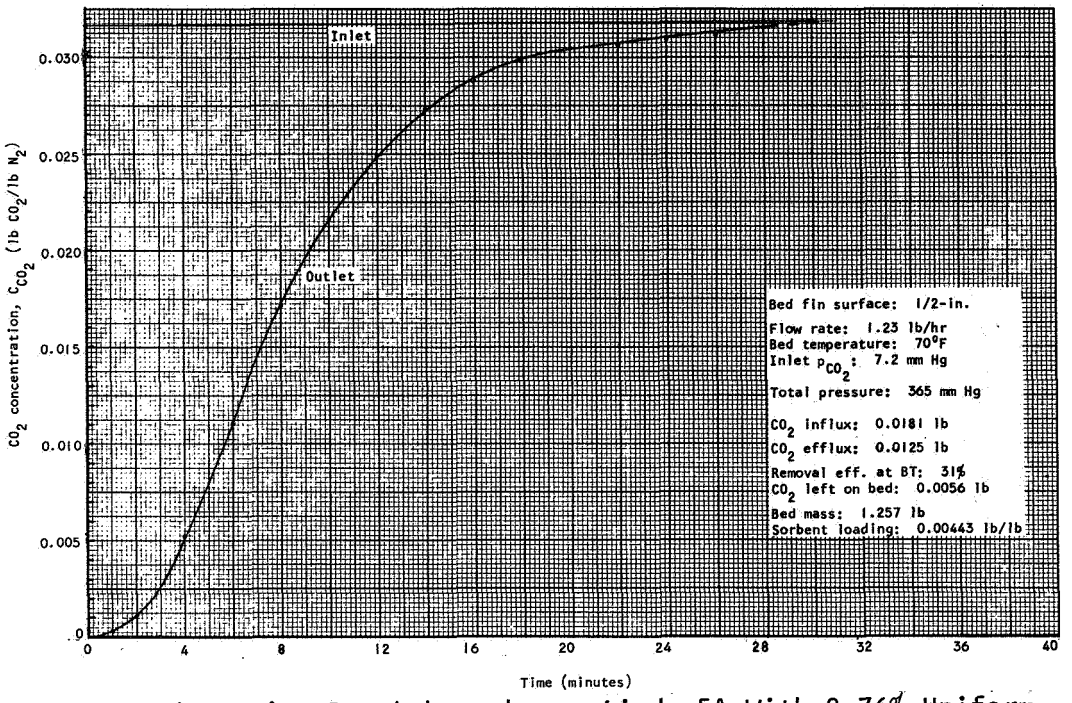

A. CO_2 Adsorption Breakthrough, on Linde 5A With 8.76% Uniform Water Preload, Run No. 5A/W-CO_2(1/2)-1

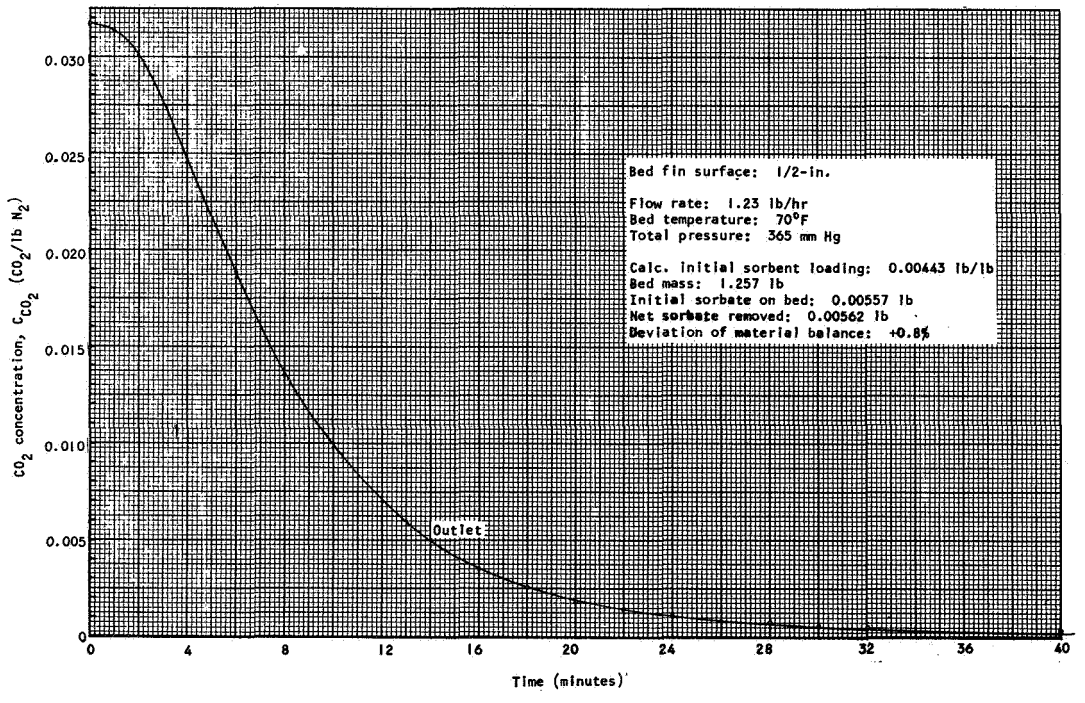

B. Gas Trip of CO_2 From Linde 5A with 8.76% Uniform Water Preload Run No. 5AW-CO_2(1/2)-2s

Figure 6-5. CO_2 Adsorption Breakthrough Run No. 5A/W-CO_2(1/2)-1 and Gas Strip Run No. 5A/W-CO_2(1/2)-2s

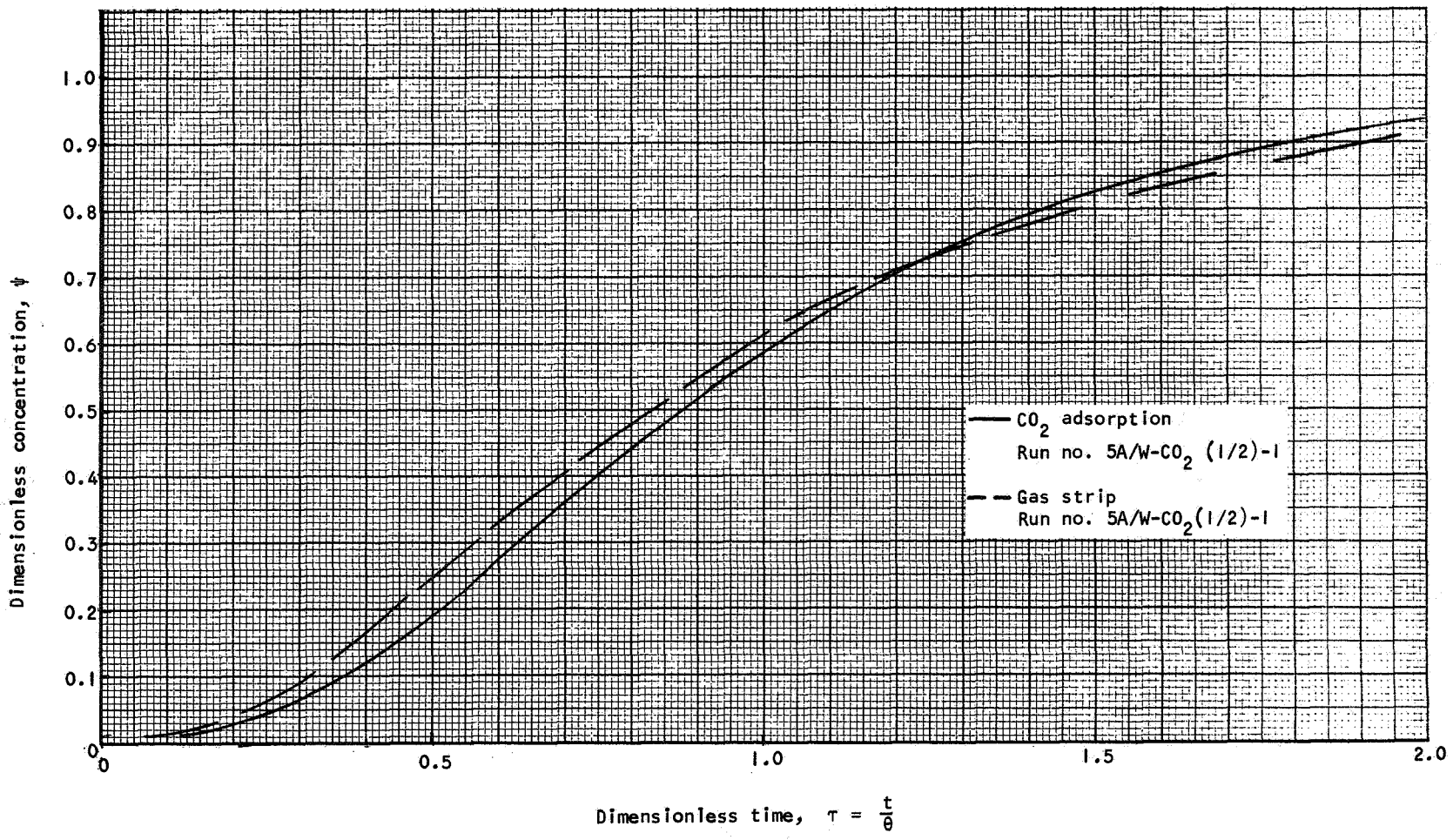

Figure 6-6. Dimensionless Breakthrough Curves; CO_2 on Linde 5A, 8.76% Uniform Water Preload

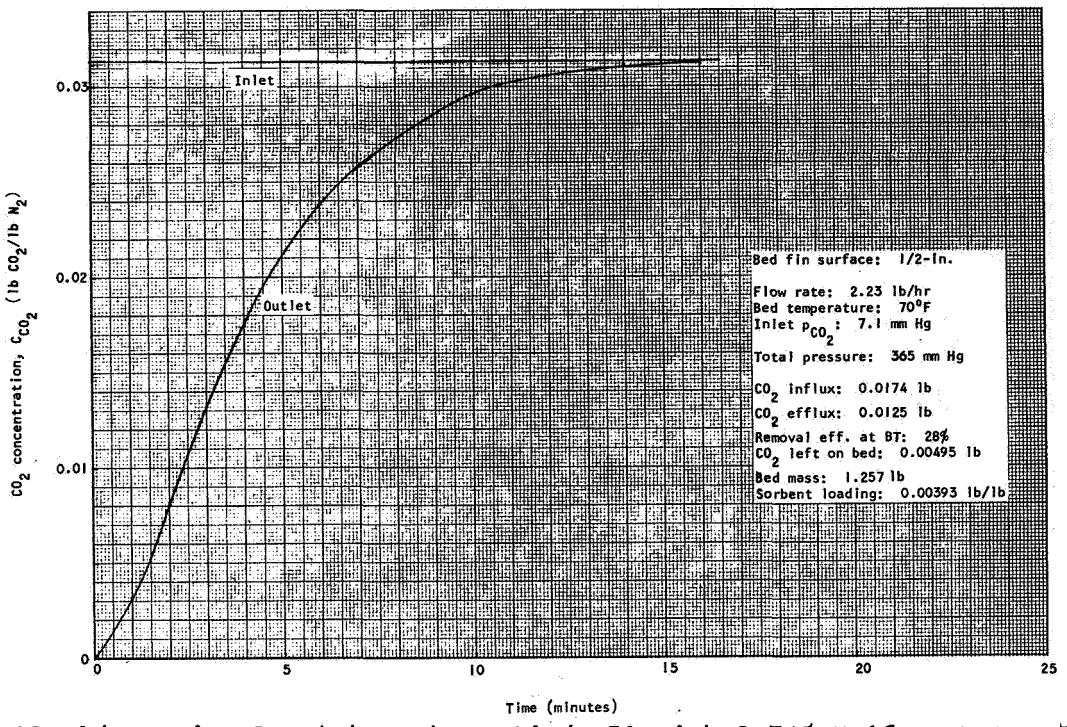

A. CO_2 Adsorption Breakthrough on Linde 5A With 8.76% Uniform Water Preload, Run No. 5A/W-CO_2(1/2)-5

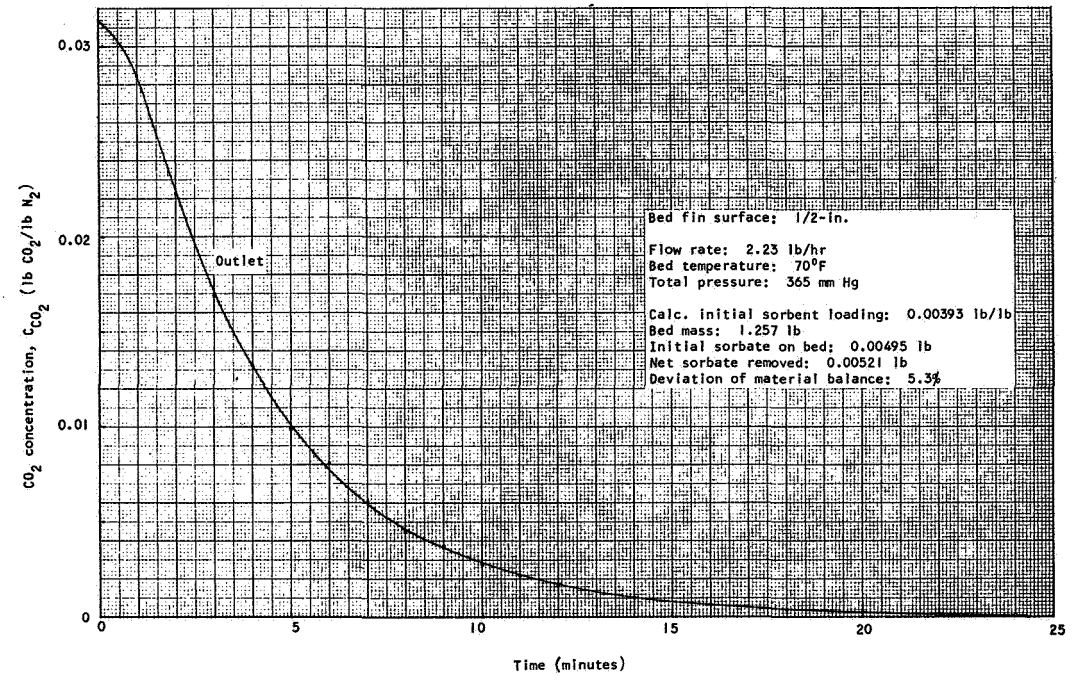

B. Gas Strip of CO_2 From Linde 5A With 8.76% Uniform Water Preload, Run No. 5A/W-CO_2(1/2)-6s

Figure 6-7. CO_2 Adsorption Breakthrough Run No. 5A/W-CO_2(1/2)-5 and Gas Strip Run No. 5A/W-CO_2(1/2)-6s

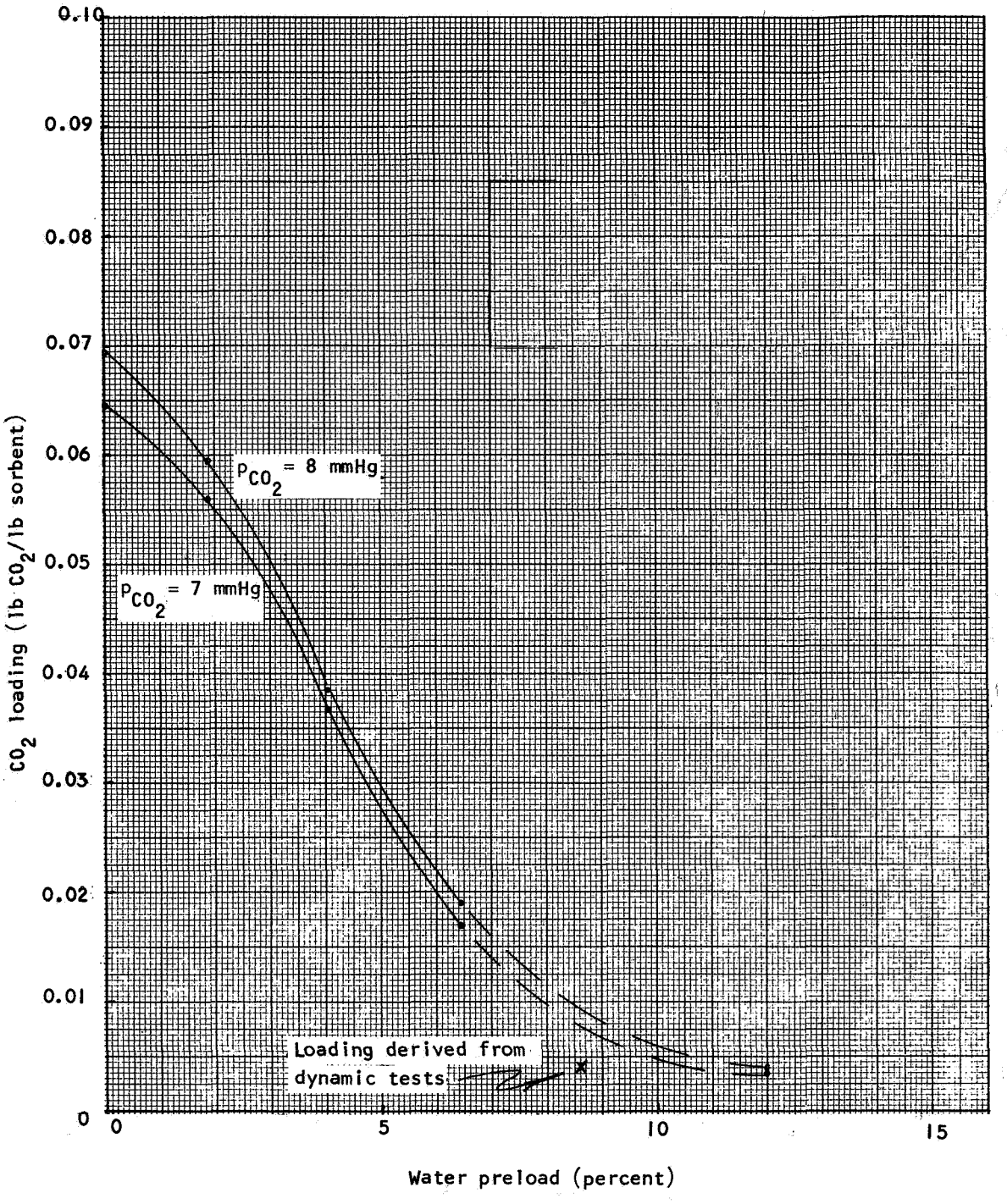

Figure 6-8. Water/CO_2 Coadsorption Equilibria for Linde 5A Molecular Sieve Pellets

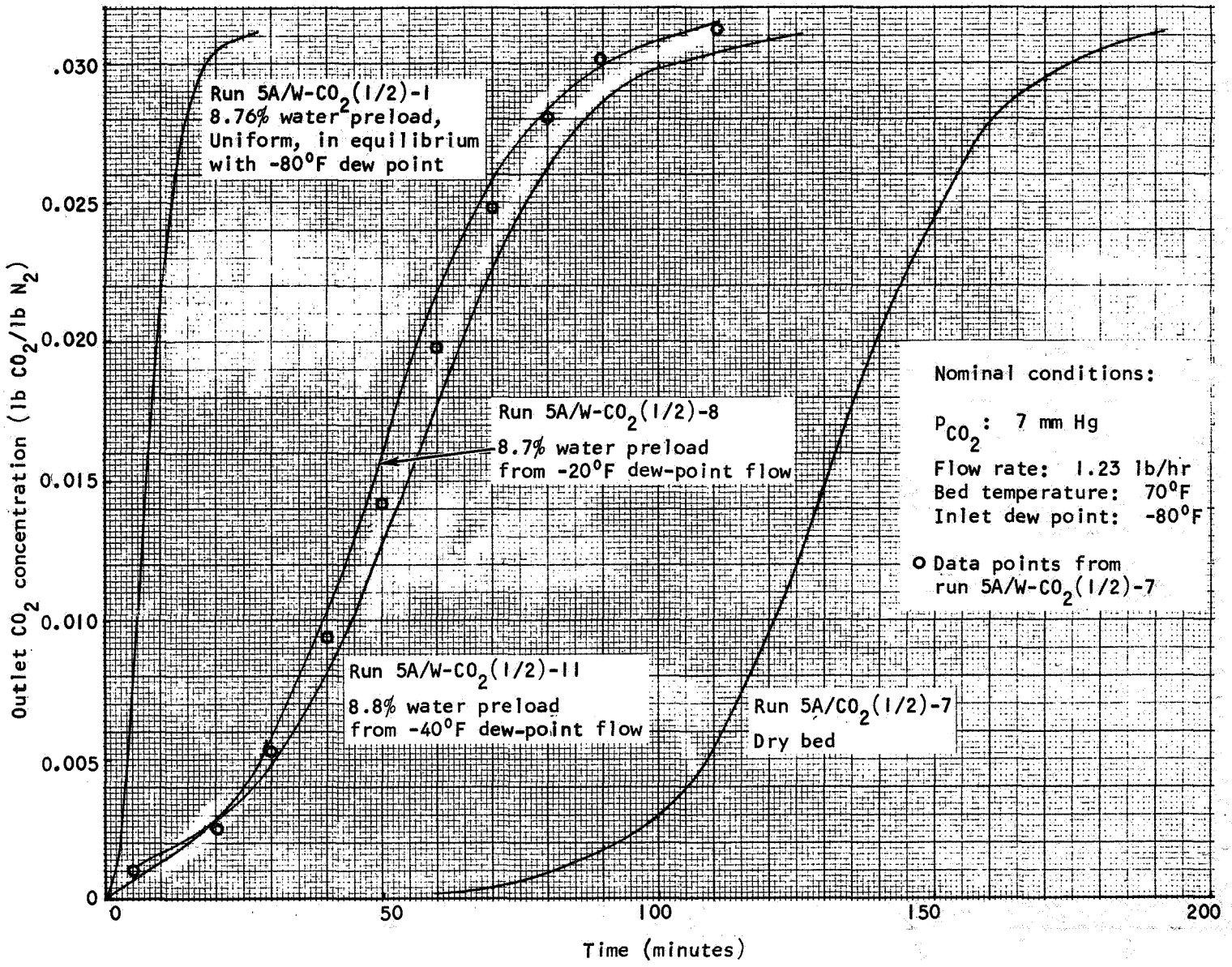

Figure 6-9. CO_2 Breakthrough Curves on Water Preloaded Linde 5A Molecular Sieve (1.23 lb/hr)

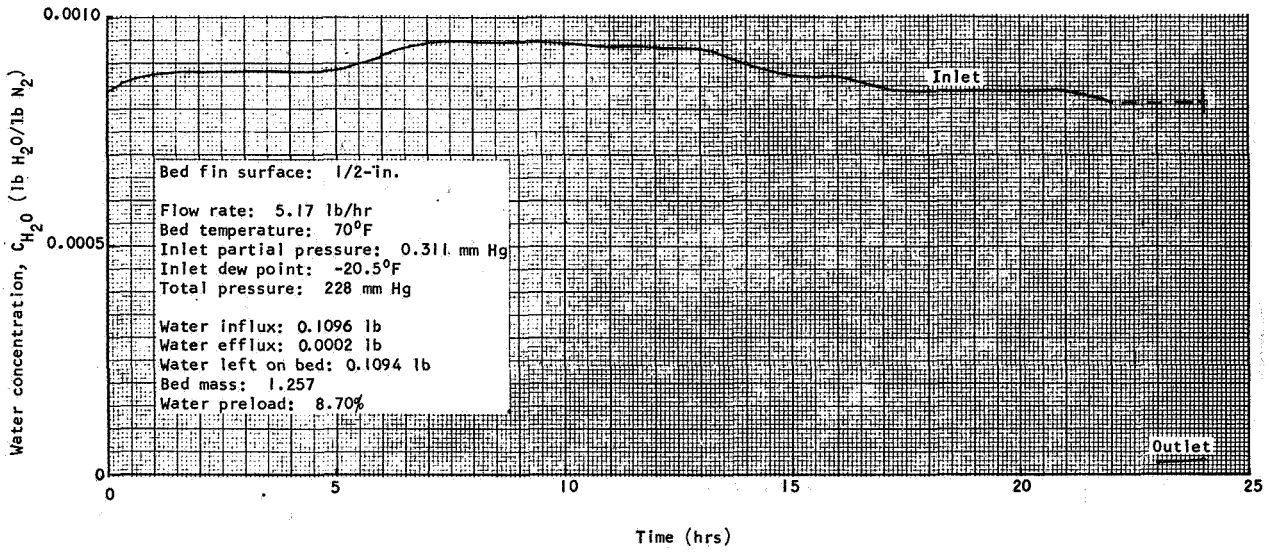

A. Water Preloading Sequence on Linde 5A, Run No. 5A/W-CO_2(1/2)-8p

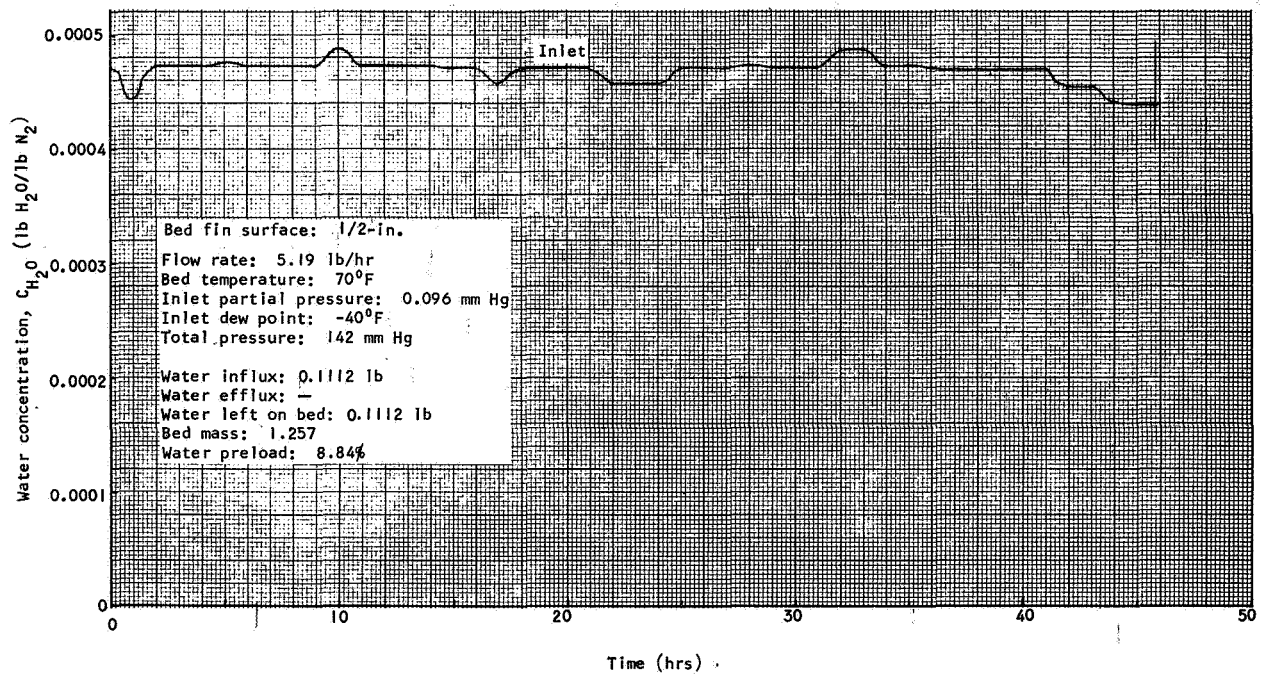

B. Water Preloading Sequence on Linde 5A, Run No. 5A/W-CO_2(1/2)-11p

Figure 6-10. Water Preloading Sequences on Linde 5A Run Nos. 5A/W-CO_2(1/2)-8p and 5A/W-CO_2(1/2)-11p

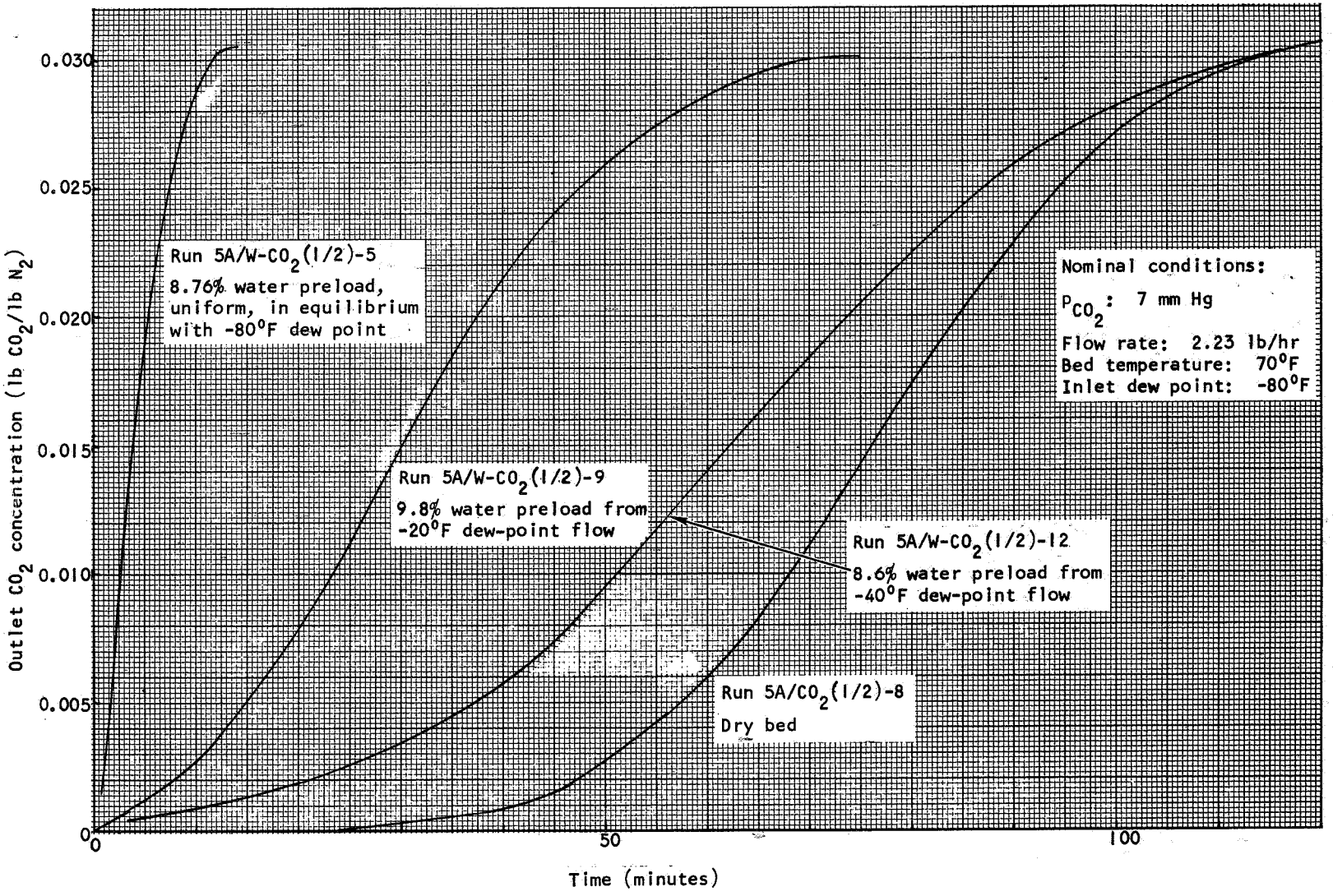

Figure 6-11. CO_2 Breakthrough Curves on Water Preloaded Linde 5A Molecular Sieve (2.23 lb/hr)

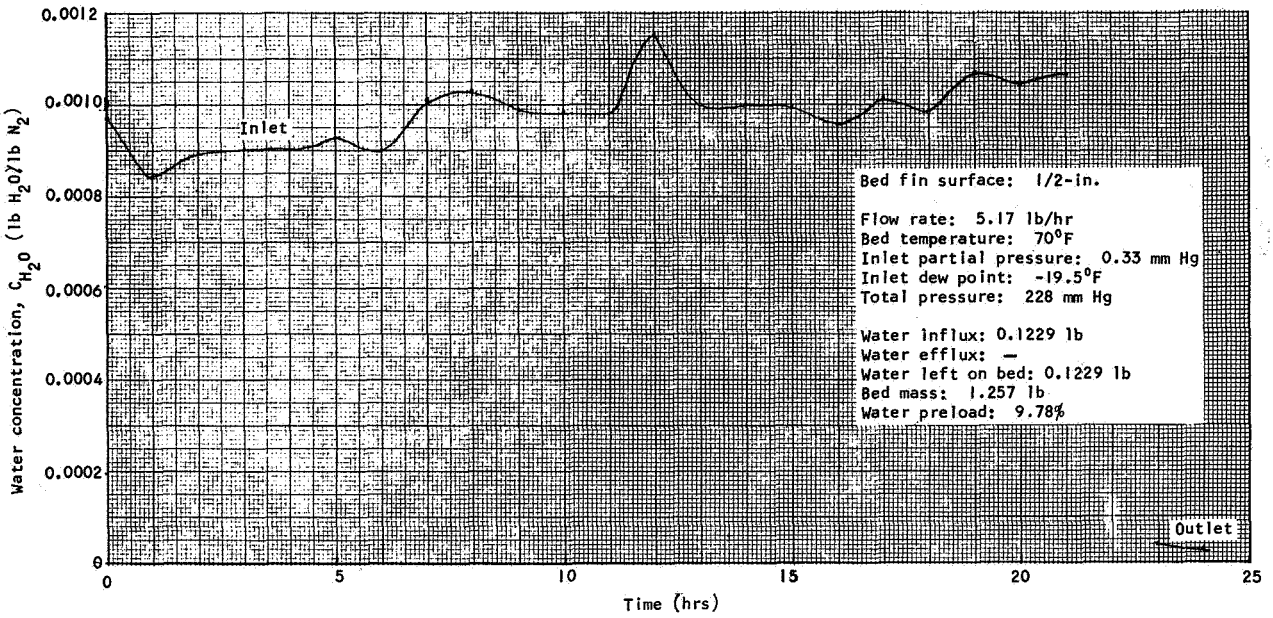

A. Water Preloading Sequence on Linde 5A, Run No. 5A/W-CO_2(1/2)-9p

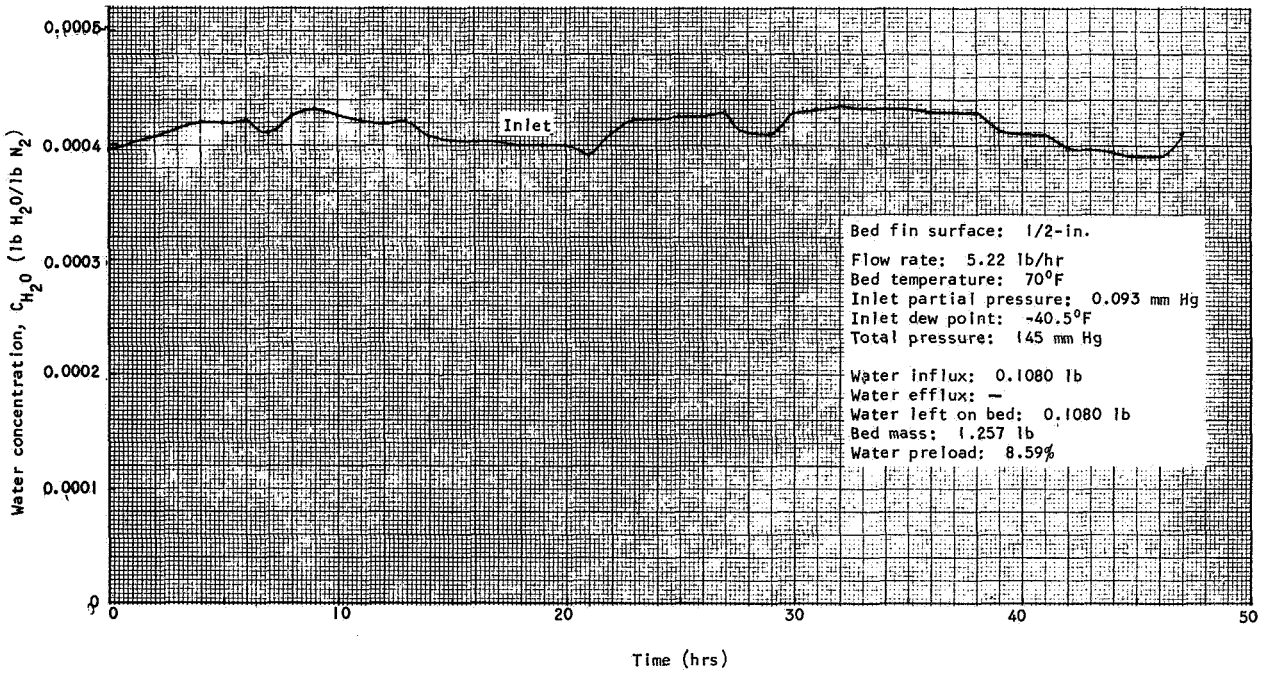

B. Water Preloading Sequence on Linde 5A, Run No. 5A/W-CO_2(1/2)-12p

Figure 6-12. Water Preloading Sequences on Linde 5A, Run Nos. 5A/W-CO_2(1/2)-9p and 5A/W-CO_2(1/2)-12p

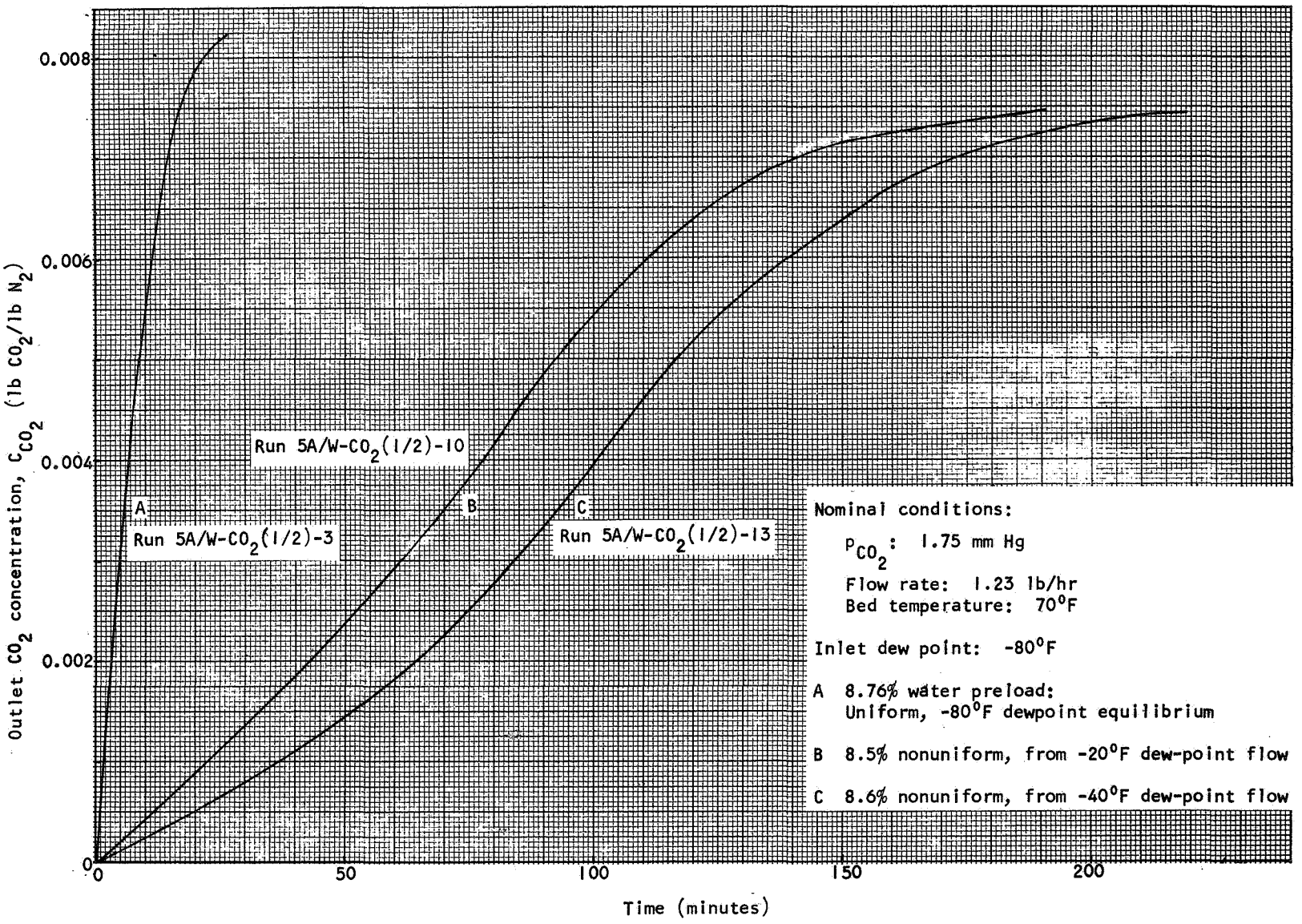

Figure 6-13. CO_2 Breakthrough Curves on Water Preloaded Linde 5A Molecular Sieve at Low CO_2 Partial Pressure

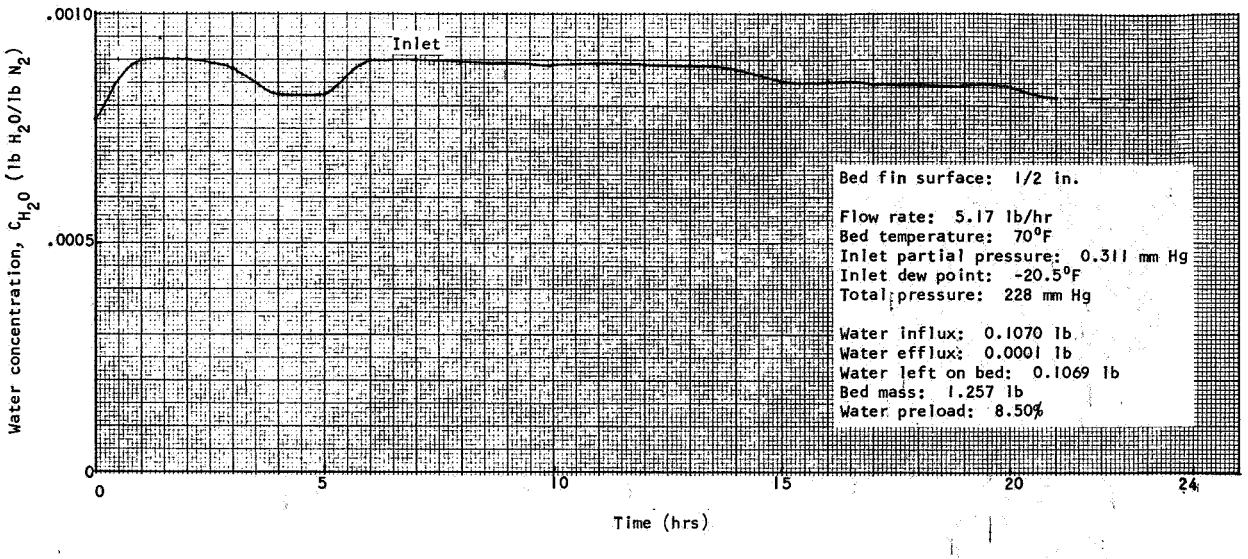

A. Water Preloading Sequence on Linde 5A, Run No. 5A/W-CO_2(1/2)-10p

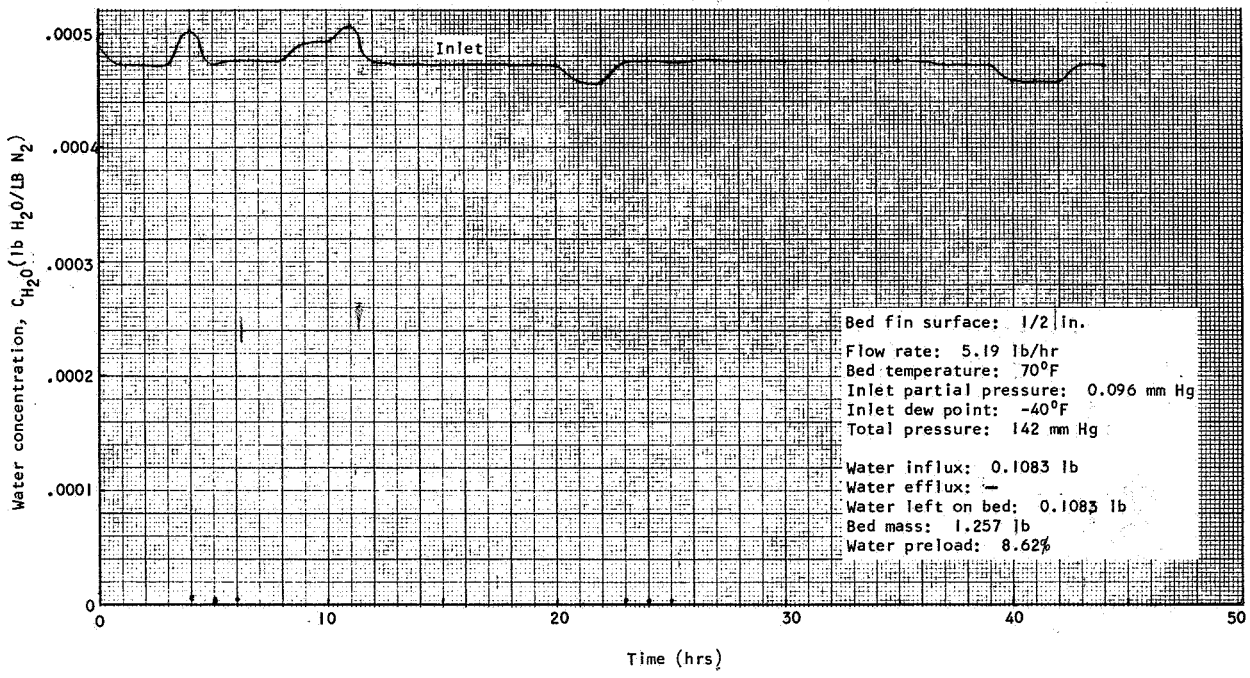

B. Water Preloading Sequence on Linde 5A, Run No. 5A/W-CO_2(1/2)-13p

Figure 6-14. Water Preloading Sequences on Linde 5A, Run Nos. 5A/W-CO_2(1/2)-10p and 5A/W-CO_2(1/2)-13p

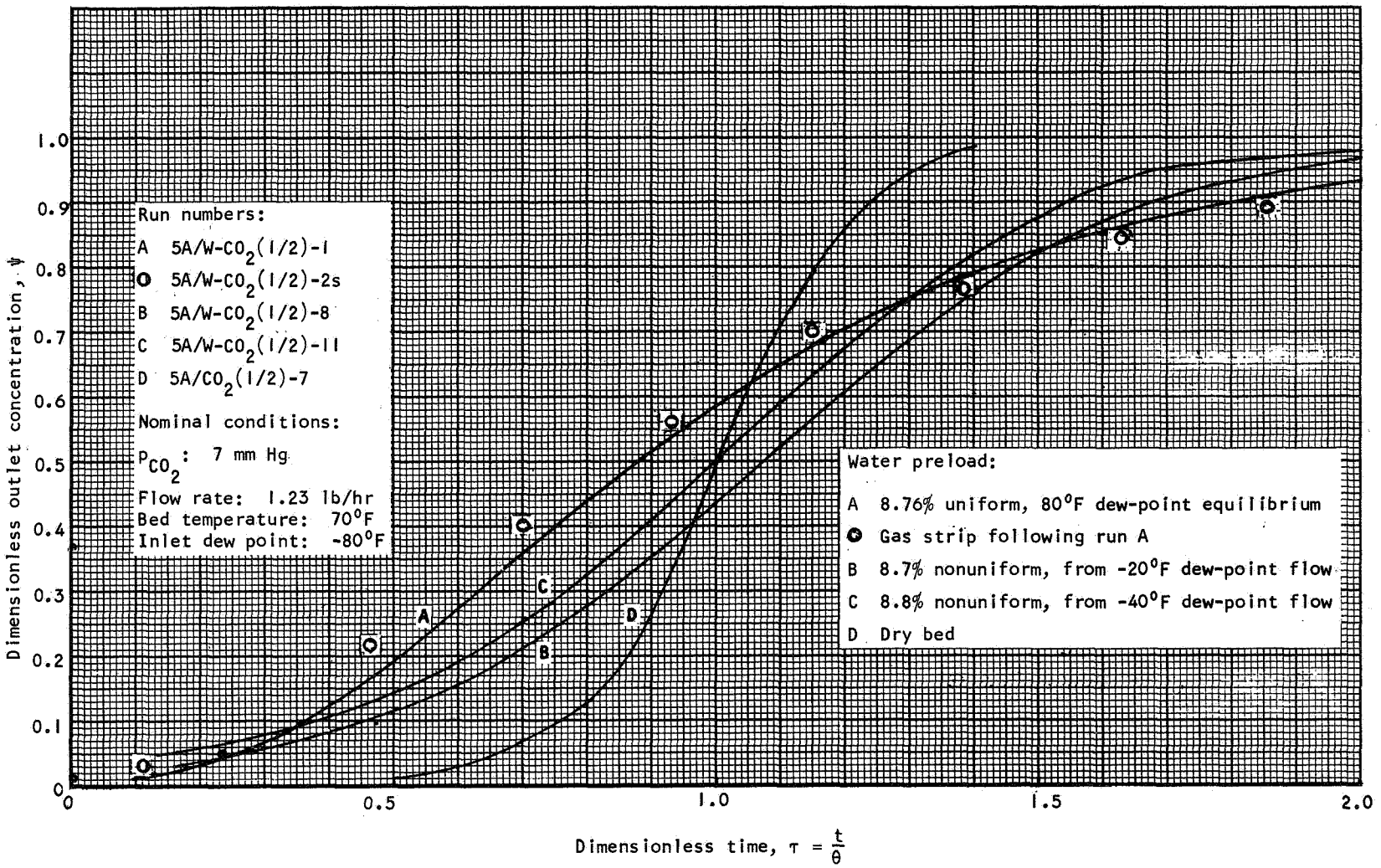

Figure 6-15. Dimensionless CO_2 Breakthrough Curves on Water Preloaded Linde 5A Molecular Sieve (1.23 lb/hr)

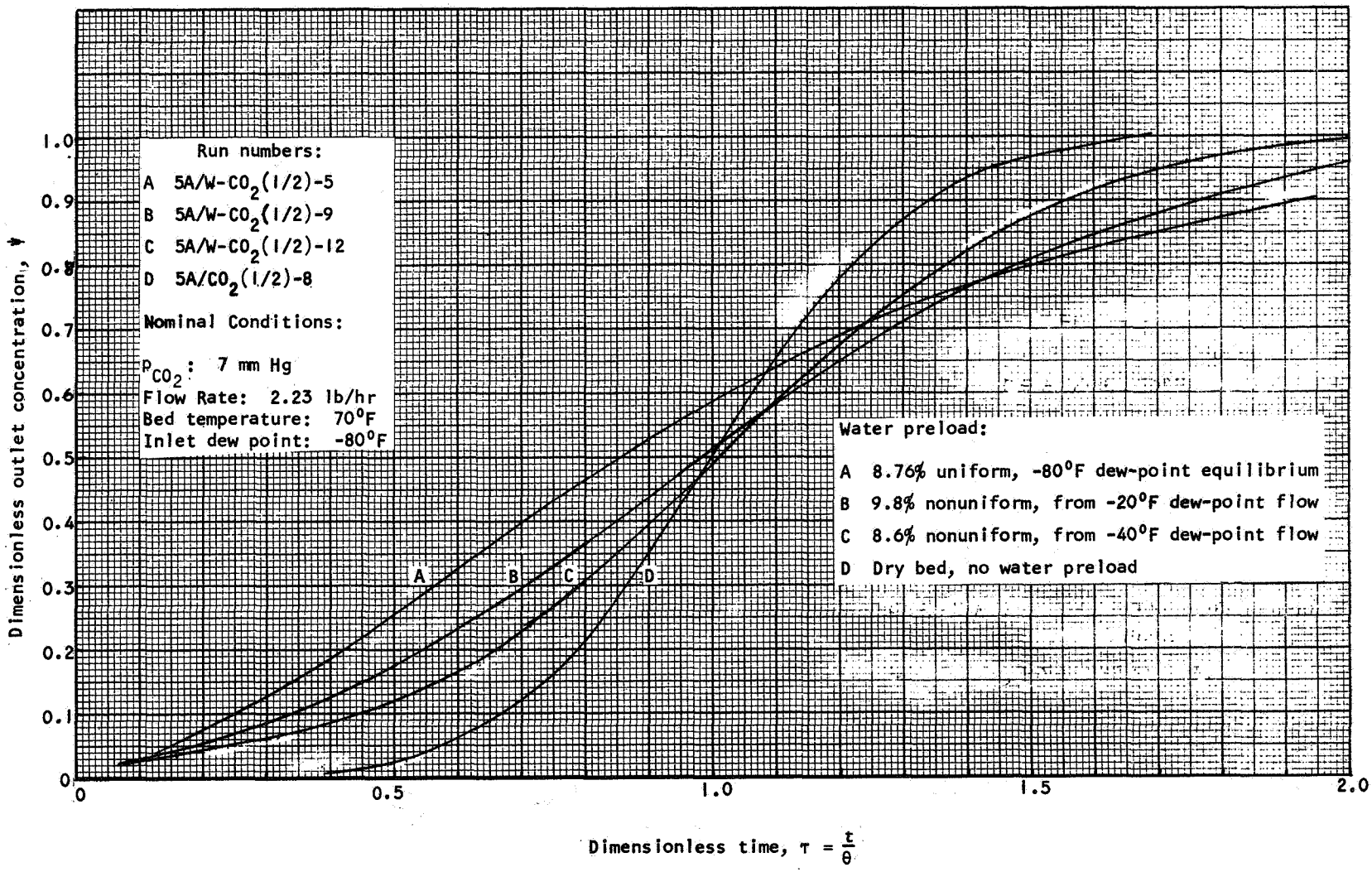

Figure 6-16. Dimensionless CO_2 Breakthrough Curves on Water Preloaded Linde 5A Molecular Sieve (2.23 lb/hr)

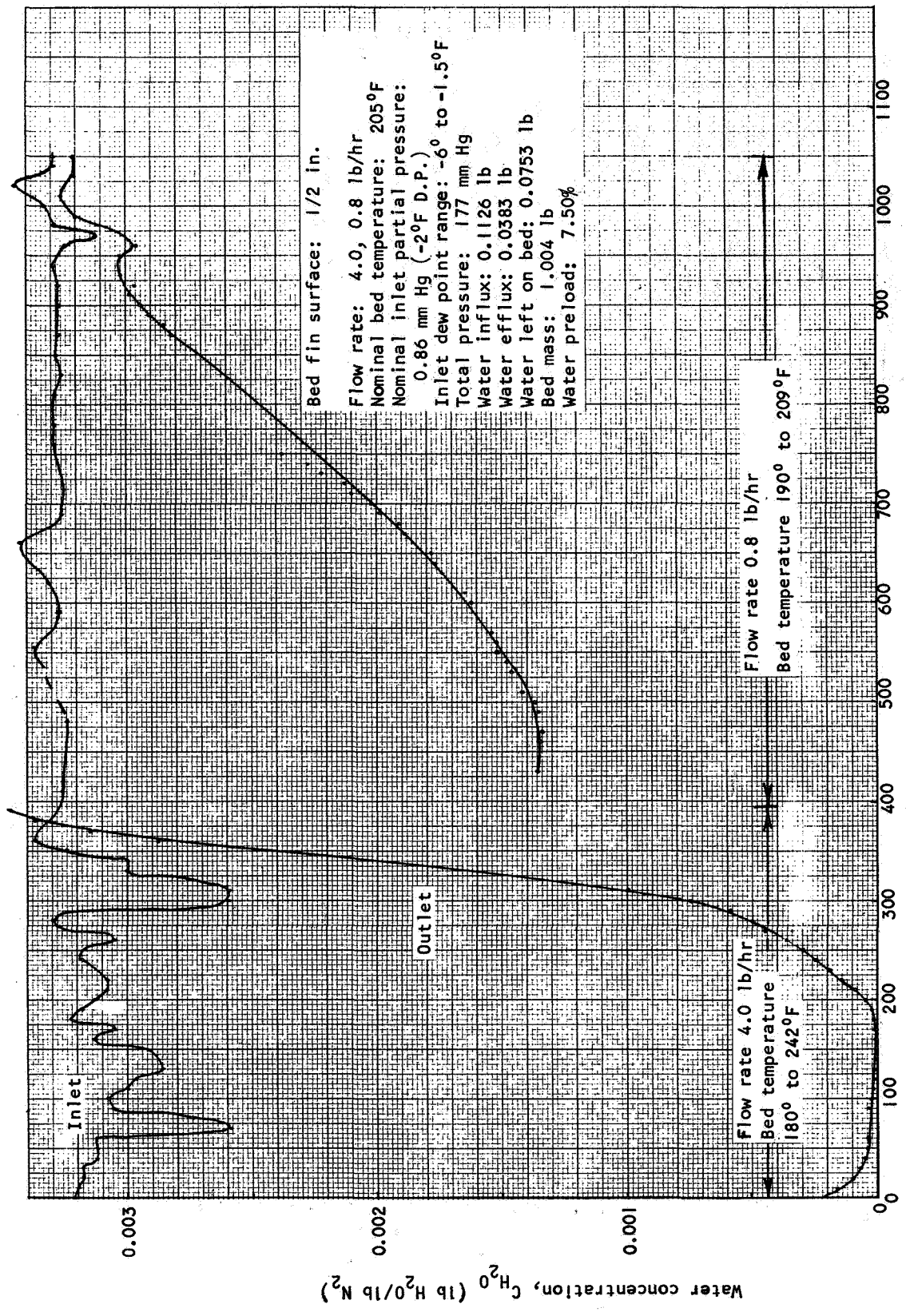

Figure 6-17. Water Preloading Sequence on Linde 13X, Run No. 13XW-CO_2(1/2)-1p

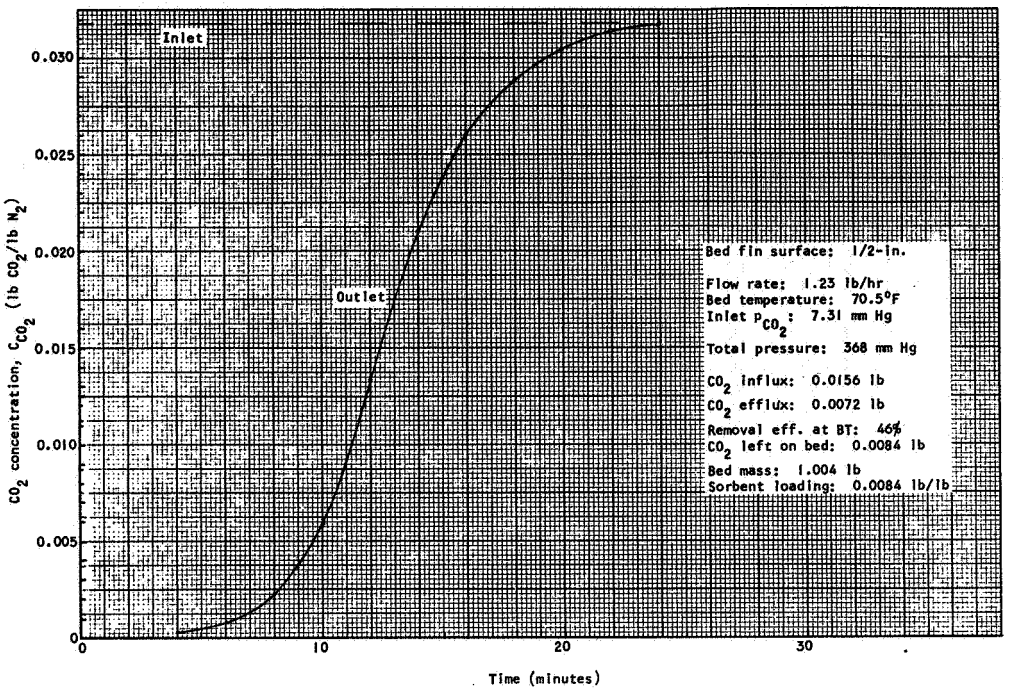

A. CO_2 Adsorption Breakthrough on Linde 13X With 7.5% Uniform Water Preload, Run No. 13X/W-CO_2(1/2)-1

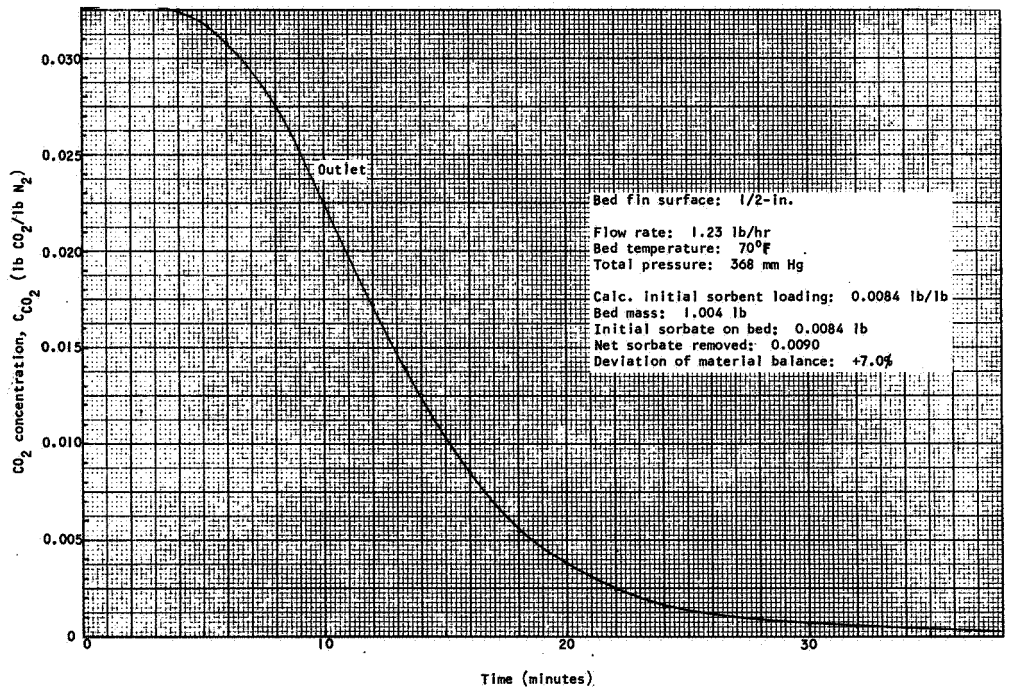

B. Gas Strip of CO_2 From Linde 13X With 7.5% Uniform Water Preload, Run No. 13X/W-CO_2(1/2)-2s

Figure 6-18. CO_2 Adsorption Breakthrough Run No. 13X/W-CO_2(1/2)-1 and Gas Strip Run No. 13X/W-CO_2(1/2)-2s

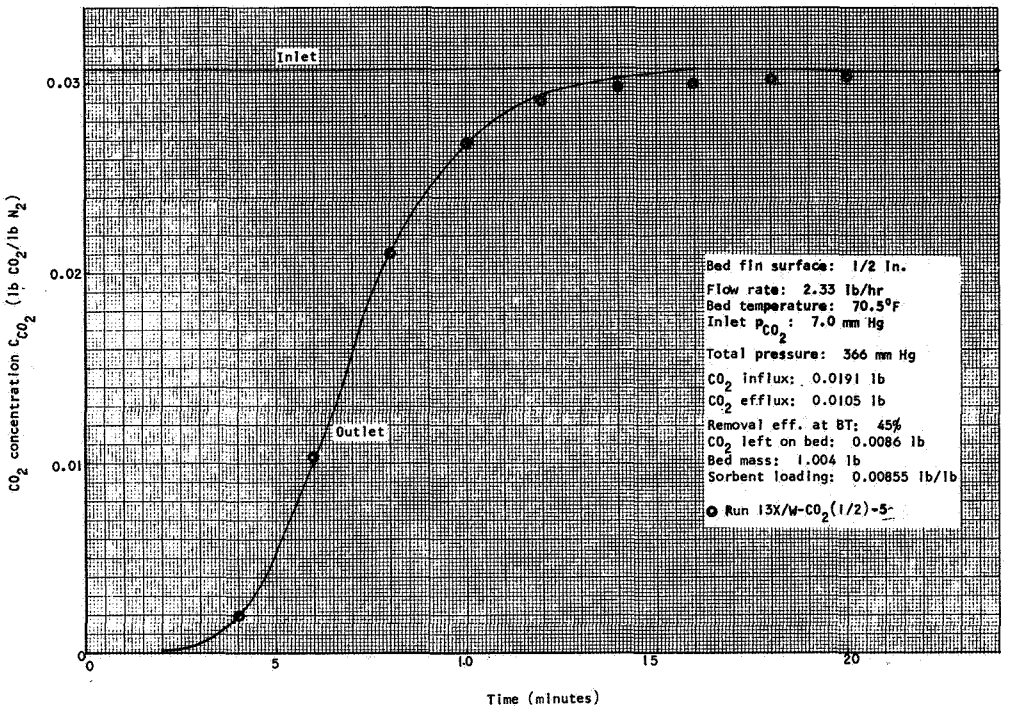

A. CO_2 Adsorption Breakthrough on Linde 13X With 7.5% Uniform Water Preload, Run No. 13X/W-CO_2(1/2)-3

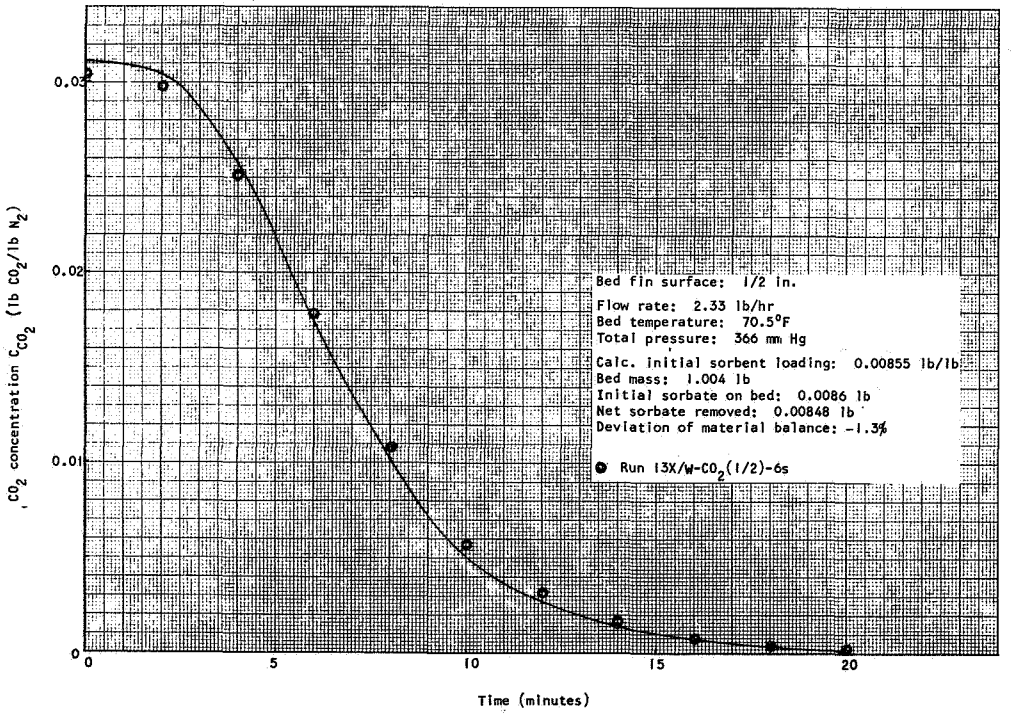

B. Gas Strip of CO_2 From Linde 5A With 7.5% Uniform Water Preload, Run No. 13X/W-CO_2(1/2)-4s

Figure 6-19. CO_2 Adsorption Breakthrough Run No. 13X/W-CO_2(1/2)-3 and Gas Strip Run No. 13X/W-CO_2(1/2)-4s

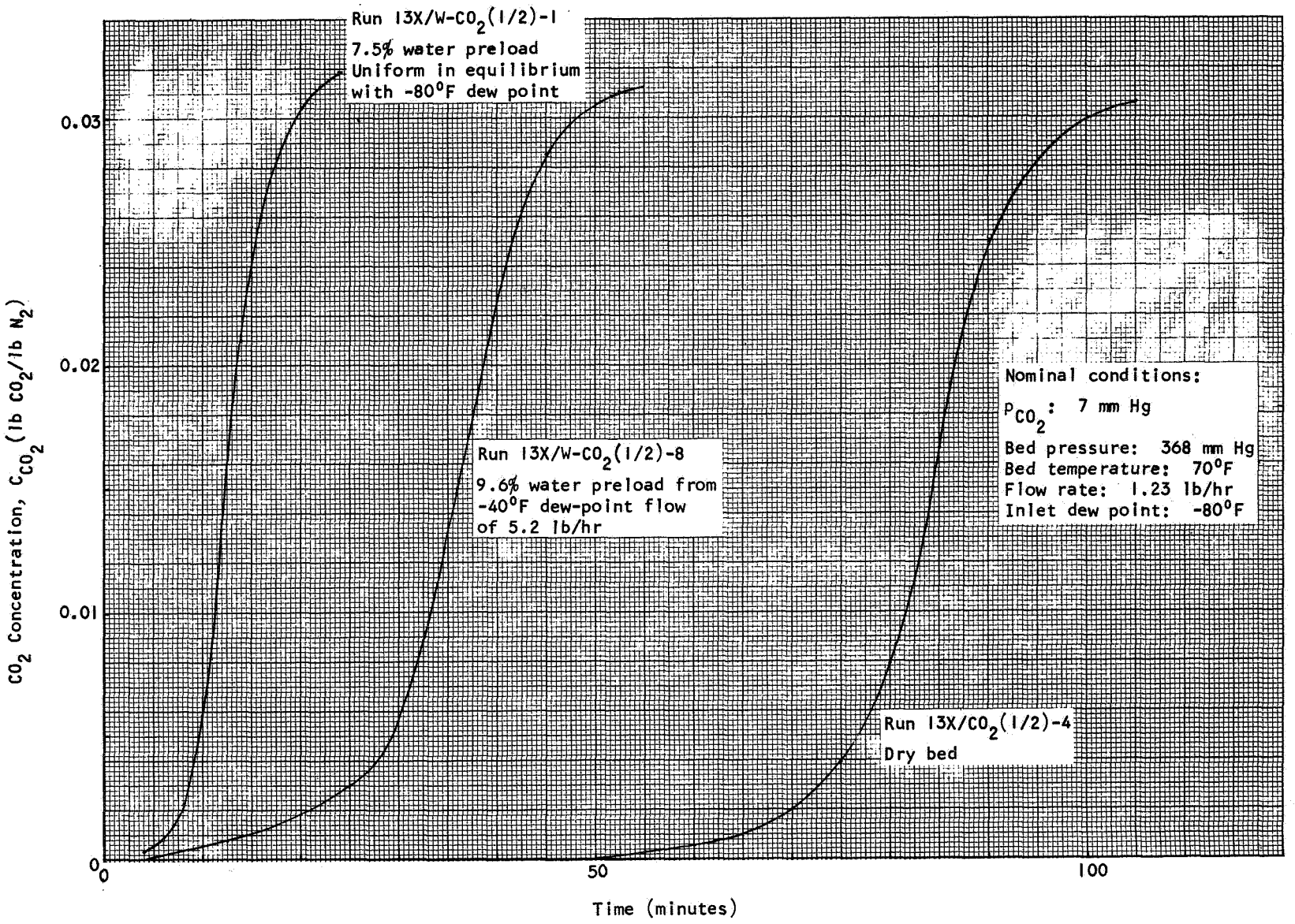

Figure 6-20. CO_2 Breakthrough Curves on Water Preloaded Linde 13X Molecular Sieve (1.23 lb/hr)

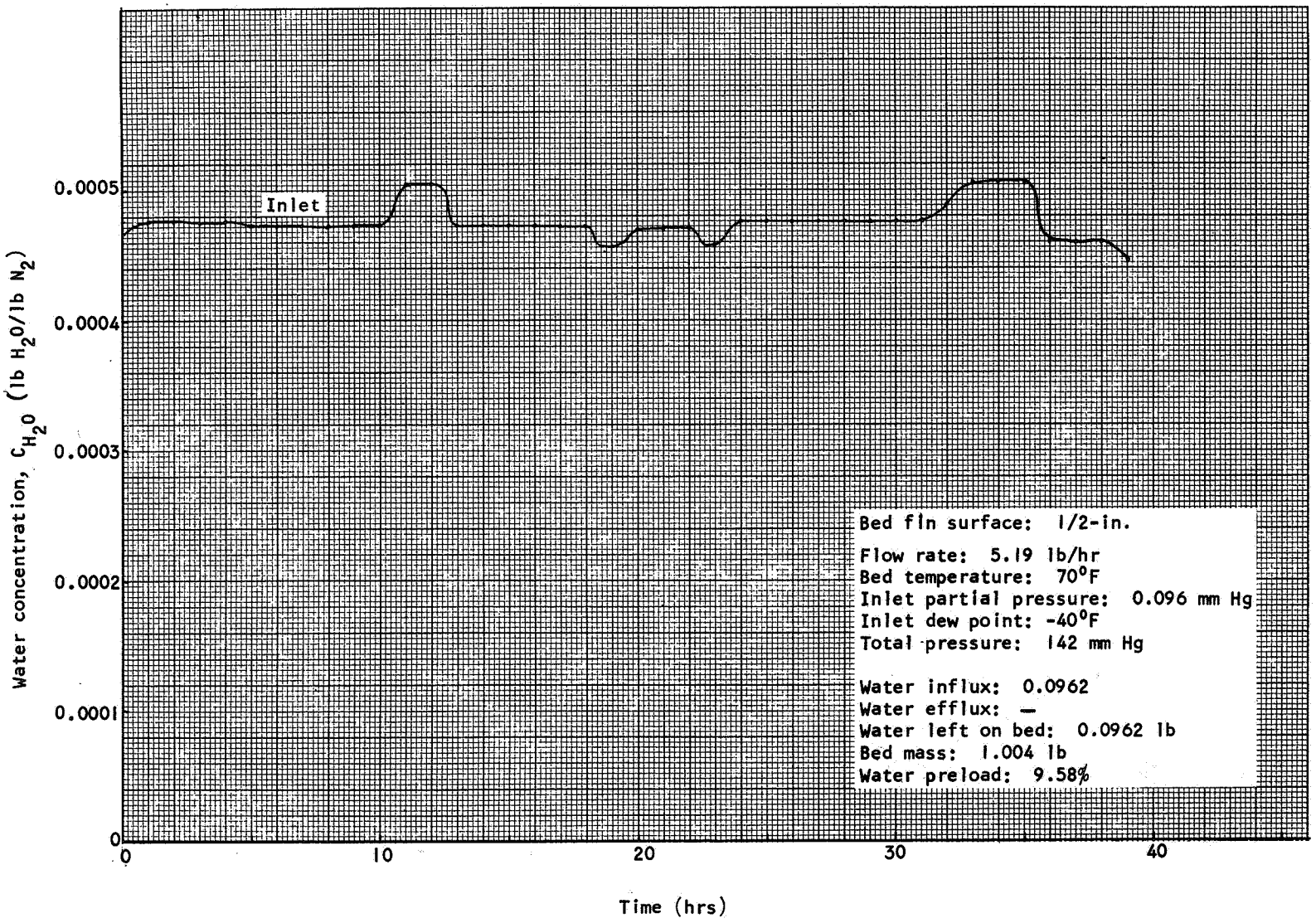

Figure 6-21. Water Preloading Sequence on Linde 13X, Run No. 13X/W-CO_2(1/2)-8p

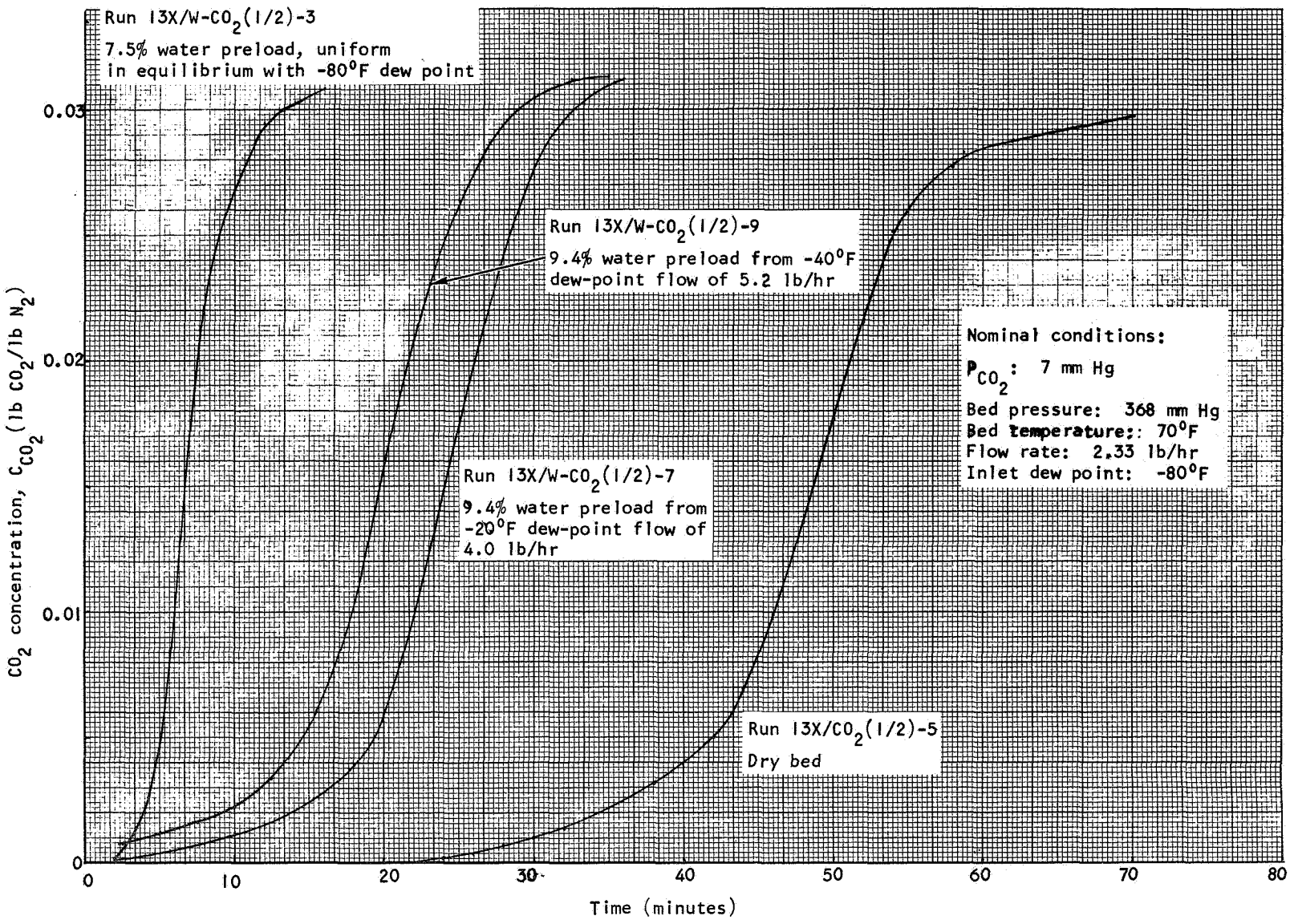

Figure 6-22. CO_2 Breakthrough Curves on Water Preloaded Linde 13X Molecular Sieve (2.33 lb/hr)

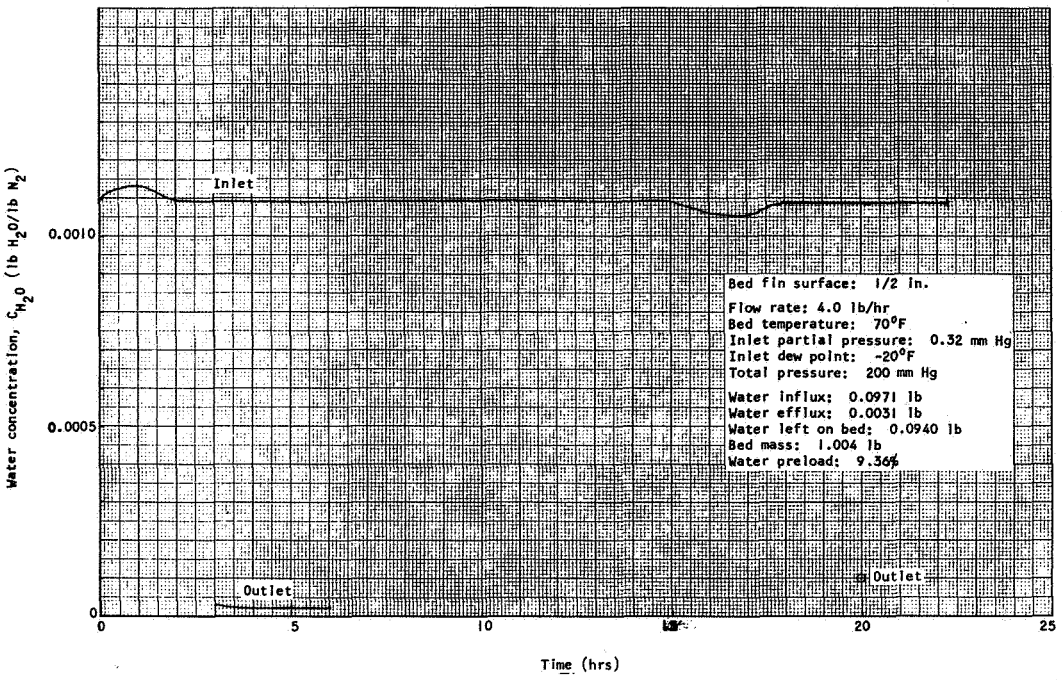

A. Water Preloading Sequence on Linde 13X, Run No. 13X/W-CO_2(1/2)-7p

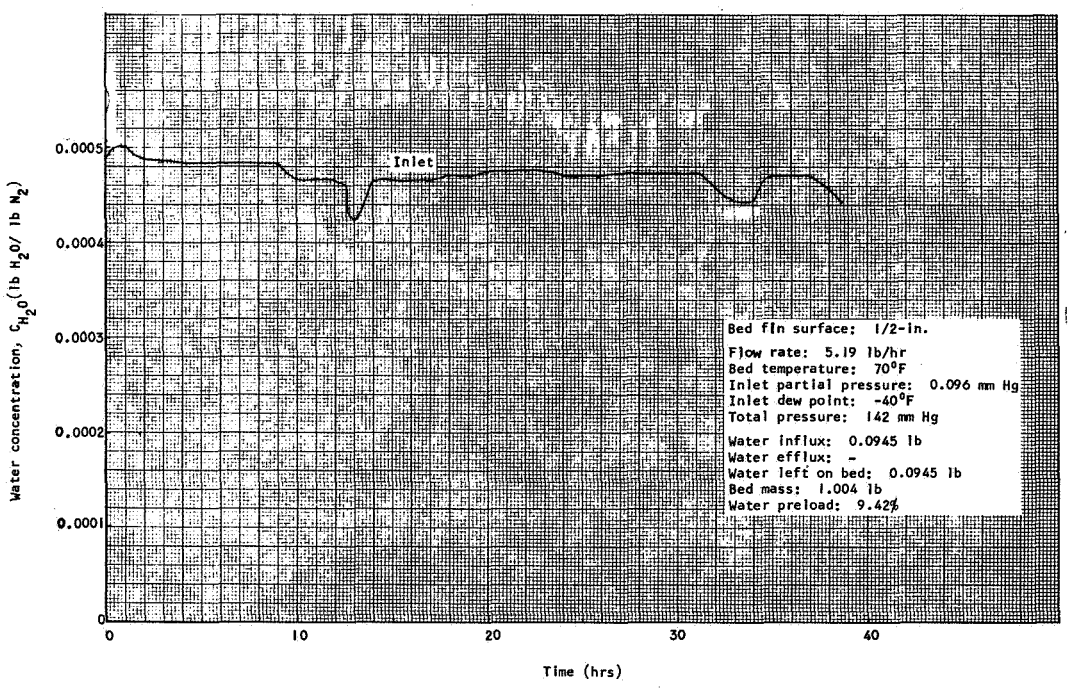

B. Water Preloading Sequence on Linde 13X, Run No. 13X/W-CO_2(1/2)-9p

Figure 6-23. Water Preloading Sequences on Linde 13X Run Nos. 13X/W-CO_2(1/2)-7p and 13X/W-CO_2(1/2)-9p

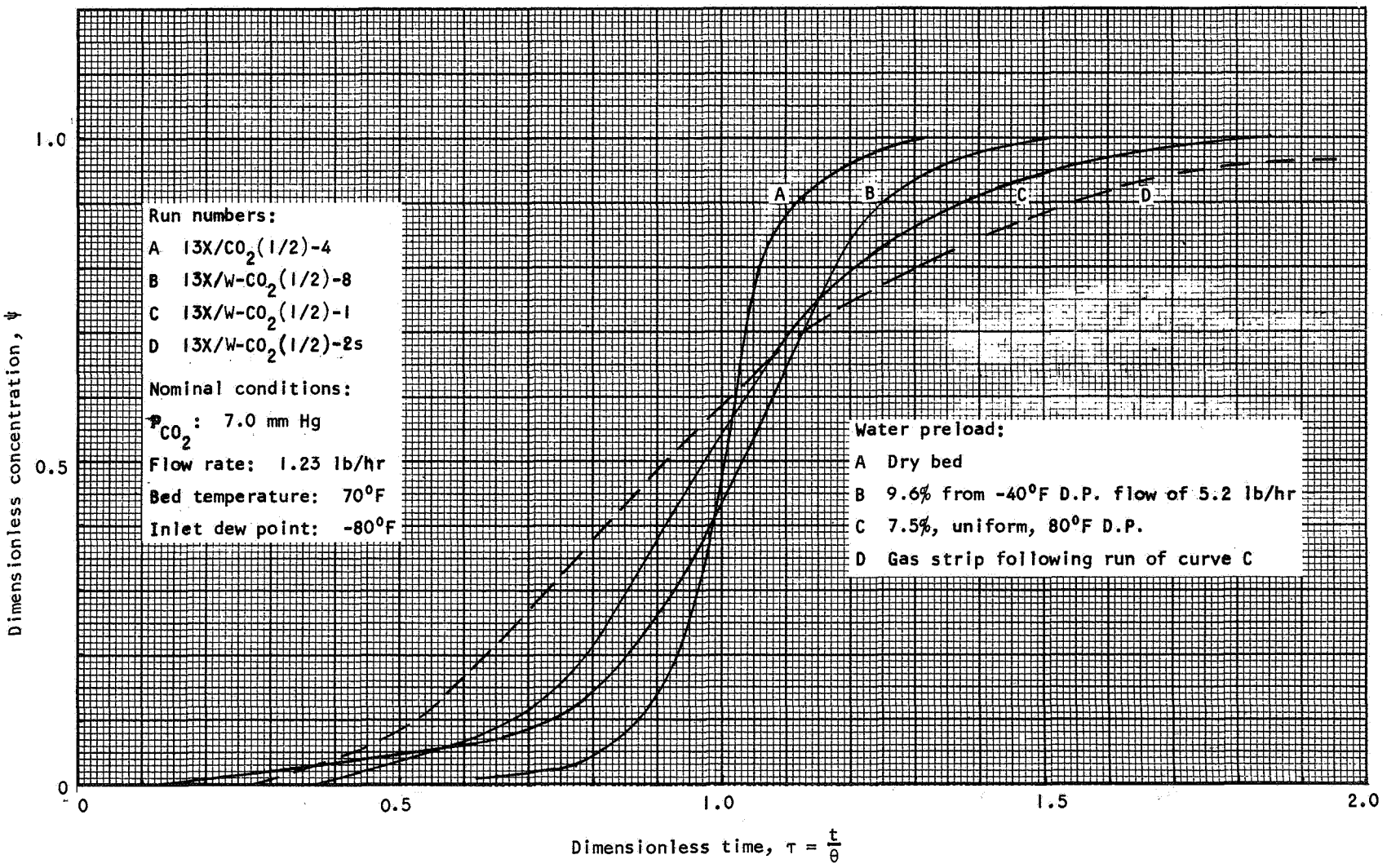

Figure 6-24. Dimensionless CO_2 Breakthrough Curves on Water Preloaded Linde 13X Molecular Sieve (1.23 lb/hr)

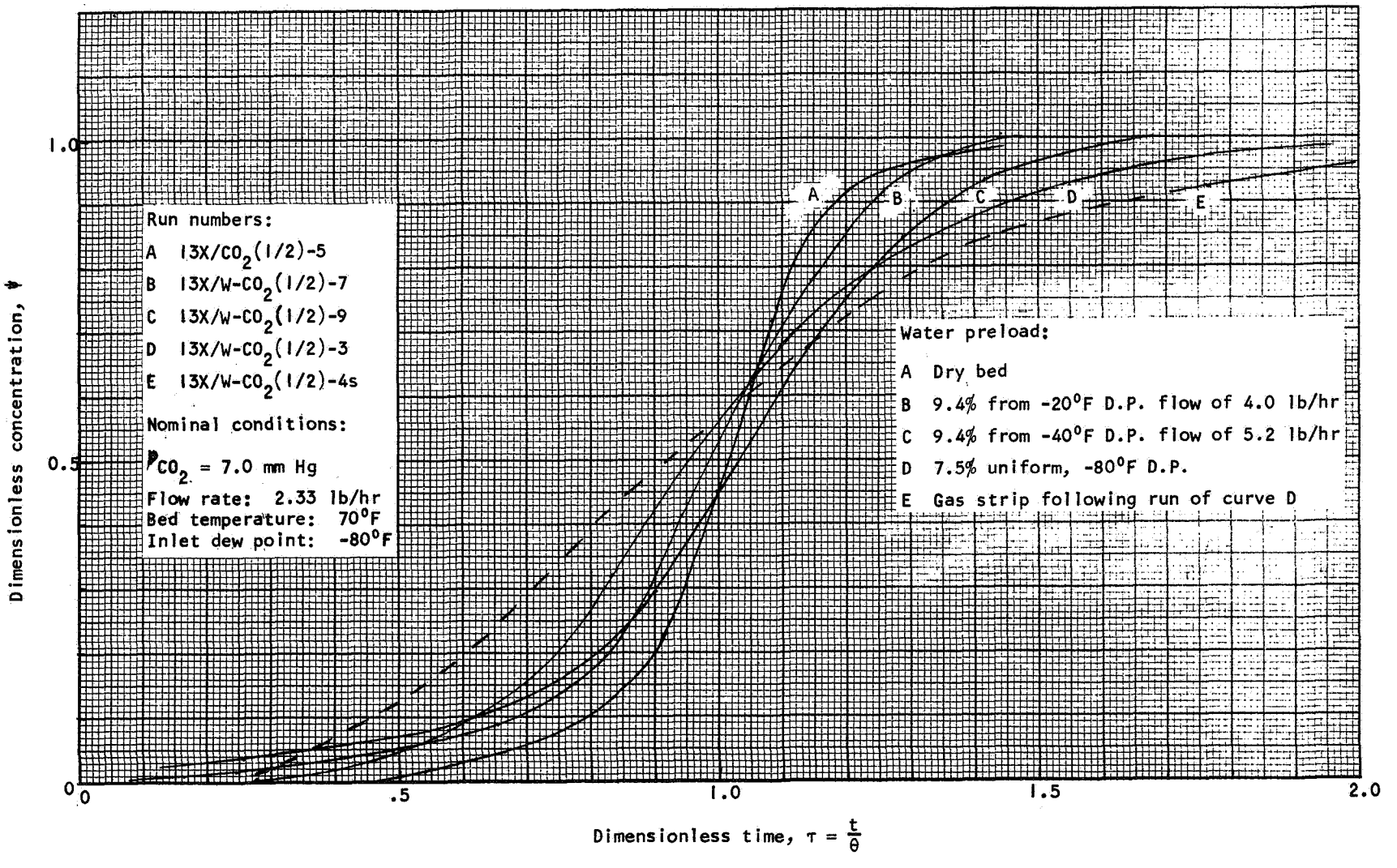

Figure 6-25. Dimensionless CO_2 Breakthrough Curves on Water Preloaded Linde 13X Molecular Sieve (2.33 lb/hr)

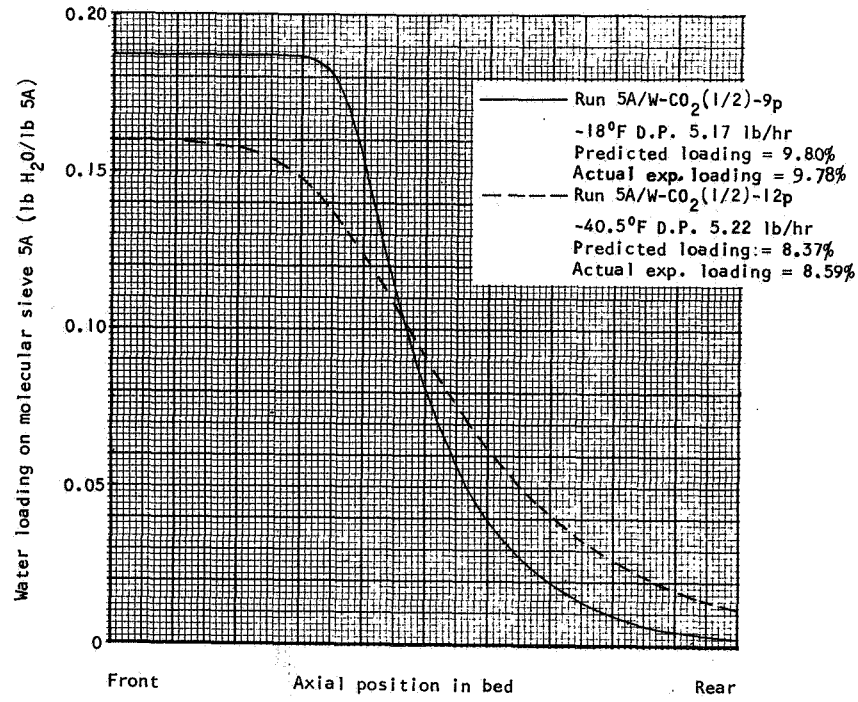

Figure 6-26. Predicted Water Preloads on Molecular Sieve 5A

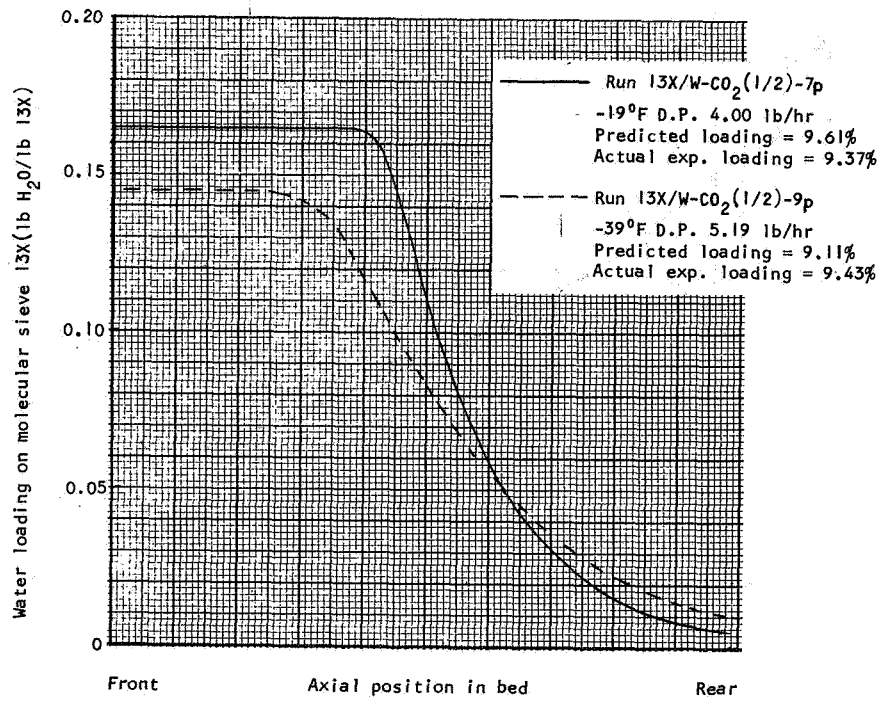

Figure 6-27. Predicted Water Preloads on Molecular Sieve 13X

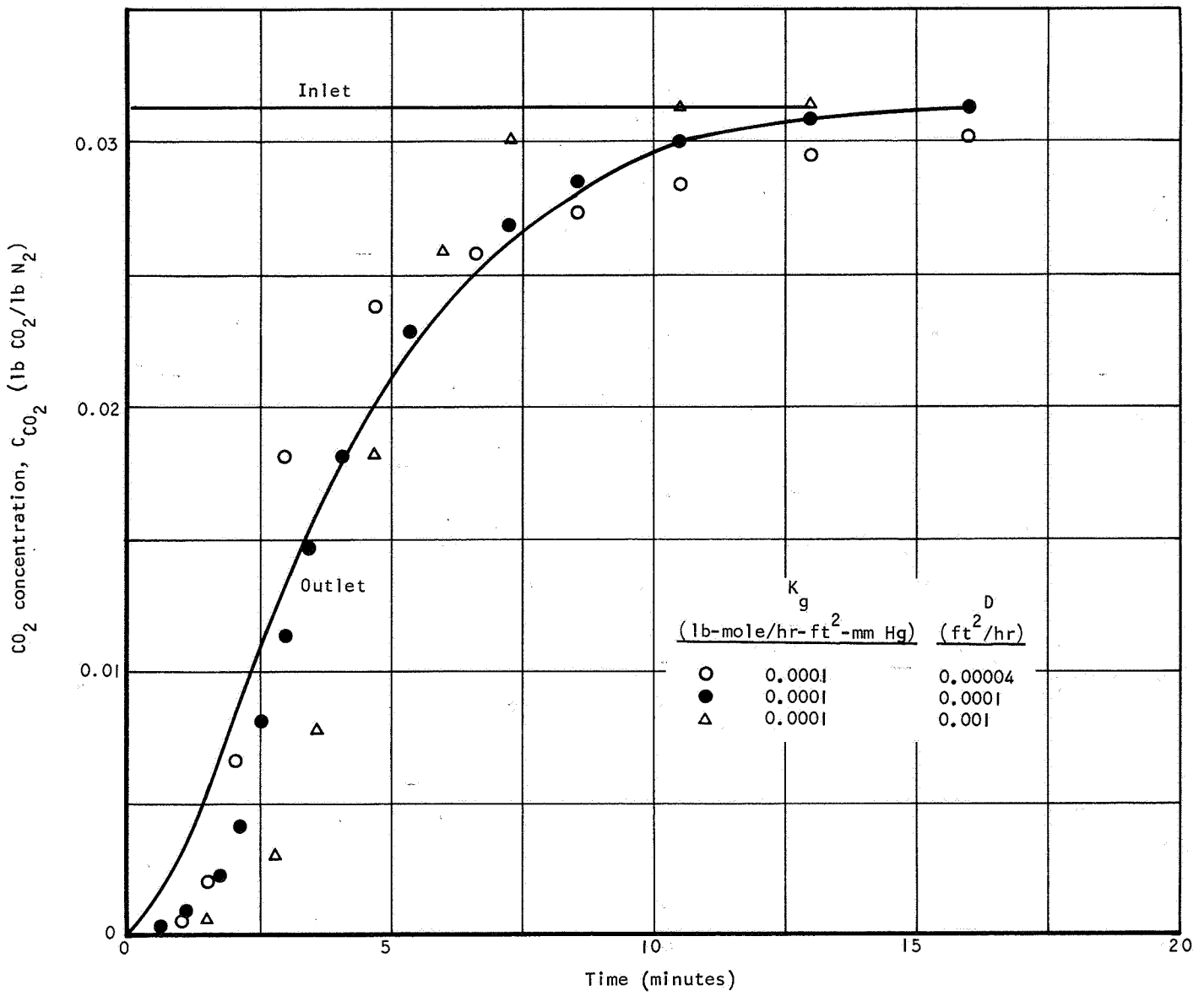

Figure 6-28. Evaluation of Mass-Transfer Parameters for Uniformly Water-Preloaded Bed of Molecular Sieve 5A, Run No. 5A/W-CO_2(1/2)-5

SECTION 7

PERFORMANCE PREDICTION COMPUTER PROGRAMS

S9960, TRANSIENT PERFORMANCE-PREDICTION FOR CO_2 REMOVAL WITH SINGLE OR COMPOSITE SORBENT BEDS

Program S9960 for water-dump/CO_2-dump composite sorbent beds (originally produced by AiResearch under another NASA contract) was the first program delivered to NASA Langley Research Center under this contract. Under this contract, some updating of the program was made and full documentation was prepared (Reference 1). It has been checked out thoroughly on CDC-6600 and Univac 1108 computer systems.

This program deals with systems such as the Skylab RCRS where both water and CO_2 are dumped to vacuum. The program optionally allows for internal coolant passages, or adiabatic beds can be simulated. Any sorbents can be employed in the desiccant and CO_2-removal sections of the bed. Vacuum desorption is the main desorption mode, but gas stripping simulations can be made by proper input data assignments.

The program was used exclusively in the mass-transfer coefficient evaluations as presented in Section 5. In this case, by input data assignments, the bed was configured to hold only one type of sorbent and only one sorbate was contained in the process gas stream. Also, for the evaluation, the particular option was specified which caused the predictions to be made for isothermal beds. If warranted, bed heat transfer could have been simulated. However, this would have introduced a great deal of complexity into the mass-transfer coefficient evaluations. For the evaluations, a specific main program and printed output program were devised. These programs make it easier to run successive breakthrough predictions with different K_g and D values; these new programs are given later in this section.

MAIN 4B, PERFORMANCE PREDICTION PROGRAM FOR CO_2-REMOVAL SORBENT SYSTEMS WITH MULTIPLE BEDS

MAIN 4B is an extended version of program S9960. All of the refinements and additions to MAIN 4B were made under this contract. The documentation of this extensive program is contained in Reference 1.

Many of the numerical schemes used by MAIN 4B are essentially the same as S9960, and it uses many subroutines written earlier. Several features are included in the program that were not considered in S9960:

- The poisoning effect of gradual water buildup on the CO_2 sorbent
- Estimation of overboard gas losses, oxygen and nitrogen
- Two- and four-bed capability

- An option to allow electric heater inclusion in the bed
- The capability to analyze desorption when vacuum pumping is included in the system

By considering (1) the poisoning of the CO_2-removal bed by water and (2) the adsorption and subsequent loss of atmospheric gases O_2 and N_2, this program treats some of the very important second-order effects due to coadsorption. Even though the program does not handle the coadsorption in a thoroughly rigorous manner, it should provide good results, which will prove quite valuable in system design and optimization work. The program is much more versatile then S9960 in that it can handle two- or four bed systems with water/CO_2-dump or -save provisions.

PROGRAM ADDITIONS TO S9960

Revised Main Program S9960 and Revised Print Subroutine PRADSB

Appendices A, B and C present computer programs which are additions to the program series S9960. The new programs have been written to facilitate the evaluation of mass-transfer coefficients from the experimental dynamic data as discussed in Section 5. In Appendix A, a new version of main program S9960 is presented. This program is used to run back-to-back adsorption half-cycle predictions, each starting with the same initial conditions, but each with a differing set of mass-transfer parameters K_g and D (Fortran variables GK and DIF). The program is intended to be used with the new PRADSB subroutine for printed output presented in Appendix B. It is, however, compatible with the original PRADSB routine (S9979), which is included in Reference 1.

The new main program requires some input by means of punched data cards. The first card of the data deck is a heading card. The information on this card is printed on the first line of each page of output during the entire computer run. Following the heading card in the data deck are the cards which specify the values of GK and DIF to be applied to the different predictions. One pair of GK and DIF values are contained on each card; the individual GK and DIF values (named locally as GKR and DIFR) are to be applied to all nodes. Thus, this main program can only be used where GK and DIF are desired to be constant throughout the bed. In order that the second and successive predictions start with the same initial conditions as given in the BLOCK DATA program (S9993), this new main program stores the initial conditions on a scratch device and restores them to core at the start of each successive run. It is also noted that the card input data for GK and DIF override the data contained in the BLOCK DATA program.

Also to be punched on each data card (in the third ten-column field) is the integer indicator IPRINT. This indicator when zero or blank, instructs the new PRADSB program to print only outlet quantities vs sorption time, giving a tremendous savings in printer time and number of pages, when only this information is desired. When greater than zero, quantities for all

finite-difference elements throughout the bed are printed by PRADSB, but with a more compact format than in the earlier version. In addition to format changes, the new PRADSB gives values for gas-phase concentration for both water and CO_2, as well as the partial pressures. The concentration values are those defined by Equations 4-1 and 4-2. For user convenience, values of GKR and DIFR are printed with the heading on each page of output.

The new version of PRADSB can be used as is with the existing program set described in Reference 1. However, heading information and the IPRINT indicator should be added to the BLOCK DATA program if one wants to use the full capabilities of the new output program.

Equilibrium Data Subroutine PKEQ

Appendix C lists the new, table-lookup PKEQ subroutine (for sorbent/sorbate equilibrium data). This routine has been used exclusively in the mass-transfer coefficient evaluations of Section 4. The table-lookup concept was resorted to when it became extremely difficult to obtain equilibrium-data curve fits with sufficient accuracy for these evaluations. In this regard, the program has worked very well; and without needing to curve-fit each equilibrium isotherm, it is much easier to prepare equilibrium data for use.

The method for using the program, and requirements on the tabled equilibrium data are contained in the comment cards included in the Fortran listing. As an example of the storage of a single equilibrium isotherm, the listing in Appendix C contains data for CO_2 on Davison 5A molecular sieve at 70^0F. Program computations are about 30 percent slower using the table-lookup version of PKEQ, but the ease of use, when adequate curve fits are not already available, more than justifies the extra computation cost.

EQUILIBRIUM DATA CURVE FITTING PROGRAM

In order to use program set S9960, the user must produce a Fortran subroutine PKEQ which upon call, for the sorbents of interest, will yield sorbate equilibrium partial pressure as a function of sorbent loading and temperature. This is discussed fully in Reference 1. The program discussed above fulfills this need with little setup being required of the program user. However, from the view point of computation speed, a closed-form algebraic expression is desired--in effect a curve fit (or a map fit) of the equilibrium data for the sorbent/sorbate pair. Experience has shown that it is often quite difficult to obtain such a curve or map fit with sufficient accuracy for design purposes. Many of the classical isotherm expressions (Langmuir, Freundlich, BET, etc.) have been tried; the usual results are curve fits that may have the correct shapes, but are not accurate enough. More success has been achieved with correlation equations which may resemble the theoretical isotherm expressions, but which possess one or more arbitrary groupings of terms and parameters.

In order to facilitate the curve-fitting of equilibrium isotherms and maps, a special program has been developed. This program and its method of use are presented in Appendix D. The program contains 35 different correlation-equation forms. The program produces coefficients and exponents for the correlation equations, and shows the deviation between the predicted values and the data used for input. If one is to be concerned with a large amount of performance-prediction computations for certain sorbate/sorbent pairs, the use of this program is suggested. If sufficiently adequate correlations result, computer time is saved. If correlations are not considered adequate, the table lookup version of PKEQ can be used.

SECTION 8

PRESSURE DROP AND PACKED-BED DENSITIES

PRESSURE DROP

The knowledge of pressure drop sustained by the process gas stream flowing through a packed bed is an essential piece of information needed in the design of any fixed-bed sorbent system. All of the sorbents studied in this program have been in large-scale commercial use for several years, and because of this, considerable information is available on pressure drop. However, because of the plate-fin heat-transfer surfaces incorporated in the test beds, a situation rarely if ever encountered in the chemical process industry, it was desired to provide accurate experimental pressure drop data. It should be noted that the effect of the plate-fin surfaces was expected to be relatively small. Generally, it would seem that the additional wall effect in the plate-fin beds would tend to produce slightly less pressure drop.

In all adsorption and gas stripping runs, bed pressure drop was measured by a precision Wallace and Tiernan differential pressure gage. With silica gel (Davison, Grade 05, 6 to 16 mesh particles), the range and number of experimental tests provided enough data to characterize pressure drop performance of the material. With Linde 5A and 13X molecular sieves (1/16-in. pellets), the experimental range was not considered as great as desired, so a separate pressure-drop test series was conducted. With these tests, both an inclined oil manometer, and a Baratron electronic pressure indicator were added to the instrumentation. For Davison 5A molecular sieve material, so little adsorption testing was accomplished, that no pressure drop data is reported here. As spherical beads, this material packed well in the test beds, and it is expected that pressure drop can be predicted easily by using correlations for packed beds of spheres. One such correlation, due to Ergun, is given by Davison (Reference 9).

In all of the information that follows it should be noted that the pressure drop of the empty bed, including that of the two 25-mesh sorbent-retention screens, was measured to be so low that it was ignored. That is, the pressure drop as measured is due entirely to the flow through the sorbent packing. Because of the inorganic nature of the sorbents, there was expected to be no effect on pressure drop due to the amount of sorbate held by the bed; no such effect was ever observed. In other words, there is no geometric change (swelling, shrinkage, etc) of these sorbents as they pick up water or CO_2.

The pressure drop data for silica gel was correlated so well by the expression given by the Davison division of W.R. Grace and Co. (Reference 10), that no data curves are presented here. The Davison pressure drop equation is

$$\frac{\Delta P}{L} = KV^m$$

where $\Delta P/L$ is the pressure drop in psi per foot of bed depth, and V, the

superficial velocity, is in ft/sec. It should be noted that in calculating V for the plate-fin beds, the bed superficial free-flow area from Table 4-12 was used. This area does not include the cross-sectional areas of the coolant passages, the plates, or the gas side fins. It is thus a net superficial area. For air, Davison gives for the coefficient K the value 0.10; for the exponent m, 1.5. These values correlated well the nitrogen pressure drops in the 1/2-in.-fin bed at 5 psia.

The test data for Linde 1/16-in. molecular-sieve pellets are shown in Figure 8-1. These data were actually taken on 13X molecular sieve; but since all of the Linde 1/16-in. pelleted materials appear dimensionally similar, these data should be valid for other molecular sieves of this configuration. The data for Figure 8-1 cover the pressure range from 5 to 14.7 psia (258 to 760 mm Hg) and the bed flow rate of 0.5 to 5.4 lb/hr. The ordinate of the figure is pressure drop (in. H_2O) per unit of flow length (ft) times the density ratio σ, which relates the actual gas density in lb/ft^3 to that at standard conditions, 0.07176 lb/ft^3. The abscissa is flow rate per unit superficial free-flow area ($lb/hr\text{-}ft^2$). Within the accuracy required for design, all of the data for both beds, at all of the test pressures, could have been represented by one line.

PACKED-BED DENSITY

Because of the plate-fin heat-transfer surfaces incorporated into the sorbent beds, packed-bed density (sometimes called bulk sorbent density) would be expected to vary with fin size and would not coincide with predicted values which are based upon the large beds as found in industry. To investigate the effect of fin size on packed-bed density, four small bed modules were constructed. Three of the beds contained offset fin surfaces of the type used in the test beds discussed in Section 4; i.e., 1/4-in. 1/2-in., and 1-in. fin height and spacing. The fourth bed was left empty. The modules were approximately 2 in. by 2 in. at the face, with a 4 in. bed depth. To facilitate the packed density measurements all of the beds were welded closed at one end.

Using the general procedure for packing described in Section 4, the beds were packed with sorbent and weighed in a nitrogen dry box. After the various packings and weighings were completed, bed free volumes were determined by filling with water and weighing.

Table 8-1 presents packed bed densities as a function of fin size, as derived from the bed modules and from the dynamic test beds. For reference, bulk density from manufacturer's literature is also given. There is some scatter in the density measurements given in the table, but a definite trend with fin size is evident. Density variations for the dynamic test beds stem from improved packing techniques as the program progressed, and the possibility that the retention screens were bulged, thus allowing more sorbent to be held. The densities of the bed modules have not been corrected for nitrogen adsorption; this could be about 1 percent for the molecular sieves. Presumably, all sorbents used for the bed modules were dry due to bakeouts previous to packing. However, it is possible that some significant water pickup could have occurred during the packing test procedure.

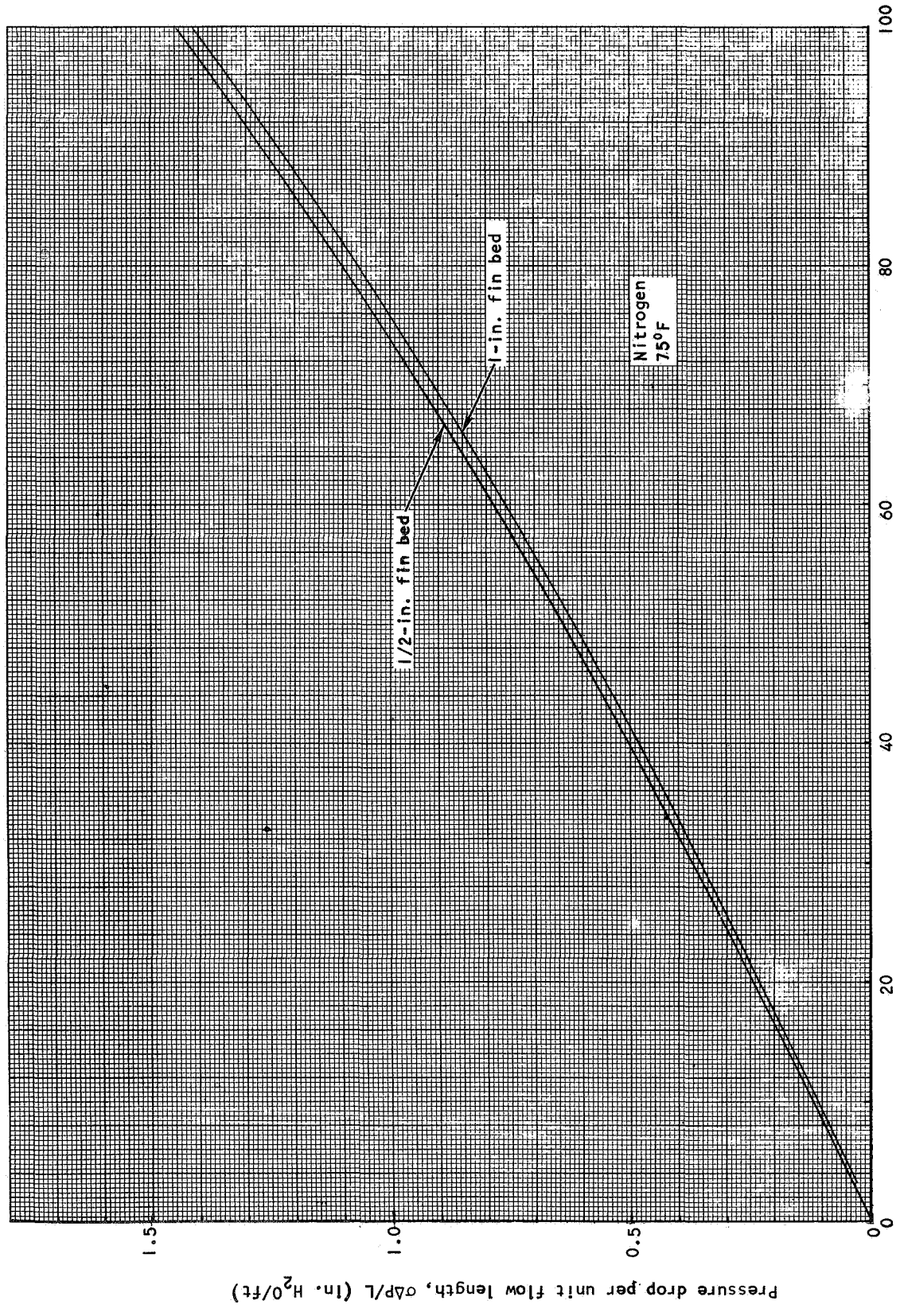

Figure 8-1. Pressure Drop in the 1/2-in.-Fin and 1-in.-Fin Test Beds for Linde 1/16 in. Molecular Sieve Pellets

TABLE 8-I

PACKED-BED DENSITIES IN FINNED SORBENT BEDS

Fin Size and Bed	Silica Gel (Davison Grade 05) 6 to 16 Mesh	Linde 13X 1/16-in. Pellets	Linde 5A 1/16-in. Pellets	Davison 5A 8 to 12 Mesh Beads
1/4-in.-fin bed module	38.8	39.3	41.8	38.5
1/2-in.-fin bed module	41.7	43.1	45.2	43.1
1/2-in.-fin test bed	43.0	39.7 41.1	43.6 49.7	43.0
1-in.-fin bed module	44.0	43.3	46.1	44.4
1-in.-fin test bed	43.2	39.0 43.2	--	--
Empty bed module	44.6	46.9	48.6	47.8
Manufacturer's bulk density	45	40	43	44

SECTION 9

CONCLUSIONS AND RECOMMENDATIONS

The efforts under this contract have provided two large-scale computer program sets to predict the transient performance of spacecraft, regenerable, CO_2-removal systems which employ molecular sieve adsorbents. The first program for two-bed, water-dump/CO_2-dump systems (Reference 1) has already seen extensive use in the design and evaluation of actual spacecraft CO_2-removal systems. The second program (Reference 1) provides a significant amplification and update of the first program. It can be used for two- or four-bed systems with either water-, or CO_2-, save or dump provisions. Further, the new program treats some coadsorption phenomena, (poisoning and atmospheric gas losses) which, although considered second-order effects, can dominate the design of such systems. Several other refinements and additions are included in this well checked-out program.

The equilibrium behavior of several sorbent/sorbate systems was investigated in one of the latest, most well-equipped, experimental setups of its kind. The investigations also produced data on the equilibrium behavior of molecular sieves when two sorbates are coadsorbed. Very little information of this nature was previously available.

The dynamic behavior of specially-constructed molecular-sieve sorbent beds was studied in a specially designed experimental setup. The test beds contain very efficient plate-fin, offset, heat-transfer surfaces, designed for sorbent bed applications. Differing sizes of fins were evaluated in the test program. In general, fin height and spacing of 1/2 in. provides good bed heat-transfer performance, while allowing good packed bed density. Although not tested, 3/8-inch fins should provide good heat- and mass-transfer performance. Fins as large as 1-inch high, spaced 1 inch apart, should be avoided. To limit channeling to a sufficiently low amount, offset fins should be provided.

On the basis of single-sorbate breakthrough tests, mass-transfer coefficient and intraparticle diffusivities were evaluated. For all tests involving molecular sieves 5A and 13X, and silica gel, intraparticle diffusion resistance is quite low. Therefore, large values of effective diffusivity should be used in performance-prediction programs. For the systems studied, mass-transfer coefficient values are recommended. These values seem somewhat low compared to published correlations. However, it is considered that the low values compensate for unavoidable nonisothermal effects (at the mass-transfer front) in the dynamic tests, and the phenomenon of axial dispersion which is not considered in the performance-prediction programs. These programs, when used with the recommended mass-transfer parameters, should provide good transient performance predictions, over a wide range of bed geometries and conditions.

The effect of coadsorbed water and CO_2 on the dynamic behavior of molecular sieve beds was studied. For predrier beds, where water pickup

is of interest, the presence of CO_2 in the gas stream may be ignored. For CO_2-removal beds, the presence of water, even in small quantities, has a large and important effect. Equilibrium capacity for CO_2 is drastically lowered when water is coadsorbed; being one-half of the dry value when water loading is about 4 percent; and practically nil when water loading reaches 8 percent. Further, as water is coadsorbed, the CO_2 adsorption rate coefficients decline markedly. It is considered that diffusion in the sorbent pellets is hindered by the presence of water.

At the present time, techniques for design and performance evaluation of regenerable CO_2-removal systems using molecular sieves are highly developed. One can feel confident that molecular sieve sorbent systems will meet the stringent objectives of space hardware, including low weight and volume penalties and reliable long life. Much of the information and many of the tools discussed in this report have already been used in the improvement of both CO_2-removal systems and the techniques used in their design. Still, with changing spacecraft conditions, there are areas where continued study and development should be undertaken. At the present time, with lower desired levels of CO_2 partial pressure (3 mm Hg) and higher cabin pressures, full system design studies should be implemented. It is acknowledged that molecular-sieve sorbents do not have large CO_2 capacities at such low partial pressure, but as demonstrated in this program with tests involving 1.75 mm Hg p_{CO_2}, molecular sieves show excellent dynamic performance even in this range. Also, many inherent qualities of molecular sieves (their inertness, dimensional stability, tolerance to vacuum, etc) are not affected by the newer conditions. Full system design/tradeoff studies would be enlightening, especially in view of the new and untried schemes for CO_2 removal that are now being considered.

Further, it is believed that basic improvements can be made in molecular-sieve CO_2-removal systems even at this stage in their development. Up to this time, molecular sieve 5A has been the choice for the CO_2 sorbent. However, at low partial pressures, (about 4 mm Hg and below) 4A has higher equilibrium capacity than 5A. It is possible that with smaller pore openings, the dynamic performance of 4A might be poorer than that of 5A. However, the comparison tests should be made. Also, at the present time, both Linde and Davison are marketing 4A and 5A molecular sieves without binder. These materials have the potential of providing an immediate 20 percent increase in capacity as compared to their clay-binder counterparts. Both equilibrium and dynamic tests would be warranted. Predrier sorbents that have low capacities for O_2 and N_2 are desired. Molecular sieve 3A, or other large-cation substituted sorbents may be useful here. There are a number of design features that need exploring. One such feature, to limit the loss of atmospheric gases (O_2 and N_2), involves the pressure equalization of closed-off desorbing and adsorbing beds before switching. It is considered that a large fraction of atmospheric gases on the adsorbing bed would be quickly desorbed and saved by this operation. Other features such as multipoint desorption bear study.

From the viewpoint of providing better basic data, more coadsorption equilibrium and dynamic testing would be fruitful. Computer program improvement could involve the effects of longitudinal or axial dispersion. More

information of rate effects with coadsorption would be welcomed. In some areas, rechecks of single-sorbate equilibrium data would be of interest.

APPENDIX A

LISTING OF REVISED MAIN PROGRAM S9950 FOR EXECUTING BACK-TO-BACK HALF-CYCLE COMPUTATIONS USING THE SAME INITIAL CONDITIONS BUT DIFFERING VALUES OF GK AND DIF.

```
      @ ELT S9950,1,700121, 59453     , 1

000001                  COMMON /HEAD/ HEADNG(20), IPRINT, NLINE
000002                  COMMON /BLOK2/ ABED(41), A(41), AVC(41),CPG(41),RHOG(41),
000003                 1HXG(41),HXS(41),HXC(41),DIF(41),F(41),C(41),VS(2),DVS(2),DVS1(2),R
000004                 2S1(2,41),RHOS(2),UG(41),WM(2),UC(41),NDXM,PS(41),RHOSB(41),DS(41),
000005                 3CS1(41),CS2(41),C1(21,41),C2(21,41),D1(21,41),D2(41),PC1(41),PC2(4
000006                 41),PC3(41),ASG(41),ASX(41),AGX(41),C1P(41),C2P(41),C3P(41),D1P(41)
000007                 5,FR(2,41),RS(2),NDX1,NDR4,DX,DT,GK(41),DH(41),SK(41),P1(41),P2(41)
000008                 6,P3(41),WS(41),CR1(2,21),CR2(2,21),CR3(2,21),C3(21,41),B(21,41),
000009                 7Q(21,41),CP1(41),CP2(41),X(41),VOIDF(41),TIME
000010                 8,AXC(41),RHOC(41),CPC(41),T268,AVX(41),TKX(41),CPX(41),RHOX(41)
000011                 9,NOG,PK(2,41),PC02I,PH20I,  GMR,GMW,TGI,PA,PT(41),CPS(41),HSG(41)
000012                  COMMON /BLOK3/ W(21,41), TG(41), TS(41), TC(41), TX(41), CYCLE
000013                  DATA III/77/
000014            C
000015                  REWIND 15
000016                  READ (5,4001) HEADNG
000017             4001 FORMAT (20A4)
000018                  IF (III.EQ.77) WRITE (15) W, TG, TS, TC, TX
000019                  REWIND 15
000020            C
000021                2 IF (III.NE.77) READ  (15) W, TG, TS, TC, TX
000022                  REWIND 15
000023                  III    = 0
000024            C
000025                  READ (5,4002) GKR, DIFR, IPRINT
000026             4002 FORMAT (2F10.0,I10)
000027                  DO 3 I=1,41
000028                  GK(I)  = GKR
000029                3 DIF(I) = DIFR
000030                  NLINE  = 100
000031                  CALL MADSOR
000032                  GO TO 2
000033                  END
```

APPENDIX B

LISTING OF REVISED PRINTED OUTPUT PROGRAM PRADSB

```
@ ELT S9979,1,700121, 59451    , 1
000001                SUBROUTINE PRADSB
000002          C
000003          C
000004                DIMENSION AVLD(41)
000005                COMMON /BLOK2/ ABED(41), A(41), AVC(41),CPG(41),RHOG(41),
000006               1HXG(41),HXS(41),HXC(41),DIF(41),F(41),C(41),VS(2),DVS(2),DVS1(2),R
000007               2S1(2,41),RHOS(2),UG(41),WM(2),UC(41),NDXM,PS(41),RHOSB(41),DS(41),
000008               3CS1(41),CS2(41),C1(21,41),C2(21,41),D1(21,41),D2(41),PC1(41),PC2(4
000009               41),PC3(41),ASG(41),ASX(41),AGX(41),C1P(41),C2P(41),C3P(41),D1P(41)
000010               5,FR(2,41),RS(2),NDX1,NDR4,DX,DT,GK(41),DH(41),SK(41),P1(41),P2(41)
000011               6,P3(41),WS(41),CR1(2,21),CR2(2,21),CR3(2,21),C3(21,41),B(21,41),
000012               7Q(21,41),CP1(41),CP2(41),X(41),VOIDF(41),TIME
000013               8,AXC(41),RHOC(41),CPC(41),T268,AVX(41),TKX(41),CPX(41),RHOX(41)
000014               9,NOG,PK(2,41),PCO2I,PH2OI,  GMR,GMW,TGI,PA,PT(41),CPS(41),HSG(41)
000015                DOUBLE PRECISION W
000016                COMMON /BLOK3/ W(21,41),TG(41),TS(41),TC(41),TX(41),CYCLE
000017                COMMON /BLOK4/ POUT(10),TIMET(10),NBCOUT,NPSET(3)
000018                COMMON /BLOK6/ NCYCLT
000019                COMMON /BLOK8/ DTO,TS1(41),TS2(41),TX1(41),TX2(41),TC1(41),TC2(41)
000020                COMMON/BLOK10/ NPRINT,DTMAX,NDTCON
000021                COMMON /BLOK11/ TOTCO2,TOTH2O,SUMPTM,WTACMS,WTSG
000022                COMMON /BLOK12/ NTEMP
000023                COMMON /BLOK13/ WI, TI
000024                COMMON /BLOK14/ NCYCLE
000025                COMMON /BLOK16/ NDXMAC, PCO2C, VOLCAB, RCO2C
000026                COMMON /BLOK17/ NSTART
000027                DIMENSION AXS(41),AXG(41),AGS(41),HSX(41),HGX(41),HGS(41),ACX(41),
000028               1HCX(41)
000029                EQUIVALENCE (ASX,AXS),(AGX,AXG),(ASG,AGS),(HXS,HSX),(HXG,HGX),(HSG
000030               1,HGS),(AXC,ACX),(HXC,HCX)
000031                EQUIVALENCE(NDX,NDX1)
000032                COMMON /HEAD/ HEADNG(20), IPRINT, NLINE
000033                DIMENSION CONCO2(41), CONH2O(41)
000034                DATA NLINE/100/
000035          C
000036              1 IF (NLINE.NE.100) GO TO 2
000037                NSPACE = 4
000038                IF ((NDX.EQ. 8).OR.(NDX.EQ.18)) NSPACE = 3
000039                IF ((NDX.EQ. 9).OR.(NDX.EQ.19)) NSPACE = 2
000040                IF ((NDX.EQ.10).OR.(NDX.EQ.20)) NSPACE = 1
000041          C
000042              2 AVPH2O = SUMPTM/TIME
000043                AVH2OP =GMR*AVPH2O*18./(PA*GMW)
000044          C
000045                IF ((IPRINT.EQ.0).AND.(NLINE.LT.60))          GO TO 10
000046                IF ((IPRINT.GT.0).AND.((60-NLINE).GE.(NDX+9))) GO TO 10
000047                WRITE (6,4000) HEADNG
000048           4000 FORMAT (1H1)16X20A4)
000049                NLINE  = 1
000050                WRITE (6,4003) GK(1),DIF(1)
000051           4003 FORMAT (1H+100X'GK(1)='F7.5,' DIF(1)='E7.2)
000052                IF (IPRINT.GT.0) GO TO 10
000053                WRITE (6,4004)
000054           4004 FORMAT (1H016X'PARTIAL PRESSURES    CONCENTRATIONS   --------TEMPE
000055               1RATURES---------   ********INTERIOR SORBENT LOADINGS*********'/
000056               25H  ADS4X'TIME'9X'(MMHG)'10X'(LB/LB PR GAS)'15X'(F)'34X'(LB/LB)'/
000057               3 ' CYCLE  (HRS)      CO2        H2O        CO2    H2O        GAS  SO
000058               4RBENT COOLANT HXCORE     AVG      1      2      3      4      5')
```

```
000059                NLINE  = NLINE + 4
000060          C
000061             10 TIMEM=60.*TIME
000062          C
000063                IF (IPRINT.EQ.0) GO TO 15
000064                IF ((NSPACE.EQ.1).AND.(NLINE.EQ.1)) GO TO 14
000065                DO 13 I=1,NSPACE
000066                WRITE (6,4013)
000067           4013 FORMAT (1H )
000068             13 NLINE  = NLINE + 1
000069             14 WRITE (6,100) NCYCLE, TIME, TIMEM, DT
000070            100 FORMAT (1H 'ADSORPTION CYCLE'I3,' --- '
000071               1            5HTIME=,F9.5,1X2HHR,F12.3,1X,3HMIN,
000072               2                                5X,15HTIME INCREMENT=F7.5,1X2HHR)
000073                NLINE  = NLINE +1
000074          C
000075             15 N1     = NDXM + 1
000076                NDR3=NDR4-1
000077                DO 20 N= 1, NDXM
000078                SUMMS=0.0
000079                SUMMS=SUMMS+0.5* (W(1,N)+W(NDR4,N))
000080                IF(NDR4.EQ.2) AVLD(N) = SUMMS
000081                IF(NDR4.EQ.2) GO TO 20
000082                DO 22 NR=2,NDR3
000083             22 SUMMS=SUMMS+W(NR,N)
000084                AVLD(N)=SUMMS/NDR3
000085             20 CONTINUE
000086                DO 30 N= N1,NDX1
000087                SUMMS=0.0
000088                SUMMS=SUMMS+0.5*(W(1,N)+W(NDR4,N))
000089                IF(NDR4.EQ.2) AVLD(N) = SUMMS
000090                IF(NDR4.EQ.2) GO TO 30
000091                DO 33 NR=2, NDR3
000092             33 SUMMS=SUMMS+W(NR,N)
000093                AVLD(N)=SUMMS/NDR3
000094             30 CONTINUE
000095                SUM=0.
000096                IF(NDXMAC .EQ. 0) GO TO 35
000097                DO 31 N= 1, NDXMAC
000098             31 SUM= SUM+AVLD(N)*ABED(N)*DX*RHOSB(N)
000099                AVMSLD = SUM/WTACMS
000100                SUM=0.
000101             35 CONTINUE
000102                IF((NDX1-NDXM) .EQ. 0) GO TO 40
000103                DO 32 N= N1,NDX1
000104             32 SUM = SUM+AVLD(N)*ABED(N)*DX*RHOSB(N)
000105                AVSGLD=SUM/WTSG
000106             40 CONTINUE
000107          C
000108          C
000109                IF (IPRINT.EQ.0) GO TO 60
000110          C
000111                WRITE (6,4049)
000112           4049 FORMAT (1HO
000113               1'      PARTIAL PRESSURES    CONCENTRATIONS   --------TEMPERATURES-
000114               2--------   ***************INTERIOR SORBENT LOADINGS***************
000115               3*'/1H
000116               4'AXIAL'6X'(MMHG)'10X'(LB/LB PR GAS)'15X'(F)'41X'(LB/LB)'      /1H
000117               5'NODE    CO2       H2O        CO2    H2O       GAS  SORBENT COOLAN
000118               6T HXCORE     AVG      1      2      3      4      5      6      7'
```

```
000119                7)
000120                 DO 50 N=1,NDX
000121                 RMW    = (PA - PK(1,N) - PK(2,N)) * GMW
000122                 CONCO2(N) = PK(1,N)*44./RMW
000123                 CONH2O(N) = PK(2,N)*18./RMW
000124               50 WRITE (6,4050) N, PK(1,N), PK(2,N), CONCO2(N), CONH2O(N), TG(N),
000125                1                TS(N), TC(N), TX(N), AVLD(N), (W(NR,N),NR=1,NDR4)
000126             4050 FORMAT (1H I3,3XG9.5,1X,G9.5,1X2F7.5,1X,4F8.1,2XF7.4,1X,7F7.4)
000127                 WRITE (6,205) AVMSLD, AVSGLD
000128              205 FORMAT(30HOAVG CO2 LOADING IN M.S. BED = F8.4,1X,5HLB/LB,7X,
000129                130H AVG H2O LOADING IN S.G. BED = F8.4, 6H LB/LB)
000130                 AVRCO2=TOTCO2/TIME
000131                 AVRH2O=TOTH2O/TIME
000132                 WRITE(6,204) AVRCO2,AVRH2O
000133              204 FORMAT(27H TIME AVG CO2 ADSORP RATE =
000134                1    F8.4, 6H LB/HR ,10X,
000135                227H TIME AVG H2O ADSORP RATE =
000136                3  F8.4, 7H LB/HR )
000137                 WRITE(6, 206) AVPH2O, AVH2OP
000138              206 FORMAT(21H TIME AVG EXIT PH2O =  , F10.4, 3H MM ,18X,
000139                140HTIME AVG RATE OF M.S. POISONING BY H2O = , G12.4,10H LB H2O/HR)
000140                 NLINE  = NLINE + 8 + NDX
000141                 RETURN
000142             C
000143             C
000144                60 RMW    = (PA - PK(1,1) - PK(2,1)) * GMW
000145                 CONCO2(1) = PK(1,1)*44./RMW
000146                 CONH2O(1) = PK(2,1)*18./RMW
000147                 WRITE (6,4060) NCYCLE, TIME, PK(1,1), PK(2,1), CONCO2(1),
000148                1                CONH2O(1), TG(1), TS(1), TC(1), TX(1),
000149                2                AVLD(1), (W(NR,1),NR=1,NDR4)
000150             4060 FORMAT (1H I3,F10.5,3X,G9.5,1XG9.5,1X2F7.5,1X4F8.1,2XF7.4,1X5F7.4)
000151                 NLINE  = NLINE + 1
000152                 RETURN
000153                 END
```

APPENDIX C

LISTING OF REVISED EQUILIBRIUM DATA PROGRAM PKEQ

```
* ELT PKEQ,1,701103, 55012     , 1
000001                FUNCTION PKEQ (K, W, T)
000002           C
000003           C    THIS VERSION OF 'PKEQ' PROVIDES TABLE-LOOKUP AND INTERPOLATION OF
000004           C    SORBENT/SORBATE EQUILIBRIUM DATA.  CURVE FITTING (OR MAP FITTING)
000005           C    IS NOT USED.
000006           C    EQUILIBRIUM DATA ARE STORED VIA 'DATA' STATEMENTS IN ARRAYS AS
000007           C    FOLLOWS...GIVEN FOR SORBENT/SORBATE COMBINATION NO.1, SAME FOR 2.
000008           C
000009           C      'T1DATA(J)'     = TEMPERATURE VALUES (F) FOR WHICH P-VS-W CURVES
000010           C                        (ISOTHERMS) ARE STORED.
000011           C      'NT1'           = NUMBER OF ISOTHERMS STORED. NOTE, WHEN THE
000012           C                        COMPUTATION TO BE PERFORMED IS FOR ISOTHERMAL
000013           C                        CONDITIONS, 'NT1' MUST BE 6 OR LESS. OTHERWISE,
000014           C                        IT MAY BE 7 OR LESS.
000015           C      'W1DATA(I)'     = LOADING VALUES (LB/LB), COMMON FOR EACH
000016           C                        ISOTHERM, MAY BE 20 OR LESS.
000017           C      'NW1'           = NUMBER OF LOADING VALUES.
000018           C      'P1DATA(I,J)'   = PARTIAL-PRESSURE VALUES (MM/HG) CORRESPONDING
000019           C                        TO THE LOADING AND TEMPERATURE VALUES STORED IN
000020           C                        'W1DATA' AND 'T1DATA'.
000021           C
000022           C    ACTUAL VALUES OF ALL DATA ARE TO BE USED IN DATA STATEMENTS.
000023           C    IF LOGARITHMIC STORAGE OF PRESSURE OR LOADING VALUES IS DESIRED,
000024           C    THE INDICATORS WHICH FOLLOW WILL AUTOMATICALLY ALLOW SAME...
000025           C      'ILOGW1'        = 0, NORMAL STORAGE OF LOADING DATA,
000026           C                      = 1, LOGARITHMIC STORAGE.
000027           C      'ILOGP1'        = 0, NORMAL STORAGE OF PARTIAL-PRESSURE DATA,
000028           C                      = 1, LOGARITHMIC STORAGE.
000029           C
000030           C    NOTE..FOR EACH ISOTHERM, A PARTIAL-PRESSURE VALUE FOR EACH VALUE
000031           C    OF 'W1DATA' MUST BE ENTERED.  BY THE NATURE OF THE METHOD BY WHICH
000032           C    EQUILIBRIUM DATA ARE TAKEN, PARTIAL-PRESSURE DATA WILL PROBABLY
000033           C    NOT BE AVAILABLE FOR ALL VALUES OF LOADING IN 'W1DATA'.  THAT IS,
000034           C    DATA WILL NOT BE AVAILABLE FOR ONE OR BOTH ENDS OF THE ISOTHERM
000035           C    WITH RESPECT TO THE DATA ENTERED IN 'W1DATA'.  TO OBTAIN,
000036           C    MISSING VALUES ONE MAY EXTRAPOLATE GRAPHICALLY THE EXISTING
000037           C    EQUILIBRIUM MAP.  ALTERNATIVELY, ONE MAY ENTER ZEROES (0.0) IN THE
000038           C    DATA STATEMENTS, IN WHICH CASE, THIS PROGRAM WILL FILL IN THE
000039           C    PRESSURE ARRAYS BY LINEAR EXTRAPOLATION. NOTE, ZEROES BETWEEN REAL
000040           C    VALUES ARE NOT ALLOWED.  ZEROES ARE NOT ALLOWED AT ALL IN 'W1DATA'
000041           C
000042           C    IF DATA FOR ONLY ONE SORBENT/SORBATE COMBINATION IS TO BE STORED,
000043           C    THE 'NT-' AND 'NW-' VALUES FOR THE OTHER COMBINATION SHOULD BE
000044           C    STORED AS ZERO.  IN THE EVENT THAT THIS PROGRAM IS ENTERED TO
000045           C    INTERPOLATE DATA WHICH HAS NOT BEEN STORED, PROGRAM EXIT WILL
000046           C    OCCUR.
000047           C
000048           C    IN THIS PROGRAM INTERPOLATION OF ISOTHERM DATA IS BY MEANS OF
000049           C    SUBROUTINE 'LAGIN2'.
000050           C    INTERPOLATION (OR EXTRAPOLATION) BETWEEN (OR BEYOND) ISOTHERM
000051           C    DATA, AT CONSTANT LOADING W, IS BY MEANS OF THE RELATION
000052           C    LN(P) = A/(T+459.6) + B.
000053           C
000054           C    WHEN ONLY ONE DATA CURVE IS STORED FOR A SORBENT/SORBATE
000055           C    COMBINATION, IT WILL BE USED DIRECTLY IN ALL CIRCUMSTANCES,
000056           C    WHEN AN ISOTHERMAL RUN IS DESIRED, AS DENOTED WHEN 'NTEMP'=0,
000057           C    AT THE FIRST CALL TO 'PKEQ', AND PROVIDED THERE ARE TWO OR MORE
000058           C    ISOTHERMS STORED, THE PROGRAM WILL GENERATE AN ISOTHERM FOR THE
```

```
000059          C     GIVEN TEMPERATURE AND STORE IT IN THE 'NT-+1' AREA OF 'P-DATA'.
000060          C     THIS CURVE WILL THEN BE USED DIRECTLY FOR ALL SUBSEQUENT CALLS.
000061          C
000062                COMMON /BLOK12/ NTEMP
000063          C
000064                DIMENSION T1DATA(7), W1DATA(20), P1DATA(20,7),
000065               1          T2DATA(7), W2DATA(20), P2DATA(20,7),
000066               2          TDATA(7,2), WDATA(20,2), PDATA(20,7,2), NTD(2), NWD(2),
000067               3          ILOGW(2), ILOGP(2)
000068          C
000069                EQUIVALENCE (T1DATA(1),TDATA(1,1)), (W1DATA(1),WDATA(1,1)),
000070               1            (T2DATA(1),TDATA(1,2)), (W2DATA(1),WDATA(1,2)),
000071               2            (P1DATA(1,1),PDATA(1,1,1)),
000072               3            (P2DATA(1,1),PDATA(1,1,2)),
000073               4            (NT1,NTD(1)), (NW1,NWD(1)),
000074               5            (NT2,NTD(2)), (NW2,NWD(2)),
000075               6            (ILOGW1,ILOGW(1)), (ILOGP1, ILOGP(1)),
000076               7            (ILOGW2,ILOGW(2)), (ILOGP2, ILOGP(2))
000077          C
000078                DATA INITL/1/
000079                DATA DELTA/0.5/
000080          C
000081          C     ********************************************************************
000082          C
000083          C     DATA FOR DAVISON-5A/CO2 AT 70F.                                    D5A/C-70
000084                DATA NT1/1/, NW1/12/                                               D5A/C-70
000085                DATA T1DATA(1)/70./                                                D5A/C-70
000086                DATA (W1DATA(I),I=1,12)                                            D5A/C-70
000087               1/ 0.0065, 0.0088, 0.0130, 0.0177, 0.0215, 0.0324, 0.0489, 0.0553, D5A/C-70
000088               2  0.0615, 0.0671, 0.0714, 0.0757/                                D5A/C-70
000089                DATA ((P1DATA(I,J),I=1,12),J=1,1)                                  D5A/C-70
000090               1/    0.1,    0.2,    0.4,    0.7,    1.0,    2.0,    4.0,    5.0, D5A/C-70
000091               2     6.0,    7.0,    8.0,    9.0/                               D5A/C-70
000092                DATA ILOGW1/1/, ILOGP1/1/                                          D5A/C-70
000093          C
000094                DATA NT2/0/, NW2/0/, ILOGW2/0/, ILOGP2/0/
000095          C
000096          C
000097          C     ********************************************************************
000098          C
000099          C
000100                IF ((NWD(K).GT.0).AND.(NTD(K).GT.0)) GO TO 1
000101                WRITE (6,4000) K
000102           4000 FORMAT (1H0  '*****ERROR -- DATA FOR SORBENT/SORBATE COMBINATION'
000103               1I2,' HAS NOT BEEN STORED IN PKEQ.')
000104                CALL EXIT
000105          C
000106          C
000107             1 IF (INITL.EQ.0) GO TO 100
000108          C
000109             2 INITL  = 0
000110          C
000111          C
000112          C     CONVERT ENTERED DATA TO LOGARITHMS (IF REQUIRED) AND FILL IN
000113          C     PARTIAL-PRESSURE ARRAYS BY EXTRAPOLATION.
000114          C
000115            10 IF ((NW1.EQ.0).OR.(NT1.EQ.0)) GO TO 20
000116          C
000117                IF (ILOGW1.EQ.0) GO TO 12
000118                DO 11 I=1,NW1
```

```
000119            11 W1DATA(I) = ALOG(W1DATA(I))
000120          C
000121            12 DO 19 J=1,NT1
000122          C
000123               IZEROA = 0
000124               IZEROB = 0
000125               II     = 0
000126          C
000127               DO 15 I=1,NW1
000128               IF (P1DATA(I,J).GT.0.0) GO TO 14
000129               IF (II.GT.0) GO TO 13
000130               IZEROA = IZEROA + 1
000131               GO TO 15
000132            13 IZEROB = IZEROB + 1
000133               GO TO 15
000134          C
000135            14 II     = 1
000136               IF (ILOGP1.GT.0) P1DATA(I,J) = ALOG(P1DATA(I,J))
000137            15 CONTINUE
000138          C
000139               IF (IZEROA.EQ.0) GO TO 17
000140          C
000141               SLOPE  = (P1DATA(IZEROA+2,J) - P1DATA(IZEROA+1,J)) /
000142              1          (W1DATA(IZEROA+2)   - W1DATA(IZEROA+1)  )
000143               DO 16 I=1,IZEROA
000144               P1DATA(I,J) = P1DATA(IZEROA+1,J) +
000145              1              SLOPE*(W1DATA(I) - W1DATA(IZEROA+1))
000146               P      = EXP(P1DATA(I,J))
000147               WRITE (6,4001) W1DATA(I), P
000148           4001 FORMAT (1H0 F5.4, E13.5)
000149               IF ((ILOGP1.EQ.0).AND.(P1DATA(I,J).LT.1.0E-7)) P1DATA(I,J)=I*1.E-7
000150            16 CONTINUE
000151          C
000152            17 IF (IZEROB.EQ.0) GO TO 19
000153               I1     = NW1 + 1 - IZEROB
000154               SLOPE  = (P1DATA(I1-2,J) - P1DATA(I1-1,J)) /
000155              1          (W1DATA(I1-2)   - W1DATA(I1-1)  )
000156               DO 18 I=I1,NW1
000157               P1DATA(I,J) = P1DATA(I1-1,J) +
000158              1              SLOPE*(W1DATA(I) - W1DATA(I1-1))
000159               P      = EXP(P1DATA(I,J))
000160               WRITE (6,4001) W1DATA(I), P
000161            18 CONTINUE
000162          C
000163            19 CONTINUE
000164          C
000165            20 IF ((NW2.EQ.0).OR.(NT2.EQ.0)) GO TO 50
000166          C
000167               IF (ILOGW2.EQ.0) GO TO 22
000168               DO 21 I=1,NW2
000169            21 W2DATA(I) = ALOG(W2DATA(I))
000170          C
000171            22 IZEROA = 0
000172               IZEROB = 0
000173               II     = 0
000174          C
000175               DO 29 J=1,NT2
000176          C
000177               DO 25 I=1,NW2
000178               IF (P2DATA(I,J).GT.0.0) GO TO 24
```

```
000179                IF (II.GT.0) GO TO 23
000180                IZEROA = IZEROA + 1
000181                GO TO 25
000182             23 IZEROB = IZEROB + 1
000183                GO TO 25
000184          C
000185             24 II     = 1
000186                IF (ILOGP2.GT.0) P2DATA(I,J) = ALOG(P2DATA(I,J))
000187             25 CONTINUE
000188          C
000189                IF (IZEROA.EQ.0) GO TO 27
000190          C
000191                SLOPE  = (P2DATA(IZEROA+2,J) - P2DATA(IZEROA+1,J)) /
000192               1           (W2DATA(IZEROA+2)   - W2DATA(IZEROA+1)  )
000193                DO 26 I=1,IZEROA
000194                P2DATA(I,J) = P2DATA(IZEROA+1,J) +
000195               1              SLOPE*(W2DATA(I) - W2DATA(IZEROA+1))
000196                IF ((ILOGP2.EQ.0).AND.(P2DATA(I,J).LT.1.0E-7)) P2DATA(I,J)=I*1.E-7
000197             26 CONTINUE
000198          C
000199             27 IF (IZEROB.EQ.0) GO TO 29
000200                I1     = NW2 +1 - IZEROB
000201                SLOPE  = (P2DATA(I1-2,J) - P2DATA(I1-1,J)) /
000202               1           (W2DATA(I1-2)   - W2DATA(I1-1)  )
000203                DO 28 I=I1,NW2
000204             28 P2DATA(I,J) = P2DATA(I1-1,J) +
000205               1              SLOPE*(W2DATA(I) - W2DATA(I1-1))
000206          C
000207             29 CONTINUE
000208          C
000209                IF (NTEMP.NE.0) GO TO 100
000210          C
000211                IF ((NT1.LE.1).AND.(NT2.LE.1)) GO TO 100
000212          C
000213          C     GENERATE ISOTHERMS FOR TEMPERATURE 'T' -- TO BE USED IN ISOTHERMAL
000214          C     PERFORMANCE PREDICATIONS.
000215             50 K1     = 1
000216                K2     = 2
000217                IF (NT1.GT.1) GO TO 51
000218                K1     = 2
000219             51 IF (NT2.GT.1) GO TO 52
000220                K2     = 1
000221          C
000222             52 DO 53 KK=K1,K2
000223                NWK    = NWD(KK)
000224                NTK    = NTD(KK)
000225                DO 53 I=1,NWK
000226             53 CALL EQMAP (KK, WDATA(I,KK), T, PDATA(I,NTK+1,KK), 0)
000227          C
000228          C     ******************************************************************
000229          C
000230          C     ACTUAL INTERPOLATION.
000231            100 WC     = W
000232                IF (W.LE.0.0) WC = 1.0E-5
000233                CALL EQMAP (K, WC, T, PKEQ, 1)
000234                RETURN
000235          C
000236          C
000237                SUBROUTINE EQMAP(L, WE, T, P, INDEX)
000238          C
```

```
000239          200 NT      = NTD(L)
000240              NW      = NWD(L)
000241        C
000242              IF (NT.GT.1) GO TO 210
000243              JT      = 1
000244              GO TO 290
000245        C
000246          210 IF ((INDEX.EQ.0).OR.(NTEMP.NE.0)) GO TO 220
000247              JT      = NT + 1
000248              GO TO 290
000249        C
000250          220 IF (T.GE.TDATA(1,L)) GO TO 230
000251              J1      = 1
000252              J2      = 2
000253              GO TO 260
000254        C
000255          230 IF (T.LT.TDATA(NT,L)) GO TO 240
000256              J1      = NT - 1
000257              J2      = NT
000258              GO TO 260
000259        C
000260          240 DO 250 J=1,NT
000261              IF (T.GT.TDATA(J+1,L)) GO TO 250
000262              J2      = J + 1
000263              J1      = J
000264              GO TO 260
000265        C
000266          250 CONTINUE
000267        C
000268          260 IF (ABS(T-TDATA(J1,L)).GT.DELTA) GO TO 270
000269              JT      = J1
000270              GO TO 290
000271        C
000272          270 IF (ABS(T-TDATA(J2,L)).GT.DELTA) GO TO 280
000273              JT      = J2
000274              GO TO 290
000275        C
000276          280 WLOOK   = WE
000277              IF (ILOGW(L).GT.0) WLOOK = ALOG(WE)
000278              CALL LAGIN2 (331, WDATA(1,L), NW, 2, WLOOK, P1, PDATA(1,J1,L))
000279              CALL LAGIN2 (332, WDATA(1,L), NW, 2, WLOOK, P2, PDATA(1,J2,L))
000280              IF (ILOGP(L).GT.0) GO TO 282
000281              P1      = ALOG(P1)
000282              P2      = ALOG(P2)
000283        C
000284          282 A       = (P2-P1) / (1./(TDATA(J2,L)+459.6)-1./(TDATA(J1,L)+459.6))
000285              B       = P1 - A/(TDATA(J1,L)+459.6)
000286              P       = EXP(A/(T+459.6) + B)
000287              RETURN
000288        C
000289          290 WLOOK   = WE
000290              IF (ILOGW(L).GT.0) WLOOK = ALOG(WE)
000291              CALL LAGIN2 (333, WDATA(1,L), NW, 2, WLOOK, P, PDATA(1,JT,L))
000292              IF (ILOGP(L).GT.0) P = EXP(P)
000293              RETURN
000294        C
000295        C
000296              SUBROUTINE LAGIN2 (M, X, NP, ND, XA, YA, Y)
000297        C
000298        C     INTERPOLATION SUBROUTINE.
```

```
000299          C     ADAPTED FROM THE GENERAL 'LAGIN2' PROGRAM,
000300          C     'X' ARRAY INCREASING, LINEAR TWO-POINT INTERPOLATION, NO MESSAGE.
000301          C
000302                DIMENSION X(2), Y(2)
000303          C
000304            300 ILO     = 1
000305                IHI     = NP
000306          C
000307          C     DETERMINE IF EXTRAPOLATION IS NECESSARY.
000308            310 IF (XA - X(1)) 320, 370, 311
000309            311 IF (XA - X(NP)) 330, 380, 321
000310          C
000311            320 I1      = 1
000312                I2      = 2
000313                GO TO 360
000314            321 I1      = NP - 1
000315                I2      = NP
000316                GO TO 360
000317          C
000318          C     BINARY LOOKUP.
000319            330 LOOK    = (ILO + IHI + 1) / 2
000320                IF (XA - X(LOOK)) 331, 390, 332
000321            331 IHI     = LOOK
000322                GO TO 340
000323            332 ILO     = LOOK
000324            340 IF ((IHI-ILO).GT.1) GO TO 330
000325          C
000326            350 I1      = ILO
000327                I2      = IHI
000328          C
000329          C     LINEAR, TWO-POINT INTERPOLATION.
000330            360 YA      = Y(I1) + (Y(I2)-Y(I1))*(XA-X(I1))/(X(I2)-X(I1))
000331                RETURN
000332          C
000333            370 YA      = Y(ILO)
000334                RETURN
000335            380 YA      = Y(IHI)
000336                RETURN
000337            390 YA      = Y(LOOK)
000338                RETURN
000339          C
000340                END
```

APPENDIX D

LEAST SQUARES PROGRAM TO CORRELATE EQUILIBRIUM DATA

INTRODUCTION

This program generates a polynominal equation to correlate equilibrium data using a stepwise multiple regression least square analysis. The polynominal equation is in the form:

$$P = C + B_1 X_1 + B_2 X_2 + \text{------} + Bn\ Xn$$

where:

P = equilibrium pressure, mm Hg

B, C = constants

X = function of T and W

T = temperature, ^{0}F

W = absorbent loading, lb sorbate/lb sorbent

The program uses a least squares subroutine (CORLAT) which is an adaptation of Share Fortran program G2 ER MPR2 No. 477. The correlation developed by this program is used in the molecular sieve adsorption/desorption program to predict regenerative carbon dioxide bed performance. The polynominal developed must have derivatives which are continuous and nonzero; therefore polynominals up to the third order were used to correlate the equilibrium data.

PROGRAM LOGIC

Main Program

The flow chart for the main program is shown in Figure D-1. The main program reads in all the control data (N,K) and the equilibrium data points (T, W, P). N is the total number of data sets (T, W, P) and K is the number of different equations to be correlated by subroutine CORLAT. The present program contains 35 equations; these equations are shown in Table D-1.

The variables for each of the thirty-five equations are defined within the main program, the constant and the coefficients for a given equation are determined by subroutine CORLAT. After the constant and coefficients have been determined, control is returned to the main program. For a given correlation the deviation at each data point and the average percent error

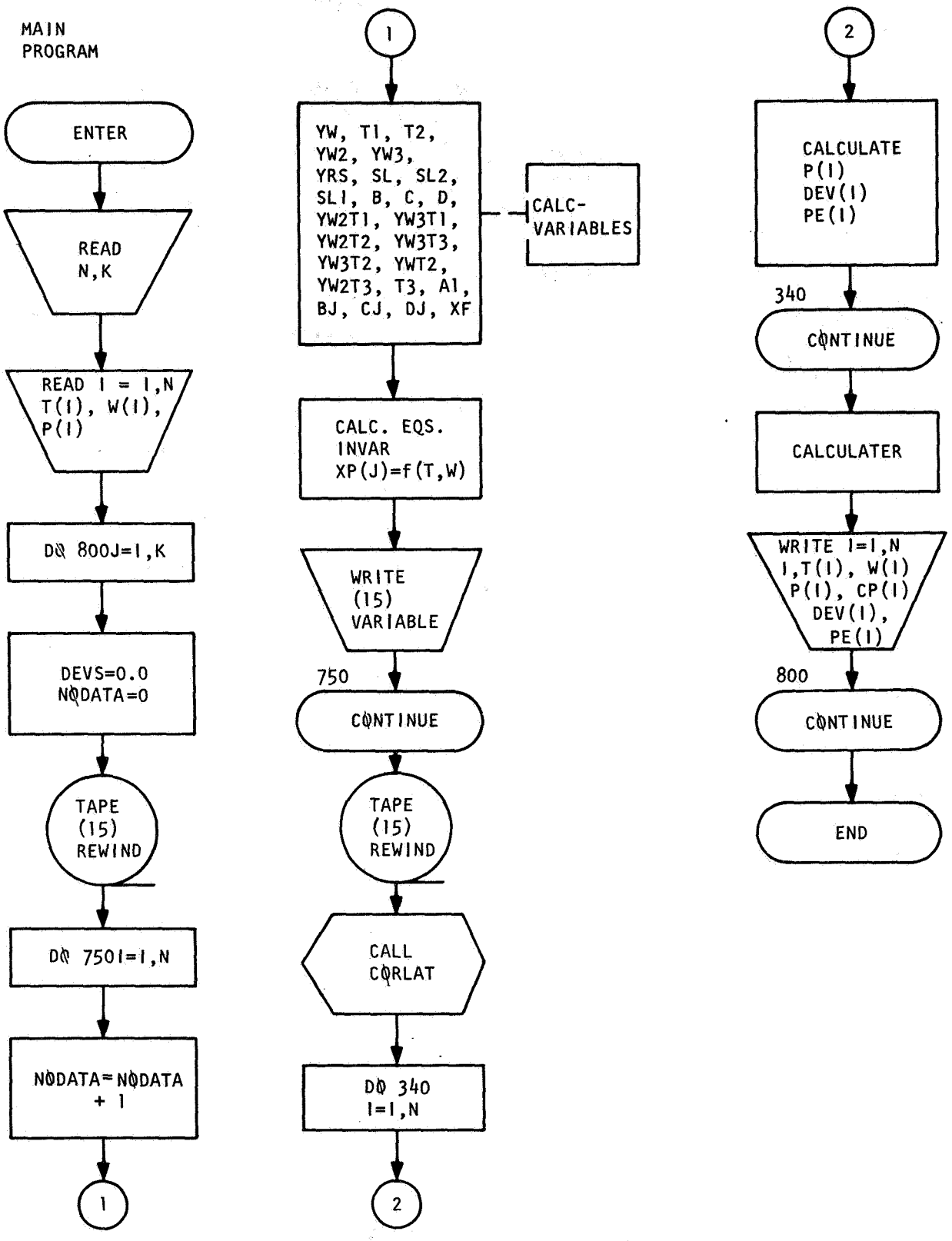

Figure D-1. Flow Chart for Main Program

APPENDIX D (Continued)

TABLE D-I

CORRELATING EQUATIONS USED IN THE MAIN PROGRAM

C=CONSTANT
LN=NATURAL LOG
P=PRESSURE, MM-HG
T=TEMPERATURE, DEG. F
W=LOAD, WT. PERCENT H2O OR CO2

EQUATIONS ATTEMPTED.

1. LN(P)=-1/(T+460)+LN(W)/(T+460)+LN(W)+LN(W)**2+C
2. LN(P)=-1/(T+460)+LN(W)/(T+460)+LN(W)+LN(W)**3+1/LN(W)**3-1/(T+460)**2+C
3. LN(P)=-1/(T+460)+LN(W)/(T+460)+LN(W)**2+LN(W)**3+C
4. LN(P)=-1/(T+460)+LN(W)+LN(W)**2+C
5. LN(P)=LN(W)/SQRT(T+460)+LN(W)+LN(W)**2+C
6. LN(P)=LN(W)/(T+460)+LN(W)+LN(W)**2+C
7. LN(P)=LN(W)+1/(T+460))+1/(T+460)**2+LN(W)**2+C
8. LN(P)=1/(T+460)**2+LN(W)**2+LN(W)+1/(T+460)+C
9. LN(P)=LOG(1/(T+460)**2+LN(W)/13.6+LN(LOG(100*W))+1/(T+460)**2(LN(W)/13.6-LN(LOG(100*W)))+C)
10. LN(P)=LOG(1/(T+460)**2+LN(W)/13.6+LN(LOG(100*W))+1/(T+460)**2(LN(W)/13.6-LN(LOG(100*W)))+C)
11. LN(P)=LOG(1/(T+460)**2(LN(W)/13.6-LN(LOG(100*W)))+C)
12. LN(P)=LN(W)/(T+460)+(LN(W)**2/(T+460))+(LN(W)**3/(T+460))+C
13. LN(P)=LN(W)/(T+460)+(LN(W)**2/(T+460)**2)+(LN(W)**3/(T+460)**3)+C
14. LN(P)=LN(W)+(LN(W)**2/(T+460))+(LN(W)**3/(T+460)**2)+C
15. LN(P)=LN(W)**3+LN(W)/(T+460)**2+LN(W)**2/(T+460)+C
16. LN(P)=LN(W)/(T+460)+LN(W)**3/(T+460)+LN(W)**2+C
17. LN(P)=LN(W)+LN(W)**2/(T+460)+LN(W)**3/(T+460)+C
18. LN(P)=1/(T+460)+LN(W)**2/(T+460)**2+LN(W)**3/(T+460)**3+C
19. LN(P)=LN(W)+LN(W)**2+LN(W)**3/(T+460)+C
20. LN(P)=LN(W)+LN(W)**2/(T+460)+LN(W)**3+C
21. LN(P)=LN(W)/(T+460)+LN(W)**2+LN(W)**3+C
22. LN(P)=1/(T+460)+LN(W)**3+LN(W)**2/(T+460)**3+C
23. LN(P)=LN(W)**3+LN(W)/(T+460)+LN(W)**2/(T+460)**2+C
24. LN(P)=LN(W)+LN(W)**2+LN(W)**3+1/(T+460)+C
25. LN(P)=LN(W)**2+LN(W)**3+LN(W)/(T+460)+1/(T+460)+C
26. LN(P)=LN(W)**3+LN(W)**2/(T+460)+LN(W)/(T+460)+1/(T+460)+C
27. LN(P)=LN(W)**3/(T+460)+LN(W)**2/(T+460)+LN(W)/(T+460)+1/(T+460)+C
28. LN(P)=LN(W)+LN(W)**2+LN(W)+1/(T+460)**2+C
29. LN(P)=LN(W)**3+LN(W)**2+LN(W)/(T+460)**2+1/(T+460)**2+C
30. LN(P)=LN(W)**2/(T+460)**2+LN(W)/(T+460)**2+1/(T+460)**2+LN(W)**3+C
31. LN(P)=LN(W)**3/(T+460)**2+LN(W)**2/(T+460)**2+LN(W)/(T+460)**2+1/(T+460)**2+C
32. LN(P)=LN(W)/(T+460)-1/(T+460)**2+1/LN(W)**3+LN(W)+1/(T+460)**3+C
33. LN(P)=LN(W)/(T+460)+1/LN(W)**3-1/(T+460)**2+LN(W)**3+LN(W)+1/(T+460)**3+C
34. LN(P)=LN(W)/(T+460)+LN(W)+LN(W)**2+LN(W)**3+1/LN(W)**3-1/(T+460)**2+1/(T+460)**3+C
35. LN(P)=-1/(T+460)+LN(W)/(T+460)+LN(W)+LN(W)**3+1/LN(W)**3-1/(T+460)**2+LN(W)**2+C

for all data points are determined. Assuming a normal error distribution, the average percent error for a correlation is determined from:

$$TER = \sqrt{\left| \sum_{N=1}^{N} \left[\frac{DEV(N)^2}{P(N)^2} \right] \right| \frac{1}{N-1}} \qquad (100)$$

where:

TER = average percent error

N = number of sets of data points

DEV(N) = deviation in pressure, at data set N

P(N) = pressure at data set N

Subroutine CORLAT

Subroutine CORLAT receives the values of the defined variables from the main program and performs the stepwise multiple regression analysis in the form of $P = B_1 X_1 + B_2 X_2 + \ldots B_n X_n + C$, where n is the number of independent variables, 59 or less. The number of sets of data points that may be analyzed at one time is 300. This restriction can be increased by enlarging the size of the dimension statement. Some properties of the stepwise regression follow:

1. A number of intermediate regression equations are obtained adding one variable at a time. The variable added is that one which makes the greatest improvement in "goodness of fit". This provides valuable statistical information at each step in the calculation.

2. A weighting factor can be assigned to each set of data. Certain sets of data may have higher reliability than others, and weighting factors can be applied in relation to their reliabilities. Weighting factors were not used for the equilibrium data.

3. Only significant variables are included in the final regression.

4. A variable which is approximately a linear combination of other independent variables is not entered into the regression. This eliminates the possibility of degeneracy and permits single precision floating point operations.

Calculation Procedure

The setpwise multiple regression procedure consists of four parts, as follows:

1. Calculation of weighted sums of squares and cross products. The following values are calculated:

a. Weighted number of data = Σw_t

b. Weighted sums of variables = $\Sigma w_t x_{i.t}$

c. Weighted sums of squares and cross products = $\Sigma w_t x_{i.t} x_{j.t}$

where

$t = 1$ to m

$i = 1$ to $n + 1$

$j = i$ to $n + 1$

Note: $x_{n+1} = y$

2. Calculation of weighted means, residual sums of squares, and residual sums of cross products.

a. Mean = $\bar{x}_i = \Sigma x_t x_{i.t} / \Sigma w_t$

b. Residual sums of squares and cross products =

$$\frac{\Sigma w_t \ \Sigma w_t x_{i.t} x_{j.t} \quad - \quad \Sigma w_t x_{i.t} \Sigma w_t x_{j.t}}{\Sigma w_t}$$

where

$t = 1$ to m

$i = 1$ to $n+1$

$j = i$ to $n+1$

$y = x_{n+1}$

3. Calculation of simple correlation coefficients, r_{ij}.

a. Definition

$x_i x_i$ = Residual sums of squares

$x_i x_j$ = Residual sums of cross products

b. Calculations

$$\sigma_i = x_i x_i$$

$$r_{ij} = \frac{x_i x_j}{\sigma_i \sigma_j} = \text{partial correlation coefficient}$$

$$r_{ji} = r_{ij}$$

$$r_{ii} = 1.000$$

where

$i = 1$ to $n+1$

$j = i+1$ to $n+1$

4. Stepwise calculation of regression coefficients and reliability.

In the stepwise procedure, intermediate results are used to give valuable statistical information at each step in the calculation. These intermediate answers are also used to control the method of calculation. A number of intermediate regression equations are obtained by adding one variable at a time, thus giving the following intermediate equations:

a. $P = B_1 X_1 + C$

b. $P = B_1 X_1 + B_2 X_2 + C$, etc.

The coefficients for each of these intermediate equations and the reliability of each coefficient are obtained by the stepwise procedure. The values and reliability may vary with each subsequent equation. The coefficients represent the best values when the equation is fitted by the specific variables included in the equation. The variable is added that makes the greatest improvement in "goodness of fit" or, stated another way, gives the greatest reduction in variance of the dependent variable.

A variable may be indicated to be significant at an early stage and enter the regression equation. After several other variables are added to the regression equation, a variable in the equation may be indicated to be insignificant. Under this situation the stepwise regression procedure will remove the insignificant variable before adding an additional variable. Thus, at the various steps in the regression procedure, only those variables which are significant will be included in the regression equation.

USAGE

Main Program

All control words must be assigned in the main program and stored in the COMMON storage area. The sequence of storage must be the same as that of CORLAT. The common statements are:

```
COMMON NTPIN, NTPOUT, TOL, EFIN, EFOUT, NOPROB, INVAR, NODATA
COMMON IFLIST, IFWT, IFSTEP, IFRAW, IFAVE, IFRESD, IFCOEN, IFPRED
COMMON IFCNST
COMMON CP
```

Tapes used by CORLAT are defined in the main program. The input tape is denoted by NTPIN, and is written by the main program in binary. The output tape is denoted by NTPOUT; it is BCD.

For later use in the main program, the constant and the coefficients obtained as a result of correlation are stored in the common area. CNST is the constant, and the coefficients B_1, B_2, etc., are stored in the array COEN. If the coefficients are to be used in the main program, CNST and COEN must appear in the COMMON statement and, in addition, COEN (60) must appear in the DIMENSION statement of the main program. The coefficients are then obtained using COEN (I), I = 1, 2 ---60.

TOL	Tolerance (normally .001)
EFIN	F level to enter variables in the regression
EFOUT	F level to remove variables in the regression
NOPROB	Problem number (up to 8 integer digits)
INVAR	The total number of variables, including the dependent variable. (If N is the number of independent variables then INVAR = N+1)
NODATA	Number of sets of data. (This need not be determined before object time, but "counted" in the main program).

The following control words should never be negative.

IFLIST	Controls listing of the input data to the subroutine. If IFLIST = 0, data are printed on the output tape. If IFLIST = 1, data are not printed
IFWT	Controls weighting of sets of data. If IFWT = 1, then all weights are 1.0 and are not to be included. If IFWT = 0, then weights are assumed to be given with the input data.
IFSTEP	Controls printing of results of intermediate steps; printed if = 0, not printed if = 1. Usually IFSTEP = 0, as this gives very valuable information.
IFRAW	Controls printing of raw sums, sums of squares, and sums of cross products; printed if = 0, not printed if = 1.
IFAVE	Controls printing of average values of the variables; printed if = 0, not printed if = 1.
IFRESD	Controls printing of residual sums and squares; printed if = 0, not printed if = 1.
IFPRED	Controls printing of predicted values and the comparison with actual values; printed if = 0, not printed if = 1.
IFCNST	Controls whether a constant appears in the regression equation. if = 1, then the constant is set to zero; if = 0, then the constant term is included and determined by the analysis.

Input Data

Data which are used by CORLAT is written by the main program (equations 1-35) in binary form and the number of this tape assigned to NTPIN; e.g., NTPIN = 15, if the data is written on tape 15. One set of data is stored in the following form: (all floating point): the run number, RUNNO; the independent variables (X_1, X_2, X_3---); and then the dependent variable (XP).

The first input card contains the number of data sets (N) and the number of equations (K) to be correlated. The following cards contain one set of equilibrium conditions (T, W, P). If variable weights are used, the weight for each set of data follows the independent variable. Sets of data are written one after the other until all data are used. Then the tape is rewound by the main program and control shifts to CORLAT by the call statement: CALL CORLAT.

Should an error occur in the execution of CORLAT, a statement is written on the output tape and control is returned to the main program by means of CORLAT statement number 910 RETURN. By suitable coding of the main program, several different regression problems can be handled sequentially. This involves proper rewinding, writing, and rewinding of the input tape, and assignment of control words in the main program. It should be noted that control words are not changed at any time by CORLAT. Thus, control words, once assigned for one problem, do not need to be reassigned for a subsequent problem, unless they are to be changed. The normal return to the main program is also by subroutine statement 910 RETURN.

Output

For each equation calculated in the main program the following is printed from:

Subroutine CORLAT

1. The number of the equation calculated.

2. The number of variables used in the equation, including the dependent variable.

3. The number of input data points and degrees of freedom.

4. The statistical level to enter and remove each independent variable.

For each variable entered into the correlation computation the following is given.

1. The computation step number
2. The variable,by number, entered into the correlation computation.
3. F level of the variable entered. This is the significance of the variable to the equation. The larger the F level, the more important the entered variable.
4. The standard error of the polynomial with the entrance of the given variable.
5. The constant C, for the polynomial.
6. The coefficients of the polynomial.
7. The diagonal elements of the final vector matrix used to develop the final polynomial.

Main Program

1. Data point sequence number.
2. Data point (T,W,P)
3. Calculated value of polynomial, per data point.
4. Deviation between the data point and its calculated value.
5. Percent error of the calculated point.
6. Average percent error of the calculated polynomial.

Operation Details

This program was written in Fortran IV for the Univac 1108 system. The core storage for the total program is 134741 octal words. Compilation and execution time for all 35 equations is one minute.

SAMPLE PROBLEM

The input equilibrium data for water on molecular sieve type 5A is shown in Table D-2, the output obtained with the two best data fits (equations 33 and 34) are shown in Table D-3. Table D-4 contains the source listing for the program.

APPENDIX D (Continued)

TABLE D-2

INPUT DATA FOR SAMPLE PROBLEM

DATA INPUT (H2O-5A)

```
43   35
      32.        .066        .001
      32.         .10       .0018
      32.         .12       .0035
      32.        .142       .0107
      32.         .16        .035
      32.         .18         .08
      77.         .04        .001
      77.         .06        .003
      77.         .08       .0076
      77.         .10       .0175
      77.         .12         .05
      77.         .14         .08
      77.         .16          .1
      77.         .18          .5
     122.        .025        .001
     122.         .04        .007
     122.         .06        .022
     122.         .08        .055
     122.         .10        .124
     122.         .12         .26
     122.         .14          .8
     122.         .16          2.0
     122.        .173          10.
     167.         .02       .0025
     167.         .04        .031
     167.         .06         .11
     167.         .08         .29
     167.         .10          .5
     167.         .12         1.39
     167.         .14          3.3
     167.         .16          9.5
     302.         .02           .1
     302.         .04         1.55
     302.         .06          3.0
     302.        .076         10.0
     392.         .02          .02
     392.        .025         1.30
     392.        .050          3.8
     392.        .095          8.6
     392.       .0395         10.0
     482.         .02         2.55
     482.        .025         7.80
     482.       .0267        10.00
```

TABLE D-3

SAMPLE PROBLEM OUTPUT DATA

```
H20 5A  LINEAR, T=32,77,122,167,302,392,482 DEG, F  4/18     0000000180469  PAGE  120

                        STEPWISE  REGRESSION

                        PROBLEM NO.      33

NO. OF DATA =   43      NO. OF VARIABLES=  7      WEIGHTED DEGREES OF FREEDOM =    43.00

                F LEVEL TO ENTER VARIABLE =   .050

                F LEVEL TO REMOVE VARIABLE=   .100
```

STA DARD ERROR OF Y = .30016310+01

STEP NO, 1
VARIABLE ENTERING 1
F LEVEL = 53,9208
STANDARD ERROR OF Y = .19966476+01
CONSTANT = .94442996+01

VARIABLE	COEFFICIENT	STD ERROR OF COEF
X 1	.26531490+04	.36131292+03

STEP NO, 2
VARIABLE ENTERING 6
F LEVEL = 439,9054
STANDARD ERROR OF Y = .60274305-00
CONSTANT = .12637710+02

VARIABLE	COEFFICIENT	STD ERROR OF COEF
X 1	.24942564+04	.10939436+03
X 6	-.82600456+09	.40798163+08

STEP NO, 3
VARIABLE ENTERING 2
F LEVEL = 23,5962
STANDARD ERROR OF Y = .48182423-00
CONSTANT = .92917259+01

VARIABLE	COEFFICIENT	STD ERROR OF COEF
X 1	.17039430+04	.18469354+03
X 2	-.16648451+02	.34273020+01
X 6	-.10959607+10	.64436851+08

STEP NO, 4
VARIABLE ENTERING 3
F LEVEL = 15,3146
STANDARD ERROR OF Y = .41209549-00
CONSTANT = .10775865+02

VARIABLE	COEFFICIENT	STD ERROR OF COEF
X 1	.14496035+04	.17081256+03
X 2	-.21731218+02	.32061649+01
X 3	.32746314+07	.83677676+06
X 6	.17452563+09	.32929590+09

STEP NO, 5
VARIABLE ENTERING 4
F LEVEL = 97,4259
STANDARD ERROR OF Y = .21910293-00
CONSTANT = .13077723+02

VARIABLE	COEFFICIENT	STD ERROR OF COEF
X 1	-.13004925+04	.29304468+03
X 2	-.44208564+02	.28445812+01
X 3	.13230781+06	.11024395+07
X 4	.12034333+00	.12192276-01

APPENDIX D (Continued)

```
H20 5A  LINEAR, T=32,77,122,167,302,392,482 DEG, F  4/18    @@@@@@180469  PAGE  122

                X  6                 ,32302199+10          ,35565812+09

STEP NO,  6
  VARIABLE ENTERING          5
  F LEVEL                =   34,7088
  STANDARD ERROR OF Y    =    ,15849377-00
  CONSTANT               =   -,14696953+01

                VARIABLE          COEFFICIENT          STD ERROR OF COEF

                X  1              ,32378223+03          ,34777606+03
                X  2             -,53695402+02          ,26128792+01
                X  3              ,74589582+07          ,12632430+07
                X  4              ,21768276-00          ,18728843-01
                X  5             -,57588499+01          ,97749766-00
                X  6              ,14777981+10          ,39327923+09

COMPLETED  6 STEPS OF REGRESSION

                DIAGONAL  ELEMENTS

                VARIABLE          VALUE

                X  1              ,14703167+03
                X  2              ,37293798+02
                X  3              ,23986429+04
                X  4              ,19688732+03
                X  5              ,85671105+03
                X  6              ,13508420+04
```

H2O SA LINE, T=12,77,122,167,302,392,482 DEG, P 4/18 @@@@@180469 PAGE 123

NO,	T	X	P	P, CALC,	P, DEVIATION	PERCENT ERROR	TOTAL PERCENT ERROR= ,144677+02
1	32,0000	,0860	,0010	,968774-03	,312959-04	,312959+01	
2	32,0000	,1000	,0019	,167939-02	,120705-03	,670585+01	
3	32,0000	,1200	,0035	,407944-02	-,579637-03	-,165610+02	
4	32,0000	,1420	,0107	,133317-01	-,243175-02	-,245958+02	
5	32,0000	,1600	,0350	,431658-01	-,816580-02	-,233308+02	
6	32,0000	,1800	,1220	,206528-00	,113472+00	,354601+02	
7	77,0000	,0400	,0010	,106333-02	-,633334-04	-,633334+01	
8	77,0000	,0600	,0030	,326916-02	-,269176-03	-,897254+01	
9	77,0000	,0800	,0076	,711907-02	,490927-03	,632799+01	
10	77,0000	,1000	,0175	,153019-01	,219814-02	,125608+02	
11	77,0000	,1200	,0350	,368021-01	-,180207-02	-,514876+01	
12	77,0000	,1400	,0960	,105938+00	-,993753-02	-,103516+02	
13	77,0000	,1600	,3100	,383266-00	-,732661-01	-,236342+02	
14	77,0000	,1800	2,5000	,182187+01	,678128-00	,271251+02	
15	122,0000	,0230	,0010	,864293-03	,135707-03	,135707+02	
16	122,0000	,0400	,0070	,746228-02	-,462277-03	-,660396+01	
17	122,0000	,0600	,0220	,225129-01	-,512877-03	-,233126+01	
18	122,0000	,0800	,0540	,463717-01	,762828-02	,136219+02	
19	122,0000	,1000	,1240	,102895+00	,211049-01	,170201+02	
20	122,0000	,1200	,2600	,245375-00	,146246-01	,562483+01	
21	122,0000	,1400	,6000	,701274-00	-,212739-01	-,312852+01	
22	122,0000	,1600	2,0000	,252136+01	-,521359-00	-,260680+02	
23	122,0000	,1750	10,0000	,100670+02	-,669597-01	-,669597-00	
24	167,0000	,0200	,0025	,230026-02	,199737-03	,798949+01	
25	167,0000	,0400	,0310	,398397-01	-,883972-02	-,285152+02	
26	167,0000	,0600	,1100	,118262+00	-,826192-02	-,751083+01	
27	167,0000	,0800	,2900	,251198-00	,388016-01	,133798+02	
28	167,0000	,1000	,6500	,529603-00	,120397+00	,185226+02	
29	167,0000	,1200	1,3900	,125379+01	,136208-00	,979914+01	
30	167,0000	,1400	3,3000	,356130+01	-,261305-00	-,791832+01	
31	167,0000	,1600	9,8000	,127362+02	-,293622+01	-,299614+02	
32	302,0000	,0200	,1000	,105946+00	-,594641-02	-,594641+01	
33	302,0000	,0400	1,9500	,172220+01	-,172203-00	-,111099+02	
34	302,0000	,0600	5,8000	,492610+01	,739031-01	,147806+01	
35	302,0000	,0760	10,0000	,886444+01	,113556+01	,113556+02	
36	392,0000	,0200	,6200	,638129-00	-,131288-01	-,292400+01	
37	392,0000	,0250	1,8000	,167915+01	-,751516-01	-,417509+01	
38	392,0000	,0300	3,8000	,391630+01	-,116295+00	-,306041+01	
39	392,0000	,0350	6,6000	,668589+01	-,856855-01	-,130130+01	
40	392,0000	,0395	10,0000	,969476+01	,305243-00	,305243+01	
41	482,0000	,0200	2,6500	,256244+01	,875615-01	,330421+01	
42	482,0000	,0250	7,4000	,746901+01	,330993-00	,424350+01	
43	482,0000	,0267	10,0000	,985629+01	,143710-00	,143710+01	

```
-20 54  LINUE, T=32,77,122,167,302,392,482 DEC, F  4/18    80469  PAGE  124
                    STEPWISE  REGRESSION
                    PROBLEM NO,      34
 NO, OF DATA =   43          NO, OF VARIABLES=  8          WEIGHTED DEGREES OF FREEDOM =   43,00
                    F LEVEL TO ENTER VARIABLE =   ,050
                    F LEVEL TO REMOVE VARIABLE=   ,100
```

```
H20 5A  LINE, T=32,77,122,167,302,392,482 DEG, F  4/18     ######180469  PAGE  125

                STANDARD ERROR OF Y =        ,30016318+01

              STEP NO,  1
                VARIABLE ENTERING          1
                F LEVEL                =   53,9208
                STANDARD ERROR OF Y =        ,19966476+01
                CONSTANT               =     ,94442996+01

                          VARIABLE          COEFFICIENT     STD ERROR OF COEF

                           X  1              ,26531480+04      ,36131292+03

              STEP NO,  2
                VARIABLE ENTERING          7
                F LEVEL                =  409,9054
                STANDARD ERROR OF Y =        ,60274385+00
                CONSTANT               =     ,12637710+02

                          VARIABLE          COEFFICIENT     STD ERROR OF COEF

                           X  1              ,24942564+04      ,10935436+03
                           X  7             -,82600456+09      ,40798163+08

              STEP NO,  3
                VARIABLE ENTERING          5
                F LEVEL                =   23,5962
                STANDARD ERROR OF Y =        ,48182423+00
                CONSTANT               =     ,92917259+01

                          VARIABLE          COEFFICIENT     STD ERROR OF COEF

                           X  1              ,17039430+04      ,18469354+03
                           X  5             -,16648451+02      ,34273020+01
                           X  7             -,10959607+10      ,64436851+08

              STEP NO,  4
                VARIABLE ENTERING          6
                F LEVEL                =   15,3146
                STANDARD ERROR OF Y =        ,41209549+00
                CONSTANT               =     ,10775865+02

                          VARIABLE          COEFFICIENT     STD ERROR OF COEF

                           X  1              ,14496035+04      ,17081256+03
                           X  5             -,21731218+02      ,32061649+01
                           X  6              ,32746314+07      ,83677676+06
                           X  7              ,17452563+09      ,32929890+08

              STEP NO,  5
                VARIABLE ENTERING          4
                F LEVEL                =   97,4259
                STANDARD ERROR OF Y =        ,21910293+00
                CONSTANT               =     ,13077723+02

                          VARIABLE          COEFFICIENT     STD ERROR OF COEF

                           X  1             -,13004925+04      ,29304668+03
                           X  4              ,12034333+00      ,12192276-01
                           X  5             -,44208564+02      ,28445812+01
                           X  6              ,13230781+08      ,11024395+07
```

X 7	.32302199+10	.35565E12+09

STEP NO. 6
VARIABLE ENTERING 2
F LEVEL = 34.7088
STANDARD ERROR OF Y = .15849377-00
CONSTANT = -.14696953+01

VARIABLE	COEFFICIENT	STD ERROR OF COEF
X 1	.32378223+03	.34777606+03
X 2	-.57568499+01	.97749766-00
X 4	.21768276-00	.16728843-01
X 5	-.53695402+02	.26126792+01
X 6	.74589582+07	.12632430+07
X 7	.14777981+10	.39327923+09

COMPLETED 6 STEPS OF REGRESSION

DIAGONAL ELEMENTS

VARIABLE	VALUE
X 1	.14703167+03
X 2	.85671105+03
X 3	.31807176-05
X 4	.19688732+03
X 5	.37293798+02
X 6	.23986429+04
X 7	.13508420+04

H2O 5A LINDE, T=32,77,122,167,302,392,482 DEG, F 4/18 ######180469 PAGE 127

NO.	T	X	P	P, CALC.	P, DEVIATION	PERCENT ERROR	TOTAL PERCENT ERROR= .144677+02
1	32,0000	.0860	.0010	.968704-03	.312961-04	.312961+01	
2	32,0000	.1000	.0018	.167929-02	.120705-03	.670585+01	
3	32,0000	.1200	.0035	.407964-02	-.579638-03	-.165611+02	
4	32,0000	.1420	.0107	.133317-01	-.263175-02	-.245958+02	
5	32,0000	.1600	.0350	.431658-01	-.816581-02	-.233309+02	
6	32,0000	.1800	.3200	.206528-00	.113472+00	.354601+02	
7	77,0000	.0400	.0010	.106333-02	-.633329-04	-.633329+01	
8	77,0000	.0600	.0030	.326918-02	-.269175-03	-.897251+01	
9	77,0000	.0800	.0076	.711907-02	.480927-03	.632799+01	
10	77,0000	.1000	.0175	.153019-01	.219814-02	.125608+02	
11	77,0000	.1200	.0350	.368021-01	-.180207-02	-.514876+01	
12	77,0000	.1400	.0960	.105938+00	-.993755-02	-.103516+02	
13	77,0000	.1600	.3100	.383266-00	-.732661-01	-.236342+02	
14	77,0000	.1800	2.5000	.182187+01	.678128-00	.271251+02	
15	122,0000	.0230	.0010	.864292-03	.135708-03	.135708+02	
16	122,0000	.0400	.0070	.746228-02	-.462276-03	-.660394+01	
17	122,0000	.0600	.0220	.225129-01	-.512877-03	-.233126+01	
18	122,0000	.0800	.0560	.483717-01	.762828-02	.136219+02	
19	122,0000	.1000	.1240	.102895+00	.211049-01	.170201+02	
20	122,0000	.1200	.2600	.245375-00	.146246-01	.562483+01	
21	122,0000	.1400	.6800	.701274-00	-.212741-01	-.312855+01	
22	122,0000	.1600	2.0000	.252136+01	-.521360-00	-.260680+02	
23	122,0000	.1780	10.0000	.100670+02	-.669597-01	-.669597-00	
24	167,0000	.0200	.0029	.230026-02	.199738-03	.798954+01	
25	167,0000	.0400	.0310	.398397-01	-.883971-02	-.285152+02	
26	167,0000	.0600	.1100	.118262+00	-.826192-02	-.751083+01	
27	167,0000	.0800	.2900	.251198-00	.388016-01	.133798+02	
28	167,0000	.1000	.6500	.529603-00	.120397+00	.185226+02	
29	167,0000	.1200	1.3900	.125379+01	.136208-00	.979914+01	
30	167,0000	.1400	3.3000	.356130+01	-.261305-00	-.791832+01	
31	167,0000	.1600	9.8000	.127362+02	-.293622+01	-.299615+02	
32	302,0000	.0200	.1000	.105946+00	-.594640-02	-.594640+01	
33	302,0000	.0400	1.5500	.172220+01	-.172203-00	-.111099+02	
34	302,0000	.0600	5.0000	.492610+01	.739031-01	.147806+01	
35	302,0000	.0780	10.0000	.886444+01	.113556+01	.113556+02	
36	392,0000	.0200	.6200	.638129-00	-.181288-01	-.292400+01	
37	392,0000	.0250	1.8000	.187515+01	-.751518-01	-.417510+01	
38	392,0000	.0300	3.8000	.391630+01	-.116296+00	-.306042+01	
39	392,0000	.0350	6.6000	.668589+01	-.858855-01	-.130130+01	
40	392,0000	.0395	10.0000	.969476+01	.305243-00	.305243+01	
41	482,0000	.0200	2.6500	.256244+01	.875612-01	.330420+01	
42	482,0000	.0250	7.8000	.746901+01	.330993-00	.424350+01	
43	482,0000	.0267	10.0000	.985629+01	.143711-00	.143711+01	

TABLE D-4
SOURCE LISTING

```
                      MAIN PROGRAM
00101     1*          DIMENSION TT(300),PP(300),WW(300),TR(300),TR2(300),WL(300),
00101     2*         1          WL2(300),CP(300),PE(300),DEV(300)
00103     3*          COMMON NTPIN,NTPOUT,TOL,EFIN,EFOUT,NOPROB,INVAR,NODATA          GAR50010
00104     4*          COMMON IFLIST,IFWT,IFSTEP,IFRAW,IFAVE,IFRESD,IFCOEN,IFPRED     GAR50020
00105     5*          COMMON IFCNST                                                  GAR50030
00106     6*          COMMON CP
00106     7*    C  PROGRAM OPERATION- DATA INPUT
00106     8*    C  FIRST DATA CARD- N=NO. SETS OF DATA POINTS (T,W,P), K=NO. OF EQUATIONS IN THE
00106     9*    C                  PROGRAM, FORMAT(2I4),
00106    10*    C  SECOND AND FOLLOWING DATA CARDS- ONE CARD FOR EACH SET OF DATA POINTS (T,W,P)
00106    11*    C                                  IN THAT ORDER, FORMAT(3F10.0),
00106    12*    C  NOTE- THE GO TO RANGE OF FORTRAN STATEMENT 76, MUST BE .LE. TO THE VALUE OF K
00106    13*    C       ON DATA CARD NUMBER 1,
00106    14*    C       SUBROUTINE CURLAT MUST BE INCLUDED
00107    15*          NTPIN=15
00110    16*          NTPOUT=6
00111    17*          TOL=.001
00112    18*          EFIN=.05
00113    19*          EFOUT=.10
00114    20*          IFWT=1
00115    21*          IFSTEP=0
00116    22*          IFRAW=1
00117    23*          IFAVE=1
00120    24*          IFRESD=1
00121    25*          IFCOEN=1
00122    26*          IFPRED=0
00123    27*          IFCNST=0
00124    28*          IFLIST=1
00124    29*    C  N=NUMBER OF SETS OF DATA POINTS (T,W,P), INPUT
00124    30*    C  K=TOTAL NUMBER OF DIFFERENT EQUILIBRIUM EQUATIONS, INPUT
00125    31*          READ(5,101) N,K
00131    32*          DO 300 I=1,N
00131    33*    C  T=TEMPERATURE, DEG. F, INPUT
00131    34*    C  W=PERCENT LOADING, INPUT
00131    35*    C  P=PRESSURE, (MM-HG), INPUT
00134    36*          READ(5,200)T,W,P
00141    37*          TT(I)=T
00142    38*          WW(I)=W
00143    39*          PP(I)=P
00144    40*          T1=1./(T+460.)
00145    41*          TR(I)=T1
00146    42*          T2=T1*T1
00147    43*          TR2(I)=T2
00150    44*          YW=ALOG(W)
00151    45*          WL(I)=YW
00152    46*          Y1=YW*YW
00153    47*          WL2(I)=Y1
00154    48*      300 CONTINUE
00156    49*          DO 800 J=1,K
00161    50*          NOPROB=J
00162    51*          DEVS=0.0
00163    52*          NODATA=0
00164    53*          REWIND 15
00165    54*          DO 470 I=1,N
00170    55*          CP(I)=0.0
00171    56*          PE(I)=0.0
00172    57*          DEV(I)=0.0
```

```
                    H20 HA  LINDE, T=32,77,122,167,302,392,482 DEG, F  4/18    0020000180469  PAGE     5

00173    58*      470 GO TO (
00175    59*         DO 750 I=1,
00200    60*         NODATA=NODATA+1
00200    61*   C  RUN NO=RUN NUMBER
00201    62*         RUN NO=I
00201    63*   C                          EQUATION VARIABLES
00201    64*   C                          LN=NATURAL LOG
00201    65*   C  YW=LN(W)
00202    66*         YW=WL(I)
00202    67*   C  T1=1/(T+460), DEG, RANKINE
00203    68*         T1=TR(I)
00203    69*   C  T2=1/(T+460)**2, DEG, RANKINE
00204    70*         T2=TR2(I)
00204    71*   C  YW2=LN(W)**2
00205    72*         YW2=WL2(I)
00205    73*   C  YW3=LN(W)**3
00206    74*         YW3=YW**3
00206    75*   C  YSR=1/LN(W)**3
00207    76*         YSR=1./YW3
00207    77*   C  TSR=SQ, ROOT(1/(T+460))
00210    78*         TSR=SQRT(T1)
00210    79*   C  SL=-LN(W)/SQ, ROOT(1/(T+460))
00211    80*         SL=-YW/TSR
00211    81*   C  SL2=LN(W)**2/SQ, ROOT(1/(T+460))
00212    82*         SL2=YW2/TSR
00212    83*   C  SL1=LN(W)/SQ, ROOT(1/(T+460))
00213    84*         SL1=-SL
00213    85*   C  B=-1/(T+460)
00214    86*         B=-T1
00214    87*   C  C= LN(W)/(T+460)
00215    88*         C=YW*T1
00215    89*   C  D=-1/(T+460)**2
00216    90*         D=-T2
00216    91*   C  YW2T1=LN(W)**2/(T+460)
00217    92*         YW2T1=YW2*T1
00217    93*   C  YW3T1=LN(W)**3/(T+460)
00220    94*         YW3T1=YW3*T1
00220    95*   C  YW2T2=LN(W)**2/(T+460)**2
00221    96*         YW2T2=YW2*T2
00221    97*   C  YW3T3=LN(W)**3/(T+460)**3
00222    98*         YW3T3=YW3*T1*T2
00222    99*   C  YW3T2=LN(W)**3/(T+460)**2
00223   100*         YW3T2=YW3*T2
00223   101*   C  YWT2=LN(W)/(T+460)**2
00224   102*         YWT2=YW*T2
00224   103*   C  YW2T3=LN(W)**2/(T+460)**3
00225   104*         YW2T3=YW2*T1*T2
00225   105*   C  T3=1/(T+460)**3
00226   106*         T3=T1*T2
00226   107*   C  AJ=1/(T+460)**2
00227   108*         AJ=TT(I)**2
00227   109*   C  BJ=LN(Y)/13.6
00230   110*         BJ=YW/13.6
00230   111*   C  CJ=LN(LOG10(100*W))
00231   112*         CJ=ALOG(ALOG10(100.*WW(I)))
00231   113*   C  DJ=(1/(T+460))-(LN/13.6-(LN(LOG10(100*W))))
00232   114*         DJ=AJ*(BJ-CJ)
00232   115*   C  XP=LN(P), DEPENDENT VARIABLE
00233   116*         XP=ALOG(PP(I))
00234   117*         GO TO(1,2,3,4,5,6,7,8,9,10,11,12,13,14,15,16,17,18,19,20,21,22,23,
```

```
                -20 53  LINE, T=32,77,122,167,302,393,482 DEG, F  4/18    @@@@@180469  PAGE     6

00234   118*          124,25,26,27,28,29,30,31,32,33,34,35                              ),J
00234   119*  C                              EQUATIONS ATTEMPTED,
00235   120*       1 CONTINUE
00236   121*         INVAR=5
00237   122*         WRITE(15) RUNNO,B,C,YW,Yw2,XP
00237   123*  C  1,  LN(P)=-1/(T+460)+LN(W)/(T+460)+LN(W)+LN(W)**2+C
00247   124*         GOTO 750
00250   125*       2 CONTINUE
00251   126*         INVAR=7
00252   127*         WRITE(15) RUNNO, B,C,Yw,YW3,YSw,D,XP
00252   128*  C  2,  LN(P)=-1/(T+460)+LN(W)/(T+460)+LN(W)+LN(W)**3+1/LN(W)**3-1/( T+460 )**2+C
00264   129*         GOTO 750
00265   130*       3 CONTINUE
00266   131*         INVAR=5
00267   132*         WRITE(15) RUNNO,B,C,Yw2,Yw3,XP
00267   133*  C  3,  LN(P)=-1/(T+460)+LN(W)/(T+460)+LN(W)**2+LN(W)**3+C
00277   134*         GOTO 750
00300   135*       4 CONTINUE
00301   136*         INVAR=4
00302   137*         WRITE(15) RUNNO,B,Yw,Yw2,XP
00302   138*  C  4,  LN(P)=-1/(T+460)+LN(W)+LN(W)**2+C
00311   139*         GOTO 750
00312   140*       5 CONTINUE
00313   141*         INVAR=4
00314   142*         WRITE(15) RUNNO,SL1,YW,YW2,XP
00314   143*  C  5,  LN(P)=LN(W)/SQRT(T+460)+LN(W)+LN(W)**2+C
00323   144*         GOTO 750
00324   145*       6 CONTINUE
00325   146*         INVAR=4
00326   147*         WRITE(15) RUNNO,C,Yw,Yw2,XP
00326   148*  C  6,  LN(P)=LN(W)/(T+460)+LN(W)+LN(W)**2+C
00335   149*         GOTO 750
00336   150*       7 CONTINUE
00337   151*         INVAR=5
00340   152*         WRITE(15) RUNNO,Yw,T1,T2,Yw2 ,XP
00340   153*  C  7,  LN(P)=LN(W)+1/(T+460)+1/(T+460)**2+LN(W)**2+C
00350   154*         GOTO 750
00351   155*       8 CONTINUE
00352   156*         INVAR=5
00353   157*         XP=ALOG10(PP(I))
00354   158*         WRITE(15) RUNNO,AJ,BJ,CJ,DJ,XP
00354   159*  C  8,  LN(P)=1/(T+460)**2+LN(W)**2+LN(W)+1/(T+460)+C
00364   160*         GOTO 750
00365   161*       9 CONTINUE
00366   162*         INVAR=4
00367   163*         XP=ALOG10(PP(I))
00370   164*         WRITE(15) RUNNO,BJ,CJ,DJ,XP
00370   165*  C  9,  LN(P)=LOG(1/(T+460)**2+LN(W)/13.6+LN(LOG(100*W))+1/(T+460)**2(LN(W)/13.6-
00370   166*  C              LN(LOG(100*W))+C)
00377   167*         GOTO 750
00400   168*      10 CONTINUE
00401   169*         INVAR=3
00402   170*         XP=ALOG10(PP(I))
00403   171*         WRITE(15) RUNNO,CJ,DJ,XP
00403   172*  C 10,  LN(P)=LOG(LN(W)/13.6 +LN(LOG(100*W))+1/(T+460)**2(LN(W)/13.6-LN(LOG(100*W
00403   173*  C              )))+C)
00411   174*         GOTO 750
00412   175*      11 CONTINUE
00413   176*         INVAR=2
00414   177*         XP=ALOG10(PP(I))
```

```
                    H20 5A  LI CE, T=72,77,122,167,302,392,482 DEG, F  4/18    0000080469  PAGE    7

00415   178*          WRITE(15) W,T,C,DD,XP
00415   179*    C 11,  LN(P)=LOG(1/(T+460)**2(LN(W)/13.6-LN(LOG(100*W)))+C)
00422   180*          GOTO 750
00423   181*       12 CONTINUE
00424   182*          INVAR=4
00425   183*          WRITE(15)W,T,C,Y,2T1,YW3T1,XP
00425   184*    C 12,  LN(P)=LN(W)/(T+460)+(LN(W)**2/(T+460))+(LN(W)**3/(T+460))+C
00434   185*          GOTO 750
00435   186*       13 CONTINUE
00436   187*          INVAR=4
00437   188*          WRITE(15)W,T,C,Y,2T2,YW3T3,XP
00437   189*    C 13,  LN(P)=LN(W)/(T+460)+(LN(W)**2/(T+460)**2)+(LN(W)**3/(T+460)**3)+C
00446   190*          GOTO 750
00447   191*       14 CONTINUE
00450   192*          INVAR=4
00451   193*          WRITE(15)W,T,C,YW,YW2T1,YW3T2,XP
00451   194*    C 14,  LN(P)=LN(W)+(LN(W)**2/(T+460))+(LN(W)**3/(T+460)**2)+C
00460   195*          GOTO 750
00461   196*       15 CONTINUE
00462   197*          INVAR=4
00463   198*          WRITE(15)W,T,C,Y,3,YW2T2,YW2T1,XP
00463   199*    C 15,  LN(P)=LN(W)**3+LN(W)/(T+460)**2+LN(W)**2/(T+460)+C
00472   200*          GOTO 750
00473   201*       16 CONTINUE
00474   202*          INVAR=4
00475   203*          WRITE(15)W,T,C,YW3T1,YW2,XP
00475   204*    C 16,  LN(P)=LN(W)/(T+460)+LN(W)**3/(T+460)+LN(W)**2+C
00504   205*          GOTO 750
00505   206*       17 CONTINUE
00506   207*          INVAR=4
00507   208*          WRITE(15)W,T,C,YW,YW2T1,YW3T1,XP
00507   209*    C 17,  LN(P)=LN(W)+LN(W)**2/(T+460)+LN(W)**3/(T+460)+C
00516   210*          GOTO 750
00517   211*       18 CONTINUE
00520   212*          INVAR=4
00521   213*          WRITE(15)W,T,C,T1,YW2T2,YW3T3,XP
00521   214*    C 18,  LN(P)=1/(T+460)+LN(W)**2/(T+460)**2+LN(W)**3/(T+460)**3+C
00530   215*          GOTO 750
00531   216*       19 CONTINUE
00532   217*          INVAR=4
00533   218*          WRITE(15)W,T,C,YW,YW2,YW3T1,XP
00533   219*    C 19,  LN(P)=LN(W)+LN(W)**2+LN(W)**3/(T+460)+C
00542   220*          GOTO 750
00543   221*       20 CONTINUE
00544   222*          INVAR=4
00545   223*          WRITE(15)W,T,C,YW,YW2T1,YW3,XP
00545   224*    C 20,  LN(P)=LN(W)+LN(W)**2/(T+460)+LN(W)**3+C
00554   225*          GOTO 750
00555   226*       21 CONTINUE
00556   227*          INVAR=4
00557   228*          WRITE(15)W,T,C,YW2,YW3,XP
00557   229*    C 21,  LN(P)=LN(W)/(T+460)+LN(W)**2+LN(W)**3+C
00566   230*          GOTO 750
00567   231*       22 CONTINUE
00570   232*          INVAR=4
00571   233*          WRITE(15)W,T,C,T1,YW3,YW2T3,XP
00571   234*    C 22,  LN(P)=1/(T+460)+LN(W)**3+LN(W)**2/(T+460)**3+C
00600   235*          GOTO 750
00601   236*       23 CONTINUE
00602   237*          INVAR=4
```

```
00603   238*          WRITE(15)RUNNO,YW3,C,YW2T2,XP
00603   239*    C 23, LN(P)=LN(X)**3+LN(Y)/(T+460)+LN(W)**2/(T+460)**2+C
00612   240*          GOTO 750
00613   241*       24 CONTINUE
00614   242*          INVAR=5
00615   243*          WRITE(15)RUNNO,YW,YW2,YW3,T1,XP
00615   244*    C 24, LN(P)=LN(X)+LN(W)**2+LN(Y)**3+1/(T+460)+C
00625   245*          GOTO 750
00626   246*       25 CONTINUE
00627   247*          INVAR=5
00630   248*          WRITE(15)RUNNO,YW2,YW3,C,T1,XP
00630   249*    C 25, LN(P)=LN(X)**2+LN(Y)**3+LN(W)/(T+460)+1/(T+460)+C
00640   250*          GOTO 750
00641   251*       26 CONTINUE
00642   252*          INVAR=5
00643   253*          WRITE(15)RUNNO,YW3,YW2T1,C,T1,XP
00643   254*    C 26, LN(P)=LN(X)**3+LN(Y)**2/(T+460)+LN(W)/(T+460)+1/(T+460)+C
00653   255*          GOTO 750
00654   256*       27 CONTINUE
00655   257*          INVAR=5
00656   258*          WRITE(15)RUNNO,YW3T1,YW2T1,C,T1,XP
00656   259*    C 27, LN(P)=LN(X)**3/(T+460)+LN(W)**2/(T+460)+LN(W)/(T+460)+1/(T+460)+C
00666   260*          GOTO 750
00667   261*       28 CONTINUE
00670   262*          INVAR=5
00671   263*          WRITE(15)RUNNO,YW3,YW2,YW,T2,XP
00671   264*    C 28, LN(P)=LN(X)**3+LN(Y)**2+LN(W)+1/(T+460)**2+C
00701   265*          GOTO 750
00702   266*       29 CONTINUE
00703   267*          INVAR=5
00704   268*          WRITE(15)RUNNO,YW3,YW2,YWT2,T2,XP
00704   269*    C 29, LN(P)=LN(X)**3+LN(W)**2+LN(W)/(T+460)**2+1/(T+460)**2+C
00714   270*          GOTO 750
00715   271*       30 CONTINUE
00716   272*          INVAR=5
00717   273*          WRITE(15)RUNNO,YW2T2,YWT2,T2,YW3,XP
00717   274*    C 30, LN(P)=LN(W)**2/(T+460)**2+LN(Y)/(T+460)**2+1/(T+460)**2+LN(W)**3+C
00727   275*          GOTO 750
00730   276*       31 CONTINUE
00731   277*          INVAR=5
00732   278*          WRITE(15)RUNNO,YW3T2,YW2T2,YWT2,T2,XP
00732   279*    C 31, LN(P)=LN(X)**3/(T+460)**2+LN(W)**2/(T+460)**2+LN(W)/(T+460)**2+
00732   280*    C           1/(T+460)**2+C
00742   281*          GOTO 750
00743   282*       32 CONTINUE
00744   283*          INVAR=6
00745   284*            WRITE(15)RUNNO,C,D,YSR,YW,T3,XP
00745   285*    C 32, LN(P)=LN(X)/(T+460)-1/(T+460)**2+1/LN(Y)**3+LN(W)+1/(T+460)**3+C
00756   286*          GO TO 750
00757   287*       33 CONTINUE
00760   288*          INVAR=7
00761   289*            WRITE(15)RUNNO,C,YSR,D,YW3,YW,T3,XP
00761   290*    C 33, LN(P)=LN(X)/(T+460)+1/LN(W)**3-1/(T+460)**2+LN(W)**3+LN(W)+1/(T+460)**3+C
00773   291*          GO TO 750
00774   292*       34 CONTINUE
00775   293*          INVAR=8
00776   294*            WRITE(15)RUNNO,C,YW,YW2,YW3,YSR,D,T3,XP
00776   295*    C 34, LN(P)=LN(X)/(T+460)+LN(W)+LN(Y)**2+LN(Z)**3+1/LN(X)**3-1/(T+460)**2+
00776   296*    C           1/(T+460)**3+C
01011   297*          GO TO 750
```

```
                    H20 54  LINDE, T=32,77,122,167,302,392,482 DEG, F  4/18    ******180469  PAGE      9

01012   298*        35 CONTINUE
01013   299*           INVAR=6
01014   300*             WRITE(15)RUNNO,B,C,Y4,YW3,YSR,D,Y 2,XP
01014   301*     C 35.  L.(P)=-1/(T+46 )+LN(W)/(T+460)+LN( )+L (W)**3+1/LN(W)**3-1/(T+460)**2+
01014   302*     C            LN( )**2+C
01027   303*           GO TO 750
01030   304*        750 CONTINUE
01032   305*           REWIND 15
01033   306*           CALL CORLAT
01034   307*           DO 340 I=1,N
01034   308*     C  CP=COMPUTED VALUE OF P, RETURNED FROM SUBROUTINE CORLAT
01037   309*           IF(J.EQ.9.OR.J.EQ.10.OR.   J.EQ.11)CP(I)=10.**(CP(I))
01041   310*           IF(J.EQ.9.OR.J.EQ.10.OR.   J.EQ.11)GO TO 339
01043   311*           CP(I)=EXP(CP(I))
01044   312*        339  CONTINUE
01044   313*     C  DEV=DEVIATION, P-CP
01045   314*           DEV(I)=PP(I)-CP(I)
01046   315*           DEVS=(DEV(I)/PP(I))**2+DEVS
01046   316*     C  PE= PERCENT ERROR PER POINT P
01047   317*        340 PE(I)= 100.*DEV(I)/PP(I)
01047   318*     C  TER =TOTAL PERCENT ERROR PER RUN NO, STANDARD DEVIATION 'ESTIMATE OF ASSUMED
01047   319*     C          NORMAL DATA DISTRIBUTION',
01051   320*           TER=SQRT(DEVS/(N-1))*100.
01052   321*           WRITE(6,360)TER
01055   322*           WRITE(6,400)(I,TT(I),WW(I),PP(I),CP(I),DEV(I),PE(I),I=1,N)
01071   323*        800 CONTINUE
01073   324*        101 FORMAT(2I4)
01074   325*        200 FORMAT( 3F10.0)
01075   326*        360 FORMAT(1H1' NO,' 6X'T',  9X'W', 9X'P', 9X'P, CALC,', 4X'P, DEVIATI
01075   327*          1ON', 2X'PERCENT ERROR', 5X'TOTAL PERCENT ERROR='E12,6//)
01076   328*        400 FORMAT(I4,3F10.4,3E15.6)
01077   329*           END

      END OF UNIVAC 1108 FORTRAN V COMPILATION,     0 *DIAGNOSTIC* MESSAGE(S)
```

```
00101   1*        SUBROUTINE CORLAT                                                    AR20010
00101   2*C       JOB                SUBROUTINE CORLAT - ROGER WRIGHT - APRIL 5, 1966
00101   3*C       SIMPLE STEPWISE REGRESSION, ADAPTED FROM G2 ER MPR2 477              GAR70010
00101   4*C       THIS ADAPTATION ALLOWS GENERATION OF DATA FROM EXISTING PROGRAMS     GAR70020
00101   5*C         AND SUBSEQUENT CORRELATION BY USE OF THIS SUBROUTINE.              GAR70030
00101   6*C       THIS SUBROUTINE IS WRITTEN FOR FORTRAN MONITOR OPERATION.            GAR70040
00101   7*C         ROGER N. WRIGHT                FEBRUARY 28, 1961                 GAR70050
00101   8*C         IFLIST = 1  DO NOT LIST INPUT DATA ON THE OUTPUT TAPE NTPOUT     GAR70060
00101   9*C         IFAT   = 1  THEN ALL WEIGHTS (WHT) = 1.0                         GAR70070
00101  10*C         IFSTEP = 1  DO NOT PRINT EACH STEP                               GAR70080
00101  11*C         IFRAW  = 1  DO NOT PRINT RAW SUMS AND SQUARES                    GAR70090
00101  12*C         IFAVE  = 1  DO NOT PRINT AVERAGES                                GAR70100
00101  13*C         IFRESD = 1  DO NOT PRINT RESIDUAL SUMS SQUARES                   GAR70110
00101  14*C         IFCOEN = 1  DO NOT PRINT PARTIAL COEFFICIENTS                    GAR70120
00101  15*C         IFPRED = 1  DO NOT CALCULATE PREDICTED VALUES                    GAR70130
00101  16*C         IFCNST = 1  DO NOT HAVE A CONSTANT TERM IN THE EQUATION          GAR70140
00103  17*C       DIMENSION DATA(300),AVE(300),SIGMA(300),COEN(300),SIGMCO(300),
00103  18*C      1   INDEX(300),VECTOR(201,201),CP(300)
00104  19*        COMMON NTPI,NTPOUT,TOL,EFIN,EFOUT,NOPROB,NVAR,NODATA               GAR50010
00105  20*        COMMON IFLIST,IFAT,IFSTEP,IFRAW,IFAVE,IFRESD,IFCOEN,IFPRED         GAR50020
00106  21*        COMMON IFCNST                                                      GAR50030
00107  22*        COMMON CP
00110  23*        NOIN=0
00111  24*        VAR=0.
00112  25*        K=0                                                                GAR70150
00113  26*        FLEVEL=0                                                           GAR70160
00114  27*        NOENT=0                                                            GAR70170
00115  28*        NOWIN=0                                                            GAR70180
00116  29*        NOVAR=1.VAR                                                        GAR70190
00117  30*        NVPI=NOVAR+1                                                       GAR70200
00120  31*        110 DO 120 I=1,NVP1                                                GAR70210
00121  32*        130 DO 120 J=1,NVP1                                                GAR70220
00124  33*        120 VECTOR(I,J)=0.0                                                GAR70230
00127  34*        121 READ NTPI                                                      GAR70240
00132  35*        DETERMINATION IF DATA POINTS ARE WEIGHTED, IFWT=1 ALL WEIGHTS =1.0 GAR70250
00133  36*C       140 IF (IFAT)900,900,150                                           GAR70260
00133  37*C       EXIT INSTRUCTION IN CASE OF CONTROL WORD ERROR                     GAR70270
00135  38*C       900 WRITE (NTPOUT,905)                                             GAR70280
00136  39*        905 FORMAT (1H0,21HCONTROL WORD ERROR//)                           GAR70290
00140  40*        RETURN                                                             GAR70300
00140  41*C       150 READ (NTPI,FMT) ((DATA(L,L=1,NOVAR)                            GAR70310
00141  42*C       FORMAT (1H0,26X,73H- - - - - - - - - - - - - - - - - - - - - - -)  GAR70320
00142  43*C      1LEM TERMINATED - - - - - - - - - - - - - - - - - - - - - - -)      GAR70330
00142  44*        GO TO 910                                                          GAR70340
00145  45*        160 DO 170 N=1,NODATA                                              GAR70350
00145  46*        READ (NTPI,NUMB)(DATA(L),L=1,NOVAR)                                GAR70360
00145  47*C       OPTIONAL PRINTOUT OF INPUT DATA, IFLIST=0 DATA IS PRINTED OUT,     GAR70370
00154  48*        162 IF (IFLIST)900,163,180                                         GAR70380
00157  49*        163 WRITE (NTPOUT,93)NUMB,(DATA(L),L=1,NOVAR)                      GAR70390
00166  50*         93 FORMAT (5H RUN ,F6.1,8E13.6/(11H ,10X,8E13.6))                 GAR70400
00167  51*        180 DO 190 I=1,NOVAR                                               GAR70410
00172  52*        200 VECTOR(I,NOVAR+1)=VECTOR(I,NOVAR+1)+DATA(I)                    GAR70420
00173  53*        210 DO 220 J=1,NOVAR                                               GAR70430
00176  54*        220 VECTOR(I,J)=VECTOR(I,J)+DATA(I)*DATA(J)                        GAR70440
00200  55*        190 CONTINUE                                                       GAR70450
```

```
                    H20 5A  LI.DE, T=32,77,122,167,302,392,482 DEG, F  4/18     #####180469  PAGE    12

00202    54*        170 VECTOR(NVP1,NVP1)=VECTOR(NVP1,NVP1)+1,0                                    GAR70460
00204    55*        230 GO TO 565                                                                  GAR70470
00204    56*  C        CALCULATION  SUMS WHEN VARIABLE WEIGHTS                                     GAR70480
00205    57*        500 DO 510 L=1,NODATA                                                          GAR70490
00210    58*        520 READ (NTPIN)RUN C,(DATA(L),L=1,NOVAR),WHT                                  GAR70500
00220    59*        522 IF (IFLIST)90,523,530                                                      GAR70510
00223    60*        523 WRITE (NTPOUT,93)RUNNO,(DATA(L),L=1,NOVAR),WHT                             GAR70520
00233    61*        530 DO 540 I=1,NOVAR                                                           GAR70530
00236    62*        550 VECTOR(I,NOVAR+1)=VECTOR(I,NOVAR+1)+DATA(I)*WHT                            GAR70540
00237    63*        560 DO 540 J=I,NOVAR                                                           GAR70550
00242    64*        540 VECTOR(I,J)=VECTOR(I,J)+DATA(I)*DATA(J)*WHT                                GAR70560
00245    65*        510 VECTOR(NVP1,NVP1)=VECTOR(NVP1,NVP1)+WHT                                    GAR70570
00245    66*  C        COMPLETED SUMS OF SQUARES AND CROSS PRODUCTS.  THESE ARE IN                 GAR70580
00245    67*  C        STORAGE IN LOCATION, VECTOR (I, J).  THESE WILL BE PRINTED OUT ON           GAR70590
00245    68*  C        OUTPUT TAPE NTPOUT UNDER CONTROL OF CONTROL WORD IFRESD, PRINTED            GAR70600
00245    69*  C        IF IFRESD=0, NOT PRINTED IF IFRESD=1,                                       GAR70610
00247    70*        565 NOVMI=NOVAR-1                                                              GAR70620
00250    71*        566 NOVPL=NOVAR+1                                                              GAR70630
00251    72*        567 WRITE (NTPOUT,90)NOPROB,NODATA,NOVAR,VECTOR(NOVPL,NOVPL),EFIN,            GAR70640
00251    73*           1EFOUT                                                                      GAR70650
00261    74*         90 FORMAT (1H1,52X,20HSTEPWISE  REGRESSION/1H0,52X,11HPROBLEM NO.,1X,GAR70660
00261    75*           1I8//1H0,9X,13HNO. OF DATA =,I6,24X,17HNO. OF VARIABLES=,I3,8X,29HWGAR70670
00261    76*           1EIGHTED DEGREES OF FREEDOM =,1X,F9.2/1H0,44X,27HF LEVEL TO ENTER VGAR70680
00261    77*           1ARIABLE =,F7.3/1H0,44X,27HF LEVEL TO REMOVE VARIABLE=,F7.3///)    GAR70690
00261    78*  C        OPTIONAL PRINTOUT OF RAW SUMS AND SQUARES                                   GAR70700
00262    79*        570 IF (IFRAW)900,580,650                                                      GAR70710
00265    80*        580 WRITE (NTPOUT,15)                                                          GAR70720
00267    81*         15 FORMAT (1H ,52X,19HSUMS  OF  VARIABLES//)                                  GAR70730
00270    82*        590 WRITE (NTPOUT,20)(I,VECTOR(I,NOVPL),I=1,NOVMI)                             GAR70740
00277    83*         20 FORMAT (1H ,9X,4HSUM X ,I2,4H  = ,E15.8,14X,6HSUM X ,I2,4H  = ,E15GAR70750
00277    84*           1.8,15X,6HSUM X ,I2,4H  = ,E15.8)                                           GAR70760
00300    85*        600 WRITE (NTPOUT,25)VECTOR(NOVAR,NOVPL)                                       GAR70770
00303    86*         25 FORMAT (1H ,9X,12HSUM  Y  = ,E15.8//)                                      GAR70780
00304    87*        610 WRITE (NTPOUT,30)                                                          GAR70790
00306    88*         30 FORMAT (1H ,40X,44HRAW  SUMS  OF  SQUARES  AND  CROSS  PRODUCTS//)GAR70800
00307    89*        620 WRITE (NTPOUT,35)((I,J,VECTOR(I,J),J=I,NOVMI),I=1,NOVMI)                   GAR70810
00322    90*         35 FORMAT (1H ,5X,2HX ,I2,6H  * X ,I2,4H  = ,E15.8,10X,2HX ,I2,6H  *GAR70820
00322    91*           1X ,I2,4H  = ,E15.8,11X,2HX ,I2,6H  * X ,I2,4H  = ,E15.8)                   GAR70830
00323    92*        630 WRITE (NTPOUT,40)(I,VECTOR(I,NOVAR),I=1,NOVMI)                             GAR70840
00332    93*         40 FORMAT (1H ,5X,2HX ,I2,12H  *  Y  = ,E15.8,10X,2HX ,I2,12H  *GAR70850
00332    94*           1Y  = ,E15.8,11X,2HX ,I2,12H  *  Y  = ,E15.8)                              GAR70860
00333    95*        640 WRITE (NTPOUT,45)VECTOR(NOVAR,NOVAR)                                       GAR70870
00336    96*         45 FORMAT (1H ,7X,14HY  *  Y  = ,E15.8//)                                     GAR70880
00337    97*           GO TO 650                                                                   GAR70890
00337    98*  C        CALCULATION OF RESIDUAL SUMS OF SQUARES AND CROSS PRODUCTS                  GAR70900
00340    99*        650 IF (IFCNST)900,651,735                                                     GAR70910
00343   100*        651 IF (VECTOR(NOVPL,NOVPL))652,652,655                                        GAR70920
00346   101*        652 WRITE (NTPOUT,654)                                                         GAR70930
00350   102*        654 FORMAT (1H0/1H0,26X,73H- - - - - - - - - ZERO NUMBER OF DATA, PROBLGAR70940
00350   103*           1EM TERMINATED, - - - - - - - - -)                                          GAR70950
00351   104*           GO TO 910                                                                   GAR70960
00352   105*        655 DO 660 I=1,NOVAR                                                           GAR70970
00355   106*        670 DO 660 J=I,NOVAR                                                           GAR70980
00360   107*        660 VECTOR(I,J)=VECTOR(I,J)-(VECTOR(I,NOVPL)*VECTOR(J,NOVPL)/VECTOR(GAR70990
00360   108*           1NOVPL,NOVPL))                                                              GAR71000
00363   109*        680 DO 690 I=1,NOVAR                                                           GAR71010
00366   110*        690 AVE(I)=VECTOR(I,NOVPL)/VECTOR(NOVPL,NOVPL)                                 GAR71020
00366   111*  C        OPTIONAL PRINTOUT OF AVERAGES                                               GAR71030
00370   112*        700 IF (IFAVE)900,710,735                                                      GAR71040
00373   113*        710 WRITE (NTPOUT,50)                                                          GAR71050
```

```
00375  114*      50 FORMAT (1H ,47X,29HAVERAGE  VALUE  OF  VARIABLES//)                GAR71060
00376  115*     720 WRITE (NTPOUT,721)(I,AVE(I),I=1,NOVMI)                            GAR71070
00405  116*     721 FORMAT (1H ,9X,6HAVE X ,I2,4H  = ,E15.8,14X,6HAVE X ,I2,4H  = ,E15GAR71080
00405  117*        1.8,15X,6HAVE X ,I2,4H  = ,E15.8)                                  GAR71090
00406  118*     730 WRITE ( NTPOUT,731)AVE(NOVAR)                                     GAR71100
00411  119*     731 FORMAT (1H ,9X,12HAVE   Y   = ,E15.8//)                           GAR71110
00411  120*  C      OPTIONAL PRINTOUT OF RESIDUAL SUMS OF SQUARES                     GAR71120
00412  121*     735 IF (IPRESD)900,740,780                                            GAR71130
00415  122*     740 WRITE (NTPOUT,55)                                                 GAR71140
00417  123*      55 FORMAT (1H ,38X,                                                  GAR71150
00417  124*        14HRESIDUAL  SUMS  OF  SQUARES  AND  CROSS PRODUCTS//)             GAR71160
00420  125*     750 WRITE (NTPOUT,35)((I,J,VECTOR(I,J),J=I,NOVMI),I=1,NOVMI)          GAR71170
00433  126*     760 WRITE (NTPOUT,45)(I,VECTOR(I,NOVAR),I=1,NOVMI)                    GAR71180
00442  127*     770 WRITE (NTPOUT,45)VECTOR(NOVAR,NOVAR)                              GAR71190
00445  128*     780 NOSTEP=-1                                                         GAR71200
00446  129*     781 ASSIGN 1320 TO NUMBER                                             GAR71210
00447  130*     782 DEFR=VECTOR(NOVPL,NOVPL)-1.0                                      GAR71220
00450  131*     790 DO 800 I=1,NOVAR                                                  GAR71230
00453  132*     791 IF (VECTOR(I,I))792,794,61                                        GAR71240
00456  133*     792 WRITE (NTPOUT,793)I                                               GAR71250
00461  134*     793 FORMAT (1HO/1HO,16X,42H- - - - - - ERROR RESIDUAL SQUARE VARIABLE,GAR71260
00461  135*        1I4,1X,44HIS NEGATIVE, PROBLEM TERMINATED, - - - - - - -)          GAR71270
00462  136*        GO TO 910                                                          GAR71280
00463  137*     794 WRITE (NTPOUT,795)I                                               GAR71290
00466  138*     795 FORMAT (1HO,38X,8HVARIABLE,I4,12H IS CONSTANT)                    GAR71300
00467  139*     796 SIGMA(I)=1.0                                                      GAR71310
00470  140*     797 GO TO 800                                                         GAR71320
00471  141*     810 SIGMA(I)=SQRT(VECTOR(I,I))                                        GAR71330
00472  142*     800 VECTOR(I,I)=1.0                                                   GAR71340
00474  143*     820 DO 830 I=1,NOVMI                                                  GAR71350
00477  144*     840 IP1=I+1                                                           GAR71360
00500  145*     841 DO 830 J=IP1,NOVAR                                                GAR71370
00503  146*     850 VECTOR(I,J)=VECTOR(I,J)/(SIGMA(I)*SIGMA(J))                       GAR71380
00504  147*     830 VECTOR(J,I)=VECTOR(I,J)                                           GAR71390
00504  148*  C      OPTIONAL PRINTOUT OF PARTIAL CORRELATION COEFFICIENTS             GAR71400
00507  149*     860 IF (IPCOEF)910,870,1000                                           GAR71410
00512  150*     870 WRITE (NTPOUT,61)                                                 GAR71420
00514  151*      61 FORMAT ( 1H ,49X,34HPARTIAL  CORRELATION  COEFFICIENTS//)         GAR71430
00515  152*     874 NOVM2=NOVMI-1                                                     GAR71440
00516  153*     875 DO 885 I=1, NOVM2                                                 GAR71450
00521  154*     880 IP1=I+1                                                           GAR71460
00522  155*     885 WRITE (NTPOUT,35)(I,J,VECTOR(I,J),J=IP1,NOVMI)                    GAR71470
00533  156*     890 WRITE (NTPOUT,45)(I,VECTOR(I,NOVAR),I=1,NOVMI)                    GAR71480
00542  157*    1000 NOSTEP=NOSTEP+1                                                   GAR71490
00543  158*    1001 IF (VECTOR(NOVAR,NOVAR))1002,1002,1010                           GAR71500
00546  159*    1002 NSTPM1=NOSTEP-1                                                  GAR71510
00547  160*         WRITE (NTPOUT,1004)NSTPM1                                        GAR71520
00552  161*    1004 FORMAT (1HO,38X,38HY SQUARE NON-POSITIVE, TERMINATE STEP ,I5)    GAR71530
00553  162*         GO TO 1381                                                       GAR71540
00554  163*    1010 SIGY=SIGMA(NOVAR)*SQRT(VECTOR(NOVAR,NOVAR)/DEFR)                 GAR71550
00555  164*    1015 DEFR=DEFR-1.0                                                    GAR71560
00556  165*    1016 IF (DEFR)1018,1018,1020                                          GAR71570
00561  166*    1018 WRITE (NTPOUT,1019)NOSTEP                                        GAR71580
00564  167*    1019 FORMAT (1HO,38X,31HNO MORE DEGREES OF FREEDOM STEP,I5)           GAR71590
00565  168*         GO TO 1381                                                       GAR71600
00566  169*    1020 VMIN=0.0                                                         GAR71610
00567  170*    1030 VMAX=0.0                                                         GAR71620
00570  171*    1035 NOIN=0                                                           GAR71630
00571  172*    1040 DO 1050 I=1,NOVMI                                                GAR71640
00574  173*    1041 IF (VECTOR(I,I))1043,1050,1060                                   GAR71650
```

```
                    FTN 5A  LINE, T=72,77,122,167,302,392,487 DEC, F  4/18    0000160469  PAGE  14

00577   174*     1043 WRITE (NTPOUT,1044)I,NOSTEP                                          GAR71660
00603   175*     1044 FORMAT (1H0,38X,9HSQUARE X ,I2,18H  NEGATIVE, SOLONG,I5,6H STEPS)    GAR71670
00604   176*     1045 GO TO 1351                                                           GAR71680
00605   177*     1050 IF (VECTOR(I,I)-TOL)1050,1080,1080                                   GAR71690
00610   178*     1060 VAR=VECTOR(I,NOVAR)*VECTOR(NOVAR,I)/VECTOR(I,I)                      GAR71700
00611   179*     1090 IF (VAR)1100,1050,1110                                               GAR71710
00614   180*     1100 NOIN=NOIN+1                                                          GAR71720
00615   181*     1120 INDEX(NOIN)=I                                                        GAR71730
00616   182*     1130 COEN(NOIN)=VECTOR(I,NOVAR)*SIGMA(NOVAR)/SIGMA(I)                     GAR71740
00617   183*     1140 SIGMCO(NOIN)=(SIGY/SIGMA(I))*SQRT(VECTOR(I,I))                       GAR71750
00620   184*     1150 IF (VMIN)1160,1170,904                                               GAR71760
00623   185*      904 WRITE (NTPOUT,906)                                                   GAR71770
00625   186*      906 FORMAT (1H0/1H0,26X,73H- - - - - - - - - - ERROR, VMIN PLUS, PROBLEMGAR71780
00625   187*        1 TERMINATED, - - - - - - - - - -)                                     GAR71790
00626   188*          GO TO 910                                                          GAR71800
00627   189*     1170 VMIN=VAR                                                           GAR71810
00630   190*     1180 NOMIN=I                                                            GAR71820
00631   191*     1190 GO TO 1050                                                         GAR71830
00632   192*     1160 IF (VAR-VMIN)1050,1050,1170                                        GAR71840
00635   193*     1110 IF (VAR-VMAX)1050,1050,1210                                        GAR71850
00640   194*     1210 VMAX=VAR                                                           GAR71860
00641   195*     1220 NOMAX=I                                                            GAR71870
00642   196*     1050 CONTINUE                                                           GAR71880
00644   197*     1230 IF (NOIN)903,1240,1245                                             GAR71890
00647   198*      903 WRITE (NTPOUT,907)                                                 GAR71900
00651   199*      907 FORMAT (1H0/1H0,26X,73H- - - - - - - - - - ERROR, NOIN MINUS, PROBLEGAR71910
00651   200*        1 TERMINATED,- - - - - - - - - -)                                    GAR71920
00652   201*          GO TO 910                                                          GAR71930
00653   202*     1240 WRITE (NTPOUT,65)SIGY                                              GAR71940
00656   203*       65 FORMAT (1H1,40X,22HSTANDARD ERROR OF Y = ,5X,E15,8)                GAR71950
00657   204*     1260 GO TO 1350                                                         GAR71960
00660   205*     1245 IF (IFCONST)900,1250,1246                                          GAR71970
00663   206*     1246 CNST=0.0                                                           GAR71980
00664   207*     1247 GO TO 1300                                                         GAR71990
00665   208*     1250 CNST=AVE(NOVAR)                                                    GAR72000
00666   209*     1270 DO 1280 I=1,NOIN                                                   GAR72010
00671   210*     1290 J=INDEX(I)                                                         GAR72020
00672   211*     1280 CNST=CNST-(COEN(I)*AVE(J))                                         GAR72030
00672   212*C         OPTIONAL PRINTOUT OF EACH STEP                                     GAR72040
00674   213*     1300 IF (IFSTEP)900,1310,1320                                           GAR72050
00677   214*     1310 IF (NOEXT)1311,1311,1313                                           GAR72060
00702   215*     1311 WRITE (NTPOUT,91)NOSTEP,K                                          GAR72070
00706   216*       91 FORMAT (1H0,38X,8HSTEP NO,,I4/1H ,40X,16HVARIABLE REMOVED,10X,I3)  GAR72080
00707   217*     1312 GO TO 1314                                                         GAR72090
00710   218*     1313 WRITE (NTPOUT,92)NOSTEP,K                                          GAR72100
00714   219*       92 FORMAT (1H0,38X,8HSTEP NO,,I4/1H ,40X,17HVARIABLE ENTERING,9X,I3)  GAR72110
00715   220*     1314 WRITE (NTPOUT,70)FLEVEL,SIGY,CNST,(INDEX(J),COEN(J),SIGMCO(J),J=1,GAR72120
00715   221*        1NOIN)                                                               GAR72130
00730   222*       70 FORMAT (1H ,40X,7HF LEVEL,13X,2H= ,E12.4/1H ,40X,22HSTANDARD ERRORGAR72140
00730   223*        1 OF Y = ,5X,E15.8/1H ,40X,8HCONSTANT,12X,2H= ,5X,E15.8/1H0,50X,8HVGAR72150
00730   224*        1ARIABLE,11X,11HCOEFFICIENT,5X,17HSTD ERROR OF COEF//(1H ,51X,2HX GAR72160
00730   225*        1I2,1H ,11X,E15.8,4X,E15.8))                                         GAR72170
00731   226*     1315 GO TO NUMBER,(1320,1580)                                           GAR72180
00732   227*     1320 FLEVEL=SIGY*COEF/VECTOR(NOVAR,NOVAR)                               GAR72190
00733   228*     1330 IF (EFOUT+FLEVEL)1350,1350,1340                                    GAR72200
00736   229*     1340 K=NOMIN                                                            GAR72210
00737   230*     1345 NOEXT=0                                                            GAR72220
00740   231*          GO TO 1391                                                         GAR72230
00741   232*     1350 FLEVEL=VMAX*COEF/(VECTOR(NOVAR,NOVAR)-VMAX)                        GAR72240
00742   233*     1360 IF (EFIN-FLEVEL)1370,1361,1380                                     GAR72250
```

```
                H20 DA  LINES, T=32,77,122,167,302,392,482 DEG, F  4/18     0000000180469  PAGE   15

00745   234*     1361 IF (EFI )1370,1360,1370                                                    GAR72260
00750   235*     1370 K=NOMAX                                                                    GAR72270
00751   236*     1390 NOEXT=K                                                                    GAR72280
00752   237*     1391 IF (K)1392,1392,1400                                                       GAR72290
00755   238*     1392 WRITE (NTPOUT,1395)NOSTEP                                                  GAR72300
00760   239*     1395 FORMAT (1H0/1H0,26X,30H- - - - - - - - - - - -  K=0, STEP,I5,1X,37HPROGRAGAR72310
00760   240*         1BLEM TERMINATED, - - - - - - - - - -)                                      GAR72320
00761   241*     1394 GO TO 910                                                                  GAR72330
00762   242*     1400 DO 1410 I=1,NOVAR                                                          GAR72340
00765   243*     1420 IF (I-K)1430,1410,1430                                                     GAR72350
00770   244*     1430 DO 1440 J=1,NOVAR                                                          GAR72360
00773   245*     1450 IF (J-K)1460,1440,1460                                                     GAR72370
00776   246*     1460 VECTOR(I,J)=VECTOR(I,J)-(VECTOR(I,K)*VECTOR(K,J)/VECTOR(K,K))              GAR72380
00777   247*     1440 CONTINUE                                                                   GAR72390
01001   248*     1410 CONTINUE                                                                   GAR72400
01003   249*     1470 DO 1480 I=1,NOVAR                                                          GAR72410
01006   250*     1490 IF (I-K)1500,1480,1500                                                     GAR72420
01011   251*     1500 VECTOR(I,K)=-VECTOR(I,K)/VECTOR(K,K)                                       GAR72430
01012   252*     1480 CONTINUE                                                                   GAR72440
01014   253*     1510 DO 1520 J=1,NOVAR                                                          GAR72450
01017   254*     1530 IF (J-K)1540,1520,1540                                                     GAR72460
01022   255*     1540 VECTOR(K,J)=VECTOR(K,J)/VECTOR(K,K)                                        GAR72470
01023   256*     1520 CONTINUE                                                                   GAR72480
01025   257*     1550 VECTOR(K,K)=1.0/VECTOR(K,K)                                                GAR72490
01026   258*     1560 GO TO 1000                                                                 GAR72500
01027   259*     1380 WRITE (NTPOUT,75)NOSTEP                                                    GAR72510
01032   260*       75 FORMAT (1H0/1H ,39X,9HCOMPLETED,3X,I3,20H STEPS OF REGRESSION)             GAR72520
01033   261*     1381 IF (IFSTEP)900,1560,1570                                                   GAR72530
01036   262*     1570 ASSIGN 1560 TO NUMBER                                                      GAR72540
01037   263*     1571 GO TO 1310                                                                 GAR72550
01040   264*     1580 WRITE (NTPOUT,1586)(L,VECTOR(L,L),L=1,NOVMI)                               GAR72560
01047   265*     1586 FORMAT (1H0/1H ,53X,18HDIAGONAL  ELEMENTS/1H0,50X,8HVARIABLE,13X,         GAR72570
01047   266*         15HVALUE//(1H ,51X,2HX ,I2,1H ,11X,E15.8))                                  GAR72580
01047   267*C        OPTIONAL PRINTOUT OF PREDICTED VALUES OF Y, PRINTED IF IFPRED=0.            GAR72590
01050   268*     1581 IF (IFPRED)900,1582,910                                                    GAR72600
01053   269*     1582 REWIND NTPIN                                                               GAR72610
01053   270*C1583 WRITE (NTPOUT,85)                                                             GAR72620
01054   271*     1583 CONTINUE                                                                   GAR72630
01055   272*       85 FORMAT (1H1/1H ,47X,29HACTUAL  VS  PREDICTED RESULTS/1H0,32X,57HRUGAR72630
01055   273*         1N NO.       ACTUAL          PREDICTED          DEVIATION//)               GAR72640
01056   274*     1590 DO 1660 L=1,NODATA                                                         GAR72650
01061   275*     1591 IF (IFRT)900,1601,1600                                                     GAR72660
01064   276*     1600 READ (NTPIN)RUNNO,(DATA(L),L=1,NOVAR)                                      GAR72670
01073   277*          GO TO 1610                                                                 GAR72680
01074   278*     1601 READ (NTPIN)RUNNO,(DATA(L),L=1,NOVAR),WHT                                  GAR72690
01104   279*     1610 YPRED=CONST                                                                GAR72710
01105   280*     1620 CONTINUE                                                                   
01106   281*          DO 1630 I=1,NOIN                                                           
01111   282*     1640 K=INDEX(I)                                                                 GAR72730
01112   283*     1630 YPRED=YPRED+COEF(I)*DATA(K)                                                GAR72740
01114   284*     1650 DEV=DATA(NOVAR)-YPRED                                                      GAR72750
01115   285*          CP(N)=YPRED                                                                
01116   286*     1660 CONTINUE                                                                   
01116   287*C1660 WRITE (NTPOUT,80)RUNNO,DATA(NOVAR),YPRED,DEV                                   GAR72760
01120   288*       80 FORMAT (1H ,32X,F6.1,3X,E15.8,3X,E15.8,3X,E15.8)                           GAR72770
01121   289*      910 RETURN                                                                     GAR72780
01122   290*          END                                                                        GAR72790

 END OF UNIVAC 1108 FORTRAN V COMPILATION,     0 *DIAGNOSTIC* MESSAGE(S)
```

REFERENCES

1. Hwang, K. C., A Transient Performance Method for CO_2 Removal With Regenerable Adsorbents, NASA CR-112098, October 1972.

2. Ruthven, D. M. and K. F. Loughlin, "Diffusion in Molecular Sieves," presented at 68th National Meeting of AIChE, March 1971.

3. Skopp, A., and J. Miceli, Investigation of Heatless Adsorption Technology for Carbon Dioxide Control for Manned Spacecraft, NASA CR-66582.

4. Perry, R. M., C. H. Chilton, S. D. Kirkpatrick, Chemical Engineers' Handbook, 4th ed. 1963, McGraw-Hill, N.Y. p. 16-13.

5. Lightfoot, E. N., et al. in New Chem. Eng. Sep. Tech. Schoen et al., ed., Interscience, N.Y. (1962).

6. Lee, H., and W. P. Cummings, "A New Design Method for Silica Gel Air Driers under Nonisothermal Conditions," Chemical Engineering Progress Symposium Series, No. 74, Vol. 63., pp. 42-49.

7. Vermeulen, T., and G. Klein, "Recent Background Developments for Adsorption Column Design, " Invited Lecture, 68th National Meeting, AIChe, March 1971.

8. Dell'Osso, L., and J. Winnick, Ind. Eng. Chem. Proc. Design Devel. 8, 469 (1969).

9. "Davison Molecular Sieves," Brochure by W. R. Grace and Co., Baltimore, Maryland.

10. The Fluid Processing Handbook, Davison Chemical Division, W. R. Grace and Co., 1966.

*U.S. GOVERNMENT PRINTING OFFICE: 1973-739-029/72